# COMPUTING IN CARDIOLOGY

**September 7-10, 2014**
**Boston, Massachusetts, USA**

**Welcome to Boston!**

# Table of Contents

Sponsors ..... ii
Computing In Cardiology 2015 ..... v
Letter from the President: ..... vii
Welcome to Boston ..... ix
Computing in Cardiolgoy 2014 Hotel and Conference Venue ..... xi
- Meeting Site and Schedule ..... xi
- Transportation ..... xi
- Registration ..... xi
- Internet ..... xii
- Meals ..... xii
- Accompanying Persons ..... xii

For Authors and Speakers ..... xii
- Oral Presentations ..... xii
- Rosanna Degani Young Investigator Award ..... xiii
- PhysioNet / Computing in Cardiology Challenge 2014 ..... xiii
- Poster Sessions ..... xiii
- Manuscripts ..... xiii

Conference Overview ..... xiv
- Sunday Symposium: Data-driven Learning, Discovery, and Innovation ..... xiv
- Scientific Sessions ..... xv
- Abstract Number Formatting ..... xv
- Social Program ..... xvi

Traveling Directions ..... xviii
- Silver Line SL1 To and From Logan Airport ..... xx
- Getting to the Sunday Symposium ..... xx
- Getting around in Boston ..... xxi

Scientific Sessions Program Overview ..... xxii
Scientific Program ..... xxv
Abstracts ..... 1

## Sponsors

We would like to thank our sponsors and those who have made generous donations:

http://www.mortara.com

PHILIPS

http://www.usa.philips.com/healthcare

mindray

http://www.mindraynorthamerica.com/

IBM

http://ibm.com

ZOLL

http://www.zoll.com

MITSUBISHI ELECTRIC
Changes for the Better

http://merl.com

IOP Publishing

http://www.iop.org

## Technical Sponsors:

imes
INSTITUTE FOR MEDICAL ENGINEERING & SCIENCE

http://imes.mit.edu

CSAIL

http://www.csail.mit.edu

PhysioNet
the research resource for complex physiologic signals

http://physionet.org

**The 41st conference of Computing in Cardiology is hosted by**

Massachusetts Institute of Technology

**The CinC 2014 Scientific Program is endorsed by:**

The Engineering in Medicine and Biology Society of the IEEE advances the application of engineering sciences and technology to medicine and biology, promotes the profession, and provides global leadership for the benefit of its members and humanity by disseminating knowledge, setting standards, fostering professional development, and recognizing excellence.

The field of interest of the IEEE Engineering in Medicine and Biology Society is the application of the concepts and methods of the physical and engineering sciences in biology and medicine. This covers a very broad spectrum ranging from formalized mathematical theory through experimental science and technological development to practical clinical applications. It includes support of scientific, technological and educational activities.


Engineering in Medicine and Biology Society
445 Hoes Lane
Piscataway, New Jersey, USA 08854
Telephone: +1 732 981 3433
Facsimile: +1 732 465 6435
E-mail: emb-exec@ieee.org, www.embs.org


**PUBLICATIONS**
IEEE PULSE
Transactions on Biomedical Engineering/Transactions on Biomedical Engineering Letters
Transactions on Information Technology in Biomedicine
Transactions on Neural Systems and Rehabilitation Engineering
Transactions on Medical Imaging
Transactions on NanoBioscience
Transactions on Computational Biology and Bioinformatics
Transactions on Biomedical Circuits and Systems
Reviews on Biomedical Engineering

**ELECTRONIC PRODUCTS**
EMBS Electronic Resource

**CONFERENCES**
Annual International Conference of the IEEE Engineering in Medicine and Biology Society (EMBC)
IEEE EMBS Special Topic Conference on Neural Engineering (NER)
International Symposium on Biomedical Imaging (ISBI)
International Conference on Biomedical Robotics and Biomechatronics (BIOROB)
International Conference on Rehabilitation Robotics (ICORR) AMA/IEEE-EMBS Medical Technology Conference (MedTech)
Grand Challenges Conference Series (GCBE)

**SUMMER SCHOOLS Sponsored by EMBS**
International Summer School on Biomedical Imaging
International Summer School on Biomedical Signal Processing
International Summer School on Biocomplexity
International Summer School on Medical Devices and Biosensors
International Summer School on Information Technology in Biomedicine

## Computing In Cardiology 2015
**September 6-9, 2015, Nice, France**

Welcome to the Heart of the French Riviera

"*When I realized I would see that light every morning, I could not believe my happiness … I decided never to leave Nice and remained here for my almost entire existence* " (Henri Matisse), … or just for a little while ?

We warmly invite you to discover with us this kind atmosphere by attending the 42th annual scientific meeting of *Computing in Cardiology*, for its second French edition. With over 300 days of sunshine a year, its own, distinct gastronomy, a stunning beach promenade facing a vast choice of hotels, Nice is an amazing combination of old (vieux Nice) and contemporary aspects of Mediterranean style, surrounded by the mountain and the sea.

Nice is easy to reach. The Nice-Cote d'Azur airport is an international gateway, the second largest airport in France, with 103 direct-flight destinations and is connected to European and International capitals (London, Frankfurt, Amsterdam, New-York, Dubaï). Conveniently located nearby the city center it will connect you to various accommodation facilities for all budgets.

For further details, please refer to cinc2015.org

# Board of Directors and Local Committee

## BOARD OF DIRECTORS

**President**
Peter Macfarlane, DSc
University of Glasgow
Glasgow, UK

**Secretary**
Leif Sörnmo, DSc
Lund University Lund, Sweden

**Treasurer**
Victor Mor-Avi, PhD
University of Chicago Chicago, IL,USA

**Past President**
Harold Ostrow, MSEE
Gaithersburg, MD, USA

Willem Dassen, PhD
Maastricht University Maastricht,
The Netherlands

Paul Kligfield, MD
Weill Cornell Medical School
New York, NY, USA

Pablo Laguna, PhD
University of Zaragoza
Zaragoza, Spain

George Moody
Massachusetts Institute of
Technology Cambridge, MA, USA

Dewar Finlay, PhD
University of Ulster
Belfast, UK

Sheryl Prucka, MSEE
Park City, UT, USA

**Ex-Officio**
ESC Representative
Marek Malik, MD, PhD University of
London, England

**Editor, Proceedings**
Alan Murray, PhD
Newcastle University
Newcastle upon Tyne, UK



## LOCAL COMMITTEE

**Faculty**
Roger Mark, MD, PhD – Professor of Health Sciences and Technology and EECS

Ary Goldberger, MD – Professor of Medicine, HMS, BIDMC

Dana Brooks, PhD - Professor of Bioengineering and Electrical Engineering, Northeastern University

Peter Szolovits, PhD - Professor of Computer Science, MIT

Rosalind Picard, PhD - Professor, Program in Media Arts and Sciences, MIT

Thomas Heldt, PhD - Assistant Professor of EECS, MIT

Riccardo Barbieri, PhD - Assistant Professor of Anesthesia (Biomedical Engineering) HMS at MGH

Madalena Costa, PhD – Assistant Professor of Medicine HMS, BIDMC

**Research Staff**
George Moody – Research Engineer, IMES

Ikaro Silva, PhD – Research Engineer, IMES

Leo Celi, MD, MS – Research Scientist, IMES

Li-wei Lehman, PhD – Research Scientist, IMES

Braiam Escobar, BS – Visiting Engineer, IMES

**Postdocs**
Mengling Feng, PhD - IMES
Sara Mariani, PhD – Wyss Institute
Mariana Meo, PhD – HMS

**Grad Student**
Mohammad Ghassemi – EECS

**Industry**
John Wang, PhD - Principal Scientist, Philips Healthcare

## Letter from the President:

Dear Participant,

Welcome to the 41st Computing in Cardiology meeting. This is the third time that the conference has been held in Cambridge, MA and it is always a pleasure to return to the vicinity of the world famous MIT, whose staff have organised previous meetings as well as this conference! This year, however, the situation has been a little different.

The CinC Board of Directors normally meet towards the end of May at which time they review abstracts and organise the programme for September. This year was no exception and the Board met in Cambridge, MA at the end of May only to learn that George Moody, who had been leading the Local Organising Committee, had suffered a severe stroke a couple of days beforehand and was thus unable to participate in the deliberations. This was a significant setback. However, I am pleased to say that George is making gradual progress, though his recovery is still continuing. It is uncertain at the time of writing whether he can join us in September. We all wish him well on the road to recovery.

The Board is therefore very grateful to Dr Roger Mark, a previous Board Member and "veteran" of many CinC Conferences, including the earlier meetings in Cambridge which he helped to organise, for stepping in and taking charge of the local organising committee (LOC). Sincere thanks are due to Roger, his "first lieutenant" Ikaro Silva and other members of the LOC whose names can be found elsewhere, for all of the work which they have done to organise the conference. Much of the team were already helping George before his illness.

This year, there were a record number of abstracts submitted for a Computing in Cardiology meeting outside of Europe and it is encouraging that the organisation goes from strength to strength. There is an exciting social programme which involves a dinner while cruising round the Boston harbor area. The usual activist and passivist programme will also take place to keep you busy while a Critical Data Marathon has been organised as a pre-conference meeting, which is not a part of the Computing in Cardiology conference, but is allied with it. The regular Sunday symposium is also on the agenda and there is a link with the pre-conference meeting in the form of data driven research.

At the end of this meeting, Sheri Prucka and Pim Dassen leave the Board. I would like to thank them for 9 years of hard work serving Computing in Cardiology, Sheri through directing our IT related work, such as abstract

submission, registration, programme compilation as well as producing this abstract book, and Pim for organising the Young Investigator's Award for several years. In addition, Harold Ostrow steps down from the role of Past President. Harold has been involved with Computers and then Computing in Cardiology essentially from their inception. He has been on the Board more than once and has faithfully assisted CinC through thick and thin! He deserves special mention for such a long, dedicated period of service to the organisation, for which he is offered our sincere thanks.

This year also marks my final year as President of the Board. The last six years have been challenging at times but there have been changes which need not all be listed here. They include a subtle change of the name of the organisation, a new website, a more sound financial footing, the first CinC conference to be organised in China and most recently, a more open method of soliciting nominations for Board membership. I would like to thank all the other members of the Board who have been a great support to me over the past six years and wish my successor, whoever that may be, every good wish for the continued success of CinC.

Next year the meeting will return to Europe and will be held in Nice from September 6$^{th}$ to 9$^{th}$, 2015. I do hope that after you go home from this meeting, you will start to think of what research you would like to present in Nice and be ready to submit an abstract by mid-April of next year.

Finally, may I wish you an academically profitable and socially enjoyable conference visit to Cambridge.

Sincerely,

Peter Macfarlane
President, Board of Computing in Cardiology

## Welcome to Boston

On behalf of the Organizing Committee it is our pleasure to welcome you once again to Boston and Cambridge, this time for the 42nd annual meeting of Computing in Cardiology. We are honored to host this important and active group of investigators from the physical sciences, engineering, computer science, medicine and physiology. We are confident that the level of social and scientific exchange will be up to the high standards of our past meetings.

It has been the goal of Computing in Cardiology from its inception to encourage engineers and computer scientists to interact closely and productively with physiologists and clinicians. This meeting is designed to foster that goal. The social events and scientific sessions are organized to facilitate technical exchange and personal collaborations. Please make this your own personal goal as well while we are together!

The sponsoring institution for the meeting this year is the MIT's Institute of Medical Engineering and Science (IMES), which shares the basic philosophy of Computing in Cardiology. IMES was established in July 2012, and serves as an integrative force across MIT, bringing together research and education efforts at the nexus of engineering, science, and clinical medicine to advance human health. IMES is also a robust new home for the Harvard-MIT Health Science & Technology (HST) program, which has a rich history of educating leaders in medicine and health-related technologies. HST was established in 1970 to focus the academic resources of the Massachusetts Institute of Technology and Harvard University (particularly the Medical School) on the resolution of important problems in medicine and the supporting sciences. Its educational programs (both MD and PhD tracks) and research activities are based on the belief that through close collaboration technology and medicine will continue to make major contributions toward better health for all.

*View of Beacon Street*

*Sailing on the Charles River*

The Boston area holds many treasures that await your exploration. We will show you some during the social program, but we encourage you to take the time to investigate the city's cultural attractions, its restaurants and shops, its major teaching and research hospitals, its universities, and its historical sites. Our conference staff is prepared to help in any way possible to make your stay an exciting and rewarding one!

Welcome!

George Moody & Roger G. Mark
Co-Chairs, Local Organizing Committee

# Computing in Cardiolgoy 2014 Hotel and Conference Venue

### *Meeting Site and Schedule*

The 41st annual conference of Computing in Cardiology will meet at the Royal Sonesta Hotel in Cambridge, Massachusetts, September 7 – 10, 2014. The hotel is located strategically at the head of the Charles River, and places guests close to the area's finest shops, museums, historic sites and restaurants. Just three miles from Logan International Airport, the Royal Sonesta is minutes from downtown Boston's financial district and the Boston Public Garden, with easy access to the historic waterfront, Faneuil Hall and the Freedom Trail. MIT and Cambridge high-tech centers are less than a mile away. The Royal Sonesta is directly across the street from the CambridgeSide Galleria, and next door to the Museum of Science.

The conference will begin on Sunday, September 7th, with an afternoon symposium on the MIT campus in the Media Lab, about a ten-minute walk from the main conference venue. The scientific sessions will begin on Monday morning with the opening plenary session of presentations by the four finalists in the Rosanna Degani Young Investigator Award (YIA) competition, followed by parallel sessions. Monday afternoon and evening will be devoted to the traditional social program with opportunities for activists and passivists to explore the Boston and Cambridge area, followed by a gala dinner cruise exploring Boston harbor. Parallel and poster sessions will continue on Tuesday and Wednesday, ending on Wednesday afternoon with a closing plenary session, including selected talks and presentations of the YIA, Challenge, and poster awards.

### *Transportation*

Cambridge is easily reached by taxi from Boston's Logan International Airport, and also by FREE public transportation (See Traveling Directions below) The Royal Sonesta Hotel is only three miles from the airport, on the Cambridge side of the Charles River, and is very close to the Science Museum that is a major landmark**.** The hotel provides shuttle service to MIT and to several Cambridge sites.

### *Registration*

The registration desk is located in the conference area on the second floor of the Royal Sonesta Hotel and will be open as follows:

| | |
|---|---|
| Sunday, September 7 | 0830 – 1800 |
| Monday, September 8 | 0800 – 1130 |
| Tuesday, September 9 | 0800 – 1600 |
| Wednesday, September 10 | 0800 – 1700 |

***Internet***
The Sonesta offers complimentary high-speed internet access (Wi-Fi and wired) in the rooms and in the conference area.

***Meals***
The Sunday Symposium will include a Reception at the MIT Media Lab. Lunch and dinner on Monday will be provided as part of the social program. Lunches on Tuesday and Wednesday will be provided during the poster sessions. Coffee breaks are scheduled regularly during the conference.

***Accompanying Persons***
The accompanying person registration allows the guest to attend the Sunday symposium and reception, and the Monday social event starting at 1300 with lunch, participation in the activist or passivist program and ending with the evening dinner cruise. All accompanying persons will have free access to the Science Museum for the entire day on Monday. The passivist program includes a short time to see the museum, but accompanying guests may wish to take advantage of a more leisurely visit earlier in the day.

## For Authors and Speakers

***Oral Presentations***
The time allocated for each presentation is 10 minutes, followed by 5 minutes for discussion except for sessions S51 and S71 (Challenge I & II). Speakers and session chairs are requested to adhere strictly to this schedule in order to finish sessions on time and to permit participants to move successfully from one parallel session to another.

All conference rooms will be equipped with a computer projection system (LCD projector and PC with Windows 7, PowerPoint 2010, Windows Media Player, and Adobe Acrobat reader). Speakers are required to allow adequate time prior to their sessions to load and check their presentations on the designated computer. If needed they may connect their own laptop and check their presentations prior to the beginning of their sessions. A local staff member will be available to help. In particular when speakers are presenting in the second of two consecutive sessions with no break scheduled between them, they should take care of these preparations before the beginning of the first session. *Any delay due to a speaker's presentation logistics will shorten the time available for that speaker's presentation.* In addition, speakers are required to meet with their session chairpersons in the scheduled conference room at least 10 minutes before the beginning of the session. It is helpful to check that the chairperson knows how to correctly pronounce your name.

***Rosanna Degani Young Investigator Award***

Computing in Cardiology runs an annual competition to encourage young investigators and to provide a living memorial to Rosanna Degani. The competition for the 2014 Rosanna Degani Young Investigator Award was open to persons under 36 years of age and in "training status" at the submission deadline of May 1st, 2014. Finalists in the competition will present their work in session M1, at 0800 on Monday, 7th September. The name of the winner will be announced during the closing plenary session on Wednesday.

***PhysioNet / Computing in Cardiology Challenge 2014***

Since 2000, Computing in Cardiology has annually issued a PhysioNet Challenge in cooperation with PhysioNet, part of the NIH sponsored Research Resource for Complex Physiologic Signals. The aim of this year's challenge is *"Robust Detection of Heart Beats in Multimodal Data".* The challenge sessions are on Tuesday, September 8th:

- S51 10:15 - 11:45
- S71 14:15 - 15:45

The time allocated for each oral presentation in these sessions is 3 minutes; the remaining time will be allocated to panel discussions. The winners will be announced during the closing plenary session on Wednesday.

***Poster Sessions***

The poster sessions will take place from 1200 - 1415 on Tuesday, September 8th and from 1245 - 1500 on Wednesday, and complimentary lunches will be served. Authors are requested to be present at their posters during that time in order to interact with other conference attendees.

Authors should hang their posters on Tuesday and Wednesday during or before the morning coffee breaks. Subject areas for the poster session will be clearly marked, and poster boards will be numbered with a card corresponding to the abstract number in this book. Authors must remove their posters promptly at the end of the poster session to avoid loss.

***Manuscripts***

Computing in Cardiology will publish the conference proceedings containing the complete manuscripts of all papers actually presented at the meeting. (No-shows will not be published.) The complete proceedings will be freely available via the CinC web site (http://www.cinc.org). Also, they will be published by the IEEE at their IEEEXplore digital library. For any questions about manuscripts consult via the CinC web site, or contact via email Prof. Alan Murray, the Editor of the proceedings. (alan.murray@ncl.ac.uk) **The deadline for submitting completed manuscripts is September 1, 2014.**

## Conference Overview

The conference begins on the afternoon of Sunday 7th with a special symposium entitled "Data-driven Learning, Discovery, and Innovation" to be held at the MIT Media Laboratory conference center. A reception starts at the end of the symposium. The scientific sessions of the conference begin on Monday morning at 0800. During the afternoon, the traditional social program will take place. Scientific sessions will continue on Tuesday and Wednesday. Sessions include both oral presentations and poster sessions.

***Sunday Symposium: Data-driven Learning, Discovery, and Innovation***
Time: Sunday, September 7th at 1400
Venue:
MIT Media Lab
MIT Campus, Building E14, 6th floor
Corner of Amherst and Carleton Streets
Cambridge, Massachusetts
(See below for walking route.)

The focus of this year's symposium is data — big data, shared data, metadata; well characterized, multidimensional, complex, physiologic and clinical data — and how data resources function as catalysts and accelerators of progress in understanding, predicting, and treating chronic and critical disorders. The program will include presentations by five outstanding researchers.

### Part I: Resources for Data-driven Research

#### The Framingham Heart Study

*Daniel Levy, MD*
Director of the Framingham Heart Study
Director of the Center for Population Studies
NIH/NHLBI
http://www.framinghamheartstudy.org/

#### PhysioNet: the Research Resource for Complex Physiologic Signals

*Ary L. Goldberger, MD*
PhysioNet Program Director
Director of the Margret & H. A. Rey Institute for Nonlinear Dynamics in Medicine, Beth Israel Deaconess Medical Center
Professor of Medicine, Harvard Medical School
http://physionet.org

### The MIMIC Intensive Care Databases

*Leo Anthony Celi, MD*
Laboratory for Computational Physiology, MIT
Assistant Clinical Professor of Medicine, Beth Israel Deaconess Medical Center
Founder and Executive Director of Sana (sana.mit.edu)
http://mimic.physionet.org/

## Part II: Closing the Loop

### Early detection of subacute potentially catastrophic illnesses using readily available bedside monitoring data

*J. Randall Moorman, MD*
Professor of Medicine, Biomedical Engineering and Molecular Physiology and Biological Physics, University of Virginia
Editor-in-Chief, *Physiological Measurement*
http://bme.virginia.edu/people/moorman.html

### Detection and treatment of apnea in preterm infants

*David Paydarfar, MD*
Professor of Neurology and Physiology, University of Massachusetts Medical School
http://wyss.harvard.edu/viewpage/206

1700 - 1900: Reception

***Scientific Sessions***

The scientific sessions of the conference are all held in the Royal Sonesta Hotel, and begin on Monday morning at 0800 with presentations by the finalists in the Rosanna Degani Young Investigators Competition, followed by parallel sessions for the remainder of the morning. The social program begins at 1300 and is described below.
Scientific presentations resume on Tuesday morning at 0815, and continue throughout the day. The Tuesday poster session is scheduled at 1200 and includes a buffet lunch. The final day of the conference, Wednesday, begins again at 0815. The Wednesday poster session starts at 1245 and also includes lunch.

***Abstract Number Formatting***
Please note that the numbering of abstracts in the abstract book are now numbered “xxx-yyy” where “xxx” represents the page number of the abstract in this book, and “yyy” represents the submission number of the

abstract. We hope that this numbering system will make it easier for authors to utilize the abstract book.

### *Social Program*

The social program is designed to provide conference attendees with an intimate view of the city of Boston, and also to provide ample time for networking and renewing old friendships. The program begins immediately after the last scientific session at 1300 with a short (10 minute) walk around the corner to the Museum of Science. Lunch will be served on the museum's pavilion with a beautiful view of the Charles River, the Esplanade, the Boston skyline, and the MIT campus. After lunch the attendees will divide into the activist and passivist groups.

*View from the Museum of Science Pavilion*

### *Passivist Program*

Immediately following lunch, the group will have a limited time to explore the fascinating exhibits in the Museum of Science. The group will next enjoy a guided exploration of the city of Boston's history. You will visit all the places that make Boston the birthplace of freedom and a city of firsts, from the golden-domed State House to Bunker Hill and the TD Banknorth Garden, Boston Common and Copley Square to the Big Dig, Government Center to fashionable Newbury Street, Quincy Market to the Prudential Tower, and more. And, as Boston unfolds before your eyes, your guide will be giving you lots of little known facts and interesting insights about our unique and wonderful city. The tour will conclude at the waterfront where you will join your activist colleagues on board the Odyssey ship for a delightful harbor Starlight Dinner Cruise. Trolley buses will return you to the hotel, probably around 2200.

*State House on Beacon Hill*

*Faneuil Hall at Quincy Market*

***Activist Program***

Immediately after lunch the activists will participate in the guided and narrated tour of Boston as described above. You will then be deposited somewhere in the city and will divide into competitive teams. An intellectually and physically challenging treasure hunt has been planned to explore the rich traditions and legends of the early 18th century freedom fighters (also known as patriots or as terrorists depending on one's point of view) in their early struggles against the British Empire. Boston was a hotbed of radicals where the American Revolution had its birth. You will explore the Boston 'massacre' , the Boston tea party, the 'Intolerable Acts', the role of Paul Revere in the Battle of Lexington and Concord, and other historical landmarks. Winning the hunt will require speed and cunning, and the race will be lots of fun. The hunt concludes at the waterfront in time to board the Odyssey ship for the Starlight Dinner Cruise. Trolley buses will return you to the hotel, probably around 2200.

*Paul Revere's House*

*USS Constitution*

*The Odyssey*

## Traveling Directions

* Public transportation from Logan airport to the Sonesta Hotel

Take the FREE SILVER LINE bus from the terminal to the SOUTH STATION stop. Change there to the RED LINE train (inbound) to PARK STREET, where you go upstairs to change to the GREEN LINE train going to LECHMERE.

From the Lechmere stop you walk 0.7 miles to the hotel.
Exit the station and follow signs to CAMBRIDGE STREET. Cross to First Street and walk along the CambridgeSide Galleria to Charles Street/Cambridgeside Place. Turn left and the Hotel will be at the end of the block. Total cost should be $0.00!

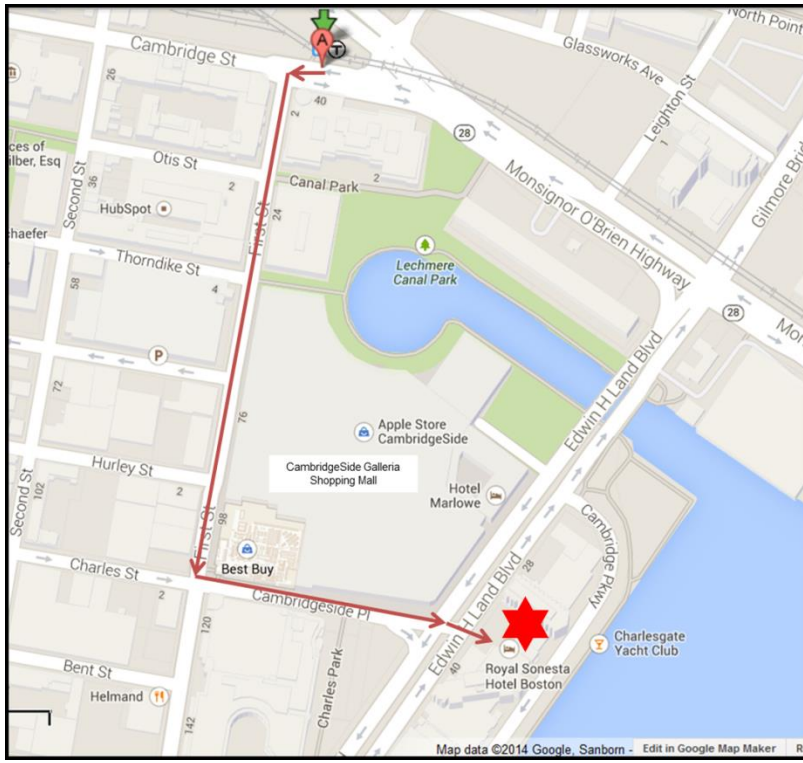


*Royal Sonesta Hotel Location*

***Silver Line SL1 To and From Logan Airport***

The Silver Line Route SL1 (Logan Airport - South Station via Waterfront) bus rapid transit service is your best direct connection to and from the Red Line at South Station, and this is your best option for transportation to:

- Cambridge
- Downtown Boston
- Harvard University
- MIT
- Massachusetts General Hospital
-

The service offered by Silver Line offers drop-off and pick-up directly in front of each Logan Terminal. There are no shuttle transfers and plenty of room to store your luggage.

For service *from* Logan Airport using the Silver Line SL1, take the FREE Silver Line Route SL1 from your terminal to the Red Line at South Station. Please use all doors to board at any Silver Line stop location. The Silver Line SL1 is handicapped-accessible and runs from approximately 5:30 a.m. to 12:30 a.m. every day of the week

***Getting to the Sunday Symposium***

Walking directions from the Sonesta Hotel to the Media Lab

The nicest route is along the bank of the Charles River. Exit the back of the hotel and walk along the river as far as the traffic light at Wadsworth St. That is a good place to cross Memorial Drive. Then continue on Wadsworth St., and in one block go left on Amherst St. Continue on Amherst St.to the Media Lab building on the right.

***Getting around in Boston***

The MBTA public transportation system runs across Boston-Cambridge from 6 a.m. until midnight on weekdays, and until 3 a.m. on weekends. http://www.mbta.com/

An alternative, fun way to explore the city is by bike sharing:
Hubway bike rental: https://www.thehubway.com/

## Scientific Sessions Program Overview

**Monday, September 8, 2014**

| | | |
|---|---|---|
| 8:00 | Welcome to CinC 2014 | Grand Ballroom |
| 8:15 | M1: Rosanna Degani Young Investigator Finals | Grand Ballroom |
| 9:45 | Coffee Break | |
| 10:15 | S21: Cardiac Mechanics | Skyline A |
| 10:15 | S22: ECG Noise Cancellation | Grand Ballroom A |
| 10:15 | S23: Cellular and Genetic Vent. Arrhythmic Modeling | Skyline C |
| 10:15 | S24: Pathophysiology of Heart Rate Variability | Grand Ballroom B |
| 11:45 | Coffee Break | |
| 12:00 | S31: Cardiac MRI & CT | Skyline A |
| 12:00 | S32: Electrophysiology Analysis | Skyline C |
| 12:00 | S33: ECG Decision Support Systems | Grand Ballroom A |
| 12:00 | S34: Physionet Inspired Studies | Grand Ballroom B |
| 1:00 | Social Event | |

**Tuesday, September 9, 2014**

| | | |
|---|---|---|
| 8:15 | S41: Repolarization and Risk | Grand Ballroom A |
| 8:15 | S42: Electrophysiology Modelling | Grand Ballroom B |
| 8:15 | S43: Algorithmic and Software Tools | Skyline A |
| 8:15 | S44: Temporal Aspects of CV Signals | Skyline C |
| 9:45 | Coffee Break | |
| 10:15 | S51: Challenge I | Grand Ballroom A |
| 10:15 | S52: Blood Pressure Systems | Grand Ballroom B |
| 10:15 | S53: Cardiovascular Ultrasound | Skyline A |
| 11:45 | Break | |
| 12:00 | P6: Poster Session with Lunch | Grand Ballroom Lobby |
| 14:00 | Break | |
| 14:15 | S71: Challenge II | Grand Ballroom A |
| 14:15 | S72: ECG Waveform Quality and Detection I | Grand Ballroom B |
| 14:15 | S73: Nonlinear Analysis of Heart Rate Variability | Skyline A |
| 14:15 | S74: Classification of CV Signals | Skyline C |
| 15:45 | Coffee Break | |
| 16:15 | S81: Ischemia and Infarction | Grand Ballroom A |
| 16:15 | S82: Fibrillation and Tachyarrhythmia | Grand Ballroom B |
| 16:15 | S83: Ventricular Modelling | Skyline A |
| 16:15 | S84: 3D Imaging | Skyline C |

**Wednesday, September 10, 2014**

| | | |
|---|---|---|
| 8:15 | S91: ECG Waveform Quality and Detection II | Grand Ballroom A |
| 8:15 | S92: Atrial Fibrillation Modelling | Skyline A |
| 8:15 | S93: Pathology of Heart Rate Variability | Grand Ballroom B |
| 8:15 | S94: Miscellaneous Medical Informatics | Skyline C |
| 9:45 | Coffee Break | |
| 10:15 | SA1: Atrial Fibrillation I | Grand Ballroom A |
| 10:15 | SA2: Inverse Problem | Skyline A |

10:15 SA3: Blood Pressure and Peripheral Pulse ..... Grand Ballroom B
10:15 SA4: Ionic Modelling in Ventricular Arrhythmia ..... Skyline C
11:15 Coffee Break
11:30 SB1: Ischemic Modelling ..... Grand Ballroom A
11:30 SB2: Atrial Fibrillation II..... Grand Ballroom B
11:30 SB3: Apnea Detection and Cardio-respiratory Interactions ..... Skyline A
12:30 Break
12:45 PC: Poster Session with Lunch .....Grand Ballroom Lobby
14:45 Break
15:00 MD: Plenary ..... Grand Ballroom
16:00 Closing Ceremony ..... Grand Ballroom
16:30 Conference Closes

# Scientific Program

**Monday, September 8, 2014, 08:15**

**M1: Rosanna Degani Young Investigator Finals**

Room: Grand Ballroom

Chair(s): Peter Macfarlane and Willem Dassen

1-113 **Identification of Myocardial Scar in Ventricular Tachycardia: Correlation between CT based results and Electro-Anatomic Map Findings**

Sofia Antunes*, Antonio Esposito, Giuseppe Macabelli, Anna Palmisano, Caterina Colantoni, Sebastiano Colombo, Paolo della Bella, Sergio Cerutti and Giovanna Rizzo

2-382 **How does Uncoupling in Ventricular Tissue Affect Conduction at Purkinje-Myocardial Junctions?**

Elham Behradfar*, Anders Nygren, Fu Siong Ng and Edward J Vigmond

3-121 **Physiology-based Regularization Improves Noninvasive Reconstruction and Localization of Cardiac Electrical Activity**

Matthijs JM Cluitmans*, Monique MJ de Jong, Paul GA Volders, Ralf LM Peeters and Ronald L Westra

4-251 **Non-invasive Detection of Reentrant Drivers during Atrial Fibrillation: a Clinical-Computational Study**

Miguel Rodrigo*, Andreu M Climent, Alejandro Liberos, Jorge Pedrón-Torrecilla, José Millet, Francisco Fernández-Avilés, Felipe Atienza, Omer Berenfeld and Maria S Guillem

**Monday, September 8, 2014, 10:15**

**S21: Cardiac Mechanics**

Room: Skyline A

Chair(s): Andrew Blaber and Elisabete Aramendi

5-374 **Using Seismocardiogram for Detection of Ischemia by Extraction of Systolic and Diastolic Time Variability**
Farzad Khosrow-Khavar, Andrew Blaber, Carlo Menon and Kouhyar Tavakolian*

6-277 **Modeling Mechanical Response of the Chest During the Cardiopulmonary Resuscitation Procedure**
Ali Jalali*, Vinay Nadkarni and C Nataraj

7-118 **Empirical Mode Decomposition for Chest Compression and Ventilation Detection in Cardiac Arrest**
Erik Alonso*, Elisabete Aramendi, Digna González-Otero, Unai Ayala, Mohamud Daya and James K Russell

8-91 **Evaluation of Aortic Flow Alterations using MRI: Associations with Left Ventricular Remodeling**
Ioannis Bargiotas*, Emilie Bollache, Alain De Cesare, Alban Redheuil, Elie Mousseaux and Nadjia Kachenoura

9-80 **ECG Analysis during Continuous-flow LVAD**
O Meste*, A Cabasson, L Fresiello, MG Trivella, A di Molfetta, G Ferrari and F Bernini

10-227 **Effects of Cardiac Resynchronization Therapy on the First Heart Sound Energy**
Ask Schou Jensen*, Samuel Emil Schmidt, Johannes Jan Struijk, John Hansen, Claus Graff, Jacob Melgaard, Tanveer Ahmed Bhuiyan, Kasper Emerek and Peter Soegaard

**Monday, September 8, 2014, 10:15**

**S22: ECG Noise Cancellation**

Room: Grand Ballroom A

Chair(s): John Wang and Aline Cabasson

11-210 **A Fexible PCA-based ECG Reconstruction Algorithm with Confidence Estimation for ECG during Exercise**
Steffen A Mann* and Reinhold Orglmeister

12-315 **Coherence as a Measure of Noise in the ECG**
Johannes Struijk*, Claus Graff, Joergen Kanters, Joel Xue, Ask Schou Jensen and Samuel Schmidt

13-386 **A Framework for ECG Signal Preprocessing based on Quadratic Variation Reduction**
Valeria Villani* and Antonio Fasano

14-381 **Electrocardiogram Artifact Cancelation based on Empirical Mode Decomposition and Peak Detection using Dual-Slope Algorithm**
Mohammadreza Ravanfar, Riadh Arefin, Kouhyar Tavakolian and Reza Fazel-Rezai*

15-111 **Extracting a Clean ECG from a Noisy Recording: A New Method based on Segmented-beat Modulation**
Angela Agostinelli*, Corrado Giuliani and Laura Burattini

16-63 **A Bayesian Filtering Framework for Accurate Extracting of the Non Invasive FECG Morphology**
Joachim Behar*, Fernando Andreotti, Julien Oster and Gari Clifford

**Monday, September 8, 2014, 10:15**

**S23: Cellular and Genetic Ventricular Arrhythmic Modeling**

Room: Skyline C

Chair(s): Marek Malik and Niels Otani

17-28 **A Boolean Network of Crosstalk between IGF and Wnt Signalling**
Lea Siegle, Ludwig Lausser, Michael Kühl and Hans A Kestler*

18-271 **Modelling the Functional Impact of KCNA5 Mutations on the Electrical and Mechanical Activities of Human Atrial Cells**
Haibo Ni*, Michael Colman and Henggui Zhang

19-73 **Simulation of Re-entrant Wave Dynamics in a 2-D Sheet of Human Ventricle with KCNJ2-linked Variant 3 Short QT Syndrome**
Kuanquan Wang*, Cunjin Luo, Yongfeng Yuan, Weigang Lu and Henggui Zhang

20-383 **The Effect of Random Cell Decoupling on Electrogram Fractionation near the Percolation Threshold in Microstructural Models of Cardiac Tissue**
Marjorie Hubbard* and Craig Henriquez

21-44 **Computational Modeling Supports Induced Pluripotent Stem Cell-derived Cardiomyocytes Reliability as a Model for Human LQT3**
Michelangelo Paci*, Stefano Severi and Jari Hyttinen

22-85 **Contribution of developmental changes in energy metabolism to excitation-contraction coupling of the ventricular cell: a simulation study**
Hitomi Sano*, Tamami Toki, Yasuhiro Naito and Masaru Tomita

**Monday, September 8, 2014, 10:15**

**S24: Pathophysiology of Heart Rate Variability**

Room: Grand Ballroom B

Chair(s): Luca Mainardi and Luca Citi

23-373 **Point Process Heartbeat Dynamics Assessment of Neurocardiogenic Syncope in Children**

Digna M González-Otero*, Ronald G García, Gaetano Valenza, Laura M Reyes and Riccardo Barbieri

24-39 **Lower Instantaneous Entropy of Heartbeat Dynamics Characterizes Cognitive Impairment in Parkinson's Disease**

Riccardo Barbieri*, Gaetano Valenza, Luca Citi, Maria Guerrisi, Stefano Orsolini, Carlo Tessa, Stefano Diciotti and Nicola Toschi

25-209 **Analysing Cardiac Aautonomic Neuropathy in Diabetes using Electrocardiogram-derived Systolic-diastolic Interval Interactions**

Mohammad Hasan Imam*, Chandan Karmakar, Ahsan Khandoker, Herbert F Jelinek and Marimuthu Palaniswami

26-132 **Long-term HRV in Critically Ill Pediatric Patients: Coma versus Brain Death**

Ana Paula Rocha*, Rute Almeida, Argentina Leite, Marta João Silva and Maria Eduarda Silva

27-105 **Automated Selection of measures of Heart Rate Variability for Detection of Early Cardiac Autonomic Neuropathy**

David J Cornforth, Mika P Tarvainen and Herbert F Jelinek*

28-206 **Coupling Between Short-Term Heart Rate and Diastolic Period is Reduced in Heart Failure Patients as Indicated by Multivariate Entropy Analysis**

Peng Li, Lizhen Ji, Chang Yan, Ke Li, Chengyu Liu* and Changchun Liu

**Monday, September 8, 2014, 12:00**

**S31: Cardiac MRI & CT**

Room: Skyline A

Chair(s): Cristiana Corsi and Victor Mor-Avi

29-325 **Volumetric Identification of Left Atrial Fibrosis from Delayed Enhancement Magnetic Resonance Imaging: Preliminary Results**

Roberta Leonardi, Federico Veronesi, Stefano Severi, Roberto Mantovan and Cristiana Corsi*

30-157 **A Practical Algorithm for Improving Localization and Quantification of Left Ventricular Scar**

Brian Zenger*, Joshua Cates, Alan Morris, Eugene Kholmovski, Alexander Au, Ravi Ranjan, Nazem Akoum, Chris McGann, Brent Wilson, Nassir Marrouche, Frederick Han and Rob MacLeod

31-390 **Fully Automated Assessment of Left Ventricular Volumes, Function and Mass from Cardiac MRI**

Marco Marino*, Federico Veronesi, Giacomo Tarroni, Victor Mor-Avi, Amit Patel and Cristiana Corsi

32-32 **Quantitative Evaluation of Myocardial Ischemia by Cardiac Magnetic Resonance Imaging**

Siyi Huang*, Jingwei Pan, Lin Yu, Xin Yang and Meng Wei

**Monday, September 8, 2014, 12:00**

**S32: Electrophysiology Analysis**

Room: Skyline C

Chair(s): Steven Swiryn and Jean-Marc Vesin

33-281 **The Maximum Electrical Fields in the Implant Regions of Implantable Cardiac Rhythm Devices for the Worst Case RF Heating during MRI Scans in 1.5 T**

Dawei Li, Xiaoyi Min*, Shiloh Sison and Ji Chen

34-98 **Cardiac Arrhythmia Discrimination Using Evolutionary Computation**

Juan Francisco Martín-García, Inmaculada Mora-Jiménez, Arcadio García-Alberola and José Luis Rojo-Álvarez*

35-96 **A Morphology-Based Spatial Consistency Algorithm to Improve EGM Delineation in Ventricular Electroanatomical Mapping**

Alejandro Alcaine, David Soto-Iglesias, David Andreu, Juan Acosta, Antonio Berruezo, Pablo Laguna*, Oscar Camara and Juan Pablo Martínez

36-254 **Localization of the Latest-Activated Areas in the Ventricles from Body Surface Potential Maps**

Jana Svehlikova*, Mark Potse and Milan Tysler

**Monday, September 8, 2014, 12:00**

**S33: ECG Decision Support Systems**

Room: Grand Ballroom A

Chair(s): Sara Mariani and Dave Mortara

37-314 **Comparison of Different Methods and Catheter Designs to Estimate the Rotor Tip Position – A Simulation Study**

Markus Rottmann*, Matthias W Keller, Tobias Oesterlein, Gunnar Seemann and Olaf Dössel

38-290 **Analysis of the QRS Alterations during Stress Test Recordings on Patients with Brugada Syndrome**

Daniel Romero*, Nathalie Behar, Alba Martín-Yebra, Juan Pablo Martínez, Pablo Laguna, Esther Pueyo, Guy Carrault, Philippe Mabo and Alfredo Hernández

39-285 **A New Phase Space Analysis Algorithm for the Early Detection of Syncope During Head Up Tilt Tests**

Nadine Khodor*, Guy Carrault, David Matelot, Hassan Amoud, Nathalie Ville, Mohamad Khalil, Francois Carre and Alfredo Hernandez

40-249 **Automatic Detection of ECG Lead-wire Interchange for Conventional and Mason-Likar Lead Systems**

Chengzong Han*, Richard Gregg and Saeed Babaeizadeh

**Monday, September 8, 2014, 12:00**

**S34: Physionet Inspired Studies**

Room: Grand Ballroom B

Chair(s): Ikaro Silva and Pilip de Chazal

41-89 **A Multi-modal Apporach to Sleep-Wake Classification in Infants using Minimally Invasive Sensors**
Gregory Cohen and Philip De Chazal*

42-340 **Classification of Sleep Disordered Breathing in the Evaluation of Acoustic Sound in Correlation with the ECG Signal**
Klaudia Kinga Proniewska*, Krzysztof Malinowski, Elżbieta Pociask and Bartosz Proniewski

43-143 **Preprocessing and Mortality Prediction: the Physionet/CinC 2012 Challenge Revisited**
Alistair E W Johnson* and Gari D Clifford

44-378 **Scaling the PhysioNet WFDB Toolbox for MATLAB and Octave**
Tristan Naumann* and Ikaro Silva

**Tuesday, September 9, 2014, 08:15**

**S41: Repolarization and Risk**

Room: Grand Ballroom A

Chair(s): Thomas Brennan and Paul Kligfield

45-47 **A Quantitative QT Hysteresis Model**
David Mortara* and Fabio Badilini

46-124 **Ventricular Arrhythmias Assessment: a New Repolarization Index of Risk**
Corrado Giuliani, Cees A Swenne, Sumche Man, Angela Agostinelli and Laura Burattini*

47-219 **QT/RR and T-peak-to-end/RR Curvatures in Chronic Heart Failure Patients**
Julia Ramírez*, Iwona Cygankiewicz, Pablo Laguna, Marek Malik and Esther Pueyo

48-119 **T-wave Alternans Rate of Change with Exercise for Cardiac Risk Assessment**
Laura Burattini*, Sumche Man, Giovanni Ottaviano, Sandro Fioretti, Francesco Di Nardo and Cees A Swenne

49-83 **Repolarization lability measured by spatial TT' angle**
Larisa Tereshchenko*

50-197 **Tensor-based Detection of T Wave Alternans in Multilead ECG Signals**
Griet Goovaerts*, Carolina Varon, Bert Vandenberk, Rik Willems and Sabine Van Huffel

**Tuesday, September 9, 2014, 08:15**

**S42: Electrophysiology Modelling**

Room: Grand Ballroom B

Chair(s): Frida Sandberrg and Trygve Eftestøl

51-359 **Controlled Cardiac Activation for Robust Interrogation of the Electrophysiological Substrate**

Joshua JE Blauer*, Fred Han, Ravi Ranjan, Nassir F Marrouche and Rob S MacLeod

52-331 **A Novel method for Quantifying Localised Correlation of Late-gadolinium Intensity with Conduction Velocity**

Rheeda L Ali*, Chris D Cantwell, Caroline H Roney, Norman A Qureshi, Phang Boon Lim, Jennifer H Siggers, Spencer J Sherwin and Nicholas S Peters

53-182 **Defibrillation Thresholds: A Generalised Polynomial Chaos Study**

Peter R Johnston*

54-241 **Formulation of ATP Sensitive K+ Current and Action Potential shape in Models of Human Ventricular Myocytes**

Mitra Abbasi* and Richard Clayton

55-169 **High Specificity IEGM Beat Detection by Combining Morphological and Temporal Classification for a Cardiac Neuromodulation System**

Antje Pohl*, Carl Henning Lubba, Maren Thore, Nima Hatam and Steffen Leonhardt

56-358 **Fitting Membrane Resistance in Single Cardiac Myocytes Reduces Variability in Parameters**

Jaspreet Kaur*, Anders Nygren and Edward Vigmond

**Tuesday, September 9, 2014, 08:15**

**S43: Algorithmic and Software Tools**

Room: Skyline A

Chair(s): Kouhyar Tavakolian and Dana Brooks

57-270 **New Additions to the Toolkit for Forward/Inverse Problems in Electrocardiography within the SCIRun Problem Solving Environment**

Jaume Coll-Font*, Brett Burton, Jess Tate, Burak Erem, Darrell Swenson, Dafang Wang, Dana Brooks, Peter van Dam and Rob MacLeod

58-171 **A Feasibility Study using Image-based Parallel Modeling for Treatment Planning**

Amanda Randles*, Michael Driscoll, Erik Draeger and Franziska Michor

59-391 **Spiral Waves Clustering Using Normalized Compression Distance**

Celal Alagoz*, Andrew R Cohen, Allon Guez and John R Bullinga

60-203 **Interactive Simulation of heart rhythm: A new educational feature of ECGSIM**

Peter M van Dam*, Eelco M van Dam, Adriaan van Oosterom and Thom F Oostendorp

61-151 **Myokit: A Framework for Computational Cellular Electrophysiology**

Michael Clerx*, Paul GA Volders and Pieter Collins

62-165 **A Novel Method for Rotor Tracking using Bipolar Electrogram Phase**

Caroline H Roney*, Chris D Cantwell, Jennifer H Siggers, Fu Siong Ng and Nicholas S Peters

**Tuesday, September 9, 2014, 08:15**

**S44: Temporal Aspects of CV Signals**

Room: Skyline C

Chair(s): Olaf Doessel and Sabine van Huffel

63-156 **Analysis of Cardiovascular Time Series using Multivariate Sample Entropy: A Comparison between Normal and Congestive Heart Failure Subjects**

Chengyu Liu*, Dingchang Zheng, Lina Zhao, Changchun Liu and Alan Murray

64-264 **Comparison of Left Ventricular Ejection Time from Echocardiography, Impedance Cardiography and Photoplethysmography**

Wenfeng Duan*, Dingchang Zheng, Christopher Eggett, Philip Langley and Alan Murray

65-342 **Simulating the Relation Between APD and QT Time in Human Ventricles**

Gunnar Seemann*, David UJ Keller and Olaf Doessel

66-140 **Assessment of Different Methodologies to Include Temporal Information in Classifying Episodes of Sleep Apnea Based on Single-Lead Electrocardiogram**

Tim Willemen*, Carolina Varon, Bart Haex, Jos Vander Sloten and Sabine Van Huffel

67-308 **An Onchip Robust Real-time Automated Non-invasive Cardiac Remote Health Monitoring Methodology**

Naresh Vemishetty, Krishna Bharadwaj Chivukula, Sandeep Tiwari, Pavana Ravi Sai Kiran Malyala, Bastin Joseph, Agathya Jagirdar, Jagadish Bandaru, Venkateswara Chowdary, Sivakrishna Y, Amit Acharyya*, Rajalakshmi Pachamuthu and Paolo Emilio Puddu

68-333 **Economic Effect of Telecare on Medical Expendirures of Patients with Choronic Diseases**

Masatsugu Tsuji* and Yuji Akematsu

**Tuesday, September 9, 2014, 10:15**

**S51: Challenge I**

Room: Grand Ballrom A

Chair(s): Riccardo Barbieri and Ikaro Silva

69-380 **Robust Detection of Heart Beats in Multimodal Data: The PhysioNet/Computing in Cardiology Challenge 2014**
George B Moody*, Benjamin E Moody and Ikaro Silva

70-159 **Heart Rate Variability Discovery: Algorithm for Detection of Heart Rate from Noisy, Multimodal Recordings**
Jan Jakub Gierałtowski*, Kamil Ciuchciński, Iga Grzegorczyk, Katarzyna Kośna, Mateusz Soliński and Piotr Podziemski

71-192 **Heart Beat Detection in Multimodal Data Using Signal Recognition and Beat Location Estimation**
Thomas De Cooman*, Griet Goovaerts, Carolina Varon, Devy Widjaja and Sabine Van Huffel

72-160 **Multimodal Information Fusion for Robust Heart Beat Detection**
Quan Ding*, Yong Bai, Yusuf Erol, Rebeca Salas-Boni, Xiaorong Zhang, Lei Li and Xiao Hu

73-188 **Predicting Heart Beats using Co-occurring Constrained Sequential Patterns**
Shameek Ghosh*, Mengling Feng, Hung Nguyen and Jinyan Li

74-324 **PhysioNet/CinC Challenge 2014: A Noise Robust Method for Recognizing the Heart Beats in Multimodal Data**
Ali Ghaffari, Seyyed Abbas Atyabi* and Mohammad Javad Mollakazemi

75-70 **Rhythm-based Accuracy Improvement of Heart Beat Detection Algorithms**
Zoltán Gilián*, Péter Kovács and Kaveh Samiee

**Tuesday, September 9, 2014, 10:15**

76-76 **Identification of a Signal for an Optimal Heart Beat Detection in Multimodal Physiological Datasets**
Johannes W Krug*, Roman Schulte and Georg Rose

77-60 **Robust Algorithm to Locate Heart Beats from Multiple Physiological Waveforms**
Lars Johannesen*, Jose Vicente, Christopher Scully, Loriano Galeotti and David Strauss

78-112 **R Peak Estimation using Multimodal Lead Switching**
Alistair E W Johnson*, Joachim Behar, Julien Oster and Gari D Clifford

79-94 **Robust Detection of Heart Beats in Multimodal Data Using Integer Multiplier Digital Filters and Morphological Algorithms**
Urska Pangerc and Franc Jager*

**Tuesday, September 9, 2014, 10:15**

**S52: Blood Pressure Systems**

Room: Grand Ballroom B

Chair(s): Roberto Sassi and Madalena Costa

80-78 **Respiratory Rate Effect in the Power of Pulse Photoplethysmogram Derived Respiration Signals**
Jesús Lázaro*, Raquel Bailón, Pablo Laguna, Ki Chon, Yunyoung Nam and Eduardo Gil

81-8 **Performance of the Low-frequency Power of the Maximal Value of the First Derivative of Arterial Pressure Waveform as a Sympathetic Activity Index**
Salvador Carrasco-Sosa and Alejandra Guillén-Mandujano*

82-310 **Sleep Stage Classification in Children Using Photoplethysmogram Pulse Rate Variability**
Parastoo Dehkordi*, Ainara Garde, Walter Karlen, David Wensley, J Mark Ansermino and Guy A Dumont

83-344 **Characterization of Pulse Transit Time and Photoplethysmogram Amplitude Dynamics in Sleep Apnea**
Aziz El-Tatar, Delphine Feuerstein, Laurence Graindorge, Guy Carrault*, Amel Amblard, Jean-Louis Pépin and Alfredo Hernández

84-238 **Changes in Short-Term Blood Pressure Regulation in Adolescents with Type-I Diabetes Mellitus and Essential Hypertension**
Eva Zavodna*, Zuzana Novakova, Magdalena Rohanova, Jana Stastna, Natasa Honzikova, Ludmila Brazdova and Hana Hrstkova

85-41 **Monitoring Arterial Blood Pressure Fluctuations during Hemorrhage**
Christopher G Scully*, George C Kramer and David G Strauss

**Tuesday, September 9, 2014, 10:15**

**S53: Cardiovascular Ultrasound**

Room: Skyline A

Chair(s): Nico Bruining and Tanveer Syeda Mahmood

86-228 **Automatic Detection of Left Ventricular Cardiac Aneurysms in Echocardiograms**

Raziuddin Mahmood, Quan Wang and Tanveer Syeda-Mahmood*

87-261 **CAPSU: a Completely Automated Method for Carotid Plaques Segmentation in Ultrasound Images**

Francesca Galluzzo*, Cristiana Corsi, Carmela Morizzo, Luca De Marchi, Nicola Testoni, Nicolò Speciale and Guido Masetti

88-263 **Near-Automated Quantification of Prenatal Aortic Intima-Media Thickness from Ultrasound Images**

Giacomo Tarroni*, Silvia Visentin, Erich Cosmi and Enrico Grisan

89-353 **Anatomical Structure Labeling in Apical Four-Chamber View Echocardiogram Images**

Yu Cao*, Colin Compas, Hongzhi Wang and Tanveer Syeda-Mahmood

90-376 **Necrotic Tissue Distribution Analysis: Preliminary Investigation for Reducing Necrosis Overestimation in Intravascular Ultrasound Virtual Histology Images**

Fernando J R Sales*, Breno A A Falcao, Joao L A A Falcao, Sergio S Furuie and Pedro A Lemos

**Tuesday, September 9, 2014, 12:00**

**P61: ECG Methods**

Room: Grand Ballroom Lobby

91-278 **Optimized Modelling of Maternal ECG Beats Using the Stationary Wavelet Transform**
Fernando Andreotti*, Hagen Malberg and Sebastian Zaunseder

92-54 **Estimation of Atrial Fibrillatory Frequency by Spectral Subtraction of Wavelet Denoised ECG in Patients with Atrial Fibrillation**
Jonathan Goodfellow*, Omar J Escalona, Philip R Walsh, Vivek Kodoth and Ganesh Manoharan

93-20 **Morphology-based QT Interval Measurement Using Frame-based Representation of ECG Signal**
Alireza Ghodrati* and Abbas Babajani-Feremi

94-19 **Wave Sequence Based Identification of Sinus Rhythm Beats on a Microcontroller**
Alexander Noack*, Rüdiger Poll and Wolf-Joachim Fischer

95-284 **A Signal Decomposition Approach to Morphological Modeling of P-wave**
Ebadollah Kheirati Roonizi and Roberto Sassi*

96-191 **Reducing ECG Alarm Fatigue Based on SQI Analysis**
Zehui Sun*, Jianwei Su, Chaocheng Xie, Jiao Yu, Wenyu Ye and Shen Luo

97-53 **Classification of Supraventricular and Ventricular Beats by QRS Template Matching and Decision Tree**
Vessela Krasteva, Remo Leber, Irena Jekova, Ramun Schmid and Roger Abächerli*

98-86 **Respiratory Rate Estimation from Multi-Lead ECGs using an Adaptive Frequency Tracking Algorithm**
Leila Mirmohamadsadeghi* and Jean-Marc Vesin

**Tuesday, September 9, 2014, 12:00**

99-154 **QRS Detectors Performance Comparison in Public Databases**

Mariano Llamedo* and Juan Pablo Martínez

100-82 **An Algorithm for the Detection of ST Segment Elevation Relating to Induced Ischemia in Body Surface Potential Maps**

Dewar Finlay*, Daniel Guldenring, Raymond Bond and Michael Daly

101-190 **Trend Strips: a New Tool to Analyze RR Time Series**

Antônio Carlos Silva Filho, Fátima Maria Helena Simões Pereira da Silva*, Júlio Cesar Crescêncio and Lourenço Gallo Júnior

102-75 **Morphological Analysis on Single Lead Contactless ECG Monitoring based on Beat-template**

Jesús Hernández-Ortega*, Francisco-Javier Gimeno-Blanes, Jose-Luis Rojo-Álvarez, Rafael Maestre-Ferriz, Jose-María López-Ayala, Juan-Ramón Gimeno-Blanes, Arcadi García-Alberola, Andrés-Lorenzo Bleda-Tomás and Jose-Antonio Flores-Yepes

103-30 **Internet based ST Map Software: A Web Service, a Decision Support System and an Educational Tool**

Raymond Bond*, Dewar Finlay and Daniel Guldenring

**Tuesday, September 9, 2014, 12:00**

**P62: ECG Repolarization**

Room: Grand Ballroom Lobby

104-65 **Normal Ventricular Repolarization Dispersion Range with Abrupt Heart Rate Changes**

Pablo Daniel Cruces, María Paula Bonomini, Marcos Javier Teperino, Ana Mincholé, Pablo Laguna and Pedro David Arini*

105-337 **Repolarization Effects of Sertindole Manifest as T-wave Flatness on the ECG**

Tanveer A Bhuiyan*, Claus Graff, Jørgen K Kanters, Jimmi Nielsen and Johannes J Struijk

106-356 **Changes in the ST- and Ventricular Gradient Vectors over a Period of 20 Years**

Marjolein De Jongh, C Cato Ter Haar, Sumche Man, Maurits Van der Heide, Roderick Treskes*, Arie C Maan, Martin J Schalij and Cees A Swenne

107-222 **Valuation of an Index Which Estimate the Heterogeneity of Ventricular Repolarization (V-index) by BSPM and Application to Patients with Early Repolarization Syndrome**

Paola De Marco* and Irene Rossi

108-177 **Lack of Specificity of the Moving Average Method for Detecting Alternans**

David Mortara*

109-389 **The Accuracy of the EASI Derived Spatial QRS-T Angle**

Daniel Guldenring*, Dewar Finlay, Raymond Bond, Alan Kennedy and James McLaughlin

**Tuesday, September 9, 2014, 12:00**

**P63: Clinical Aspects of ECG**

Room: Grand Ballroom Lobby

110-229 **Electrocardiographic Abnormalities in Hypertrophic Cardiomyopathy**

Ana Mincholé*, Rina Ariga, Stefan Neubauer, Hugh Watkins and Blanca Rodriguez

111-375 **Low Level and High Frequency Fragmentation of the QRS Changes During Acute Myocardial Ischemia in Patients with and without Prior Myocardial Infarction**

Pedro Gomis* and Pere Caminal

112-58 **Assessing the Accuracy of Limited Lead Recordings for the Detection of Atrial Fibrillation**

Kerri Griffiths, Elaine Clark, Brian Devine* and Peter Macfarlane

113-1 **QRS and T Loops Area Changes During Haemodialysis**

Iana Simova, Ivaylo Christov*, Liliana Kambova, Giovanni Bortolan and Tzvetana Katova

114-37 **Left Ventricular Hypertrophy Index based on a Combination of Frontal and Horizontal Planes in the ECG and VCG: Diagnostic Utility of Cardiac Vectors**

María Paula Bonomini, Fernando Ingallina, Valeria Barone, Max Valentinuzzi and Pedro David Arini*

115-130 **The Loss of Multifractality as Evidence of Impaired Left Ventricular Ejection Fraction in Patients after Acute Myocardial Infarction**

Fátima Maria Helena Simões Pereira da Silva*, Antonio Carlos da Silva Filho, Julio Cesar Crescencio, Valéria Papa and Lourenço Gallo Júnior

**Tuesday, September 9, 2014, 12:00**

**P64: Nonlinear Analysis of Heart Rate Variability**

Room: Grand Ballroom Lobby

116-318 **Extended Parabolic Phase Space Mapping (EPPSM): The Novel Quadratic Function for Representation of Heart Rate Variability Signal**

Sadaf Moharreri*, Nader Jafarnia Dabanloo and Saman Parvaneh

117-193 **HRV Spectral and Fractal Analysis in Heart Failure Patients with Different Aetiologies**

Elisa Fornasa*, Agostino Accardo, Martino Cinquetti, Marco Merlo and Gianfranco Sinagra

118-303 **The analysis of human heart rate for healthy and ill patients using the recently published method Multiscale Multifractal Analysis**

Dorota Kokosińska*, Jan Gierałtowski, Jan Żebrowski, Rafał Baranowski and Ewa Orłowska - Baranowska

119-205 **Time-domain, Frequency Domain and Non-linear Measurements in Infant's Heart Rate Variability with Clinical Sepsis**

E Godoy, J Lopez, L Bermudez, A Ferrer, N Garcia, C Garcia Vicent, EF Lurbe and J Saiz*

120-247 **Nonlinear Features of Neonatal Heart Rate Dynamics**

Barbora Czippelova*, Lenka Chladekova, Zuzana Turianikova, Ingrid Tonhajzerova, Kamil Javorka, Zuzana Uhrikova, Mirko Zibolen and Michal Javorka

121-56 **Continuous Information Extraction from Blood Pressure Data Using Reconstruction of Attractors**

Philip Aston*, Manasi Nandi, Mark Christie and Ying Huang

122-153 **Analysis of Maternal-Fetal Heart Rate Coupling with High Resolution Joint Symbolic Dynamics**

Ahsan Khandoker, Andreas Voss*, Steffen Schulz, Miyuki Endo, Yoshitaka Kimura and Marimuthu Palaniswami

**Tuesday, September 9, 2014, 12:00**

123-272 **Recurrence Quantification Analysis of Heart Rate and Blood Pressure Variability in Obese Children and Adolescents**

Zuzana Turianikova*, Ingrid Tonhajzerova, Barbora Czippelova, Kamil Javorka, Zuzana Lazarova and Michal Javorka

124-110 **Multiscale Cardiovascular Autonomic Modulation Following Treatment in Patients with Anorexia Nervosa**

Herbert F Jelinek*, David J Cornforth, Sera P Lam, Janice Russell and Ian Spence

**Tuesday, September 9, 2014, 12:00**

**P65: Informatics**

Room: Grand Ballroom Lobby

125-327 **An Android Application for ECG Processing**

Rene Ivan Gonzalez-Fernandez* and Margarita Mulet-Cartaya

126-341 **Design and Optimization of an ECG Holter Hybrid System for Mobile Systems based on DSPIC**

Flavio Pineda-López*, Andrés Martínez-Fernández, José Luis Rojo-Álvarez and Manuel Blanco-Velasco

127-46 **Analysis of Heart Rate Changes in Newborns to Investigate the Effectiveness of Bag-Mask Ventilation**

Huyen Vu*, Trygve Eftestøl, Kjersti Engan, Joar Eilevstjønn, Jørgen Linde and Hege Ersdal

128-233 **Proof of Concept for an International Long-time Preservation ECG format**

Roberto Sassi*, Luca Sparagino, Norman L Stockbridge, Juan Guadiana and Fabio Badilini

129-21 **Encoding the Electrocardiogram Details in the Host Record's Bandgap for Authorization-Dependent ECG Quality**

Piotr Augustyniak*

130-158 **A Low-Cost Solution to Follow the Evolution of Arrhythmic Patients**

Rene Gonzalez-Fernandez*, Margarita Mulet-Cartaya, Juan Dayron Lopez-Cardona, Alejandro Lopez-Reyez, Rolando Lopez-Rodriguez and Rolando Lopez-Creagh

131-34 **Telemedicine Network for Collaborative Diagnosis and Care of Heart Malformations**

Alessandro Taddei*, Andrea Gori, Tiziano Carducci, Giuseppe Augiero, Alessio Ciregia, Emiliano Rocca, Giacomo Piccini, Nadia Assanta, Giorgio Ricci and Bruno Murzi

**Tuesday, September 9, 2014, 12:00**

132-163 **Telemedical Human Activity Monitoring System based on a Wearable Sensors Network**

Eliasz Kańtoch*

133-207 **Effect of Telehealth on Self-Care Behavior of Heart Failure Patients**

Carolina Varon*, Jan Minter, Michelle Stapleton, Stuart Thomson, Siegfried Jaecques, Hans-Peter Brunner-La-Rocca and Sabine Van Huffel

134-108 **Optimization of Shifts and On-Call Coverage of Cardiologists Working in a Hospital Complex Structure by Using Free Software**

Eugenio Cervesato*, Giovanni Righini, Gian L Rellini, Matteo Cassin, Rita Piazza and Gian L Nicolosi

135-379 **European Patient Summary Guideline and Continuity of Care Document: A Comparison**

Ana Estelrich, Harold Solbrig, Marcello Melgara, Giorgio Cangioli and Catherine Chronaki*

136-230 **Automated Measurement of Fetal Isovolumic Contraction Time from Doppler Ultrasound Signal without Using Fetal Electrocardiography**

Faezeh Marzbanrad*, Yoshitaka Kimura, Miyuki Endo, Marimuthu Palaniswami and Ahsan H Khandoker

137-262 **Assessment of Dynamic Autonomic Changes with Posture using Instantaneous Entropy Measures**

Gaetano Valenza*, Luca Citi, Enzo Pasquale Scilingo and Riccardo Barbieri

138-253 **Heart Murmur Detection Using Ensemble Empirical Mode Decomposition and Derivations of the Mel-Frequency Cepstral Coefficients on 4-Area Phonocardiographic Signals**

Joe A Jimenez, Miguel A Becerra* and Edilson Delgado-Trejos

**Tuesday, September 9, 2014, 12:00**

139-134 **Towards Semantic Interoperability for Cardiovascular Risk Stratification into the Electronic Health Records Using Archetypes and SNOMED-CT**

Alfonso Sanchez-Cano, Cristina Soguero-Ruiz, Inmaculada Mora-Jiménez, Luis Lechuga, Javier Ramos-Lopez, Arcadi García-Alberola, Pablo Serrano-Balazote and José Luis Rojo-Álvarez*

140-38 **Clinical Decision Support System for Post-Procedure Management of Transcatheter Aortic Valve Replacement**

Stefan Nelwan*, Mark Ronkes, Jeroen van den Berg and Teus van Dam

**Tuesday, September 9, 2014, 12:00**

**P66: Tools for Simulation and Modelling**

Room: Grand Ballroom Lobby

141-258 **New Algorithm to Identify Focus of Atrial Ectopic Activity from Multi-lead ECG Systems – Insights from 3D Virtual Human Atria and Torso**

Erick Andres Perez Alday, Michael A Colman*, Philip Langley and Henggui Zhang

142-323 **Huge Reduction of Defibrillation Thresholds using Four Electrode Defibrillators**

Ana Simic*, Inma R Cantalapiedra, Jorge Elorza and Jean Bragard

143-348 **Quantitative Insights into the Closed-loop Cardiovascular System Using an Electrical Lumped Element Physiological Model**

Athanasios Tsanas*, Gari Clifford, Vassiliki Vartela and Petros Sfirakis

144-311 **Modeling of the Human Heart Rate Variability Enhanced Using Stochastic Sleep Architecture Properties**

Mateusz Solinski*, Jan Gieraltowski and Jan Zebrowski

145-104 **A simple 2D Whole Heart Model for simulating Electrocardiogram**

Minimol Balakrishnan*, V Srinivasa Chakravarthy and Soma Guhathakurta

146-257 **Parameter Sensitivity Analysis of a Human Atrial Cell Model using Multivariate Regression**

Eugene TY Chang* and Richard H Clayton

147-13 **Detection of Abnormal Cardiac Activity using Principal Component Analysis**

Ariel Greisas* and Sharon Zlochiver

**Tuesday, September 9, 2014, 12:00**

148-185 **Quantifying Tikhonov Regularization Uncertainty in the Inverse Problem of Electrocardiography**
Jessie J France*, Yaniv Gur, Robert M Kirby and Chris R Johnson

149-178 **How Accurately Can Cardiac Conductivity Values Be Determined From Heart Potential Measurements?**
Barbara Johnston* and Peter Johnston

150-245 **Accuracy of Inverse Solution Computation of Dominant Frequencies and Phases during Atrial Fibrillation**
J Pedron-Torrecilla, AM Climent, A Liberos, M Rodrigo*, E Perez-David, J Millet, F Fernandez-Aviles, O Berenfeld and MS Guillem

151-173 **Fecgsyn: A Graphical User Interface for the Simulation of Maternal-Foetal Activity Mixtures on Abdominal Electrocardiogram Recordings**
Mohsan Alvi*, Joachim Behar, Fernando Andreotti, Julien Oster and Gari D Clifford

152-125 **Correlation Dimension as a Measure of the AF Capture during Atrial Septal Pacing**
Adrian Luca* and Jean-Marc Vesin

**Tuesday, September 9, 2014, 14:15**

**S71: Challenge II**

Room: Grand Ballroom A

Chair(s): Franc Jager and Ikaro Silva

153-399 **Robust Detection of Heart Beats in Multimodal Data: The PhysioNet/Computing in Cardiology Challenge 2014 (II)**
George B Moody, Benjamin E Moody and Ikaro Silva*

154-147 **PhysioNet/CinC Challenge**
Abid K and Deepu Vijayasenan*

155-97 **Fusion of Multimodal Physiological Signals using Cepstrum Analysis for Robust Heart Beat Detection**
Yongwei Zhu*

156-319 **Robust ECG Beat Detection in Multimodal Data**
Mahdi Bazarghan, Ruhallah Amandi, Ahmad Marofkhani* and Mohammad Farhadi

157-293 **PhysioNet/CinC Challenge 2014: The Noise Robust Method for Beat Detection in Continuous long-term Electrocardiogram Signal and Blood Pressure Signal**
Hamid Ebrahimi Orimi*

158-181 **Hidden Semi-Markov Model-based Heartbeat Detection using Multimodal data and Signal Quality Indices**
Marco Pimentel, Mauro Santos, David Springer* and Gari Clifford

159-126 **Robust Multichannel QRS Detection**
Filip Plesinger*, Juraj Jurco, Josef Halamek and Pavel Jurak

160-152 **Heuristic Algorithm for Multiparametric Beat Detection**
Jesús Presedo*, Constantino A García, Daniel Castro, Tomás Teijeiro, Abraham Otero and Paulo Félix

161-84 **Heart Beat Detection Method with Estimation of Regular Intervals between ECG and Blood Pressure**
Jongmin Yu, Taegyun Jeon* and Moongu Jeon

**Tuesday, September 9, 2014, 14:15**

162-200 **Robust Detection of Heart Beats Using ECG, BP and EEG Signals**

Soo-Kng Teo, Bo Yang, Bart Hoeben, Dong Huang, Monterola Christopher and Yi Su*

163-137 **PhysioNet/CinC Challenge**

Sachin Vernekar and Deepu Vijayasenan*

164-33 **Robust Detection of Heart Beats using Dynamic Thresholds and Moving Windows**

Marcus Vollmer*

165-68 **Heart Beat Detection in Multimodal Data via Information Synthesis**

Henian Xia*, Raj Baljepally and Xiaopeng Zhao

**Tuesday, September 9, 2014, 14:15**

**S72: ECG Waveform Quality and Detection I**

Room: Grand Ballroom B

Chair(s): Shen Luo and Raymond Bond

166-52 **Lead Quality Monitoring for Detection of the Optimal Snapshot Time to Record Resting ECG**

Irena Jekova, Remo Leber, Vessela Krasteva, Ramun Schmid and Roger Abächerli*

167-199 **Study of ECG Quality using Self Learning Techniques**

Gianfranco Toninelli*, Alfonso Gerevini, Martino Vaglio and Fabio Badilini

168-102 **ECG Recording Sites for Improving Signal to Noise Ratio during Atrial Depolarisation**

Alan Kennedy*, Dewar Finlay, Daniel Guldenring and James McLaughlin

169-226 **New method for J-point Location in Subjects with Electrocardiographic Early Repolarization**

Jacob Melgaard*, Johannes J Struijk, Jørgen K Kanters, Samuel E Schmidt, Ask S Jensen, John Hansen, Tanveer A Bhuiyan and Claus Graff

170-14 **Automatic Real-Time Quality Assessment of a 12-Lead ECG Recording**

Reza Firoozabadi*, Rich Gregg, Beth Zengo and Saeed Babaeizadeh

171-360 **Serial ECG Analysis: Can we Detect Faulty ECG Recordings?**

Arie C Maan*, C Cato Ter Haar, Sumche Man, Roderick Treskes, Marjolein De Jongh, Maurits Van der Heide, Martin J Schalij and Cees A Swenne

**Tuesday, September 9, 2014, 14:15**

**S73: Nonlinear Analysis of Heart Rate Variability**

Room: Skyline A

Chair(s): Olivier Meste and Pablo Laguna

172-269 **Analysis of Non-linear Respiratory Influences on Sleep Apnea Classification**
Alexander Caicedo*, Carolina Varon and Sabine Van Huffel

173-166 **Rank-based Multi-Scale Entropy analysis of Heart Rate Variability**
Luca Citi*, Giulia Guffanti and Luca Mainardi

174-167 **A Methodological Assessment of Phase-Rectified Signal Averaging through Simulated Beat-to-Beat Interval Time Series**
Massimo W Rivolta, Tamara Stampalija, Daniela Casati, Enrico Ferrazzi, Axel Bauer and Roberto Sassi*

175-291 **QT-Interval Adaptation to Changes in Autonomic Balance**
Ehimwenma Nosakhare*, George Verghese, Robert Tasker and Thomas Heldt

176-103 **Separating Respiratory Influences from the Tachogram: Methods and their Sensitivity to the Type of Respiratory Signal**
Devy Widjaja*, Carolina Varon, Dries Testelmans, Bertien Buyse, Luca Faes and Sabine Van Huffel

177-370 **Dynamic Network Interactions of the Cardiac System**
Ronny P Bartsch, Amir Bashan, Kang KL Liu, Chunhua Bian, Gustavo Zampier dos Santos Lima and Plamen CH Ivanov*

**Tuesday, September 9, 2014, 14:15**

**S74: Classification of CV Signals**

Room: Skyline C

Chair(s): Piotr Augustyniak and Philip Warrick

178-179 **Robust Heart Rate Estimation from Noisy Phonocardiograms**
David Springer*, Thomas Brennan, Jens Hitzeroth, Bongani Mayosi, Lionel Tarassenko and Gari Clifford

179-347 **A Novel Technique for Analyzing Noisy Noninvasive Fetal Electrocardiogram Signals**
Mohammad Javad Mollakazemi, Seyyed Abbas Atyabi* and Ali Ghaffari

180-22 **Subject-Optimized Feature Selection for Accurate Classification of Cardiac Beats**
Piotr Augustyniak*

181-215 **Evaluation of FHR Recordings based on Clustering**
Václav Chudáček*, Jiří Spilka and Tereza Janíčková

182-175 **Support Vector Machine Hidden Semi-Markov Model-based Heart Sound Segmentation**
David Springer*, Lionel Tarassenko and Gari Clifford

**Tuesday, September 9, 2014, 16:15**

**S81: Ischemia and Infarction**

Room: Grand Ballroom A

Chair(s): Goran Krstacic and Cees Swenne

183-350 **Acute Ischemia Detection using a QRS Angle-based Method**

Daniel Romero*, Juan Pablo Martínez, Pablo Laguna and Esther Pueyo

184-352 **Serial ECG Analysis for Ischemia Detection: How Representative Is a Reference ECG?**

Roderick Treskes*, C Cato Ter Haar, Sumche Man, Marjolein De Jongh, Maurits van der Heide, Arie C Maan, Martin J Schalij and Cees A Swenne

185-141 **Improving Automatic Detection of Acute Myocardial Infarction in the Presence of Confounders**

Richard Gregg* and Saeed Babaeizadeh

186-368 **A Real-time ST-segment Monitoring Algorithm based on a Multi-channel Waveform-length-transformation Method for Q-onset and J-point Setection**

Wei Zong*, Scott Kresge, Haisheng Lu and John Wang

187-244 **Wavelet Based Method For Localization Of Myocardial Infarction Using Vector Electrocardiogram**

Nader Jafarnia Dabanloo, Azadeh Nooriyan and Saman Parvaneh*

**Tuesday, September 9, 2014, 16:15**

**S82: Fibrillation and Tachiarrhythmia**

Room: Grand Ballroom B

Chair(s): Guy Carrault and José Rojo

188-107 **A Platform to guide Catheter Ablation of Persistent Atrial Fibrillation using Dominant Frequency Mapping**

Xin Li*, João Loures Salinet, Tiago Paggi de Almeida, Frederique Jos Vanheusden, Gavin S Chu, G André Ng and Fernando S Schlindwein

189-161 **Spatiotemporal Behaviour of High Dominant Frequency during Persistent Atrial Fibrillation**

Nawshin Dastagir*, Joao L Salinet, Frederique J Vanheusden, Tiago P Almeida, Xin Li, Gavin S Chu, Andre G Ng and Fernando S Schlindwein

190-335 **Distinctive Patterns of Dominant Frequency Trajectory Behaviour in Persistent Atrial Fibrillation: Spatio-temporal Characterisation**

Joao Salinet*, Jiun Tuan, Angela Salinet, Xin Li, Peter Stafford, G Andre Ng and Fernando Schlindwein

191-31 **Detection of Atrial Fibrillation Using Contactless Facial Video Monitoring**

Jean-Philippe Couderc*, Survi Kyal, Lalit Mestha, Beilei Xu, Derick Peterson, Xiaojuan Xia and Burr Hall

192-115 **Towards Impedance Optimised Transcutaneous Atrial Defibrillation**

Philip R Walsh*, Paola A Rodrigues, Niall Watermann, David McEneaney and Omar J Escalona

193-366 **Specific Patterns of Premature Beats Tend to Initiate Ventricular Tachyarrhythmias in Human Patients**

Anna RM Gelzer, Robert F Gilmour Jr and Niels F Otani*

**Tuesday, September 9, 2014, 16:15**

**S83: Ventricular Modelling**

Room: Skyline A

Chair(s): Flavio Featon and Henggui Zhang

194-131 **A Computational Investigation into the Effect of Infarction on Clinical Human Electrophysiology Biomarkers**

Louie Cardone-Noott*, Alfonso Bueno-Orovio, Ana Mincholé, Kevin Burrage, Mikael Wallman, Nejib Zemzemi, Erica Dall'Armellina and Blanca Rodriguez

195-172 **Inverse Estimation of Left Ventricular Purkinje Network Pathways from Sequence of Depolarization**

Ruben Cardenes, Rafael Sebastian*, Oscar Camara and Antonio Berruezo

196-265 **Sensitivity Study of Fiber Orientation on Stroke Volume in the Human Left Ventricle**

Lukas Baron*, Thomas Fritz, Gunnar Seemann and Olaf Dössel

197-377 **Modeling the Takeoff Voltage of the Action Potential during Fast Pacing**

Diandian Chen*, Richard Gray and Flavio Fenton

198-354 **Verification of a Defibrillation Simulation Using Internal Electric Fields in a Human Shaped Phantom.**

Jess Tate*, Thomas Pilcher, Kedar Aras, Brett Burton and Rob MacLeod

199-343 **Quantitative Analysis of Rate Dependent of Human Heart Failure Action Potential Model on Alternans Onset and Arrhythmias**

Mohamed Elshrif*, Elizabeth Cherry and Pengcheng Shi

**Tuesday, September 9, 2014, 16:15**

**S84: 3D Imaging**

Room: Skyline C

Chair(s): Rob MacLeod and Cristiana Corsi

200-239 **Automatic Extraction of Arterial Centerline from Whole-body Computed Tomography Angiography**

Xinpei Gao*, Shengxian Tu, Michiel de Graaf, Liang Xu, Pieter Kitslaar, Arthur Scholte, Bo Xu and Johan Reiber

201-365 **Fusion Imaging of Computed Tomography and 3D Echocardiography: Combined Assessment of Coronary Anatomy and Myocardial Function**

Francesco Maffessanti*, Karima Addetia, Gillian Murtagh, Lynn Weinert, Amit Patel, Roberto Lang and Victor Mor-Avi

202-187 **Automatic Correction of Motion Artifacts in 4D Left Ventricle Model Reconstructed from MRI**

Yi Su*, May-Ling Tan, Chi-Wan Lim, Soo-Kng Teo, Senthil Kumar Selvaraj, Liang Zhong and Ru-San Tan

203-338 **3D Echocardiographic Quantification of Ejection Fraction and Cardio-toxicity Onset**

Cinzia Lorenzini*, Michele Aquilina, Claudio Lamberti and Cristiana Corsi

204-361 **Temporal Sparse Promoting Three Dimensional Imaging of Cardiac Activation**

Long Yu*, Zhaoye Zhou and Bin He

205-294 **An Iterative method for solving the inverse problem in Electrocardiography imaging : From body surface to heart potential**

Nejib Zemzemi*, Hamed Bourenane and Hubert Cochet

**Wednesday, September 10, 2014, 08:15**

**S91: ECG Waveform Quality and Detection II**

Room: Grand Ballroom A

Chair(s): Eric Helfenbein and Ivaylo Christov

206-40 **A Pattern-Recognition Approach for Lead-Selection in Heartbeat Detection**
Mariano Llamedo*, Juan Pablo Martínez and Pablo Laguna

207-224 **Adaptive Beat-to-Beat Mathematical Morphology Approach for QRS detection in the ECG**
Sasan Yazdani* and Jean-Marc Vesin

208-23 **An Adaptive Heart-beat Classification System Based on Learning from Difficult Cases**
Philip de Chazal*

209-55 **A Real-time QRS Detector Based on Higher-order Statistics for ECG Gated Cardiac MRI**
Marcus Schmidt, Johannes W Krug*, Andreas Gierstorfer and Georg Rose

210-196 **QRS Detection Optimization in Stress Test Recordings using Evolutionary Algorithms**
David Hernando*, Raquel Bailón, Rute Almeida and Alfredo Hernández

211-339 **A Vector-based Pace Pulse Detection Algorithm for the surface ECG**
Simon C Chien*, Po-Cheng Chang, Hong-Ta Wo, Eric Helfenbein, Chun-Chieh Wang and Ming-Shien Wen

**Wednesday, September 10, 2014, 08:15**

**S92: Atrial Fibrillation Modelling**

Room: Skyline A

Chair(s): Adrian van Oosterom and Gunnar Seemann

212-35 **Optimization of Pharmacotherapy for Familial Atrial Fibrillation in a Numerical Model of Human Atrial Electrophysiology**

Axel Loewe*, Yannick Lutz, Mathias Wilhelms, Eberhard P Scholz, Olaf Dössel and Gunnar Seemann

213-36 **Atrial Spiral Wave Drifting Under Applied Spatial Temperature Gradients**

Guy Malki* and Sharon Zlochiver

214-50 **A Simulation Study of Electrotonic Coupling between Human Atrial Myocytes and Mechanosensitive Fibroblasts**

Honglian Su, Heqing Zhan, Yinglan Gong, Dingchang Zheng* and Ling Xia

215-202 **Accurate Characterization of Rotor Activity during Atrial Fibrillation Depends on the Properties of the Multi-electrode Grid**

Laura Martinez, Lucia Romero, Catalina Tobon, Jose M Ferrero, Jose Jalife, Omer Berenfeld and Javier Saiz*

216-296 **Constructing Human Atrial Electrophysiological Models Mimicking a Patient-Specific Cell Group**

Anna Muszkiewicz*, Alfonso Bueno-Orovio, Xing Liu, Barbara Casadei and Blanca Rodriguez

217-266 **Evaluating Effects of Fibrosis on Atrial Re-entry Using 3D Computational Modelling**

Ross Morgan*, Michael Colman, Martin Kruger, Gunnar Seemann, Kawal Rhode and Oleg Aslanidi

**Wednesday, September 10, 2014, 08:15**

**S93: Pathology of Heart Rate Variability**

Room: Grand Ballroom B

Chair(s): Valentina Corino and Andreas Voss

218-162 **Age- and Gender-related Shift in Cardiovascular Variability in Healthy Volunteers**

Hagen Malberg*, Hendrik Bonnemeier, Andreas Müller, Sebastian Zaunseder and Niels Wessel

219-282 **Causality of Heart Rate – Blood Pressure Interactions during Mental and Orthostatic Stress**

Michal Javorka*, Barbora Czippelova, Lenka Chladekova, Zuzana Turianikova, Zuzana Visnovcova, Zuzana Lazarova, Kamil Javorka and Ingrid Tonhajzerova

220-26 **Heart Rate Variability Associated with Different Modes of Lower Abdominal Muscle Tension during Zen Meditation**

Masaki Hoshiyama* and Asagi Hoshiyama

221-88 **Impacts of labour first and second stages on Hurst parameter based intrapartum fetal Heart Rate analysis**

Jiri Spilka*, Patrice Abry, Paulo Goncalves and Muriel Doret

222-357 **Phase Transitions in Independent Forms of Cardio-Respiratory Coupling across Sleep Stages**

Ronny P Bartsch, Kang KL Liu, Qianli DY Ma and Plamen CH Ivanov*

223-372 **Time-Domain and Spectral Analysis of Heart Rate Variability in Rats Challenged with Hypoxia**

Stanislaw Zajaczkowski*, Maria Smolinska, Piotr Badtke and Tomasz Wierzba

**Wednesday, September 10, 2014, 08:15**

**S94: Miscellaneous Medical Informatics**

Room: Skyline C

Chair(s): Gari Clifford and Peter Szolovits

224-10 **CrowdLabel: A Crowd-sourcing Platform for Electrophysiology**

Tingting Zhu*, Joachim Behar, Tasos Papastylianou and Gari D Clifford

225-301 **Increasing the Dynamic Range of a Pulse Oximeter Using Heart Rate Characteristics**

Chris J Brouse*, Ronald Gatzke, Daniel K Freeman and Yu Chen

226-312 **Noise and Spatial-resolution effect of Electrode Array on Rotor Tip Location during Atrial Fibrillation: A Simulation Study**

Miguel A Becerra*, Juan P Murillo, Laura C Palacio and Catalina Tobón

227-139 **Risk Assessment of Atrial Fibrillation: a Failure Prediction Approach**

Jelena Milosevic, Andreas Dittrich, Alberto Ferrante*, Miroslaw Malek, Camilo Rojas Quiros, Rubén Braojos, Giovanni Ansaloni and David Atienza

228-142 **Multimodal Sensor Fusion of Cardiac Signals via Blind Deconvolution: A Source-Filter Approach**

Christoph Hoog Antink*, Christoph Brüser and Steffen Leonhardt

229-392 **A Data Driven Approach to Patient Cohort Identification**

Thomas Brennan*, Marco Pimental, Mengling Feng, Li-Wei Lehman, Mohammad Ghassemi and Roger Mark

**Wednesday, September 10, 2014, 10:15**

**SA1: Atrial Fibrillation I**

Room: Grand Ballroom A

Chair(s): José Millet and Leif Sörnmo

230-317 **Altered Nonlinear Dynamics of Atrial Fibrillation Detected After Ablation**

Kevin Sunderland*, Adam Berman and Autumn Schumacher

231-77 **A Novel P-wave Duration Estimation Method to Assess the Impact of the Hybrid Procedure for Atrial Fibrillation Ablation**

Pietro Bonizzi*, Narendra Kumar, Stef Zeemering, Ralf Peeters and Laurent Pison

232-4 **Atrial Fibrillation Substrate Characterization and Catheter Ablation Acute Outcome Prediction: Comparative Analysis of Spectral and Nonlinear Indices from Right Atrium Electrograms**

Luigi Yuri Di Marco*, Daniel Raine, John P Bourke and Philip Langley

233-93 **Modification of Atrioventricular Node Conduction Increases RR Variability but not RR Irregularity nor Atrial Fibrillation Rate in Atrial Fibrillation Patients**

Valentina DA Corino*, Sara R Ulimoen, Steve Enger, Luca T Mainardi, Arnljot Tveit and Pyotr G Platonov

**Wednesday, September 10, 2014, 10:15**

**SA2: Inverse Problem**

Room: Skyline A

Chair(s): Dewar Finlay and Peter van Dam

234-250 **Using a new Time-Independent Average Method for Non-Invasive Cardiac Potential Imaging of Endocardial Pacing with Imprecise Thorax Geometry**

Jaume Coll-Font*, Burak Erem and Dana H Brooks

235-138 **Localization of Three-Dimensional Sources in Cardiac Tissue Using Optical Mapping**

Gwladys Ravon*, Yves Coudière, Angelo Iollo, Olivier Bernus and Richard D Walton

236-349 **Noninvasive Identification of Three-dimensional Myocardial Infarctions from Inversely Reconstructed Equivalent Current Density**

Zhaoye Zhou*, Chengzong Han and Bin He

237-305 **Local Regularization of Endocardial and Epicardial Surfaces for better Localization of Ectopic Beats in the Inverse Problem of ECG**

Danila Potyagaylo*, Walther Schulze and Olaf Dössel

**Wednesday, September 10, 2014, 10:15**

**SA3: Blood Pressure and Peripheral Pulse**

Room: Grand Ballroom B

Chair(s): Dingchang Zheng and Brian Anthony

238-81 **Validation of a Blood Pressure Simulator that Regenerates Oscillometric Cuff Pressure Waveforms**

Dingchang Zheng*, Chengyu Liu, John Amoore, Stephan Mieke and Alan Murray

239-259 **Validation of a Smartphone-based Photoplethysmographic Beat Detection Algorithm for Normal and Ectopic Complexes**

Lenn Drijkoningen, Frederic Lenaerts, Jo Van der Auwera, Christophe Smeets, Julie Vranken, Valerie Storms, Dieter Nuyens, Pieter Vandervoort and Lars Grieten*

240-123 **Oscillometric Waveform Difference between Cuff Inflation and Deflation during Blood Pressure Measurement**

Chengyu Liu*, Dingchang Zheng, Clive Griffiths and Alan Murray

241-220 **Estimation of Respiratory Information from the Built-In Pressure Sensors of a Dialysis Machine**

Frida Sandberg*, Mattias Holmer, Bo Olde and Kristian Solem

**Wednesday, September 10, 2014, 10:15**

**SA4: Ionic Modelling in Ventricular Arrhythmia**

Room: Skyline C

Chair(s): Javier Saiz and Jose Mario Ferrero

242-69 **Pro-arrhythmic Effects of Increased Late Sodium Current In Failing Human Heart**

Jieyun Bai*, Kuanquan Wang, Xiangyun Bai, Yongfeng Yuan and Henggui Zhang

243-351 **Late Sodium Current Inhibition Counteracts Pro-arrhythmic Mechanisms in Human Hypertrophic Cardiomyopathy**

Elisa Passini*, Alfonso Bueno-Orovio, Ana Mincholé, Raffaele Coppini, Elisabetta Cerbai, Stefano Severi and Blanca Rodriguez

244-279 **Theoretical Study of the Role of Funny Current (If) and the Background Inward Current (Ib) in Atrioventricular Nodal Conduction**

Jue Li* and Mark R Boyett

245-267 **Effect of Inter-Subject Variability in Determining Response to IKr Block in Human Ventricular Myocytes**

Oliver J Britton*, Alfonso Bueno-Orovio, Laszlo Virag, Andras Varro and Blanca Rodriguez

**Wednesday, September 10, 2014, 11:30**

**SB1: Ischemic Modelling**

Room: Grand Ballroom A

Chair(s): Stefan Nelwan and Daniel Guldenring

246-164 **Ischemia Alters Sensitivity of Action Potential to the Sodium-Potassium Pump**
Sanjay Kharche, Edward Vigmond, Michael Colman* and Henggui Zhang

247-101 **Dynamic Computational Simulations of Alternans in Acute Myocardial Ischemia**
Antonio Felix de Castro, Adriano Giovanni and Jose M Ferrero*

248-90 **Effects of Acute Myocardial Ischemia in Mathematical Models of Heterogeneous Myocardium**
Anastasia Vasilyeva*, Nathalie Vikulova, Olga Solovyova, Dmitry Zamaraev and Vladimir S Markhasin

249-234 **Metabolic but not Hypoxemic Stimuli are Related to the Apparent Recruitment of Capillaries in the Muscle**
Vito Starc*

**Wednesday, September 10, 2014, 11:30**

**SB2: Atrial Fibrillation II**

Room: Grand Ballroom B

Chair(s): Mariana Meo and Philip Langley

250-92 **Non-invasive Evaluation of the Effect of Metoprolol on the Atrioventricular node during Permanent Atrial Fibrillation**

Valentina DA Corino*, Frida Sandberg, Luca T Mainardi, Sara R Ulimoen, Steve Enger, Arnljot Tveit, Pyotr G Platonov and Leif Sörnmo

251-95 **Principal Component Analysis of Body Surface Potential Mapping in Atrial Fibrillation Patients Suggests Additional ECG Lead Locations**

Stef Zeemering*, Theo Lankveld, Pietro Bonizzi, Harry Crijns and Ulrich Schotten

252-79 **Is it Possible to Detect Atrial Fibrillation by Simply Using RR Intervals?**

Sándor Hargittai*

253-71 **Joint Entropy for Spatial Information Retrieval from Orthogonal Heart Planes Improves Catheter Ablation Outcome Prediction in Persistent Atrial Fibrillation**

Meo Marianna*, Vicente Zarzoso, Olivier Meste, Decebal G Latcu and Nadir Saoudi

**Wednesday, September 10, 2014, 11:30**

**SB3: Apnea Detection and Cardio-respiratory Interactions**

Room: Skyline A

Chair(s): Ary Goldberger and Carolina Varon

254-168 **An approach to the enhacement of Sleep Apnea Detection by means of Detrended Fluctuation Analysis of RR intervals**

Antonio Gabriel Ravelo García*, Ubay Casanova Blancas, Juan Luis Navarro Mesa, Sofía Martín González, Eduardo Hernández Pérez, Pedro Quintana Morales and Niels Wessel

255-42 **Automated Detection of Obstructive Sleep Apnoea by Single-lead ECG through ELM Classification**

Nadi Sadr* and Philip de Chazal

256-369 **Development of Analytical Approach for an Automated Analysis of Continuous Long-Term Single Lead ECG for Diagnosis of Paroxysmal Atrioventricular Block**

Muammar Kabir* and Larisa Tereshchenko

257-235 **Transient Behavior of Cardiorespiratory Interactions towards the Onset of Epileptic Seizures**

Carolina Varon*, Katrien Jansen, Lieven Lagae, Luca Faes and Sabine Van Huffel

**Wednesday, September 10, 2014, 12:45**

**PC1: Imaging**

Room: Grand Ballroom Lobby

258-334 **In Vivo T2-mapping and Segmentation of Carotid Artery Plaque Components Using Magnetic Resonance Imaging at 1.5T**

Bartosz Proniewski*, Tomasz Miszalski-Jamka and Przemysław Jaźwiec

259-99 **Fusion of Edge Enhancing Algorithms for Atherosclerotic Carotid Wall Contour Detection in CTA**

Florentino Luciano Caetano dos Santos*, Atte Joutsen, Juha Salenius and Hannu Eskola

260-237 **Myocardium Segmentation Improvement with Anisotropic Anomalous Diffusion Filter Applied to Cardiac Magnetic Resonance Imaging**

Antonio Carlos Senra Filho, Gustavo Barizon and Luiz Otávio Murta Junior*

261-221 **Automated Algorithm for Computing Left Ventricle Volume Changes from Cine-MR Images**

Soo-Kng Teo, Wan Min, Chi-Wan Lim, Liang Zhong, Ru-San Tan and Yi Su*

262-180 **A Local Phase-Based Algorithm for Registration of CMR Scans from Multiple Visits**

Christopher Kelly*, Stefan Neubauer, Robin Choudhury, Erica Dall'Armellina and Vicente Grau

263-45 **Defining Angular and Radial Positions and Parameters for Myocaridial Pixels in Cardiac MR Images**

Kjersti Engan*, Leik Woie and Trygve Eftestøl

**Wednesday, September 10, 2014, 12:45**

264-242 **Tissue Characterization from Myocardial Perfusion and Autonomic Innervation using MRI and SPECT images in Chagas Disease**

Gustavo Barizon, Antonio Carlos Senra Filho*, André Schmidt, Marcus Vinicius Simões, Leonardo Gadioli and Luiz Otávio Murta Junior

265-252 **Variance stabilizing transformations in the reduction of Poisson noise in 3D Nuclear Medicine images**

Edward Flórez Pacheco* and Sergio Shiguemi Furuie

266-24 **Optical Ballistocardiography for Gating and Patient Monitoring during MRI: An Initial Study**

Johannes W Krug*, Falk Lüsebrink, Oliver Speck and Georg Rose

267-3 **Automatic Segmentation of Intravascular Ultrasound Images based on Temporal Texture Analysis**

Chi Hau Chen* and Adithya G Gangidi

268-133 **A New Method for Intraoperative Quantification of Mitral Leaflet Segment Prolapse**

Sandy Engelhardt*, Raffaele De Simone, Norbert Zimmermann, Matthias Karck, Hans-Peter Meinzer, Diana Nabers and Ivo Wolf

269-260 **Ambulatory Impedance Pneumography Device for Quantitative Monitoring of Volumetric Parameters in Respiratory and Cardiac Applications**

Marcel Młyńczak, Wiktor Niewiadomski, Marek Żyliński and Gerard Cybulski*

270-286 **The Application of Different Metrics of Signal Shape for Automatic Identification of Artifacts in Impedance Cardiography Traces**

Gerard Cybulski* and Piotr Piskulak

**Wednesday, September 10, 2014, 12:45**

**PC2: System Studies**

Room: Grand Ballroom Lobby

271-388 **Antipsychotic Medication Influences Cardiovascular Coupling in Patients Suffering from Acute Schizophrenia**

Steffen Schulz*, Karl-Juergen Baer and Andreas Voss

272-326 **Study of Induced Emotion by Color Stimuli: Power Spectrum Analysis of Heart Rate Variability**

Sadaf Moharreri*, Nader Jafarnia Dabanloo and Saman Parvaneh

273-198 **In-vivo and Isolated Heart HRV Analysis by Hidden Markov Model**

Oto Janoušek*, Marina Ronzhina, Peter Scheer, Jana Kolářová, Ivo Provazník and Marie Nováková

274-345 **Detection of Electrocardiographic and Respiratory Signals Using a Wearable Transthoracic Bioimpedance Monitor for Improved Home-Based Disease Management in Congestive Heart Failure Patients**

Silviu Dovancescu* and Jarno Riistama

275-398 **Heart Rate Variability Analysis of Pre and Post-awakening of 10 Year Old Children**

Taher Biala*, Syamil Muhammad, Fernando Schlindwein and Michael Wailoo

276-371 **Global Optimization Approaches for Parameter Tuning in Biomedical Signal Processing: A Focus of Multi-scale Entropy**

Mohammad Ghassemi*, Li-Wei Lehman and Shamim Nemati

277-145 **Heart Rate Variability in Ultra-Trail Runners**

*Umberto Melia, Montserrat Vallverdu, Emma Roca, Daniel Brotons, Alfredo Irurtia, Joan A Cadefau, Pere Caminal and Alexandre Perera (Alexandre Perera)

**Wednesday, September 10, 2014, 12:45**

278-385 **Discrimination of Normal and At-Risk Populations from Fetal Heart Rate Variability**

Philip A Warrick* and Emily F Hamilton

279-223 **Investigation of Baroreflex Autonomic Control by Spectral Coherence of fMRI Independent Components and Neck Suction Stimulation Signal**

Matteo Mancini*, Eugenio Mattei, Federica Censi, Barbara Basile, Marco Bozzali and Giovanni Calcagnini

280-214 **Influence of Psychological Stress on QT Interval**

Chandan Karmakar, Mohammad Hasan Imam*, Ahsan Khandoker and Marimuthu Palaniswami

281-11 **Cardiac Autonomic Reinervation Following Aorto-Coronary Bypass Evaluated by High Resolution Heart Rate Variability**

Dimiter Simov, Maria Milanova, Mikhail Matveev, Vessela Krasteva and Ivaylo Christov*

**Wednesday, September 10, 2014, 12:45**

**PC3: Simulation**

Room: Grand Ballroom Lobby

282-287 **Linking a Novel Mutation to its Short QT Phenotype through Multiscale Computational Modelling**
Chiara Bartolucci, Cristina Moreno, Alicia de la Cruz, Pier Lambiase, Stefano Severi* and Carmen Valenzuela

283-273 **Ionic Mechanisms of Triggered Activity in Atrial Cell Models**
Marta Varela, Nooshin Ghavami, Stuart James, Ross Morgan* and Oleg Aslanidi

284-276 **Solution of the Bidomain Equations with a Composite Backward Differentiation Formula**
Wenjun Ying* and Craig Henriquez

285-195 **The Effect of Low Potassium in Brugrada Syndrome. A Simulation Study**
Karen Cardona, Juan Francisco Gómez, Javier Saiz*, Wayne R Giles and Beatriz Trenor

286-176 **Simple Ablation Guided by Approximate Entropy Mapping in a 2D Atrial Fibrillation Model**
Catalina Tobón*, Laura C Palacio, Juan E Duque, Esteban A Cardona, Juan P Ugarte, Andrés Orozco-Duque, Miguel A Becerra, John Bustamante and Javier Saiz

287-212 **The Modified Bidomain Model with Periodic Diffusive Inclusions**
Andjela Davidovic*, Clair Poignard and Yves Coudiere

288-136 **Myocardial Electrophysiological, Contractile and Metabolic Properties of Hypertrophic Cardiomyopathy: Insights from Modelling**
Ismail Adeniran*, Gareth Jones and Henggui Zhang

**Wednesday, September 10, 2014, 12:45**

289-87 **Role of Fiber Orientation in Atrial Arrythmogenesis**

Sanjay Kharche, Jichao Zhao, Simon Castro, Michael Colman*, Robert Stevenson, Jonathan Jarvis, Bruce Smail and Henggui Zhang

290-64 **Propagation Malfunctions due to Gap Junction Dysregulation**

Inmaculada R Cantalapiedra*, Angelina Peñaranda and Blas Echebarria

291-48 **Simulation of an Electro-mechanical Resuscitation Device for Cardiopulmonary Resuscitation**

Alejandro Mendoza Garcia*, Stefan Eichhorn, Marcin Polski and Alois Knoll

292-18 **Action Potential Abnormalities due to Loss- or Gain-of-Function Mutations in KCNJ2**

Ronald Wilders*

**Wednesday, September 10, 2014, 12:45**

**PC4: ECG Methods II**

Room: Grand Ballroom Lobby

293-49 **Robust Derivative-Based Method to Determine Filtered QRS Limits in High Resolution Electrocardiography**

Olivassé Nasario-Junior, Paulo Benchimol-Barbosa and Jurandir Nadal*

294-106 **Assessment of Electrocardiograms with Pretraining and Shallow Networks**

Vicent Ribas Ripoll*, Anna Wojdel, Pablo Ramos, Enrique Romero and Josep Brugada

295-7 **Variability of the Maximal Amplitudes of Impedance Cardiography and of its First Derivative during Supine, Standing, Controlled Breathing, and Exercise**

Salvador Carrasco-Sosa and Alejandra Guillén-Mandujano*

296-328 **Post Extrasystolic T Wave Change in Subjects With Structural Healthy Ventricles - Measurement and Simulation**

Gustavo Lenis*, Yannik Lutz, Gunnar Seemann, Arcadi García-Alberola, José Luis Rojo-Álvarez, Oscar Baquero-Pérez, Eduardo Gil and Olaf Doessel

297-6 **Comparative Study of Signal Decomposition Methods for Enhancement of the Accuracy of T-wave End Localisation**

Ivaylo Christov*, Velislav Batchvarov, Iana Simova, Nikolay Dimitrov and Elijah Behr

298-330 **A Portable Device for a Modular System of Patient Monitoring**

Daniel Campillo*, Hector Torres, Rene Gonzalez, Katia Valdes and Rolando Lopez

299-2 **Cardiac Telemetry System Intended for Flexible Patient Monitoring**

Gay Meissimilly*, Mary Cartaya and Diolkis Ruiz

**Wednesday, September 10, 2014, 12:45**

300-307 **Personalised System-on-chip for Standard 12-lead Reconstruction from the Reduced 3-lead System Targeting Remote Health Care**

Utkalika Panda, Sidharth Maheshwari, Gayathri Padma, Murugaiyan Thendral, Agathya Jagirdar, Venkateswara Chowdary, Naresh Vemishetty, Amit Acharyya*, Paolo Emilio Puddu and Michele Schiariti

301-292 **QRS Complex Detection in Experimental Orthogonal Electrograms of Isolated Rabbit Hearts**

Jiří Kozumplík, Marina Ronzhina, Oto Janoušek, Jana Kolářová*, Ivo Provazník and Marie Nováková

302-61 **High-frequency Noise Filtration in Stress Test ECG**

Giovanni Bortolan and Ivaylo Christov*

**Wednesday, September 10, 2014, 12:45**

**PC5: Cinical Aspects of ECG II**

Room: Grand Ballroom Lobby

303-149 **High Resolution ECG Differences between Hospital Survivors and Non-survivors of Out-of-Hospital Cardiac Arrest during Mild Therapeutic Hypothermia**

Martin Rauber*, Dušan Štajer, Marko Noč, Todd Schlegel and Vito Starc

304-280 **Susceptibility of Isolated Rabbit Hearts with various Left Ventricular Mass to Short Ischemic Periods**

Veronika Olejnicková*, Marina Ronzhina, Hana Paulova, Miroslava Hlavacova, Tibor Stracina and Marie Novakova

305-288 **Effects of Left Ventricle Enlargement on QRS of Rabbit Isolated Heart Electrogram**

Marina Ronzhina*, Veronika Olejníčková, Oto Janoušek, Tibor Stračina, Tomáš Potočňák, Jana Kolářová, Marie Nováková and Ivo Provazník

**Wednesday, September 10, 2014, 12:45**

**PC6: Cardiac Mechanics**

Room: Grand Ballroom Lobby

306-174 **Comparison of Time and Frequency Domain Methods for the Feedback on Chest Compression Rate**

Digna M González-Otero*, Erik Alonso, Jesús Ruiz, Sofía Ruiz de Gauna, Elisabete Aramendi, Unai Ayala, James K Russel and Mohamud Daya

307-62 **Three-dimensional Apex-seismocardiography**

Samuel E Schmidt*, Ask Schou Jensen, Jacob Melgaard, Claus Graff, John Hansen, Tanveer A Bhuiyan and Johannes J Struijk

308-194 **Filtering Chest Compression Artifacts Improves the Performance of VF-detection Parameters.**

Unai Ayala*, Unai Irusta, Jesús Ruiz, Felipe Alonso-Atienza, Erik Alonso, Digna González-Otero, Jo Kramer-Johansen and Trygve Eftestøl

309-186 **Feasibility of Non-invasive Blood Pressure Estimation Based on Pulse Arrival Time: a MIMIC Database Study**

Braiam Escobar* and Róbinson Torres

310-232 **Measurement of Pulse Wave Velocity during Valsalva and Mueller Maneuvers by Whole Body Impedance Monitor**

Magdalena Matejkova*, Vlastimil Vondra, Josef Halamek, Ladislav Soukup, Filip Plesinger, Ivo Viscor and Pavel Jurak

**Wednesday, September 10, 2014, 12:45**

**PC7: Electrophysiology Modelling**

Room: Grand Ballroom Lobby

311-299 **Analysis of Electrogram Complexity during Atrial Fibrillation for Ablation Procedure Duration Prediction**

Katarzyna Kośna*, Piotr Podziemski, Lauren Wilson, Simon Stolcman, Prashanthan Sanders, Jan Jacek Żebrowski and Paweł Kuklik

312-397 **Frequency Spectrum Correlation along Atria to Study Atrial Fibrillation Recurrence**

Raquel Cervigon*, Javier Moreno, Jorge García-Quintanilla, Julián Pérez-Villacastín, Francisco Castells and José Millet

313-255 **Loss of Transverse-Tubules Promotes the Development of Ectopic Activity in Guinea-pig Ventricle**

Michael Alan Colman*, Sanjay Kharche and Henggui Zhang

314-362 **Point-to-Pixel Tracking Cancellation Pipeline for Motion Artifact Compensation in Uncoupler-Free Non-Ratiometric Experimental Optical Mapping Studies**

Jaime Yagüe-Mayans, Conrado J Calvo*, Francisco J Chorro and José Millet

315-240 **The Effect of Scar Tissue on Complexity of Activation Patterns in Simulated Human Ventricular Fibrillation**

Sathyavani Malyala* and Richard Clayton

316-275 **Motion Analysis Method for Determining Cardiomyocyte Beating Properties Based on Digital Image Correlation and Templates**

Antti Ahola*, Paruthi Pradhapan, Eeva Laurila, Katriina Aalto-Setälä and Jari Hyttinen

**Wednesday, September 10, 2014, 15:00**

**MD: Plenary**

Room: Grand Ballroom

Chair(s): Roger Mark and Olivier Meste

317-367 **Discovering and Interpreting Dynamic Behaviors in Cardiovascular Time Series from a Heterogeneous Patient Cohort**

Li-Wei Lehman*, Shamim Nemati, Matthew Johnson, George Moody, Thomas Heldt and Roger Mark

318-57 **Ethnic Variation in Prevalence of End QRS Notching and Slurring in Apparently Healthy Populations**

Elaine Clark* and Peter Macfarlane

319-17 **Bidomain Simulations of Subendocardial Ischemia: The Forward and Inverse Problems**

Marius Lysaker, Bjørn Fredrik Nielsen and Samuel Wall*

# Abstracts

M1

# Identification of Myocardial Scar in Ventricular Tachycardia: Correlation between CT based results and Electro-Anatomic Map Findings

Sofia Antunes*, Antonio Esposito, Giuseppe Macabelli, Anna Palmisano, Caterina Colantoni, Sebastiano Colombo, Paolo della Bella, Sergio Cerutti and Giovanna Rizzo

Politecnico di Milano
Segrate (Milano), Italy

In the last years multi-detector computed tomography (MDCT) had a great development in terms of spatial and temporal resolution. For this reason, it has been investigating as an important alternative to the delayed enhanced magnetic resonance imaging (DE-MRI) for the preprocedural planning and guidance of ventricular tachycardia (VT) ablation procedures. The main reasons are related to the reliability in visualizing epicardial fat distribution, the reduced artefacts caused by the metallic cardioverter, as well as the higher spatial resolution when compared to DE-MRI. During substrate mapping of left ventricular myocardial endocardium or epicardium, the myocardium needs to be mapped in terms of voltage differences. Today, bipolar and unipolar voltage are used as indexes of detection of scars (usual site for re-entry channels). However, the process is time consuming and leads to wrong maps; in the endocardium mainly due to bad contact with the endocardial surface and in the epicardium caused by a thick epicardial fat layer. The purpose of this work was to compare an image-based parametric myocardium mesh automatically segmented from MDCT with the findings of electro-anatomic maps (EAM) constructed previously to radiofrequency ablation procedures. The myocardium mesh presents distance information about myocardial thickness, as well as the localization of scar detected using a delayed enhanced DE-MDCT scan. Additionally, possible zones of epicardial fat with thickness greater than 3mm were also identified on patients that underwent an epicardial intervention. The comparison was performed on 5 patients with recurrent VT undergoing angiographic and DE-MDCT scan before EAM and RFa, of which 3 patients underwent endocardial and 2 patients an epicardial procedure. We compared the findings of the myocardium mesh against EAM and our results suggest that the mesh could be an important tool for the prediction of myocardial scar localization.

M1

# How does Uncoupling in Ventricular Tissue Affect Conduction at Purkinje-Myocardial Junctions?

Elham Behradfar*, Anders Nygren, Fu Siong Ng and Edward J Vigmond

Canada

**Background:** The Purkinje system (PS) is the specialized conduction system of the ventricles, which contacts with ventricular myocytes and activates them through Purkinje-Myocardial Junctions (PMJs). There are limited data on number and distribution of PMJs, but it is known that a large portion of these junctions are not functional during normal rhythm.

**Objective:** We hypothesized that uncoupling in ventricular tissue, which happens during ischemia, facilitates propagation across PMJs, leading to more functional PMJs, and thereby accelerated activation of ventricles.

**Methods:** The hypothesis was explored by performing experiments on ischemic rabbit hearts and by computer simulation of uncoupling in the rabbit ventricular model.

**Results:** In a simple model of ventricular tissue and PS, uncoupling was modeled by reduced conductivity. We found that after only 6% reduction in tissue conductivity, normally quiescent PMJs were capable of activating myocytes. In a detailed model of the rabbit ventricles and PS, simulations were performed with varying percentage of functional PMJs and tissue conduction. Increasing the number of active PMJs accelerated propagation of activation over the surface and could compensate for the slowing of propagation due to reduced conductivity. Results of optical mapping of the endocardial surface of ischemic rabbit hearts revealed that the percentage of area with activation time less than 5 ms increased during ischemia and returned to the normal value after reperfusion. We defined a parameter based on the divergence of conduction velocity on the ventricular surface to quantify the complexity of the activation pattern and incidence of breakthroughs. The integral of divergence over the endocardial area increased for higher percentage of functional PMJs, demonstrating the occurrence of more breakthroughs and wave collisions.

**Conclusion:** Our results indicate that a higher percentage of functional PMJs can speed activation of tissue and compensate for effects of uncoupling in terms of activation time of the ventricles.

.

# Physiology-based Regularization Improves Noninvasive Reconstruction and Localization of Cardiac Electrical Activity

M1

Matthijs JM Cluitmans, Monique MJ de Jong, Paul GA Volders, Ralf LM Peeters, Ronald L Westra

Maastricht University
Maastricht, the Netherlands

Epicardial electrograms: measured (left), Tikhonov-reconstructed (middle) and physiology-based reconstructed (right).

The objective of the inverse problem of electrocardiography is to noninvasively reconstruct information about electrical activity at the heart surface (epicardium), from electrical measurements on the body surface and a patient-specific torso-heart geometry. This is complicated by the ill-posedness of the inverse problem, making reconstructions imperfect. Previously, we have shown that a realistic basis can be created from (simulated) epicardial training potentials. Reconstructions from traditional methods can be projected onto this basis, improving the quality of reconstructions. Here, we propose a novel superior method called 'physiology-based regularization' that renders traditional (e.g. Tikhonov) reconstruction and projection unnecessary. Instead, reconstruction of epicardial electrograms is achieved directly, by pursuing a sparse representation in terms of this realistic basis. This approach differs radically from the traditional regularization methods, which apply mathematical or physical constraints. By using a realistic epicardial basis, it is possible to include physiological knowledge as constraint. We validate this method by simultaneously recording 67 invasive epicardial electrograms in a canine experiment. The correlation between physiology-based reconstructed and *in vivo* measured electrograms (Pearson's $r = 0.60$) is similar to those of traditional reconstruction methods such as Tikhonov regularization ($r$=0.59). We further demonstrate that by creating a realistic basis for a specific pathology, this method can answer clinical questions with improved accuracy.

Ultimately, physiology-based regularization would improve patient care by yielding patient-specific results, inspired by electrophysiological knowledge and optimized to answer clinically relevant questions.

M1

# Non-invasive Detection of Reentrant Drivers during Atrial Fibrillation: a Clinical-Computational Study

Miguel Rodrigo, Andreu M Climent, Alejandro Liberos, Jorge Pedrón-Torrecilla, José Millet, Francisco Fernández-Avilés, Felipe Atienza, Omer Berenfeld, Maria S Guillem

Universitat Politècnica de València, València, Spain
Hospital General Universitario Gregorio Marañón, Madrid, Spain
University of Michigan, Ann Arbor, MI, USA

Reentrant drivers or mother rotors have been defined as a mechanism responsible of atrial fibrillation (AF) maintenance. Previous studies have shown that the location and ablation of the reentrant drivers allow detaining the AF episodes. This study presents a novel non-invasive approach to identify those reentrant drivers based on the analysis of the phase maps obtained from surface potential recordings.

High-density surface potential recordings were obtained from 14 paroxysmal and persistent AF patients simultaneously to intracardiac electrograms (EGM) recordings. Singularity points (SP) were detected in torso phase maps after band-pass filtering at the highest dominant frequency (HDF) found on the torso and in both atria. Besides, an atrial-torso computer model was used to investigate the effect of the band-pass filtering on the surface potential signal produced by atrial reentrant activity.

Stable SPs were found during 73.1±16.8% of time after HDF-filtering vs. 8.3±5.7% on raw signals on the entire cohort of patients ($p<0.01$). The average duration of each rotational pattern was also higher in HDF-filtered than in unfiltered AF signals (342±138 ms. vs. 160±43 ms., $p<0.01$). After band-pass filtering at the HDF from the left and right atria, the surface SPs were distributed in regions related with the torso projection of the atrial activity found on previous studies. Mathematical models allowed us to observe the mechanisms underlying the HDF-filtering which attenuate the activity provoked by atrial regions other than the atrial drivers reflecting on the torso only the rotatory activity.

HDF-filtering allows detecting atrial drivers in torso phase maps during AF, and the position of the detected SPs is related with the location of the rotor in the atria. This novel technique may improve the AF diagnosis, helping in planning the best therapy strategies by non-invasively locating the ablation targets.

# Using Seismocardiogram for Detection of Ischemia by Extraction of Systolic and Diastolic Time Variability

Farzad Khosrow-Khavar, Andrew Blaber, Carlo Menon and Kouhyar Tavakolian*

University of North Dakota
Grand Forks, United States

S21

**Objective:** The main objective of this project is to use seismocardiogram to extract hemodynamic parameters related to systolic and diastolic time interval in order to distinguish between ischemic and non-ischemic cases.

**Method:** While the electrocardiogram (ECG) signal captures the electrical activity of the heart, seismocardiogram (SCG) is designed to capture mechanical vibration penetrated to the surface of the chest. A small accelerometer mounted on the chest is used to measure cardiac vibration. It is known that peaks of the SCG signal correspond to specific mechanical activity of the heart. In particular, mitral valve closure (MC) aortic valve opening (AO) and aortic valve closure (AC) can be extracted. The ECG can be used as a reference signal in order to find these peaks. The interval of ECG-Q wave to SCG-AC corresponds to the systolic period and the interval of SCG-AC to ECG-Q of the next cycle corresponds to the diastolic period. The interval of ECG-Q wave to SCG-AO corresponds to PEP and the interval of SCG-AO to SCG-AC corresponds to LVET. The cycle to cycle cardiac variability of the systolic (SYS-VAR), diastolic (DIA-VAR), PEP (PEP-VAR), LVET (LVET-VAR) and PEP/LVET (PEP/LVET-VAR) period were used as features to distinguish between ischemic and non-ischemic patients. The same procedure as heart rate variability parameters were used for this research. Various classifications models such as linear discriminant analysis, random forest, support vector machine and neural networks were used to classify between non-ischemic and ischemic patients. The data were manually annotated for training purposes.

**Database:** The database contained total of 60 individuals including 30 ischemic heart patients from Burnaby General Hospital. Both ECG and SCG signals were simultaneously captured.

**Conclusion-** The cycle to cycle variability parameters extracted from SCG can be used to diagnose between non-ischemic and ischemic patients.

# Modeling Mechanical Response of the Chest During the Cardiopulmonary Resuscitation Procedure

S21

Ali Jalali*, Vinay Nadkarni and C Nataraj

Villanova University
Villanova University, United States

The cardiopulmonary resuscitation procedure in its current form is far from optimized and needs to be improved. The first step in improving the CPR procedure is to understand how the force applied on the chest relates to the resulting blood pressure. In order to capture the mechanical properties of the chest and abdomen accurately, we propose a nonlinear damped oscillator model which consists of a nonlinear spring, a combination of viscous and hysteresis damping mechanisms and a variable mass to account for dynamic changes in the effective mass during the CPR. We then nondimensionalize the proposed model in order to enable a parametric study of the model. In the next step we use the gradient decent optimization method to identify the model parameters for force-compression data of 427 CPR cycles collected from different pigs at the Children's Hospital of Philadelphia (CHOP). We use the mean square error (MSE) between the estimated force and actual force for each cycle as an objective function to be minimized. Using the above method we were able to estimate the model parameters for each cycle; however, since the proposed model is nonlinear and since data can be affected by noise and different experimental conditions, the estimated parameters are not consistent and vary cycle by cycle. In order to find a best set of estimated parameters we emply the K-nearest neighbor (K-NN) method. K-NN is an unsupervised learning technique which clusters the data into different groups based on the distance metric. The cluster center with lowest MSE is selected as the estimated parameter set for the entire period. The resulting mean squared errors have a mean value of 0.0046 and a standard deviation of 0.0068. Results show that the proposed model is the most accurate model of the pig chest during the CPR as yet reported.

# Empirical Mode Decomposition for Chest Compression and Ventilation Detection in Cardiac Arrest



Erik Alonso, Elisabete Aramendi, Digna González-Otero, Unai Ayala, Mohamud Daya, James K. Russell

University of the Basque Country, UPV/EHU
Bilbao, Spain

Latest resuscitation guidelines emphasize the delivery of high quality cardiopulmonary resuscitation (CPR), including chest compressions (CCs) with rates $\geq$100 min$^{-1}$ and ventilations at 8-10 min$^{-1}$. During basic life support, lay-rescuers use automated external defibrillators which record ECG and thoracic impedance (TI) signals. CCs and ventilations cause fluctuations in the TI, which can be used to report CC-rate and ventilation-rate. Inclusion in review of cardiac arrest episodes would contribute to improve CPR quality metrics.

**Aim:** To develop a method based on empirical mode decomposition (EMD) to compute CC-rate and ventilation-rate using exclusively the TI.

**Materials:** Twenty out-of-hospital cardiac arrest episodes were extracted from a database collected using the Philips HeartStart MRx monitor/defibrillator between 2006-2010 in Oregon (USA). Each episode comprised the TI, compression depth (gold standard for CC-rate), and capnography (gold standard for ventilation-rate) signals. A total duration of 1777 s, 2781 CCs and 221 ventilations were analyzed.

**Methods:** The EMD decomposed the TI signal into intrinsic mode functions (IMFs). Hilbert transform was applied to calculate the instantaneous frequencies of the oscillations within each IMF. IMFs were combined based on their median instantaneous frequency to reconstruct separately the CC and the ventilation signals. Independent CC and ventilation detectors were developed based on fixed thresholds for durations and dynamic thresholds for the amplitudes. Sensitivity and positive predictive value (PPV) was reported for each detector. CC-rate and ventilation-rate were computed as the inverse of the median interval between instants of CCs and ventilations respectively. The mean (SD) errors were reported.

**Results:** Sensitivity/PPV values were 99.35%/98.75% and 93.21%/82.40%, and mean errors 0.57(0.55) min$^{-1}$ and 1.10(1.19) min$^{-1}$ for CC and ventilation detection respectively.

**Conclusions:** CC-rate and ventilation-rate can be accurately estimated from the CC and ventilation signals reconstructed using EMD. This could be useful for CPR metrics in debriefing of cardiac arrest episodes.

## Evaluation of Aortic Flow Alterations using MRI: Associations with Left Ventricular Remodeling

S21

Ioannis Bargiotas*, Emilie Bollache, Alain De Cesare, Alban Redheuil, Elie Mousseaux, Nadjia Kachenoura

Sorbonne Universités, UPMC University Paris 06, UMR 7371, UMR_S 1146, Laboratoire d'Imagerie Biomédicale, Paris, France

**Aims:** Aortic stiffening including structural and hemodynamic changes is known to have deleterious effects on the left ventricle (LV), since afterload increases with the underlying wave reflections. This study aimed to: 1) design indices of ascending aorta (AA) flow alterations from MRI data and 2) assess their associations with LV remodeling, defined as LV-mass (LVM) divided by end-diastolic volume (EDV), in comparison with tonometric stiffness indices.

**Methods:** We studied 70 healthy volunteers (age 46.3±15.8 years; 40 males) who underwent MRI through-plane AA velocity and LV cine data, as well as carotid and femoral applanation tonometry providing central pressures and stiffness indices such as carotid-femoral pulse wave velocity (PWV) and carotid augmentation index (AIx). After an automated segmentation of AA lumen on MRI images, velocity and flow curves were estimated and used to derive indices reflecting their late systolic morphological changes, such as a) time-interval required for flow ($T^F_{1/2}$) or velocity ($T^V_{1/2}$) deceleration to reach half of systolic peak, normalized by systolic deceleration time-interval (DT), and b) decrease in flow ($DR^F_{1/2}$) or velocity ($DR^V_{1/2}$) during half of DT, expressed in percentage of systolic peak.

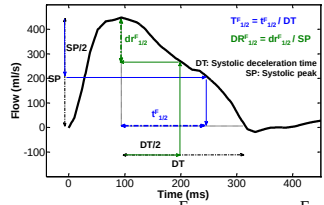

Illustration of $T^F_{1/2}$ and $DR^F_{1/2}$ estimation on flow curve.

**Results:** Significant correlations were found between LVM/EDV and the newly proposed MRI parameters with a slight superiority for flow indices, as compared to velocity indices ($T^F_{1/2}$: r=-0.46, $T^V_{1/2}$: r=-0.39, $DR^F_{1/2}$: r=0.43, $DR^V_{1/2}$: r=0.35, p<0.002). Such associations remained significant after adjustment for age, gender, weight, height, heart-rate and systolic blood pressure. PWV (r=-0.25) was the only conventional stiffness index which was significantly associated (p<0.04) with LVM/EDV but did not remain significant after adjustment.

**Conclusion:** Local indices of AA flow alterations are stronger correlates of LV remodeling than global indices of arterial stiffness. Such indices might be of usefulness in understanding subclinical arterial-ventricular coupling alterations especially in patients with LV hypertrophy, secondary to hypertension, which is a widespread disease.

## ECG Analysis during Continuous-flow LVAD

O Meste*, A Cabasson, L Fresiello, MG Trivella, A di Molfetta, G Ferrari and F Bernini

Université Nice Sophia Antipolis, CNRS
France

S21

**Aim:** The current use of left ventricular assist devices (LVADs) as destination therapy is associated with the clinical need of monitoring patient-pump interaction. The present work investigated the possibility of getting useful information about the status of the assisted left ventricle using non-invasive data, such ECG. To our knowledge this is the first study where this relationship is focused on R wave magnitude, confirming in a different manner the pioneering results of MR Franz.

**Method:** 6 pigs undergoing LVADs implantation (Gyro Centrifugal Pump C1E3 and Synergy CircuLite Micropump) in atrio-aortic connection, were analysed. Data refer to different LVADs speeds with consequently different levels of ventricular unloading. From ECG signal the R wave peak (RWP) was individuated together with the corresponding left ventricular volume (LVV). Both signals are strongly affected by the assisting ventilation. Thus an adequate smoothing processing was performed in order to get rid of its effect. In addition, using a method already proposed for T wave analysis assessed the shape changes of the QRS during the changes of the pump speed.

**Results:** A correlation analysis and linear regression performed on RWP and LVV, evidenced that the R wave peak and the ventricular volume are strictly correlated. Correlation coefficients ranged from -0.83 to -0.95. More in details, any change of LVAD speed, inducing a change in ventricular volume, is associated with an opposite change in R wave peak value. The QRS shape analysis did not exhibit such correlation with LVV but evidenced the interplay with the heart rate, variable within the experiment.

**Conclusions:** The present work is a first step in investigating the usefulness of the ECG signal during LVAD therapy. The correlation found between the ECG and the ventricular volume can be a promising starting point for possible future non invasive LVAD patient monitoring.

# Effects of Cardiac Resynchronization Therapy on the First Heart Sound Energy

S21

Ask S Jensen*, Samuel E Schmidt, Johannes J Struijk, John Hansen, Claus Graff, Jacob Melgaard, Tanveer A Bhuiyan, Kasper Emerek, Peter Soegaard

Aalborg University
Aalborg, Denmark

**Introduction:** Pacemaker programming is important in optimization of cardiac resynchronization therapy (CRT). The optimization procedure requires real-time evaluation of cardiac function, for which various methods have been applied. The first heart sound (S1) carries important information about ventricular function which may be clinically useful in CRT optimization. We developed a method of measuring the effects of CRT on S1 energy.

**Methods:** For 10 patients with activation induced heart failure (age 64±8.4 years), the heart sound was recorded using a microphone placed at the left sternal border in the 4$^{th}$ intercostal space, synchronously with the three lead ECG. With the patient in the supine position, two recordings were made with the pacemaker turned off and on, respectively (Fs=5000 Hz). An automated algorithm was used for beat segmentation and alignment. ECG beats were extracted following R wave peak detection, and a median ECG beat was calculated. ECG beats were aligned to the median, and synchronous heart sound recordings were aligned to corresponding ECG beats. After removal of noisy beats, 132 beats were included for each recording on average. An envelope of the median heart sound (50-500 Hz) was calculated using the Hilbert transform, and a 0.2s interval centered on S1 was extracted. The energy of the S1 envelope was calculated as the integral of the square. Statistical analysis was carried out using the Wilcoxon signed-rank test.

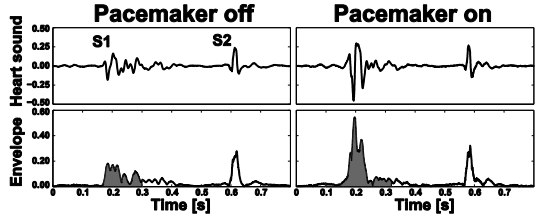


**Heart sound and envelope with pacing on/off.**

**Results:** Activation of the pacemaker resulted in an increase in S1 energy of 419.6±623.4%. This was statistically significant with $p<0.01$. Out of ten cases, the energy increased by >40% in nine and >74% in eight. In the remaining case there was a -4.5% reduction.

**Conclusion:** CRT causes clinically relevant change in S1 energy, and methods of real-time measurement may be useful in CRT optimization.

# A flexible PCA-based ECG-reconstruction algorithm with confidence estimation for ECG during exercise

Steffen A Mann, Reinhold Orglmeister

Electronics and Medical Signal Processing, TU-Berlin
Berlin, Germany

S22

**Aims:** Holter monitoring during everyday situations is prone to movement artefacts and declining skin-electrode contact. This study aimed at automatically detecting and reconstructing leads that have been compromised on a beat-to-beat basis. As a clean reference cannot always be recorded, the quality of the reconstruction was evaluated using only the least disturbed leads.

**Methods:** A wireless body-sensor-network, encompassing active ECG electrodes with accelerometers, was used to record 12-lead ECGs during everyday situations. These recordings include motion intensive activities such as climbing stairs and jogging. Beat-to-beat quality evaluation of ECG-leads was realised using the electrodes' accelerometric data together with selected ECG-signal features from the 'PhysioNet/CinC-Challenge-2011', which were adapted for beat-to-beat processing.
Situation specific reconstruction matrices $A$ can be determined by principal component analysis, for e.g. inhalation/exhalation or different heart-rates. Using $A$, the first principal components of leads with high quality can be transformed into substitutes for low quality leads.
Lacking an undisturbed reference during exercise, a confidence estimation was achieved by considering the reconstruction accuracy for undisturbed leads in the same segment by means of the Pearson Correlation and the overall segment quality.

**Results:** In this preliminary study, four hours of 12-channel ECG recordings from six healthy subjects, totalling in 17480 recorded heartbeats per lead, containing different activities including exercise, were evaluated. The overall reconstruction quality according to the Pearson Correlation in segments classified as suitable for reconstruction, i.e. at least four of eight leads had only minor to medium disturbances, was 0.94.

**Conclusion:** The algorithm is able to detect disturbances in recorded ECGs on a beat-to-beat level. Leads with the lowest disturbances in a segment are automatically detected and used for reconstructing all leads in that segment. The quality of the reconstruction can then be assessed without the need for a clean reference.

# Coherence as a Measure of Noise in the ECG

S22

Johannes J Struijk*, Claus Graff, Jørgen K Kanters, Joel Q Xue, Ask Schou Jensen, Samuel Schmidt

Aalborg University, Aalborg, Denmark

**Introduction:** The normal 12-lead ECG can be described as the projection of a time-varying dipole on the lead vectors. This dipole-source assumption of the ECG implies that the different leads must show a very high coherence and that deviations from values close to unity may indicate the presence of noise.

**Methods:** We evaluated the average coherence in the band of 5 Hz to 45 Hz in 309 ECGs, both normal and with various abnormalities, and compared the coherence measure with an automatic out-of-band noise evaluation by GE Healthcare, quantified at a 10 level scale from 0 (clean) to 10 (very noisy).

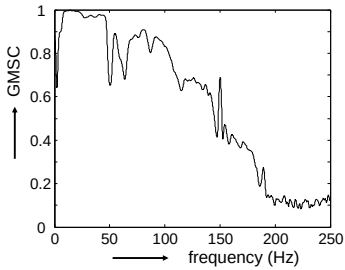


The coherence measure used was the generalized magnitude squared coherence (GMSC) as described by Ramirez et al. (2008). The generalized coherence is a measure of the linear relationship among the leads. The GMSC gives a measure of the coherence among all leads based on the largest eigenvalue of the matrix of all pairwise coherences. In addition a pairwise analysis among the leads was performed.

**Results:** A high coherence (GMSC>0.95) was always associated with very low noise (level 0 or 1) and 0.9<GMSC<0.95 was associated with levels 0-2. For noise levels > 2 the GMSC was <0.87 in all cases. There were no cases of high noise level and a high coherence, however, in 32% of the cases with noise level 0 or 1 the GMSC was <0.8.

**Conclusion:** For normal noiseless ECGs the GMSC is close to unity, with a good correlation between noise level and GMSC for normal ECGs. However, a low coherence also seems to be associated with abnormalities in the ECG, which will be subject for further study.

# A Framework for ECG Signal Preprocessing based on Quadratic Variation Reduction

Valeria Villani* and Antonio Fasano

Università Campus Bio-Medico di Roma
Rome, Italy

S22

**Aims:** In this paper we propose a novel framework for ECG signal preprocessing, which is general, effective and fast. In this regard, LTI filtering is the only general method that can handle any noise and artifact corrupting the ECG. However, it suffers from some important limitations. In particular, it cannot cope with transient noise, and may introduce unacceptable distortions in the ECG. Moreover, sophisticated filters can hardly be implemented on handheld devices.

**Proposed Approach:** The framework is based on the notion of quadratic variation, introduced as a measure of variability. Noise and artifacts are jointly removed by solving a convex optimization problem which selectively reduces the quadratic variation of the measured ECG. The framework is very general, since it is able to cope with all kinds of noise and artifacts that corrupt ECG signals, like baseline wander, narrowband artifacts (e.g., power-line interference), electromyographic and thermal noise. It can be used to smooth single waves (P-waves and T-waves) as well as entire ECG records. The framework relies on a single algorithmic structure, which can be easily adapted to cope with the different kinds of noise. Moreover, it is fast and efficient, even on long recordings.

**Results:** Performances were extensively investigated in several other papers, considering all kinds of noise and artifacts that usually corrupt an ECG. The algorithms within the framework outperform state-of-the-art approaches, in terms of both effectiveness in removing noise and artifacts, and ability to preserve ECG morphology.

**Conclusion:** The proposed framework can cope with any kind of noise and artifact affecting the ECG. It is effective in improving signal quality without altering ECG morphology, in particular the ST segment. It is very fast, thus being suitable for real-time applications and for implementation on devices with reduced computational power, e.g., handheld devices.

# Electrocardiogram Artifact Cancelation based on Empirical Mode Decomposition and Peak Detection using Dual-Slope Algorithm

S22

Mohammadreza Ravanfar, Riadh Arefin, Kouhyar Tavakolian, Reza Fazel-Rezai

University of North Dakota,
Grand Forks, ND, USA

During past decades, due to advances in signal processing methods, there has been more attention to the use of electrocardiogram (ECG) in noninvasive diagnosis procedures. Nonetheless, intrinsic and extrinsic sources of artifacts degrade the quality of ECG recordings and consequently constrain the potentials of ECG in medical diagnoses. Low frequency ECG artifacts change the signal offset. In addition, high frequency artifacts and power-line interference negatively impact on the semantic changes of ECG and create challenging problems in ECG processing algorithms. After removing the baseline and power-line artifacts, R peak detection has particular importance in the subsequent processing. Therefore, designing an algorithm with great ability in baseline removing, denoising, and R peak detection provides insights for identifying the patterns of different arrhythmias and solving arrhythmia classification problem. Due to nonlinear origins of ECG and the undesirable artifacts, nonlinear signal processing has great potential to reach creditable outcomes. Empirical mode decomposition (EMD) is one of most popular non-stationary and non-linear methods which has found a broad application in biomedical processing. In this paper, EMD was properly applied to ECG for denoising and baseline removing where EMD-based polynomial fitting was utilized for baseline estimation. The power-line interference was removed using high oscillatory modes. Then, R peaks were detected by a fast dual-slope algorithm. In addition, doubly iterative-EMD (DI-EMD) was used to obviate the EMD border effects. The algorithm was applied to MIT-BIH database for evaluation and showed 192 false negative diagnosis, 491 false positive diagnosis, and total error of 0.62% out of 109,508 beats. The figure represents the detected R peaks after the artifact cancelation.

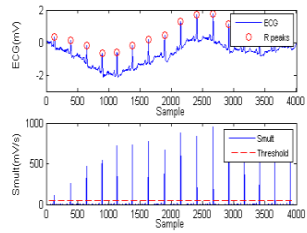


R peak detection for sample 105 of MIT-BIH showing different variables of the algorithm.

# Extracting a Clean ECG from a Noisy Recording: A New Method based on Segmented-beat Modulation

Angela Agostinelli*, Corrado Giuliani and Laura Burattini

Università Politecnica delle Marche
Ancona, Italy

S22

Electrocardiogram (ECG) testing represents a simple, economic and non-invasive diagnostic tool to identify heart diseases. Generally, an ECG recording is corrupted by different types of noise and artifacts, including power line interference, baseline drifts, motion artifacts, muscle contractions, electrode contact noise, electronic noise and electrical interferences. Such noisy components may alter the ECG morphological characteristics, jeopardizing the clinical evaluation. Hence, to extract useful information from the ECG, this needs to be filtered in order to get rid of the noise without distortions. The aim of the present study is to introduce a new method, termed segmented-beat modulation method (SBMM), for extracting a clean ECG signal from a noisy recording. The SBMM uses modulated beats to construct a template-beat which is then concatenated to obtain the filtered, clean ECG. More specifically, each cardiac cycle (CC) is segmented into two segments, the QRS segment and the TUP segment, respectively independent and proportional to preceding RR interval. TUP-segment modulation (compression or stretch) is initially used to force all CC to have the same duration. Such condition is indeed required for computing the template-beat as the median beat. Then, filtered ECG is obtained by concatenating the template-beat after TUP-segment demodulation (stretch or compression) in order to obtain reconstructed beats whose duration matches that of the corresponding beats in the original noisy recording. Optimization procedures are performed to take into account small inter-beat morphological ECG variations independent from actual heart rate. The SBMM was tested in two applications respectively involving an ECG corrupted by motion artifacts; and an abdominal recording from a woman in labor. Results clearly demonstrate the SBMM ability to provide a clean, and thus clinically useful, ECG tracing from a noisy recording.

# A Bayesian Filtering Framework for Accurate Extracting of the Non Invasive FECG Morphology

S22

Joachim Behar*, Fernando Andreotti, Julien Oster and Gari Clifford

Oxford
Oxford, United Kingdom

**Introduction:** The electrocardiogram (ECG) allows for interpretation of the electrical activity of the heart. The information which can be derived from the foetal ECG (FECG) goes beyond heart rate and heart rate variability. However morphological analysis of the FECG waveform is usually not performed in clinical practice.

**Methods:** A Bayesian Filtering Framework based on an extended Kalman filter (EKF) for extracting the FECG from a single abdominal channel is described using a training database of 20, one minute maternal-foetal mixtures and evaluated on 200, one minute mixtures. (Data were generated using the simulator, fecgsyn, used to generate a subset of the signals of the Physionet Challenge 2013.) A single pass of the EKF (EKFS) was performed to cancel out the maternal ECG (MECG) in order to build an average FECG morphology. A dual EKF (EKFD, i.e. where both the MECG and FECG cycle morphology were modelled) was then applied to separate the three sources present in the signal mixture (noise, MECG and FECG). A normalised root mean square error and absolute QT error after EKFS and EKFD were calculated.

**Results:** An SNR improvement of 5.04 db after EKFS and 15.9 db after EKFD on the test set were achieved. Median absolute error on QT measurement was 24 ms for the EKFS and 4 ms for the EKFD.

**Conclusion:** This work is a proof of concept that the EKFD allows accurate extraction of the FECG morphology from abdominal recordings.

# A Boolean Network of Crosstalk between IGF and Wnt Signalling

Lea Siegle, Ludwig Lausser, Michael Kühl and Hans A Kestler*

Germany

S23

Various Wnt homologues are expressed in distinct temporal stages and tissues during heart development. Wnt signalling is divided into a canonical b-catenin dependent pathway and other non-canonical b-catenin independent pathways. During heart development, wnt/b-catenin signalling is known to inhibit terminal differentiation of cardiomyocytes while non-canonical Wnt/JNK and Wnt/PKC pathways are essential for formation of myocardial tissue. Simultaneously Wnt/b-catenin signalling is necessary for endocardial cushion development and thus valve formation, neural crest development and cell-cell contact fromation. Dysregulation of Wnt pathways leads to malformation of the embryonic heart. In the adult heart Wnt signalling is associated with cardiac hypertrophy. Cardiac hypertrophy is accompanied by an increased Wnt expression and thus higher concentration of b-catenin. Wnt signalling has also been shown to be involved during cardiac remodelling after injury. Insulin-like growth factor 1 (IGF-1) is a key regulator of metabolism, autophagy and cell survival (not only) in the heart. IGF-1 deficiency or insulin resistance are associated with dysregulation of calcium signaling, heart failure and cardiohypertrophy (p.e. caused by obesity or diabetes mellitus) while an increase in IGF-1 activity is known to improve heart function. IGF-1, just like Wnt signaling, is necessary for proliferation of cardiomyocytes. In this context we analysed a potential crosstalk and interregulation between IGF and Wnt signalling. We generated a dynamical network model of Wnt and IGF pathways from natural language statements of local interactions found in literature using the Boolean paradigm. Boolean networks can be regarded as the most basic type of dynamic networks. They consist of On/Off-rules for every node of the network. Analysis of Boolean networks results in attractors - steady states that correlate with phenotypes. With this Boolean network we are now able to simulate the interactions between the IGF and Wnt pathways and answer questions regarding the knock-down of compounds.

# Modelling the Functional Impact of KCNA5 Mutations on the Electrical and Mechanical Activities of Human Atrial Cells

S23

Haibo Ni, Michael A. Colman, Henggui Zhang

Biological Physics Group, University of Manchester
Manchester, UK

**Introduction:** Atrial fibrillation (AF) is the most common sustained cardiac arrhythmia in the developed world. Lone-AF is associated with inherited genetic mutations. A recent study identified six mutations in the KCNA5 channel (encoding for the ultra-rapid potassium current, $I_{Kur}$) associated with lone-AF. However, the impact of the mutations on electro-mechanical function is unclear. In this study, we use a coupled electro-mechanical model of the human atrial action potential to investigate this functional impact.

**Methods:** The formulation of $I_{Kur}$ in the previously developed atrial model was updated to fit the data for control and the six mutations. A myofilament model was then updated and incorporated into the atrial model to replicate experimental data regarding the force-$Ca^{2+}$ relationship. Electrical feedback was introduced by incorporating the stretch-activated current, $I_{SAC}$. The functional impacts of the KCNA5 mutations were evaluated by modelling the isometric and isotonic stretch tests.

**Results:** All mutations demonstrated marked effects on the contraction forces. Loss-of-function mutations prolonged action potential durations (APD), increased the magnitude of calcium transients and promoted contraction. Gain-of-function mutations demonstrated more complex behaviour due to the complex $I_{Kur}$ dynamics and action potential effects. All gain-of-function mutations resulted in reduced force and shortening, despite prolonging the APD in some cases. In isometric simulations, inclusion of $I_{SAC}$ prolonged APD for the gain-of-function mutations, whereas it had small effects on the loss-of-function mutations. In isotonic simulations, activation of $I_{SAC}$ abbreviated APD in most cases.

**Conclusions:** The KCNA5 mutations exhibited heterogeneous effects on human cardiac electrical activities and contractile function through the effects on the magnitude and duration of the intracellular calcium transient; loss-of-function mutations promoted larger amplitude calcium transients and therefore greater shortening whereas gain-of-function mutations reduced calcium transients and cellular contraction. Furthermore, it was demonstrated that $I_{SAC}$ played an important role in modulating action potential and calcium transient.

# Simulation of Re-entrant Wave Dynamics in a 2-D Sheet of Human Ventricle with KCNJ2-linked Variant 3 Short QT Syndrome



Kuanquan Wang*, Cunjin Luo, Yongfeng Yuan, Weigang Lu and Henggui Zhang

China

**Aims:** Recent studies suggested that short QT syndrome (SQT) is liable to cause malignant ventricular arrhythmia possibly due to high-frequency re-entrant waves (rotors). Our goal was to study the dynamical behaviours of rotors associated with a KCNJ2-linked variant 3 short QT syndrome (SQT3).

**Methods and results:** We utilized a two-dimensional (2-D), heterogeneous, isotropic sheet (10 × 6 cm2, consisting of 500 × 300 nodes, ENDO: M: EPI=25%: 35%: 40%) model of human ventricular tissue to create a short QT syndrome substrate. Electrical action potential of each node was simulated by the ten Tusscher et al. model (TNNP2006), which was modified to incorporate changes of Ik1 based on experimentally observed data of Kir2.1 function, including wild type (WT), heterozygous (WT-D172N) and homozygous (D172N) scenarios. Rotors were initiated by the standard S1-S2 stimulation protocol, with a coupling time interval of 410 ms, 380 ms and 360 ms for the WT, WT-D172N and D172N condition respectively (the stimulation duration of the S2 was 3 ms. Furthermore, we tested the minimal length of the S2 stimulus which provided a sufficient substrate for maintaining rotors. It was shown that WT-D172N and D172N mutant Ik1 led to abbreviated APD and ERP, resulting in a reduced minimal length of the S2 stimulus to sustain re-entry. The computed minimal S2 length was ~7.16 cm, ~6.28 cm, ~5.84 cm for WT, WT-D172N and D172N respectively. It was also shown that re-entrant waves broke up under the mutation conditions, implicating a transition from ventricular tachycardia to ventricular fibrillation, due to an increased functional heterogeneity of electrical properties of the tissue.

**Conclusion:** Due to an increased Ik1 arising from the SQT3 Kir2.1 mutation, the simulated rotors can be more easily initiated and sustained as compared to the WT condition in a 2-D model of the human ventricle. The simulated rotors in the mutation condition also breaks up, forming complex multiple wavelets. These simulation results provide novel insights into the ionic bases of an increased incidence of ventricular fibrillation, which may cause sudden cardiac death.

# The Effect of Random Cell Decoupling on Electrogram Fractionation near the Percolation Threshold in Microstructural Models of Cardiac Tissue

S23

Marjorie Hubbard* and Craig Henriquez

Duke University
Durham, United States

Random clusters of decoupled cells caused by cell death in diseased cardiac tissue can increase structural heterogeneity and give rise to abnormal patterns of propagation; however, the relationship between the underlying cardiac microstructure and the pattern of wavefront activation as the substrate transitions from well-connected to disconnected is poorly studied. The objective of this study was to use computer models of adult monolayers to study the effect of increasing the fraction of decoupled cells on wavefront propagation and electrogram fractionation at the microscale level. Two-dimensional 0.6 cm x 0.6 cm microstructural computer models (dx=10 μm) of ventricular monolayers that incorporated discrete, uniformly distributed gap junctions (gj) were randomly generated. A fraction of individual cells (~100um x30 um) between 0 and 0.60 were randomly decoupled. The LRD membrane model of guinea pig cardiac cells was used to represent the ionic properties. The tissue was stimulated along the left longitudinal axis or along the bottom transverse axis. Unipolar electrograms were measured at 25 distinct sites using point electrodes at the center of the tissue. As the fraction of decoupled cells increased, the pattern of propagation shifted from a plane wave to localized sites of retrograde propagation as the wave traveled around clusters of decoupled cells. Near the percolation threshold of 0.40, wavefront propagation in the cardiac tissue substrate became more tortuous at the microscale level resulting in conduction delays and wavefront microcollisions that manifested as fractionation and asymmetry in unipolar electrograms. The degree of fractionation was correlated not only with the dimensions of the decoupled cluster but also with the zig-zag pattern of decoupled cells near the recording electrode. Analysis of electrogram morphology may be useful for identifying regions of tissue near the percolation threshold that may be vulnerable to long conduction delays and wavefront reentry.

# Computational Modeling Supports Induced Pluripotent Stem Cell-derived Cardiomyocytes Reliability as a Model for Human LQT3



Michelangelo Paci*, Stefano Severi and Jari Hyttinen

Tampere University of Technology
Finland

Long QT 3 (LQT3) is a specific LQT syndrome, induced by defects in the SCN5A gene, encoding for the Na+ channels. Its effect is a Na+ current (INa) gain-of-function, resulting in a sustained late current and in an action potential (AP) duration (APD) prolongation. LQT3 can cause lethal cardiac events in resting condition or sleep. We developed a computational model of LQT3 in human induced pluripotent stem cell-derived cardiomyocytes (hiPSC-CMs) based on recent data (Ma et al. 2013), showing how hiPSC-CMs represent a promising in-vitro model for this pathology. Data include the INa (i) I/V curve, (ii) steady state activation and inactivation, (iii) recovery from inactivation and (iv) late INa measurements. Specifically, LQT3 shifts the steady state inactivation towards positive potentials and speed the recovery from inactivation, resulting in an increment of the sustained Na+ current (~5-folds). We used these data to develop a control and a LQT3 AP models. The control model showed (simulations vs experiments) (i) AP amplitude: 94.0 VS 86.0+/-1.4 mV, (ii) maximum diastolic potential: -64.0 VS -61.4+/-1.4 mV, (iii) APD90: 458.3 VS 434.0+/-31.1 ms, (iv) rate of spontaneous beating: 67.6 VS 69.1+/-11.3 bpm. In simulations, the LQT3 INa induced the experimentally observed AP changes: APD30(+26.5%), APD50(+33.4%), APD70(+41.5%), APD90(+32.4%) prolongation and slower rate (-33.0%). Moreover, we used our model to simulate mexiletine effects by reproducing the experimental reduction of the sustained INa: the consequent simulated APD90 shortening (-16.0%) is in agreement with the experiments (~-20%). Finally, by simulating a 5-fold INa late increment in the O'Hara-Rudy adult model we got APD prolongations similar to those reproduced by our LQT3 model, APD30(+30.9%), APD50(+33.6%), APD70(+34.1%) and APD90(+30.2%). Our results show that hiPSC-CMs and computational models derived from their electrophysiological traces represent in-vitro and in-silico models comparable to adult cardiomyocytes for LQT3, suitable for personalized studies on this pathology.

## Contribution of developmental changes in energy metabolism to excitation-contraction coupling of the ventricular cell: a simulation study

S23

Hitomi Sano*, Tamami Toki, Yasuhiro Naito and Masaru Tomita

Keio University
Japan

The heart develops and gains new functions while continuously pumping blood, and heart abnormalities during the early developmental stages progress to congenital heart malformations; therefore, the developmental program of the heart, including the expression of the genes responsible for various ionic channels, is likely to be tightly regulated. Here, we integrated developmental changes in 1) ionic systems and 2) energy metabolism on the basis of the mathematical models. 1) The quantitative changes in individual ionic systems were represented as relative current densities. We switched the relative current densities of 9 ionic components between early to late embryonic stages in the Kyoto model, and showed that the increase in inward rectifier current before the disappearance of funny current was predicted to result in abnormally high intracellular Ca(2+) concentrations. 2) The developmental changes in glycolytic enzymatic activities and those in concentrations of glycogen and total creatine were implemented accordingly to the model to represent specific stages in development. We then simulated effects of hypoxic condition to dynamic changes in contractile force and ATP concentration. As a result, our model showed that the fetal ventricular cells maintained ATP for longer periods of time than the adult ventricular cells, which is consistent with the reported dynamics of the ventricular cells under hypoxic condition.

# Point Process Heartbeat Dynamics Assessment of Neurocardiogenic Syncope in Children

Digna González-Otero, Ronald G. García, Gaetano Valenza, Laura M Reyes, Riccardo Barbieri

Massachusetts General Hospital - Harvard Medical School, Boston, USA
University of the Basque Country (UPV/EHU), Bilbao, Spain



**Introduction:** Neurocardiogenic syncope (NCS) is the most common cause of unexplained syncope in children. Mechanisms that lead to syncope are still unclear. For this reason, we have applied an inhomogeneous point-process model to estimate instantaneous heartbeat dynamics during a head up tilt table test (HUT) leading to syncopal events in children.

**Methods:** Twenty-six children with history compatible with NCS and a positive HUT were included in the study. ECG and blood pressure signals were recorded during rest and during the diagnostic HUT. A decrease $> 30\%$ of the median systolic blood pressure during HUT compared to rest was selected as the onset of the syncopal event. ECG peak detection and ectopic beat correction were performed with in-house software. The time between R-wave events was modeled using a history-dependent inverse Gaussian. A point-process framework was applied to compute measures for heartbeat dynamics for each subject independently and averaged across subjects. We tested for significant changes in these measures in the 6 minutes previous to the syncopal event.

**Results:** Our results confirmed previous findings of autonomic changes with HUT as well as time varying evolution of spectral HRV indices before syncope. In addition, the mean of the heart rate probability density function, $\mu_{HR}$, and the scale parameter of the RR interval probability density function, $\xi_0(t)$, computed by the point process were the only indices with statistically significant changes prior to syncope.

**Conclusions:** Our study is the first in reporting a continuous estimation of autonomic indexes during HUT in children with NCS. The point process framework also provided unique novel features associated with the statistical properties of heartbeat generation that could be critical to predict and explain the occurrence of syncope.

# Lower Instantaneous Entropy of Heartbeat Dynamics Characterizes Cognitive Impairment in Parkinson's Disease

S24

Riccardo Barbieri*, Gaetano Valenza, Luca Citi, Maria Guerrisi, Stefano Orsolini, Carlo Tessa, Stefano Diciotti and Nicola Toschi

United States

**Introduction:** While the classical hallmarks of Parkinson's disease (PD) are motor symptoms that include resting tremor, balance problems, limb rigidity, bradykinesia and gait abnormalities, it has been estimated that the incidence of cognitive deficits in PD, ranging from Mild Cognitive Impairment (MCI) to frank dementia, is six-fold compared to that in the general population. PD involves postganglionic sympathetic failure and, in 25% of patients, autonomic failure, and we have previously demonstrated that the complexity of autonomic dynamics is altered in PD patients vs. healthy controls. In this paper we investigate the relationship between instantaneous autonomic complexity and cognitive impairment in PD.

**Methods:** Physiological signals were recorded from 16 PD patients, 8 cognitively preserved (PD_NC, 4M/4F, age 68.67 +/- 3.05 years), and 8 with mild cognitive impairment (PD_MCI, 6M/2F, age 64.15 +/- 5.91 years). Subjects were placed horizontally in a supine position during the entire recording (600 s). We computed mean values (over the whole recording period) of conventional heart rate variability (HRV) features as well as of novel instantaneous point process Approximate and Sample Entropy (ipApEn and ipSampEn, respectively) and tested for significant effects of group (PD_MCI vs. PD_NC) using nonparametric statistics after regressing out the effects of age and gender using a general linear model.

**Results:** All conventional HRV features were highly nonsignificant between the PD_MCI and PD_NC groups. Standard ApEn and SampEn were also nonsignificant ($p=0.23$ and $p=0.50$ respectively). Conversely, ipApEn was lower ($p=0.065$) and ipSampEn was significantly lower ($p<0.05$) in PD_MCI vs. PD_NC (ipApEn: 0.211 +/- 0.075 vs. 0.403 +/- 0.027; ipSampEn: 0.134 +/- 0.092 vs. 0.372 +/- 0.038).

**Conclusions:** Our results suggest that cognitive impairment in PD is associated with a decrease in heartbeat complexity, possibly pointing toward subtle autonomic changes (not detected by conventional HRV) which accompanying the initial stage of cognitive impairment in PD.

# Analysing Cardiac Aautonomic Neuropathy in Diabetes using Electrocardiogram-derived Systolic-diastolic Interval Interactions



Mohammad Hasan Imam*, Chandan Karmakar, Ahsan Khandoker, Herbert F Jelinek and Marimuthu Palaniswami

University of Melbourne
Melbourne, Australia

Systole and diastole are the fundamental periods of the cardiac cycle and their relative duration is used to evaluate heart function in various physiological and pathological conditions. In clinical practice, systolic-diastolic interval is generally measured using echocardiography. However, recent studies have shown that the QT and TQ intervals of the electrocardiogram (ECG) signal can be used as surrogate systolic and diastolic intervals respectively and the ratio of beat-to-beat QT-TQ intervals can be used as the systolic-diastolic interval interaction (SDI) parameter. In this study, we propose a new parameter, beat-to-beat TQ-RR ratio, to investigate the SDI. Performance of both QT-TQ and TQ-RR based SDI measures were analyzed using a case study to detect and monitor the progression of cardiac autonomic neuropathy (CAN) in diabetes. ECGs recorded in supine resting condition of 72 diabetic subjects with no CAN (CAN-) and 70 diabetic subjects with CAN were analyzed in this study. Fifty-five subjects of the CAN group had early level of CAN (ECAN) and 15 subjects were at the severe or definite stage of CAN (DCAN). The results show that variability of the TQ-RR based SDI measure can significantly ($p<0.001$) differentiate all three groups (CAN-, ECAN and DCAN) and the level of CAN. In contrast, the variability of the QT-TQ based SDI measures showed significant difference only between CAN- and DCAN groups. This result suggested that TQ-RR based SDI analysis was more sensitive in tracking progression of CAN than the QT-TQ based approach, which is crucial for the early detection of CAN.

## Long-term HRV in critically ill pediatric patients: comma versus brain death.

S24

Ana Paula Rocha, Rute Almeida, Argentina Leite, Marta João Silva, Maria Eduarda Silva

CMUP, Porto University
Porto, Portugal

Dysfunctions of the autonomic nervous system in critically ill patients with acute brain injury (ABI) lead to changes in Heart Rate Variability (HRV) which appear to be particularly marked in patients subsequently declared in brain death (BD). Although the study of HRV series may be useful in differentiating the progression of the individual patient disease process, its clinical applicability has not yet been established. HRV series are non-stationary, exhibit long memory in the mean and time-varying conditional variance, characteristics that are well modelled with Fractionally Integrated AutoRegressive Moving Average (ARFIMA) models with Generalized AutoRegressive Conditional Heteroscedastic (GARCH) errors. The long memory is estimated by the parameter $d$ of the ARFIMA-GARCH model, whilst the time-varying conditional variance parameters, $u$ and $v$ characterize the short-range and the persistence, respectively, in the conditional variance. In this work, the ARFIMA-GARCH approach is applied to HRV series of 15 pediatric patients with ABI admitted in a pediatric intensive care unit: 6 patients for which BD has been confirmed; 9 patients Survived (S).

Previous analysis of HRV series for normal subjects indicate that during sleep, the values for $d$,$u$,$v$ (mean + 3 std) are 0.5, 0.4 and 0.8, respectively. For S and BD groups, the percentage of beats with $d > 0.5$ are ($mean \pm std$): ($45.05 \pm 22.88$) and ($77.77 \pm 14.63$), respectively. The corresponding results for $u > 0.4$ and $v > 0.8$ are: S ($13.40 \pm 9.79$), BD ($36.66 \pm 18.99$) and S ($22.98 \pm 11.43$), BD ($10.77 \pm 9.13$). Additionally, the percentage of beats with $u > v$ was obtained: S ($27.22 \pm 14.69$), BD ($51.77 \pm 15.89$). For patients in BD $d$ and $u$ increase, while $v$ decreases for this group. Statistically significant differences between groups were found applying the Wilcoxon rank sum test for all 4 percentages (5% level).

The long memory and time-varying conditional variance parameters estimated by ARFIMA-GARCH modeling seem able to contribute to characterize disease severity in ABI children.

# Automated Selection of measures of Heart Rate Variability for Detection of Early Cardiac Autonomic Neuropathy



David J Cornforth, Mika P Tarvainen and Herbert F Jelinek*

Charles Sturt University
Australia

Heart rate variability (HRV) analysis begins with the relatively non-invasive and easily obtained process of ECG recording, yet provides a wealth of information on cardiovascular health. Measures obtained from HRV use time-domain, frequency-domain and non-linear approaches. These measures can be used to detect disease, yet from the large number of possible measures, it is difficult to obtain an objective method to select which measures provide the best separation between disease and health. This work reports on a case study using a variety of measures to detect the early stages of Cardiac Autonomic Neuropathy (CAN). CAN affects the correct operation of the heart and in turn leads to associated co-morbidities. We examined time-domain measures including the standard deviation of the RR interval, pNN50, triangular interpolation of the interval histogram (TINN), parameters of the Poincaré plot; frequency domain measures including the peak and sum of components at low and high frequencies, and non-linear measures such as sample entropy and Renyi entropy. In all, 81 variables were extracted from the RR interval time series. We applied machine learning methods to separate participants with early CAN from healthy aged-matched controls, while using a Genetic Algorithm to search the 81 variables for the subset that provided the maximum separation between these two classes. Results show good discrimination of early CAN from normal patients using a range of variables based only on measurement of the RR interval or heart rate. Using a reduced feature set selected using a Wrapper algorithm and GA, the best performance was found for the Support Vector classifier. This gave a correct classification of up to 70% of unseen data.

## Coupling Between Short-Term Heart Rate and Diastolic Period is Reduced in Heart Failure Patients as Indicated by Multivariate Entropy Analysis

S24

Peng Li, Lizhen Ji, Chang Yan, Ke Li, Chengyu Liu* and Changchun Liu

Shandong University
China

The analyses of cardiac dynamics appear to be very promising in assessing the cardiovascular health. Short-term analysis well meets the increasing clinical needs for point-of-care diagnosis, portable monitoring, personal healthcare, etc. In one of our previous CinC articles, we have proved that there is a inherent coupling between short-term heart rate variability (HRV) and diastolic period variability (DPV). Besides, the coupling is reduced at their small temporal scales in healthy aging subjects. We thus aimed to investigate the HRV–DPV coupling in heart failure (HF) patients in this work. Fifty healthy volunteers and 52 HF patients were studied. Multiscale multivariate fuzzy entropy (MMFE) analysis was performed in each bivariate signal (short-term HRV and simultaneous recorded DPV) to probe into the their within- and cross-channel correlations. Results show that the coupling between short-term HRV and DPV is reduced at both small and large temporal scales in HF patients compared with healthy volunteers. It should probably indicate that the cardiac loses both the immediate mechanical response to the changes of heart period and its long-range compliance, which is very different from the effects of healthy aging. It thus show great potential of short-term HRV–DPV coupling analysis in the noninvasive and nondestructive detection of HF. An increased specificity of the so-constructed HF detection indices should also be expected.

# Volumetric Identification of Left Atrial Fibrosis from Delayed Enhancement Magnetic Resonance Imaging: Preliminary Results

Roberta Leonardi, Federico Veronesi, Stefano Severi, Cristiana Corsi

DEI, Cesena Campus, University of Bologna
Bologna, Italy



Delayed gadolinium enhancement magnetic resonance (DE-MR) imaging can be used for in vivo detection of left atrium (LA) fibrosis and scarring, whose identification is important for atrial fibrillation (AF) treatment. This study presents a new tool for 3D visualization of cardiac LA fibrosis based DE-MR imaging and its qualitative validation by comparison with electro-anatomic mapping (EAM), currently considered the gold standard for fibrosis evaluation. Angio-MR (MRA) and DE-MR images were acquired and registered applying a multimodality affine transformation. Automatic left atrium segmentation from MRA images was obtained applying a 2D segmentation method based on the intra-class variance minimization and a density-based spatial clustering. Gray level intensities of DE-MR images in a fixed thickness around the LA, were used as texture for the LA 3D surface model (figure, panel A). To better visualize regions with fibrosis on the LA surface a color map was used (figure, panel B) and the result was compared with the 3D bipolar voltage maps measured with an EAM system (Ensite Velocity, St. Jude Medical Inc.). An example of the qualitative comparison between our 3D LA fibrosis map and the corresponding electro-anatomic map is shown in the figure (panel B and C). The comparison in 4 patients, pre and post AF ablation, between the maps of fibrosis from MR and the EAM confirmed the qualitative correspondence between the low-potential areas and the high-enhanced areas showing LA fibrosis in DE-MR. Preliminary results on volumetric visualization of LA fibrosis based on DE-MR and MRA data processing have shown promising results and simply thresholding our color-coded map could lead to a fast 3D quantification of LA fibrosis location and extent.

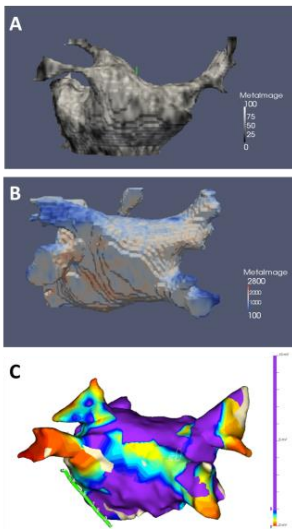

# A Practical Algorithm for Improving Localization and Quantification of Left Ventricular Scar

Brian Zenger*, Joshua Cates, Alan Morris, Eugene Kholmovski, Alexander Au, Ravi Ranjan, Nazem Akoum, Chris McGann, Brent Wilson, Nassir Marrouche, Frederick Han and Rob MacLeod

University of Utah
United States

S31

Current automated algorithms for left ventricular (LV) segmentation and scar detection use atlas-based and computationally costly approaches with variable accuracy. For this study we evaluated whether a semi-automated, LV segmentation and scar quantification method would improve the accuracy and speed of LV segmentation and scar detection. We obtained a high-resolution magnetic resonance angiogram (MRA) and late-gadolinium enhanced magnetic resonance imaging (LGE-MRI) 1.5 Tesla (T) or 3T scan (Siemens Healthcare, Malvern, PA) in 14 pa-tients who had ventricular scar from a prior myocardial infarction (MI). We used (1) a combination of the MRA and LGE-MRI to segment the myocardi-um and (2) an automated signal intensity algorithm (Otsu method) to charac-terize ventricular scar compared to two blinded, expert observers. We as-sessed accuracy of the LV segmentation by comparing the semi-automated method to the manual segmentation in 5 patients. The scar detection algo-rithm was evaluated in patients with MI scar and compared to observer val-ues. Comparison of segmentation approaches trended towards increased efficiency using the semi-automated method (mean semi-automated = 46 min ± 8.9 mean; manual = 50.6 min ± 7.5, NS). The LV geometry using the semi-automated method had a high degree of correlation with the manual segmen-tation images (88.1% overlap ± 2.9). The ventricular segmentation scar vol-umes (7.0 ± 5.8 cm3) obtained with the Otsu method correlated with the scar volumes obtained by manual segmentation (7.13 ± 6.49 cm3) (r2=0.95). Our results confirm that our semi-automated LV segmentation and scar detection method has a high degree of accuracy while showing a trend towards increased time efficiency. Three-dimensional segmentation of ven-tricular scar that does not require atlases holds promise for integration into future research for ventricular tachycardia ablation and risk stratification of sudden death. Ongoing studies will determine the best parameters using this pipeline to ensure faster segmentation times while maintaining quality.

# Fully Automated Assessment of Left Ventricular Volumes, Function and Mass from Cardiac MRI

Marco Marino, Federico Veronesi, Giacomo Tarroni, Victor Mor-Avi, Amit R. Patel, Cristiana Corsi

University of Bologna, Bologna, Italy and University of Chicago, Chicago, Illinois, U.S.A.



**Background.** The importance of quantification of left ventricular (LV) size, function and mass is increasingly recognized through growing evidence about the prognostic value of these indices in a variety of pathologies and their diagnostic role in follow up of patients during therapy. However, quantitative evaluation from cardiac magnetic resonance (CMR) images relies on manual tracing of LV endo- and epicardial boundaries, which is subjective and time-consuming. Accordingly, our goal was to develop a fully automated technique for the detection of LV endo- and epicardial boundaries from CMR images to assess LV volumes, ejection fraction (EF) and mass.

**Methods.** Our fully automated approach consists of the following steps: 1) identification of the LV cavity based on the detection of moving and circular structures; 2) endocardial detection using a region-based probabilistic level set model to allow volume measurement throughout the cardiac cycle; 3) epicardium detection at end-diastole based on an edge-based level set model to allow LV mass measurement. This approach was tested on short-axis CMR images obtained in 10 patients (8-14 slices per patient, 30 frames per cardiac cycle). The automatically detected myocardial borders (total 110 slices) were compared with manual tracing by an experienced cardiologist on end-diastolic (ED) and end-systolic (ES) frames using standard similarity metrics. Linear regression and Bland-Altman analyses were used to validate LV volumes, EF and mass measurements derived from these borders.

**Results.** Automated detection of the endo- and epicardial boundaries took <5 minutes per patient on a standard PC. The detected boundaries were in good agreement with manual tracing (figure): Dice coefficient =0.92±0.07, Jaccard index =0.86±0.11 and Hausdorff distance =1.8±0.38 mm. As a result, LV volumes, EF and mass showed good inter-technique concordance, reflected by minimal biases and narrow limits of agreement (table).

**Conclusions.** The proposed technique allows fully automated, fast and accurate measurements of LV volumes, EF and mass from CMR images, which may address the growing clinical need for quantitative assessment.

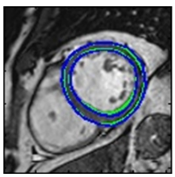

Automated detection — Manual tracing

| | Bias | Bias (% of Mean) | 95% LOA |
|---|---|---|---|
| **EDV** | -7.5 ml | 4.1% | -22 ÷ 7 ml |
| **ESV** | -3 ml | 3.4 % | -23 ÷ 17 ml |
| **EF** | 0.18 % | 0.35 % | -10 ÷ 11 % |
| **Mass** | -8.4 g | 7.4 % | -24 ÷ 7.1 g |

## Quantitative Evaluation of Myocardial Ischemia by Cardiac Magnetic Resonance Imaging

Siyi Huang*, Jingwei Pan, Lin Yu, Xin Yang and Meng Wei

the sixth Shanghai People's hospital affiliated to Shanghai Jiao Tong University
China

S31

The objective of this study was to evaluate the significance of transmural gradient perfusion (TGP) method with 3.0T MRI to detect coronary artery disease (CAD). Traditional quantitative analysis of transmural myocardial perfusion, such as myocardial blood flow (MBF) and relative myocardial perfusion reserve (MPR), neglects the fact that subendocardium is more vulnerable to ischemia than subepicardium. TPG and relative TPG reserve (TPGR) can take the inhomogenous perfusion impairment in account and should be useful for CAD diagnosis. 44 patients(35 men, age 61.5±7.8 years) with known or suspected CAD underwent adenosine-stress CMR scan. Quantification of myocardial perfusion was based on exponential model by deconvolution technique. Quantitative coronary angiography (QCA) was measured in all main coronary arteries and ≥70% QCA stenosis was considered anatomically significant. MBF and relative MPR of both subendocardium (MBF: 1.41±0.42 vs 1.90±0.36, p = 0.002; relative MPR: 0.69±0.24 vs 1.02±0.23, p < 0.001) and transmural myocardium (MBF: 1.67±0.49 vs 1.98±0.36, p = 0.038; relative MPR: 0.76±0.24vs 0.98±0.23, p = 0.001) reveled significant difference between impairment perfusion territories and normal territories while there was no difference in same analysis of subepicardium. The TPG (0.72±0.14 vs 0.95±0.18 P <0.0001) and relative TPGR (0.82±0.13 vs 1.09±0.11 P <0.0001)) also showed significant difference between ischemia and normal territories. Sensitivity and specificity for CAD diagnosis were 82.14%/ 81.15% and 89.66%/ 92.00% for TPG (cut-off 0.79) and relative TPGR (cut-off 0.95) respectively. Area under curve was 0.87 for TPG and 0.94 for relative TPGR. Relative TPGR yielded significantly better sensitivity and specificity of CAD diagnosis compared to MBF, relative MPR and TPG (P<0.0001) and appeared to be the most meaningful parameter to detect anatomical significant CAD.

# The Maximum Electrical Fields in the Implant Regions of Implantable Cardiac Rhythm Devices for the Worst Case RF Heating during MRI Scans in 1.5 T

Dawel Li, Xiaoyi Min*, Shiloh Sison and Ji Chen

University of Houston
United States

S32

MRI scans have been contraindications for patients with pacemakers or ICDs due to safety reasons. Induced currents along the leads due to radio frequency (RF) fields during MRI scans pose high risks for causing direct rapid cardiac pacing and heating in the tissue. The ISO/IEC Joint Working Group (JWG) has developed the tiered approaches to establish the worst case RF heating conditions for active implantable devices utilizing computer simulations. Lower in tier, the more stringent is the criteria amongst the four tiers. The tier 2 utilizes the maximum electric field over 10 gram average (max E) in the implant regions. We evaluated the applicability of the ISO/IEC JWG tier 2 approach to implantable cardiac rhythm devices in five human body models of obese male (Fats), adult male (Duke), adult female (Ella), girl (Billie), and boy (Thelonius). The SEMCAD software package was used to calculate the electric field distribution within five human subject models due to RF fields from high pass and low pass MRI birdcage coils. The simulation conditions also included body positions inside RF coils, tissue properties, loading positions and RF coil size etc. All the fields were averaged over 10 gram and scaled to 4 W/kg whole body SAR (IEC 60601-2-33) with a head SAR limit of 3.2 W/kg. The maxE values were obtained in the implant regions (vein, heart, left jugular, right jugular, left pectoral, and right pectoral region) extracted from the simulations. Results show that the max E in the heart was the minimum among the six regions (267.9 V/m). The highest max E was from left jugular region (639.4 V/m). The max E values in the sub regions could provide the worst RF heating criteria for small devices such as leadless pacers inside right ventricle etc.

# Cardiac Arrhythmia Discrimination Using Evolutionary Computation

JF Martín-García[a], I Mora-Jiménez[a], A García-Alberola[b], JL Rojo-Álvarez[a]
[a] Signal Theory and Communications Dept., Rey Juan Carlos University, Spain
[b] Arrhythmia Unit, Virgen de la Arrixaca Hospital, Murcia, Spain

S32

**Background.** The use of Implantable Cardioverter Defibrillators (ICD) for cardiac arrhythmia treatment implies a search for efficiency in terms of discrimination quality and computational complexity.

**Materials and Methods.** Evolutionary computation is a discipline emulating natural mechanisms as a means of achieving the solution of a problem. It is characterized by a population of individuals (possible solutions) which evolve generation after generation to provide fitter solutions. Genetic programming (GP) was chosen here to discriminate between ventricular and supraventricular tachycardia (VT/SVT) because GP solutions, coded as decision trees, can be both computationally simple and clinically interpretable.

We considered electrograms (EGM) from episodes registered by ICDs in spontaneous/induced tachycardia, previously classified as VT/SVT by clinical experts. Data were 38 real-valued samples, arranged as the concatenation of two beat segments (Fig. 1): a sinus rhythm template immediately previous to the arrhythmic episode (19 samples, basal reference), and the arrhythmic episode template.

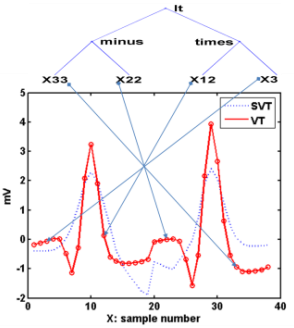


Fig.1. Best tree found, confronted with related samples, SVT:= (X33-X22)<(X12*X3). Plotted signals resemble medians for SVT/VT templates.

**Results**. Episodes from six Spanish healthcare centers were considered for application of GP with populations of 100 individuals. Training set (used for classifier design) was composed by 38 SVT-68 VT episodes from 16 patients with ICD, whereas the test set (used for evaluation) was composed by 284 SVT-1057 VT episodes from 28 patients. Many low complexity solutions yielded error probabilities around 5%, and some of them allowed physiological interpretation. The best tree found (Fig. 1) yielded an error probability of 1.8%, with both sensitivity and specificity above 98%. This solution compared two samples from the end of the arrhythmic pulse with another two samples from the sinus rhythm, pointing out to a relevant discrimination role of the lasting EGM, which had not been suggested until now in the literature.

**Conclusion.** Qualitative analysis of several solutions shows that, besides the ventricular activation onset, the end also carries relevant information for VT-SVT discrimination.

# A Morphology-Based Spatial Consistency Algorithm to Improve EGM Delineation in Ventricular Electroanatomical Mapping

Alejandro Alcaine*, David Soto-Iglesias, David Andreu, Juan Acosta, Antonio Berruezo, Pablo Laguna, Oscar Camara, Juan Pablo Martínez

BSICoS Group, I3A, Universidad de Zaragoza.
Zaragoza, Spain.



**Aims:** Activation mapping (AM) using electroanatomical mapping systems help to guide catheter ablation treatment of common arrhythmias. In focal tachycardias, the earliest activation area becomes the ablation target. Recently, a wavelet-based algorithm was proposed for automatic identification of bipolar electrogram (EGM) activation onsets. Under the assumption of a high-density mapping of the area of interest (AOI), we propose an EGM morphology-based spatially-consistent algorithm to improve AM.

**Materials:** We studied 15 electroanatomical maps (a total of 1763 mapping points) of patients with idiopathic ventricular outflow tract tachycardia admitted for ablation procedure at Hospital Clínic (Barcelona, Spain). Signal acquisition was made point-by-point at 1 kHz sampling frequency using the CARTO® system. Each mapping point consist of 2.5 seconds of 12-lead standard ECG and bipolar EGM signals.

**Methods:** The algorithm begins by delineating each mapping point using a previously presented wavelet-based strategy. Then, it searches for previously analysed mapping points in a neighbourhood of the current one. Those neighbour points with similar morphology are grouped and aligned for checking if the detected activation onsets are synchronized up to a tolerance of $\pm$ 5 ms with the current one. If they are not synchronized, a weighted average EGM signal was delineated and the new identified onset is reassigned to the current mapping point and to each point of the neighborhood, compensating the delay between points.

**Results:** Evaluation was done by means of the difference between the automatic onsets with those manually obtained during the intervention by an expert technician. The algorithm modifies a total of 548 (31%) mapping points. Onset identification of those modified points by the presented algorithm reduces the difference from 5.1 $\pm$ 13 ms to 4.3 $\pm$ 11.6 ms.

**Conclusions:** The presented algorithm improves AM by averaging spatially close and morphologically similar EGMs for better identification of the AOI in catheter ablation treatments of focal ventricular tachycardias.

# Localization of the Latest-Activated Areas in the Ventricles from Body Surface Potential Maps

Jana Svehlikova[1], Mark Potse[2] , Milan Tysler[1]

[1]Institute of Measurement Science, SAS, Bratislava, Slovakia
[2]Center for Computational Medicine in Cardiology, Università della Svizzera italiana, Lugano, Switzerland

S32

Background: Identification of the latest depolarized site of the ventricles has information with direct clinical applicability for lead positioning in cardiac resynchronization therapy (CRT).

Method: The very last depolarization of the ventricles is reflected in the final part of the QRS complex in the ECG. In normal activation such areas are either on lateral sides at the base of both ventricles, or at the lateral base of one of them. It can be assumed that at the very end of the depolarization these areas are so small that their electrical activity can be approximated by one dipole. Therefore we computed the integral body surface potential map (IBSPM) of the 10ms time interval before the J point and used it as the input data for an inverse solution using one or two dipoles as the equivalent cardiac electric generator. We used the simulated IBSPMs of normal myocardial activation from two well-defined simulation codes: The first one was a normal male model in the simulation tool ECGSIM, the second was propag-4, a high-resolution reaction-diffusion model of the human heart and torso developed at Université de Montréal. The very last activated points in both ventricular models were known.

The IBSPMs for both models were computed for the Amsterdam 62-lead system. The possible location of the dipoles representing the very last activated area was searched in a 5mm grid within the modeled ventricular myocardium.

Results: In the first model the localization error of the single area on the lateral wall of the right ventricle was 2cm. In the second model two areas on lateral sides of both ventricles were localized with an average error of 2.4cm (2.9 and 1.8cm resp.).

Conclusions: The proposed method seems promising for the preliminary noninvasive assessment of the latest-activated ventricular areas, which are of great interest for CRT.

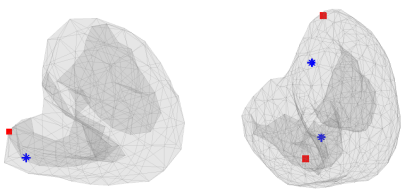

Centers of the very last depolarized areas (red dots) vs. inverse solutions (*) for both heart models.

# Comparison of Different Methods and Catheter Designs to Estimate the Rotor Tip Position – A Simulation Study

Markus Rottmann, Matthias W. Keller, Tobias Oesterlein, Gunnar Seemann, Olaf Dössel

Institute of Biomedical Engineering, Karlsruhe Institute of Technology, Karlsruhe, Germany



Aims: The detection of reentry patterns, such as rotors, is an unsolved task in the context of the therapy of atrial arrhythmias. The aim of this work was the analyzing of typical signal characteristics near a rotor center, the comparison of different features, maps and virtual catheters to estimate the rotor center.

Methods: Rotors were simulated on a 2D patch geometry (100mm x 100mm x 1mm) with spatial resolution of 0.1mm. For simulations the finite difference method and the parallel solver acCELLerate were used and extracellular signals were obtained by forward calculation. Based on extracellular potentials, different features were evaluated: Local activation time, peak to peak amplitude, steepest negative slope and approximate entropy were compared regarding their ability to indicate the rotor tip location. Furthermore, typical signal patterns of virtual mapping catheters (PentaRay and Inquiry Optima) centered at the rotor tip position were analyzed.

Results: Due to the limited coverage of the circular catheter, centered at the rotor tip position, the virtual PentaRay catheter provided more informations about amplitude changes. The tracked rotor center determined by phase singularity moved in an area (2.7mm x 6mm). Maximum distances between the focal point of phase singularities and estimated centers by the peak to peak amplitudes were 1.7 mm and between rotor centers estimated by the steepest negative slope 0.7 mm. The trajectory described by the maximum values of the approximate entropy showed a high degree of agreement with the phase singularities.

Discussion: In this simulation study rotor centers estimated by the peak to peak amplitudes and by the steepest negative slope are consistent with the referenced phase singularities. Also the approximate entropy might be a parameter to detect the rotor center. These results may perform assistance in clinical diagnosis in regarding of signal characteristics near a rotor center.

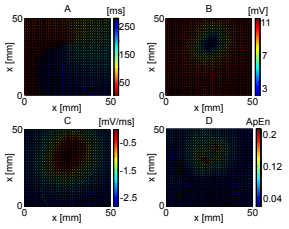


Map of: (A) LAT.
(B) Peak to Peak.
(C) Steepest negative slope.
(D) Approximate entropy.

# Analysis of the QRS Alterations during Stress Test Recordings on Patients with Brugada Syndrome

Daniel Romero*, Nathalie Behar, Alba Martín-Yebra, Juan Pablo Martínez, Pablo Laguna, Esther Pueyo, Guy Carrault, Philippe Mabo and Alfredo Hernández

Université de Rennes 1
France

S33

**Background:** Brugada syndrome (BrS) is characterized by the occurrence of syncope and sudden death due to cardiac arrhythmia in patients with apparently structural normal heart. To date, one supported hypothesis underlying the pathophysiological mechanism of Brugada ECG pattern is based on depolarization disorders.

**Methods:** A study population of 46 patients with suspected or diagnosed BrS was analyzed. Six patients presented clinical symptoms including VF/ACC or syncope (symptomatic group), 13 were diagnosed as having the syndrome, but did not present clinical symptoms (asymptomatic group), and in the other 27, the coved-type ECG pattern of BrS was not discovered under any diagnostic test (non-diagnosed group). Stress test ECG recordings acquired for all the patients were analyzed by evaluating a QRS-angle-based method during the entire duration of the test. Changes in the angles were measured as the difference between different stages of the stress test and its beginning and were statistically compared among the three patient groups.

**Results:** The R-wave angle showed the biggest changes in augmented leads aVL (11.9±10.9º) and aVR (7.9±11.7º) rather than in precordial leads at the time of maximum effort. A similar delta values were observed in both asymptomatic and non-diagnosed patient groups, but these were slightly different to the symptomatic group, in particular during the active (AR) and passive (PR) recovery phases. Statistically significant differences were found between symptomatic and asymptomatic groups in such phases (AR: p=0.0125, PR: p=0.0194 in aVR), but not between asymptomatic and suspected BrS subgroups (AR, p=0.2039, PR: p=0.5826).

**Conclusion:** This study shows that morphologic changes during depolarization induced by stress test are associated with the BrS, particularly during the recovery phases, which are characterized by an increased parasympathetic tone. This finding should be considered, in combination with the analysis of repolarization changes, in further studies to characterize the electrophysiological modifications on BrS patients.

# A New Phase Space Analysis Algorithm for the Early Detection of Syncope During Head Up Tilt Tests

Nadine Khodor*, Guy Carrault, David Matelot, Hassan Amoud, Nathalie Ville, Mohamad Khalil, Francois Carre and Alfredo Hernandez

University of Rennes 1
France

S33

**Aims:** Head Up Tilt Test (HUTT) is a well-established procedure, commonly used to diagnose syncope, which originates from a malfunction in the region of the nervous system that regulates heart rate and blood pressure. Here, we study the ability to automatically predict syncope and differentiate between positive and negative test groups, using only 12-min RR-interval time series for the supine position (6 minutes at rest and 6 minutes for controlled respiration at 0.25 Hz), preceding HUTT.

**Methods:** An original method, based on the analysis of heart rate variability dynamics and a combination of phase space (PS) analysis and kernel support vector machine (KSVM), is proposed. The dynamic behavior of the RR-interval time series was analyzed using phase space reconstruction (PSR). The embedding dimension (d) and time delay ($\tau$) of the PSR were determined using false nearest neighbor and mutual information methods. The normalized PS area is then divided into 1000 equal sized cells and the density matrix is obtained by computing the percentage of PS points in each cell. Cells, displaying a statistical difference (Mann-Whitney test), are used for further classification using KSVM.

**Results:** 66 subjects participated in the study and standard HUTT diagnosis criteria were used to identify negative and positive patients. Among them, 35 subjects developed a vasovagal syncope. Parameters d and $\tau$ were both estimated to 3 and the Gaussian kernel was optimized over the whole database. By applying a cross validation procedure repeated 10 times using only 1/3 of the population in the training step, we determined the capability of correctly classify positive patients. A sensitivity of 100% with a specificity around 50% were observed. PSR combined with KSVM demonstrate the interest to take into account the dynamics of the RR series and their capability to predict tilt test's outcome using only pre-HUTT data.

# Automatic Detection of ECG Lead-wire Interchange for Conventional and Mason-Likar Lead Systems

Chengzong Han*, Richard Gregg, Saeed Babaeizadeh

Advanced Algorithm Research Center
Philips Healthcare, Andover, MA, USA

S33

Misconnection of ECG lead-wires could generate abnormal ECG and erroneous diagnosis. In this work we developed an automatic lead-wire interchange detection algorithm that works equally well on either conventional or Mason-Likar (ML) electrode placement.

Our method is a decision tree classifier which uses beat morphology features including P-wave axis, P-wave vector loop rotation, QRS axis, and QRS vector loop rotation. These measurements are done automatically using Philips DXL ECG algorithm. The classifier was trained on a database (n=23,540) containing ECG recordings in conventional lead system from multiple clinical centers on patients with or without a known cardiac disease. Different lead-wire misconnections were simulated using ECG recordings with correct lead placement. The algorithm was evaluated on an independent database (n=1,439) which included both conventional and ML ECG recordings for each subject.

Defining a positive event as detecting lead reversal, the table below summarizes the algorithm performance in detecting lead-wire interchange in the evaluation database.

| | Conventional System | | Mason-Likar System | |
|---|---|---|---|---|
| Lead Swaps | Sensitivity (%) | Specificity (%) | Sensitivity (%) | Specificity (%) |
| LA-LL | 65.4 | 99.2 | 65.1 | 99.0 |
| LA-RA | 93.0 | 98.3 | 92.2 | 98.2 |
| RA-LL | 88.3 | 97.7 | 90.7 | 98.1 |

*LA: left arm; LL: left leg; RA: right arm*

There was no statistically significant difference ($P>0.05$, paired student's t-test) in algorithm performance between the conventional ECG and ML lead systems.

Evaluating on this unique ECG database which includes both conventional and ML ECGs for each subject, our morphology-based lead reversal detection algorithm showed similarly high performance for either lead system. Therefore, in practice, the same algorithm can be used with either setting without a need for a special configuration.

# A Multi-modal Apporach to Sleep-Wake Classification in Infants using Minimally Invasive Sensors

Gregory Cohen and Philip De Chazal*

University of Western Sydney
Sydney, Australia



As sleep/wake state classification is an important and widely used metric in evaluating infant health and in the detection and scoring of sleep apnea, there is a clear need for lower-cost and less invasive methods for the automated classification of sleep stages. In this study, we evaluate the potential of a combination of electrocardiogram (ECG), pulse-oximetry (SpO2) and actigraphy features in the automated classification of sleep state in infants. These sensors were chosen as they are far less invasive than the current gold-standard method based on electroencephalography (EEG) analysis and are also routinely used in the detection of sleep-related breathing disorders. Full overnight polysomnogram data from 396 infants was extracted from the National Collaborative Home Infant Monitoring Evaluation (CHIME) database along with hand-scored sleep state annotations. The CHIME database contains infant polysomnograms from four distinct screening categories; healthy infants, infants diagnosed with apnea, premature infants and siblings of SIDS infants and this study evaluates the performance of the system on each screening condition. A comprehensive artefact rejection step was performed on both the data and the annotations, after which time and frequency-based features were extracted. Combinations of these features were then used to train a linear discriminants classifier. The performance of the system was evaluated using a leave-one-out cross-validation scheme on the 396 recordings. When discriminating active sleep, quiet sleep and wake states we achieved an overall accuracy of 58.2% with a specificity of 62.59%, a sensitivity to active sleep of 81.58% and a sensitivity to quiet sleep of 33.49%. When discriminating sleep from wake states our system achieved an accuracy of 74.1%, a sensitivity of 60.9% and a specificity of 82.0%.

# Classification of sleep disordered breathing in the evaluation of acoustic sound in correlation with the ECG signal

Klaudia Proniewska[1], Krzysztof Malinowski[2], Elżbieta Pociask[1], Bartosz Proniewski[1]

[1]AGH University of Science and Technology, Krakow, Poland
[2]Krakow Cardiovascular Research Institute, Krakow, Poland

S34

**Aims:** The aim of the study was to investigate the predictive capability of a dual-modality analysis scheme for the detection of sleep disordered breathing, specifically for automatic detection of sleep disorders such as snoring, wheezing or sleep apnea in the evaluation of acoustic sound in correlation with the electrocardiography (ECG) signal during sleep.
**Methods:** Breathing sounds and ECGs of 15 study subjects with different degrees of disordered breathing were captured and analyzed. These source data provided a database of parameters that, after the statistical analysis and supported by the subjective sleep evaluation made by tests subjects, guided the system-supported sleep evaluation. In this work 5 ECG- and 29 acoustic-derived parameters were used. Two logistic regressions were proposed to show types of probabilistic statistical classification models where breathing events were divided into normal vs. all events and where just the disordered breathing was divided into severe snoring vs. other events. Using Akaike information criterion in conjunction with the analysis of receiver operating characteristic (ROC) curves (measure of area under curve, AUC), the number of classifiers were minimized.
**Results:** Optimized classifiers in both considered cases showed that the selected parameters can discriminate normal vs. abnormal events during the night with high sensitivity and specificity (AUC=0.99453, cut-off point - 0.37). Similar holds true for determining, whether these events were incidents of severe snoring or had a different background (AUC=0.99025, cut-off point - 0.35).
**Conclusion:**. Statistical analysis of ROC curves yielded very good results with visible strong association between parameters. This suggests the proposed parameters have a very high predictive value in differentiating causes and severity of respiratory events during sleep. Results can be used as an introduction for designing a system for automatic analysis of breath based on acoustic and cardiac parameters and show perspectives for data mining methods, i.e. random forests.

# Preprocessing and Mortality Prediction: the Physionet/CinC 2012 Challenge Revisited

Alistair E W Johnson* and Gari D Clifford

University of Oxford
Headington, Oxford, United Kingdom

S34

The Physionet/CinC 2012 challenge focused on improving patient specific mortality predictions in the intensive care unit. While most of the focus in the challenge was on applying sophisticated machine learning algorithms, little attention was paid to the preprocessing performed on the data a priori. We compare four standard pre-processing methods with a novel Box-Cox outlier rejection technique and analyze their effect on machine learning classifiers for predicting the mortality of ICU patients. The best machine learning model utilized the proposed preprocessing method and achieved an AUROC of 0.848. In general, the AUROC of models using our novel preprocessing method increased, and this increase was as much as 0.02 in some cases. Furthermore, the use of preprocessing improved the performance of regression models to a higher level than that of non-linear techniques such as random forests. We demonstrate that proper preprocessing of the data prior to use in a prognostic model can significantly improve performance. This improvement can be even greater than that provided by more complex non-linear machine learning algorithms.

## Scaling the PhysioNet WFDB Toolbox for MATLAB and Octave

Tristan Naumann* and Ikaro Silva

MIT
United States

S34

The PhysioNet WFDB Toolbox for MATLAB and Octave is a collection of functions for reading, writing, and processing physiologic signals and time series used by PhysioBank databases. Using the WFDB Toolbox, researchers have access to over 50 PhysioBank databases consisting of over 3TB of physiologic signals. These signals include ECG, EEG, EMG, fetal ECG, PLETH (PPG), ABP, respiration, and others. The WFDB Toolbox provides support for local concurrency; however, it does not currently support distributed computing environments. Consequently, researchers are unable to utilize the additional resources afforded by popular distributed frameworks. The present work improves the scalability of the WFDB Toolbox by adding support for distributed environments. Further, it aims to supply several best-practice examples illustrating the gains that can be realized by researchers leveraging this form of concurrency.

## A Quantitative QT Hysteresis Model

David Mortara* and Fabio Badilini

Mortara Instrument and UCSF School of Nursing
Milwaukee, United States

We report on a model of the QT/RR relationship based on the preceding 255 RR intervals to predict the current QT interval. The parameters of the model are sufficiently stable across two study populations to suggest the possibility of a broadly applicable quantitative model. All data is from 12-lead 24-hour Holter recordings with a sampling rate of 1000 Hertz. The study population includes 33 Mortara company employees and 383 recordings from a large trial on chronic heart failure patients (the GISSI-HF study). Each hour of RR and QT interval data, measured by an automatic algorithm, was fitted with a linear QT/RR model in which the preceding RR interval of each (normal beat) QT interval is replaced by a weighted average (RRc) of the preceding 255 RR intervals. The parameters of the model are the slope, intercept, and weights applied to the prior RR intervals. Common weights are used for successively doubled numbers (powers of two) of RR intervals, going backward in time from the current beat, resulting in 8 weights (with a sum of unity) for 255 beats. Hours with insufficient normal beats or rate variation were omitted. Out of a total of 9770 hours of data, 8114 were acceptable. Illustrating the importance of the RR history, the weighted RR improved QT prediction by reducing the root mean squared prediction error (rms) from 5.74ms (only considering the prior RR) to 2.94ms. A composite set of weights, taken from the average of all results, and applied to each hour resulted in an rms prediction error for QT of 3.12ms, with the largest observed mean difference (between universal and hourly optimized weights) of rms errors for any single recording of 0.90ms, suggesting that a universal set of RR weights may apply to a diverse population.

## Ventricular Arrhythmias Assessment: a New Repolarization Index of Risk

Corrado Giuliani, Cees A Swenne, Sumche Man, Angela Agostinelli and Laura Burattini*

Università Politecnica delle Marche
Ancona, Italy

S41

**Introduction:** Defects in the cardiac repolarization are known to be associated to several life-threatening diseases. In the electrocardiogram (ECG) such defects appear as abnormalities of the ST segment and T wave, which can be non-invasively characterized by means of several indexes, none of which has yet shown sufficient sensitivity and specificity to justify preventive interventions. Thus, the aim of the present study was to propose a new repolarization frequency-based index, termed f99, and to test its predictive power on exercise 15-lead (X, Y, Z, V1 to V6, I to III, aVr, aVl, aVf) ECG recordings from 266 ICD patients (Leiden University Medical Center Database), of which 76 developed ventricular tachycardia or fibrillation during the 4-year follow-up (ICD_Cases), and 190 did not (ICD_Controls).

**Methods:** After performing the frequency-content evaluation of the repolarization signal (RPS) at the maximum heart-rate reached during exercise, f99 was computed as the frequency at which the RPS energy first reaches or overcomes 99%. This parameter was first computed in each single lead, and then f99 single-lead values were maximized over the Frank's orthogonal XYZ leads (MaxXYZ), over the 6 precordial leads (MaxV1-V6) and over the 12 standard leads (Max12L). Predictive power of MaxXYZ, MaxV1-V6 and Max12L for the occurrence of ventricular arrhythmia was evaluated by computing the area-under the receiver operating curve (AUC).

**Results:** Compared to the ICD_Controls, the ICD_Cases showed significantly higher values of MaxXYZ (38 Hz vs. 27 Hz, $P<0.05$; AUC=0.61), MaxV1-V6 (42 Hz vs. 33 Hz, $P<0.05$; AUC=0.60) and Max12L (46 Hz vs. 37 Hz, $P<0.01$; AUC=0.65).

**Conclusion:** Thus, the new f99 represents a promising tool to identify the risk of ventricular tachycardia or fibrillation, with Max12L showing the best predictive power.

# QT/RR and T-peak-to-end/RR Curvatures in Chronic Heart Failure Patients

Julia Ramírez, Iwona Cygankiewicz, Pablo Laguna, Marek Malik, Esther Pueyo

University of Zaragoza
Zaragoza, Spain



**Background:** The majority of previous studies investigated the QT/RR relationship by means of fixed regressions between simultaneously measured QT and RR intervals. However, the QT/RR pattern does not necessarily follow the same regression relationship in different subjects. The QT/RR pattern is known to be frequently but not always steeper at faster heart rates compared to slower heart rates. Curvatures of QT/RR patterns were previously investigated in healthy subjects but not in cardiac patients.

**Methods:** Holter ECG recordings of 651 patients with chronic heart failure (CHF) from the "MUSIC" database were analyzed. ECGs were delineated using a single-lead procedure over the first principal component to emphasize the T-wave. RR, QT and $T_{pe}$ series were obtained and for each patient, the regression equation was fitted: y = $\chi$ + $\phi$(1-$RR^{\gamma}$) + $\varepsilon$, where y is either QT or $T_{pe}$ while RR represents the underlying heart rate after removing the hysteresis effect. $\gamma$ is the y/RR curvature, and $\varepsilon$ is a normally distributed zero-centered error. The y/RR slope was evaluated at the medium RR value: $\Delta = -\phi\gamma RR^{\gamma-1}|_{RR=\bar{RR}}$

**Results:** The mean ± standard deviation (SD) slope was $\Delta^{QT}$ = 0.201 ±0.138, and $\Delta^{T_{pe}}$ = 0.060 ± 1.074. The mean ± SD curvature was $\gamma^{QT}$ = 0.227 ± 3.696 and $\gamma^{T_{pe}}$ = 0.836 ± 7.081, respectively. The histograms of slope and curvature distributions showed non-normally distributed values.

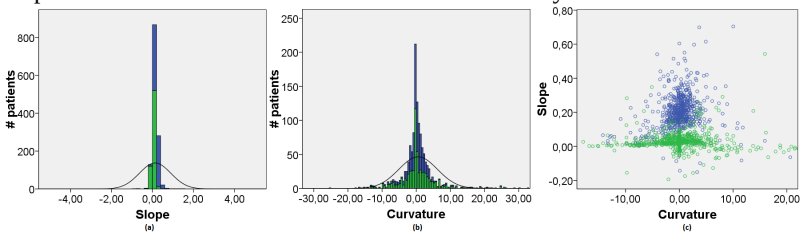


Histogram of slope (a) and curvature (b) values, and their scatter diagram (c) for QT(blue) and $T_{pe}$ (green) series.

**Conclusions:** In CHF patients, the curvatures of QT/RR and $T_{pe}$/RR showed that the regression QT/RR and $T_{pe}$/RR patterns are highly individual and, consequently, any generalized assumption about their mathematical description may lead to inappropriate conclusions. The values of slopes showed smaller inter-individual variability.

## T-wave Alternans Rate of Change with Exercise for Cardiac Risk Assessment

Laura Burattini*, Sumche Man, Giovanni Ottaviano, Sandro Fioretti, Francesco Di Nardo and Cees A Swenne

Università Politecnica delle Marche
Ancona, Italy

S41

Microvolt T-wave alternans (TWA), an every-other-beat fluctuation of the T-wave amplitude, is associated to cardiac instability, so that its amplitude is usually considered an index of the risk of arrhythmic events. TWA increases with heart rate (HR) so that its evaluation is often performed under exercise conditions. Still, at high HRs, TWA is also induced in healthy subjects, so that TWA predictive power not necessarily increases with HR. Aim of the present study was to investigate if, beside TWA amplitude, TWA rate of change with HR can be also used for risk assessment. To this aim our HR adaptive match filter for automatic TWA identification was applied to exercise ECG recordings of 266 patients with implanted cardio-defibrillator, 76 of which developed ventricular arrhythmias during the 4-year follow-up (ICD_Cases), and 190 did not (ICD_Controls). TWA was measured at 80 bpm (TWA80) and at 115 bpm (TWA115). The rate of change of TWA with exercise was evaluated by computing the ratio (TWAratio) and the difference (TWAdiff) between TWA115 and TWA80. Predictive power of these parameters was evaluated by measuring the area under the receiver operating curve (AUC) when discriminating the two ICD groups. Compared to the ICD_Controls, the ICD_Cases showed significantly higher TWA80 (median: 22 μV vs. 16 μV; $P<0.01$) but not TWA115 (median: 30 μV vs. 24 μV vs; $P=0.4032$). Moreover, the latter group also showed significantly higher TWAratio (median: 1.63 vs. 1.05; $P<0.05$) and TWAdiff (median: 11 μV vs. 1 μV; $P<0.05$). TWAratio showed the highest AUC (0.6914) followed by TWAdiff (0.6816), TWA80 (0.6414) and TWA115 (0.4547). Thus, parameters measuring the rate of TWA increment with HR provided better risk assessment for the occurrence of ventricular arrhythmias than TWA amplitude at both high (115 bpm) and low (80 bpm) HR.

# Repolarization lability measured by spatial TT' angle

Larisa G. Tereshchenko

Oregon Health & Science University, Knight Cardiovascular Institute. Portland, OR, USA



Aims: Increased repolarization lability is a marker of the risk of life-threatening ventricular arrhythmias (VA). I recently developed method of dynamic vectorcardiography for three-dimensional assessment of repolarization lability. Relatively large T peaks cloud volume was shown associated with increased risk of VA in patients with structural heart disease and systolic dysfunction. Beat-to-beat changes in both spatial T vector orientation (spatial TT' angle) and T vector magnitude contribute into T peaks cloud volume. This study aimed to evaluate the associations of (1) spatial TT' angle with VA, and (2) variance of spatial T vector amplitude with VA, and to compare the strength of associations.

Methods: Baseline orthogonal ECGs were recorded during 5 min at rest in 523 patients with structural heart disease [mean age 59.8±12.5; 70% whites; 74% men] before implantation of implantable cardioverter-defibrillator (ICD) for primary prevention of sudden cardiac death.

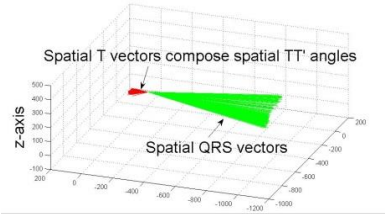


Figure 1. Spatial TT' angles of consecutive 300 beats

The crosspoint between QRS and T loops, and peak of spatial T vector was identified for each beat automatically. The spatial TT' angle (Figure 1) between consecutive spatial T vectors was calculated using the definition of the inner product:

$$TT'angle = \arccos\frac{T * T'}{|T| * |T'|}$$

Results: During a mean follow-up time of 18.4±12.5 months, 66 patients (8.4% per person-year of follow-up) experienced sustained VA with appropriate ICD therapies. In the multivariable Cox regression model after adjustment for age, sex, race, type of cardiomyopathy (ischemic vs. non-ischemic), left ventricular ejection fraction, QRS duration and renal function (blood urea nitrogen), spatial TT' angle was associated with VA (HR 1.02; 95%CI 1.00014-1.047; P=0.049).

Conclusion: Relatively wide spatial TT' angle, a measure of increased repolarization lability, is associated with increased risk of VA in patients with structural heart disease and systolic dysfunction.

# Tensor-based Detection of T Wave Alternans in Multilead ECG Signals

Griet Goovaerts[1,2], Carolina Varon[1,2], Bert Vandenberk[3], Rik Willems[3], Sabine Van Huffel[1,2]

[1] KU Leuven, Department of Electrical Engineering-ESAT, STADIUS Centre for Dynamical Systems, Signal Processing and Data Analytics, Belgium.
[2] iMinds, Medical IT Department, Belgium.
[3] Department of Cardiology, KU Leuven, Leuven, Belgium

S41

**Introduction** T wave alternans (TWA), a periodic variation of the T wave amplitude in a ABAB-pattern, is a widely recognized indicator for sudden cardiac death. While many methods exist for TWA detection in single lead ECG signals, most are very sensitive to noise. The use of tensors (multi-dimensional matrices) allows to combine the information present in all channels, making detection more robust.

**Methods** To construct a 3D tensor from a 2D ECG signal, the T wave is first roughly segmented by detecting the QRS complex with a wavelet based method and taking a fixed interval of 40 ms after each QRS complex. The intervals are then placed after each other to obtain a 3D structure with dimensions time, space and heartbeats. The tensor is decomposed using Canonical Polyadic Decomposition. The result is 1 rank-one tensor consisting of 3 loading vectors (which match the 3 dimensions of the original tensor). The third loading vector corresponds to the heartbeats dimension and gives information about the behavior of the T wave in different heartbeats. The Fourier transform of this loading vector can then be used to examine the presence of TWA

**Results and conclusion** The methods have been tested on a subset of the T wave alternans database available on Physionet. The subset consists of 10 subjects with and 10 subjects without TWA. Results show a very clear distinction between loading vectors of signals from both groups: the power of the loading vector in the TWA group is on average 100 times larger than in the control group. This suggests that tensors are an effective way of detecting TWA in multilead signals.

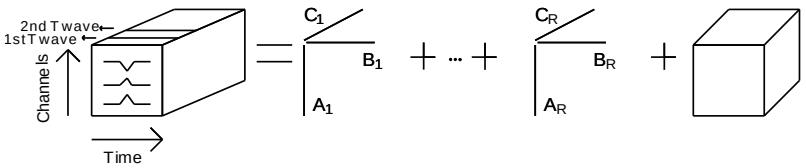


Illustration of tensor construction and decomposition

# Controlled Cardiac Activation for Robust Interrogation of the Electrophysiological Substrate

Joshua JE Blauer*, Fred Han, Ravi Ranjan, Nassir F Marrouche, Rob S MacLeod

University of Utah, CARMA Center, Salt Lake City, UT, USA



**Introduction** - Mapping of electrophysiological substrate is critical to analyzing and treating cardiac arrhythmias, however, current approaches have persistent limitations. One such limitation is the inability to alter the direction of wave front propagation from that in sinus rhythm. Consequently, pro-arrhythmic substrates that present during non-sinus activation may go undetected when mapping in sinus rhythm. We have developed a novel approach for mapping indicators of substrate remodeling, *e.g.,* conduction velocity, during multiple variably oriented activation patterns by pacing and recording with trackable, multi-electrode, mapping catheters.

**Methods** - Prior to pulmonary vein isolation for atrial fibrillation, trackable, 10 pole, loop catheters were positioned flat on the posterior wall of the left atrium. Bipolar pacing (5 mA, 2 ms pulse width, 500 ms cycle length) was used to capture the atria from subsequent pairs of electrodes around the loop. A clinical electroanatomical mapping system was used to track the position of all loop electrodes during pacing, while also recording unipolar and bipolar electrograms (2.5 sec duration). Non-pacing channels demonstrating clear activation signals were analyzed for activation times in order to calculate conduction velocities. Finally, the mapping data was registered to late gadolinium enhanced MRIs in which the amount of structural remodeling had been determined.

**Results** - Qualitative examination of conduction velocity vectors indicates that even modest perturbations of activation patterns can substantially altered conduction speed. This study establishes a pipeline that capitalizes on the spatial distribution, and active tracking, of multi-electrode diagnostic catheters to robustly interrogate local properties of conduction and activation. Combining these results with MRI derived structural features offers a novel method with which to study pro-arrhythmic myocardial substrates.

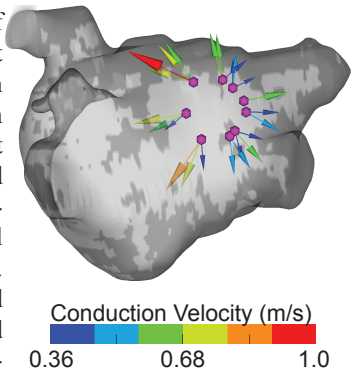

# A novel method for quantifying localised correlation of late-gadolinium intensity with conduction velocity

Rheeda L Ali, Chris D Cantwell, Caroline H Roney, Norman A Qureshi, Phang Boon Lim, Jennifer H Siggers, Spencer J Sherwin, Nicholas S Peters

Imperial College London, London, UK

S42

**Aims:** Patient-specific computer models of the human atria have the potential to aid clinical intervention in the treatment of cardiac arrhythmias. Quantification and integration of the structural aspects of the myocardium through imaging is particularly challenging. We have developed a technique to test the hypothesis that scar based on late-gadolinium enhanced magnetic resonance imaging (LGE-MRI) data influences or affects localised conduction velocity and can therefore be used for model calibration.

**Methods:** The maximum LGE-MRI intensity within 3mm normal to the atrial wall was projected onto a reference segmented left-atrial surface to create a patient-specific scar map. Intensities $>$ 3 S.D. above the mean blood-pool intensity were defined as scar. Endocardial electrogram data were exported from the Ensite Velocity system for paced cycle lengths (CL) of 600ms and 300ms. The electroanatomic surface was registered to the reference surface via landmark and surface transformations using the IRTK toolkit. Electrogram positions were then mapped onto the reference atrial surface, triangulated and conduction velocities calculated. The area-weighted average of the underlying LGE-MRI intensity for each triangle was computed and the relationship between the conduction speed and average scar intensity was assessed using Pearson's correlation coefficient.

**Results:** Speed values are quoted in terms of median (M) and inter-quartile (IQR). At CL $600ms$, M=$0.58ms^{-1}$ and IQR=$0.54ms^{-1}$ and at CL $300ms$ M=$0.45ms^{-1}$ and IQR=$0.45ms^{-1}$. These speeds were calculated over a range of S.D. of intensities between 0.0051 and 3.911. Correlation analysis showed little correlation $\rho = 0.29$ (CL=$600ms$) and $\rho = -0.05$ (CL=$300ms$).

**Conclusion:** Our study suggests that one cannot quantifiably assert reduced conductivity from intensities obtained from LGE. Further work will be focused on determining the conduction direction, relative to the fibre direction.

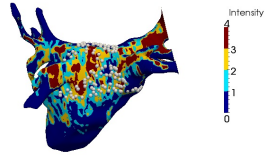


Patient-specific scar map with endocardial electrograms

# Defibrillation Thresholds: A Generalised Polynomial Chaos Study

Peter R. Johnston

Griffith University
Brisbane, Queensland, Australia



**Aims:** This study aims to understand the effect variations in cardiac conductivity values have on defibrillation thresholds in a simple heart-in-a-bath model.

**Methods:** A generalised polynomial chaos approach was used to generate 41 sets of four cardiac conductivity values based on the three commonly used data sets (Clerc (1976), Roberts, Hersh and Scher (1979) and Roberts and Scher (1982)). Intracellular and extracellular longitudinal and transverse conductivity values were calculated by assuming that each value could be sampled from a uniform range between the maximum and minimum values from the three experimentally determined data sets, respectively. Simulations, based on the bidomain equations, were performed on an isolated heart placed in a bath with defibrillation paddles at the sides of the bath. Varying potential differences were applied across the defibrillation paddles for all 41 conductivity sets. The polynomial chaos approach allowed the calculation of mean and variance extracellular potentials within the heart, as well as mean and variance potential gradient fields.

**Results:** The aim of defibrillation is to expose the heart tissue to an extracellular potential gradient of 0.6V/mm over 90% of the heart tissue volume. Simulations revealed that with a potential difference of 160V between the electrodes this threshold was met by none of the 41 conductivity sets. Alternatively, with a potential difference of 230V, the threshold was met by all conductivity sets. The study also showed that the regions of lowest potential gradient were in the left ventricular wall and the regions of greatest variance in the potential and potential gradient were near the surface of the heart and within the tissue near the paddles.

**Conclusions:** Conductivity values have a significant effect on the thresholds required to defibrillate the heart. In particular, there is up to a 70V difference between defibrillation thresholds depending on the conductivity values.

# Formulation of ATP Sensitive K+ Current and Action Potential shape in Models of Human Ventricular Myocytes

Mitra Abbasi* and Richard Clayton

University of Sheffield
Sheffield, United Kingdom

S42

**Introduction:** The contribution of the ATP-sensitive K^+ (K_ATP^+) current to the action potential is an important component of cardiac ischaemia. The purpose of this study was to investigate how the formulation of I_(K(ATP)) influences cell excitability and action potential duration in the Ten Tusscher-Panfilov 2006 model of human ventricular myocytes.

**Methods:** We studied three different formulations of the ATP activated K^+ current I_(K,ATP) (Shaw and Rudy, 1997; Matsuoka et al, 2003; Ferrero et al., 1996) based on animal heart data, and one formulation (Kazbahnov et al., 2014) based on human heart data. To study restitution of these models, we used a 2D monodomain tissue model (TP06 model). The 2D monodomain model was solved with an explicit finite difference approach with a fixed space step of 0.02 mm and time step of 0.2 ms. Action potential duration (APD) and conduction velocity (CV) restitution were measured using an S1S2 protocol with S1=1000ms. Ischaemia was simulated by reducing intracellular ATP concentration from 6.8 mM to 6.0, 5.0, 4.5 and 4.0 mM in Shaw and Rudy and Matsuoka et al. models. Similar changes were produced by the factor f_ATP in the modified version of Ferrero et al. and Kazbahnov et al. formulations to simulate APT depletion.

**Results:** The results demonstrate that inserting I_(K(ATP)) in the cell models shortens APD as intracellular ATP concentration is reduced, consistent with experimental findings. Although the current-voltage properties of each I_(K(ATP)) formulation was different, the effect of hypoxia of each formulation was similar on the properties of the tissue model.

**Conclusion:** The similarity of the simulated electrical behavior observed, by using all I_(K,ATP) models presented in this study, supports the hypothesis that I_(K,ATP) is a major current responsible for action potential duration shortening during acute ischemia.

# High Specificity IEGM Beat Detection by Combining Morphological and Temporal Classification for a Cardiac Neuromodulation System

Antje Pohl*, Carl Henning Lubba, Maren Thore, Nima Hatam and Steffen Leonhardt

Philips Chair for Medical Information Technology, RWTH Aachen University, Aachen, Germany
Aachen, Germany



Elevated heart rate is known to be an independent risk factor for a higher overall mortality, especially for patients suffering from coronary artery diseases, e.g. from heart failure. Since pharmacological approaches can not exclusively address heart rate, we investigate a cardiac neuromodulation technique lowering elevated heart rate by means of electrical neurostimulation. The idea is to exclusively stimulate the parasympathetic tone in the sinoatrial node area to decrease heart rate. However, electrical stimulation of the heart may pose a specific risk as one temporally misplaced stimulation can cause atrial fibrillation. Accordingly, we aim to trigger on the intracardiac electrogram in the high right atrium and present two algorithms satisfying the requirements of high specific, secure, real-time detection within one heart beat: Decision tree and neural network. Both algorithms were combined with a heart rate prediction estimating upcoming action potentials to maximize beat recognition against artifacts. The combined algorithms are validated on human intracardiac electrograms from electrophysiological examinations with promising results (specificity: 100%, sensitivity(tree): 70.2%, sensitivity(net): 87.3%) for secure neurostimulation.

# Fitting membrane resistance in single cardiac myocytes reduces variability in parameters

Jaspreet Kaur*, Anders Nygren, Edward J. Vigmond

University of Calgary, Canada

S42

**Introduction -** Fitting the sets of non-linear equations in cardiac single cell ionic models to reproduce experimental behavior is complicated. Usually, only the net current is fit for single cell models to reproduce isolated action potentials (APs). However, extremely different sets of parameters can produce similar APs. Furthermore, even with a good AP match in the case of a single cell, tissue behavior may be different due to electrotonic interactions among neighboring cells. We hypothesize that this uncertainty can be reduced by also fitting membrane resistance ($R_m$).

**Methods -** $R_m$ was calculated at three different time points during the AP cycle. The AP was simulated in zero current clamp protocol until it reached the $V_m$ of interest, and then clamped to 10 mV above and below the $V_m$ of interest. The membrane current $I_m$ was measured 5 ms after that point and $R_m$ calculated as

$$R_m = \frac{\Delta V_m}{\Delta I_m} = \frac{V_{m,+10} - V_{m,-10}}{I_{m,+10} - I_{m,-10}}$$

A genetic algorithm was developed incorporating $R_m$ calculated at a few time points during the AP, in addition to AP shape. A human ventricular myocyte ionic model was fit to another human ventricle model. Performance was compared to a genetic algorithm using only AP morphology data.

**Results -** Including $R_m$ as one extra objective in addition to AP shape in the model fit improves the fit to the desired AP while reducing variability by at least two-fold for the majority of parameters (figure). Thus, $R_m$ can provide information regarding ionic currents that is not sufficiently provided by the shape of the AP on its own.

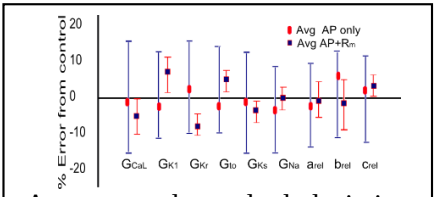


Average and standard deviation for parameter estimates.

# New Additions to the Toolkit for Forward/Inverse Problems in Electrocardiography within the SCIRun Problem Solving Environment

Jaume Coll-Font*, Brett Burton, Jess Tate, Burak Erem, Darrell Swenson, Dafang Wang, Dana Brooks, Peter van Dam and Rob MacLeod

Northeastern University
Boston, United States



Electrical cardiac imaging often requires the examination of different forward and inverse problem formulations in order to find the methods that best suit the problem of observing a physiological even that is otherwise inaccessible or unethical to explore. These formulations require a mathematical and then numerical approximation of the underlying source that can generate the associated voltages on the surface of the body. If the goal is to recover the source on the heart from body surface potentials, the solution strategy must include appropriate numerical techniques that can incorporate appropriate constraints and recover useful solutions, even when the problem is badly posed. Creating complete software solutions to such problems is a daunting undertaking, and in order to make such tools more accessible to a broad array of researchers, the Center for Integrative Biomedical Computing (CIBC) has compiled a forward/inverse toolkit within the open source SCIRun system. Here we report on three new methods added to the cardiac inverse suite of the toolkit. These new algorithms consist of two inverse methods that take advantage of the temporal structure of the heart potentials and one that uses the spatial characteristics of the transmembrane potentials to regularize. The first algorithm approximates the manifold defined by the cardiac potentials in time with smooth non-linear fitting of all ECG leads. This manifold is then used to reconstruct the complete sequence of heart potentials from a reduced set inverse solutions. The second algorithm imposes temporal constraints such that only monotonically non-decreasing solutions are allowed for the transmembrane potentials. Finally, the algorithm based on spatial characteristics applies Total Variation regularization to the transmembrane potentials, thus favoring solutions that are sparse in their first derivative in space. These three methods further expand the possibilities of researchers in cardiology to explore possible existing solutions to their particular imaging problem.

# A Feasibility Study using Image-based Parallel Modeling for Treatment Planning

Amanda Randles[1], Michael Driscoll[2], Erik Draeger[1], and Franziska Michor[3]

[1] Lawrence Livermore National Laboratory, Livermore, CA, USA
[2] University of California Berkeley, Berkeley, CA, USA
[3] Dana-Farber Cancer Institute, Boston, MA, USA

S43

**Aims:** This study aimed to assess the accuracy of image-based parallel model to study treatment planning options for patients presenting coarctation of the aorta. These surgical options can allow physicians to reduce the pressure gradient across the narrowing to below the clinical risk cutoff.

**Methods:** A patient-specific geometry was modified to create a virtual post-surgical geometry. In order to assess the merits of using the computational fluid dynamics tool, HARVEY, to study patient-specific risk factors based on prospective analysis of treatment procedures, the pressure drop is calculated for a range of physiological conditions over the course of the full cardiac cycle.

**Results:** We demonstrate that *in silico* treatment planning yields more than a 50% decrease in the pressure drop across the coarctation throughout systole. In both physiological states, the resulting gradient was below the clinically accepted risk cutoff.

**Conclusion:** This comparison of pre- and post-virtual operative hemodynamics demonstrates the potential application of the proposed framework in optimizing patient-specific CoA treatment planning. These results can feed directly back to the virtual surgery component to adjust the post-operative mesh and optimize the surgical reconstruction *in silico*. In this initially feasibility study we focus on the aortic arch but in future work we will extend this research to look at medications with larger region and more patients.

## Spiral Waves Clustering Using Normalized Compression Distance

Celal Alagoz*, Andrew R Cohen, Allon Guez and John R Bullinga

Drexel University
Philadelphia, United States

Cardiac fibrillatory dynamics are identified with spiral waves in mathematical modeling of cardiac electrical propagation. An automatic identification of the spiral wave dynamics is essential for patient specific cardiac modeling. In our work we used normalized compression distance (NCD), an information theoretical distance measure, in order to cluster the simulated spiral waves as stable, meandering and break up. Different representation of the data was introduced to NCD in the form of raw time series, fast fourier transform (FFT), feature summarization and symbolic quantization of the simulated electrograms. Clustering was done in an unsupervised way using spectral method. Clustering analysis was performed using different validation methods. Gap statistics was used to find optimal number of groups. Jaccard coefficient was used in order to evaluate accuracy of clustering. We had a perfect evaluation results from the raw data representation and fourier transformation with a jaccard index of 1, and a very good performance of feature summarization with a jaccard index of 0.98.

# Interactive Simulation of heart rhythm: A new educational feature of ECGSIM

PM van Dam*, EM van Dam, A van Oosterom, TF Oostendorp

Radboud University Medical Center, Nijmegen, the Netherlands

S43

ECGSIM is an interactive open source software package aimed at supporting ECG education and research. In this package, the local transmembrane potential may be changed interactively, and the resulting ECG changes are displayed instantaneously. In the previous versions of ECGSIM only a single heartbeat could be simulated, limiting its possibilities in investigating changes in ECG morphology. This contribution introduces a new version in which a sequence of heart beats changes can be simulated.

The educational possibilities are considerably extended by this new feature. Its potential is demonstrated by the simulation of atrial tachycardia, developing ischemia and the typical changes in the ECG of a Brugada patient elicited by the administration of Ajmaline. In the new release of ECGSIM a case is included describing a patient undergoing an Ajmaline stress-test. The development of the ECG changes during this test can be observed on a beat-to-beat basis. Another educational application is the simulation of atrial activations originating from the pulmonary veins region with intact intrinsic AV conduction. The behavior of the AV node can be simulated by the adjusting the delayed propagation time as well as accounting for the refractory period of the AV node. The application that will be presented is the simulation of developing ischemia over time, i.e. the combination of changes over time in action potential duration, resting potential elevation and propagation velocity in the acute phase of a heart attack.

This new feature enhances the educational application of ECGSIM, both for medical and technical students. As before, the clinical data used for the new cases will be made available at the ECGsim website (www.ecgsim.org). We feel confident that these new applications will increase even further the interest in ECGSIM and stimulate further the present collaboration with other educators and researchers in identifying and new applications.

*ECG of different atrial and ventricular activations, i.e. an atrial tachycardia from the pulmonary veins, normal ventricular activation, and 2 different PVCs*

# Myokit: A Framework for Computational Cellular Electrophysiology

Michael Clerx*, Paul GA Volders and Pieter Collins

Maastricht University
Netherlands



Computational cellular electrophysiology uses ODE models to study the electrical behavior of cardiomyocytes, and by extension of the heart. This paper introduces Myokit, an open source framework for development and analysis of such models. The framework consists of a dedicated modeling language and a set of tools for simulation, analysis and post-processing. Models are stored in a plain text file containing a model definition section and optional sections for a pacing protocol and a reference or sample experiment. This set-up allows an entire experiment to be stored in a single file suitable for text editors and version control systems. The model definition language is designed to be simple, unambiguous and easy to write. To provide structure, variables are grouped into components, and variables can define private child-variables for temporary use. External inputs can be accessed by binding variables to specific keywords and providing a default value for environments where no such input is defined. This allows the same model to be re-used in different contexts. The language has support for simple meta data, as well as units and unit checking. The framework is written in Python but runs performance critical operations entirely in C. A single cell simulation engine is provided that uses the CVODE solver to obtain high performance. Multi-cell simulations are run using OpenCL for parallel execution on GPUs or multi-core CPUs and a tool to examine the influence of a single model parameter is provided. Additional tools build on this core functionality and perform common analysis and post-processing tasks. Import from CellML is provided, as well as export to C, Matlab, CUDA, OpenCL and other formats. The combination of a clear modeling language, a high-level API and a freely available toolkit can serve to reduce model development and debugging times, freeing valuable resources for physiological investigation.

# A Novel Method for Rotor Tracking using Bipolar Electrogram Phase

Caroline H Roney*, Chris D Cantwell, Jennifer H Siggers, Fu Siong Ng, Nicholas S Peters

Imperial College London, London, UK

S43

**Aims:** Assessing the location and stability of rotors can help target ablation therapy for atrial fibrillation (AF). Phase singularity (PS) tracking techniques have been applied to unipolar electrogram and action potential (AP) data, but not to bipolar electrogram (BE) data, which contains local activation only. We developed and tested a technique to track PSs from simulated BE data.

**Methods:** Simulated AP data (0.25 mm resolution, 10 seconds) with two stable rotors and fibrillatory activity at the interface were postprocessed to generate BEs with two interelectrode spacings of 2mm and 4.5mm. The BEs were filtered and the moving-mean removed from the signal in such a way as to conserve deflections that were small in amplitude due to wavefront direction. Phase was calculated, and PS trajectories and lifetimes were determined using automated algorithms. Wavefront dynamics and singularity positions computed using BE data were compared to those calculated directly from AP data.

**Results:** Wavefront patterns were qualitatively similar for phase from both BE resolutions compared to full resolution AP data and agreed well with activation time maps calculated from either AP or BE data. Average AP and BE rotor core locations differed by 1.2mm (rotor 1: AP vs BE 2mm), 0.97mm (rotor 2: AP vs BE 2mm), 2.5mm (rotor 1: AP vs BE 4.5mm) and 0.80mm (rotor 2: AP vs BE 4.5mm). Similar fibrillatory dynamics were observed, and average PSs per frame were 6.0 (AP), 5.7 (BE 2mm) and 6.1 (BE 4.5mm). The overall distribution of PSs for the duration of the simulation was similar in each case (AP vs BE 2mm: r=0.74, AP vs BE 4.5mm: r=0.76).

**Conclusion:** BE phase is as effective as AP phase for rotor tip detection when using simulated data, and may be used clinically as an alternative method to unipolar phase to locate rotor PSs in AF.

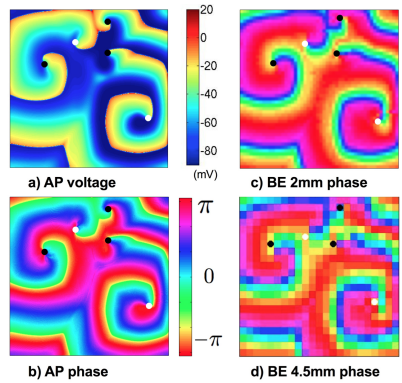


Phase singularities (black and white dots) calculated using AP phase (a, b), and BE phase at interelectrode spacings of 2mm (c) and 4.5mm (d).

# Analysis of Cardiovascular Time Series using Multivariate Sample Entropy: A Comparison between Normal and Congestive Heart Failure Subjects

Chengyu Liu*, Dingchang Zheng, Lina Zhao, Changchun Liu and Alan Murray

Newcastle University
United Kingdom



The cardiovascular (CV) system typically exhibits complex dynamical behavior, which is reflected not only within a single data channel, but more importantly across data channels. Multivariate sample entropy (MSE) has been proven as a useful tool to analyze both the within- and cross-channel coupled dynamics, providing an insight into the underlying system complexity and coupling relationship. In this study, we used the MSE method to monitor both the univariate and multivariate CV time series variability, focusing on identifying the differences between normal and congestive heart failure (CHF) subjects. Electrocardiogram, phonocardiogram and radial artery pressure waveforms were simultaneously recorded from 30 normal and 30 CHF subjects to determine three time series: RR interval, cardiac systolic time interval (STI) and pulse transit time (PTT). The MSE method was applied to univariate (RR, STI, PTT), bivariate (RR & STI, RR & PTT, STI & PTT) and trivariate (RR & STI & PTT) time series. The results showed that all MSE values in the CHF group were significant lower than those in the normal group (all $P<0.05$, except for the univariate PTT series $P=0.49$), which indicates that the complexity of univariate series decrease and the coupled degrees of multivariate series weaken for CHF subjects. Moreover, the statistical significance between the two subject groups increased from using univariate to multivariate time series (with $P<0.05$ to $P<0.001$), confirming that the multivariate analysis could give a better understanding of the underlying CV system dynamics.

## Comparison of Left Ventricular Ejection Time from Echocardiography, Impedance Cardiography and Photoplethysmography

Wenfeng Duan*, Dingchang Zheng, Christopher Eggett, Philip Langley and Alan Murray

China

S44

This study compared left ventricular ejection time (LVET) measured from cardiac imaging, impedance cardiography (ICG) and photoplethysmography (PPG). Twelve healthy subjects were studied. Cardiac aortic valve movement and valve blood flow were examined by M-mode and Doppler echocardiography, and cardiac responses from thoracic impedance changes and peripheral pulse output. Data were recorded for 15 s on each subject. To reduce the uncertainty caused by physiological variation, the measurement devices were connected together to allow the images and physiological signals to be recorded simultaneously. Further synchronization was implemented offline to align the 15 s recordings from the separate devices exactly in time. The measurement of LVET from each recording device was analysed. Finally, the beat-by-beat variability for LVET measurement from each technique was assessed, and the average values across all beats were compared. The LEVT measured from Doppler imaging had the smallest mean beat-by-beat SD across all subjects (9 ms), which was better than that from M-mode echocardiography and PPG (both were 12 ms). ICG had the largest mean beat-by-beat SD (23 ms). The mean LEVT across all subjects from the M-mode echocardiography was 336 ms, which was longer than that from Doppler imaging (313 ms). Mean LVETs from ICG (364 ms) and PPG (358 ms) were both significantly longer those from the echo images ($P < 0.001$). In conclusion, with simultaneously recorded cardiac images and physiological signals, we have compared the left ventricular ejection time measured from M-mode echocardiography, Doppler imaging, ICG and PPG. The ICG and PPG not only gave longer LVET measurements, but also had larger measurement variability than the M-mode and Doppler imaging. These results show that although physiological measurements from ICG and PPG have the potential to provide easier ways for left ventricular ejection time measurement, the results were significantly longer and more variable.

# Simulating the Relation Between APD and QT Time in Human Ventricles

Gunnar Seemann*, David UJ Keller and Olaf Doessel

Karlsruhe Institute of Technology
Karlsruhe, Germany



Heterogeneities of the ventricular electrophysiology play a major role in the generation of the T-wave morphology, amplitude and duration. The heterogeneities are known to be at least transmural and apico-basal leading to a distribution of action potential durations (APD) in the ventricles. In a previous study, we developed a heterogeneous electrophysiological setup that is able to reproduce the 64 channel T-wave of a volunteer with a correlation coefficient of 0.896 and a RMSE of 0.08 mV. The aim of this work is to investigate how APD changes are reflected in the QT time. Activation and repolarization of the heterogeneous model was calculated using the ten Tusscher model of human ventricular electrophysiology in combination with the monodomain approach. The body surface potentials were calculated using the bidomain model on an anatomical model of a volunteer generated on the basis of MRI data. In order to generate different APD distributions and heterogeneities in the ventricle, we changed the maximum conductance of both IKr and IKs by +/-25% compared to the standard heterogeneous setup. As IKr is homogeneously and IKs is heterogeneously distributed in the model, these configurations not only shift the APD distribution but also change the dispersion of repolarization. In the standard setup, mean APD was 318 ms leading to a QT time of 382 ms. The +/-25% IKr configurations led to mean APDs of 309/328 ms and QT times of 353/409 ms, respectively. The +/-25% IKs setups generated mean APDs of 304/341 ms and QT times of 366/398 ms. The results show, that there is no direct relation between APD distribution and QT time. Therefore, it has to be investigated in more detail how e.g. drugs that are single or multi-channel blocker influence the QT time, which is still one of the major discriminator of drug safety.

# Assessment of Different Methodologies to Include Temporal Information in Classifying Episodes of Sleep Apnea Based on Single-Lead Electrocardiogram

Tim Willemen*, Carolina Varon, Bart Haex, Jos Vander Sloten and Sabine Van Huffel

KU Leuven
Leuven, Belgium

S44

Automated analysis of sleep apnea based on single-lead electrocardiogram would make its diagnosis much more accessible and would allow for cost-effective population-wide screening. Over the years, several algorithms have been proposed in the literature. In most of them, one or several temporal averaging techniques are used to improve classifier performance. A comprehensive comparison between those techniques however has never been published. Four different temporal averaging techniques, as well as overlapping of segments, were independently assessed using a database of 70 night-time recordings, originally released for the Computers in Cardiology challenge in 2000. Classification was performed with an LDA classifier. Multiple problem-specific feature sets of 10 features were selected out of a complete set of 304 using a two-step approach. Averaging classifier input features over neighboring segments led to the highest agreement values on the test set, outperforming the best automatic entry during the original competition (90.4% vs 89.4%). When combining classifier output values, an odd amount of segments should be used. Calculating features on larger segments (> 1-min) led to the worst results, possibly explained by its higher susceptibility to noise. Overlapping of segments improved overall agreement by about 1%. Future work will consist of improving the calculation of the RR interval and EDR signals by applying more robust methodologies (e.g. kPCA for EDR calculation), using the LDA-based extracted feature sets in a more versatile LS-SVM classifier, and increasing the amount of possible neighboring segments used.

## An Onchip Robust Real-time Automated Non-invasive Cardiac Remote Health Monitoring Methodology

Naresh Vemishetty, Krishna Bharadwaj Chivukula, Sandeep Tiwari, Pavana Ravi Sai Kiran Malyala, Bastin Joseph, Agathya Jagirdar, Jagadish Bandaru, Venkateswara Chowdary, Sivakrishna Y, Amit Acharyya*, Rajalakshmi Pachamuthu and Paolo Emilio Puddu

IIT HYDERABAD
HYDERABAD, India



Recent surveys on Cardiovascular diseases (CVD) risk management, fortified the upsurge of CVDs especially in under-developed and developing nations. To confront the issues of the poor healthcare infrastructure of these countries and deficit of medical professionals, health monitoring had to be done remotely with a device which is affordable and reliable. Considering this, we propose here, Onchip Real-time Automated Non-invasive Unobtrusive yet Robust methodology for Cardiac Remote Health Monitoring. The medical terminology of prognosis, diagnosis, intermediate intervention and the technical challenges like low-power, unobtrusive, non-invasive portable devices should be addressed considering the contradictory terms of low-power and reliability. The system here has a four folded modeling. After the data sensing, firstly, the classification which prompts the condition of the patient, is done at the outset to avoid any further processing for normal patient and to initiate further processing, if detected otherwise. Secondly, if there is an abnormal detection by classifier, the feature extraction (FE) which is the identification of P,Q,R,S,T from ECG frames has to be done. As there is demand of P,Q,R,S,T frames, a robust boundary detection (BD) mechanism is introduced to identify such frames. The f-QRS feature is also introduced as our third contribution, which enhances the diagnostic accuracy of several common but fatal heart diseases like Myocardial infarction, cardiac sarcoidosis, non-ischemic cardiomyopathy, etc. The fourth step is communicating the abnormal data to the nearest health care center by incorporating the concept of an adaptive rule engine (ARE) based classifier in low complex way. The proposed methodology is tested on 100 patients from PTBDB (MITBIH), CSE and in house IITH DB and percentage of accuracy of 98% and 97.33% for FE+BD and classifier respectively obtained.

# Economic Effect of Telecare on Medical Expendirures of Patients with Choronic Diseases

Masatsugu Tsuji* and Yuji Akematsu

University of Hyogo
Kobe, Japan

S44

This paper analyzes for what kind of diseases telecare is effective to reduce medical expenditures. The main interests are focused on patients with four chronic diseases, namely, heart diseases, high blood pressure, diabetes, and strokes. This study applies a regression analysis to estimate the effect of telecare to users who have these diseases and then calculate the monetary effect of telecare in reduction of medical expenditures. In so doing, cross terms of telecare users times above diseases are introduced to examine how telecare affects to particularly diseases. As a result, telecare is verified to provide the largest effect to heart diseases patients and the medical expenditures of heart diseases are reduced by approximately JPY 39,080.90 yen (US$390.00) per year per user, which is the largest in comparison with patients with high blood pressure and diabetes. These results are expected to strongly valid for establishment of evidence-based policy such as reimbursement from the medical insurance which we do not have yet in Japan. .

# Robust Detection of Heart Beats in Multimodal Data: The PhysioNet/Computing in Cardiology Challenge 2014

George B Moody*, Benjamin E Moody and Ikaro Silva

MIT
Cambridge, United States

The 15th annual PhysioNet/CinC Challenge aims to encourage the exploration of robust methods for locating heart beats in continuous long-term data from bedside monitors and similar devices that record not only ECG but usually other physiologic signals as well, including pulsatile signals that directly reflect cardiac activity, and other signals that may have few or no observable markers of heart beats. Our goal is to accelerate development of open-source research tools that can reliably, efficiently, and automatically analyze data such as that contained in the MIMIC II Waveform Database, making use of all relevant information. Data for this Challenge are 10-minute (or occasionally shorter) excerpts ("records") of longer multiparameter recordings of human adults, including patients with a wide range of problems as well as healthy volunteers. Each record contains four to eight signals; the first is an ECG signal in each case, but the others are a variety of simultaneously recorded physiologic signals that may be useful for robust beat detection. We prepared and posted 100 training records, and retained 300 hidden test records for evaluation of Challenge entries. Participants in the Challenge were required to create and submit open-source software that is able to read the test data and record the times of occurrence of the beats in PhysioBank-compatible annotation files, without user interaction, in a predefined sandbox environment. We prepared two sample entries for use by participants, and we also developed software that accepted uploaded entries, evaluated them using the hidden records, and returned scores to their authors. Each participant-team was allowed to receive scores for up to five entries in each of three phases, allowing a limited amount of iterative refinement. In Phase I of the Challenge (January - April), 39 participant-teams received scores for 156 entries; 10 outscored the sample entries.

# Heart Rate Variability Discovery: Algorithm for Detection of Heart Rate from Noisy, Multimodal Recordings

Jan Jakub Gierałtowski*, Kamil Ciuchciński, Iga Grzegorczyk, Katarzyna Kośna, Mateusz Soliński and Piotr Podziemski

Warsaw University of Technology
Poland

S51

Starting point for the heart rate variability analysis is the ECG signal, which ensures the most precise way of detecting heartbeats. Methods for detecting heartbeats from the ECG are well developed and robust. But very often devices used to record ECG also record at the same time many other physiological signals. These other signals could contain an information about heartbeats, because of their physiological correlation with the ECG (e.g. blood pressure or stroke volume) or because of the unintended imposition (e.g. in electrooculograms). In the case of the poor ECG quality or its absence information about heartbeats is lost. This raises the need for robust, open-source algorithms which could locate heart beats in continuous long-term data from bedside monitors, allowing reliable, automatic analysis of the data such as that contained in the MIMIC II Waveform Database. We analyzed 100 multi-channel recordings from PhysioNet Challenge 2014 database. Each recording has 3 to 6 channels, sampling rate of 250 Hz and duration of 10 min. Detected RR interval peaks were compared with reference annotations. Our algorithm focuses on detecting the most prominent part of a QRS complex i.e. RS slope in four of the channels provided: ECG, BP, EEG and EOG. First we remove long-range trends. Then, we localize decelerations with the required characteristics (adequate amplitude and slope). Note, that algorithm is adaptive and finds by itself optimal RS slope characteristics for every recording. After this final steps of a "fine-tuning" are done, i.e. removal of incorrect detections and in the case of missing ones re-check with lower requirements. These steps allowed us to obtain accurate and reliable results of R peak detection, even in the case of very noisy data. The preliminary test score of the PhysioNet Challenge was 70.88.

# Heart Beat Detection in Multimodal Data Using Signal Recognition and Beat Location Estimation

Thomas De Cooman[1,2], Griet Goovaerts[1,2], Carolina Varon[1,2], Devy Widjaja[1,2], Sabine Van Huffel[1,2]

[1]KU Leuven, Department of Electrical Engineering-ESAT, STADIUS Center for Dynamical Systems, Signal Processing and Data Analytics, Belgium
[2] iMinds, Medical IT Department, Belgium



**Aims:** Typically, only ECG is used for the localization of heart beats. However, when ECG is contaminated, R peak detection can become very hard. By adding information of other signals, heart beats can be detected more robustly in multimodal datasets.

**Methods:** First, a noise-free training period is extracted using an autocorrelation similarity matrix based on the ECG. Next, one signal with the same periodic character as the ECG (like blood pressure or stroke volume) is found by taking the highest correlation coefficient between the power spectral density around the average heart rate of the ECG and the other signals. Subsequently, the noise-free training period is used to learn the delay between the peaks of the periodic signal and the R peaks. After this training phase, two different peak detection algorithms are used: a differentiation method for ECG and a scalogram method for the periodic signal. The R peaks located by both methods are examined one by one in order to examine which peak results in the most logical RR sequence. Peaks that are closer to the estimated heart beat locations are favored and peaks are added if they result in a decrease of Hjorth's mobility parameter for the heart rate signal.

**Results:** A total performance of 99.99% was obtained on the training set, compared to 99.90% performance if only ECG is used. A lower total performance of 84.80% was however reached for the hidden test set. The results show that there is a large difference in performance between different patients, either due to the incapability of handling certain problems or due to extremely long computation time for these patients.

**Conclusions:** The proposed algorithm is able to improve R peak detection in noisy multimodal data. It can for example be used in order to increase the accuracy of polysomnographic analyses.

# Multimodal Information Fusion for Robust Heart Beat Detection

Quan Ding*, Yong Bai, Yusuf Bugra Erol, Rebeca Salas-Boni, Xiaorong Zhang, Xiao Hu

University of California, San Francisco, CA, USA



**Aims**

As part of the Physionet/Computing in Cardiology Challenge 2014, this study aimed to build a multimodal information fusion scheme that automatically extracts reliable information from monitoring signals for heart beat detection.

**Methods**

A training data set of 100 records with each record containing 10-minute long ECG signal plus a variety of simultaneously recorded physiological signals was analyzed. All the signals were sampled at a rate of 250 samples/second for the training data. We proposed a robust heart beat detection scheme consisting of three steps: 1) QRS detection using ECG signal, 2) removal of spurious beat detections using non-ECG signals, 3) interpolation of missing beats using both ECG and non-ECG signals. The robust heart beat detection scheme was tested with 100 hidden records, sampled at rates between 120 and 1000 samples/second, as a result for phase I of the challenge.

**Results**

Tested with 100 hidden records, the scheme achieved gross sensitivity of 85.52%, grosss positive predictivity of 93.02%, average sensitivity of 85.42%, and average positive predictivity of 91.65%. The overall score was 88.90%, which was the average of the four performance statistics.

**Conclusions**

In addition to ECG signal, non-ECG signals also contain useful information about heart beats, which can be used for robust heart beat detection, especially when ECG signal is corrupted by artifacts or missing. Step 2 in the proposed approach removes spurious beat detections due to corrupted ECG signal, and step 3 fills in missing beats due to missing ECG signal. Further improvement of steps 2 and 3 is being pursued.

# Predicting Heart Beats using Co-occurring Constrained Sequential Patterns

Shameek Ghosh, Mengling Feng, Hung Nguyen, Jinyan Li

University of Technology Sydney Australia
Massachussets Institute of Technology, USA
Institute for Infocomm Research, Singapore



**Aim**: The aim of this study is to develop and evaluate a robust method for heart beat detection using a sequential pattern mining framework, based on the multi-modal Physionet 2014 challenge dataset.
**Method**: Each multi-modal patient time series was initially transformed to a symbolic sequence using Symbolic Aggregation Approximation (SAX). A training set was created, by randomly selecting 70% of the data and the rest 30% was used as the test set. Later, all segments of length 100 were extracted, for annotated beat occurrences. Subsequently, an algorithm was used to extract repetitive frequent subsequences, where consecutive symbols are separated by a pre-defined gap range. The patterns for ECG and BP were then ranked based on length and frequency support. For tests, the highest ranked patterns were used to mark beat segments. True beat occurrences were only considered when patterns co-occurred for both ECG and BP within a width of 150 time points.
**Results**: Our results comprise two parts viz. extracted top ranked sequences and gross test statistics. An interpretive highest ranked sequential pattern for ECG looks like [7,7,7,5,5,5,5,5,4,3,10,10,10,2,2,3,3,4,3,4,5,5,5,6,7], for 10 discrete symbols which identify regional signal activity, with a gap range of [2,4] between contiguous elements. As per our test results, the method gives us a sensitivity of 51.66% and a positive predictivity (PPV) of 67.15%.

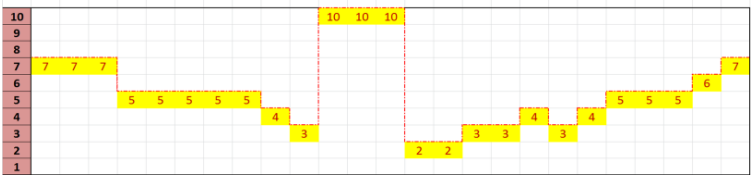


Figure I: SAX Approximated Long Range Sequential Pattern

**Conclusion**: The novelty of mining gap constrained co-occurring frequent sequential patterns lies in its ability to capture approximate co-occurring long clinical episodes across multiple variables, even if the quality of one signal suffers for a certain period of time. A higher PPV indicates that our method did not have a lot of false positives (detecting non-beats). The method is still being improved and will be further tested in the next stages of the Physionet Challenge 2014.

## *A Noise Robust Method for Recognizing the Heart Beats in Multimodal Data*

*Ali Ghaffari, Seyyed Abbas Atyabi, Mohammad Javad Mollakazemi*

*CardioVascular Research Group (CVRG), K.N.Toosi University of Technology, Tehran, Iran*

**Background**: Taking into account that electrocardiogram signal (ECG) is one of the most valuable noninvasive tools for monitoring of the heart electrical activity, reliable processing and detection of its parameters especially from the noisy ones has still remained to be a challenging task.



**Aim**: This study aims to develop a noise robust method for detecting the exact location of heart beats in continuous long-term data including electrocardiogram signal (ECG) and blood pressure signal (BP) that directly reflect cardiac activity.

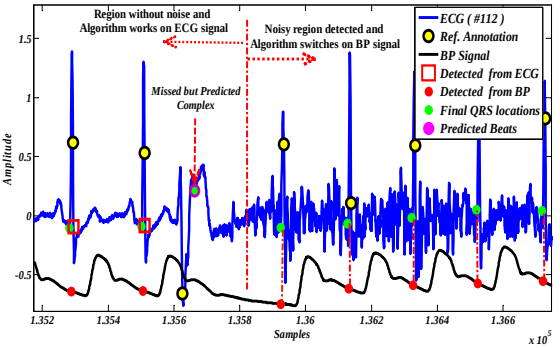


**Method:** In this study a wavelet based preprocessing technique is first implemented to the ECG signals. Then the proposed noise detecting algorithm is used to identify the remaining noisy parts of the signals. The algorithm is based on the estimation of noises of the detailed coefficients in the discrete wavelet transform. The QRS complexes in the ECG section with good quality are then identified from ECG signals. The exact locations of the heart beats in the noisy parts of the ECG signals are identified by switching the heart beat processing algorithm on the BP signals. The remained beat locations are predicted based on the criterion of the RR-interval of the earlier beats. As a final check, if some of detected beats are too close to each other, the wrong beat is identified based on the minimum error rate compared with the previous RR-intervals and is eliminated.

**Results:** Our proposed method was applied to the CinC challenge 2014 dataset. We participated to the challenge based on Octave entry and the preliminary average scores of this algorithm is 89.09% which shows better performance than the 88.89% accuracy obtained using the sample entry in octave.

## Rhythm-based Accuracy Improvement of Heart Beat Detection Algorithms

Zoltán Gilián*, Péter Kovács and Kaveh Samiee

Hungary

**Aims:** Our aim is to improve the accuracy of existing ECG-based heart beat detection algorithms in order to provide reliable heart beat locations for a multi-modal beat detection scheme.

**Methods:** Given an ECG signal, the QRS locations provided by the gqrs algorithm are processed by rejecting out-of-rhythm annotations and filling in gaps according to the median RR interval in a time window.

**Results:** The method was submitted to the first phase of the PhysioNet/CinC Challenge 2014 contest. On the corresponding training data set consisting of 100 records it has 99.55% gross sensitivity and 99.53% gross positive predictivity. On the hidden data set, the algorithm achieves 82.58% gross sensitivity and 94.85% gross positive predictivity.

**Conclusions:** Positive predictivity is still high in spite of the fact that the algorithm is based solely on ECG, however there is plenty of room for improvement regarding sensitivity. Since there are obvious cases where following rhythm is suboptimal, it is advisable to integrate other methods and signal modalities, such as blood pressure pulse intervals, into a multi-modal detection framework as our original aim suggested. Future work: To improve the aforementioned method, a novel beat detection algorithm based on rational modelling of ECG signals is being developed. Rational functions are fitted to the QRS complexes by means of numerical optimization and orthogonal expansion with respect to the Malmquist-Takenaka system. The model parameters provide features as a basis of detection.

# Identification of a signal for an optimal heart beat detection in multimodal physiological datasets

Johannes W Krug, Roman Schulte, Georg Rose

Department of Medical Engineering,
Otto-von-Guericke University of Magdeburg, Magdeburg, Germany



*Introduction:* This work is part of the PhysioNet/Computing in Cardiology Challenge 2014. The aim of this challenge was to improve the detection of heart beats based on simultaneously acquired physiological signals. The quality of one or more of these signals can be temporarily decreased by improper sensor placement, abrupt body movements, arrhythmic periods or environmental noise. Such segments need by automatically identified and other, simultaneously acquired signals which contain information about the cardiac activity should be used instead. The proposed algorithm combines the information of multimodal physiological signals to improve heart beat detection.

*Methods:* Depending on which physiological signals were available in the provided datasets, the proposed algorithm used a combination of the ECG, the blood pressure (BP) or the stroke volume (SV) signals. Due to the temporal nature of the signal distortions, each record was divided into several subsegments of the same length. Different peak detection algorithms were applied to the different signals of each subsegment. Each signal was rated with a quality index. It was used to identify one signal to be used for the heart beat detection. The quality index was estimated from the number of peaks and their location within the subsegment. Once each signal of a subsegment was rated with the quality index, the best rated signal was considered for the final peak detection. This identification procedure was then repeated for every new subsegment.

*Results:* In phase I of this challenge, the proposed method achieved an overall score of 99.98 % on the training dataset and of 90.04 % on the test dataset.

*Discussion:* For phases II and III of the challenge, additional signal features will be included to enhance the identification of a signal which is best suited for the heart beat detection. Peak detection algorithms will be modified to improve the detection quality in the identified signals.

# Robust Algorithm to Locate Heart Beats from Multiple Physiological Waveforms

Lars Johannesen*, Jose Vicente, Christopher Scully, Loriano Galeotti and David Strauss

CDRH, US FDA, Silver Spring, MD, USA
United States



**Introduction:** Alarm fatigue is a major issue in patient monitoring that could be reduced by merging physiological information from multiple sensors, minimizing the impact of a single sensor failing. We developed a heart beat detection algorithm utilizing multimodal physiological waveforms (e.g. ECG, blood pressure (BP), photoplethysmogram (PPG)) as part of the Physionet Challenge 2014. Algorithm Description: A 100 record training set from the Physionet Challenge 2014 was used for development. Heart beats are detected on ECG using a QRS detector based on a non-linear filter (U3). Pulses in BP and PPG traces are detected using a custom derivative-based peak finder. ECG annotations are first selected and beat-beat intervals that are longer than a pre-defined threshold are identified as gaps. Annotations from the BP and PPG signals, if available, are used to fill the gaps.

**Validation Method:** The algorithm was applied to the annotated training set. A true positive was declared if a beat was detected within 150 ms of an annotation. Gross and average sensitivity (Se) and positive predictive value (PPV) were determined from the true positives, false positives and false negatives.

**Results:** Gross and average PPV on the training set were 99.97% for the ECG detector alone as well as total algorithm. The Se of the algorithm (gross and average 99.82%) was higher than the ECG detector alone (gross 99.47%, average 99.49%). Applying the algorithm to the test set we achieved gross Se of 86.57%, gross PPV of 95.72%, average Se of 85.46%, and average PPV of 87.97%.

**Conclusion:** We developed a robust heart beat detector that fuses detections from BP and PPG signals with ECG annotations. The algorithm obtained equivalent PPV as the ECG detector alone but improved Se on the training set indicating it was able to fill annotation gaps. Data fusion approaches could improve patient monitoring.

# R Peak Estimation using Multimodal Lead Switching

Alistair E W Johnson*, Joachim Behar, Julien Oster and Gari D Clifford

University of Oxford
Headington, Oxford, United Kingdom

S51

**Introduction:** Most severely ill patients in the hospital are continuously monitored by both invasive and non-invasive equipment. These monitors provide synchronous waveforms with both complementary and independent information. Much work has been performed on R peak detection of the Electrocardiogram (ECG). Comparatively little has been done integrating estimates other signals, which has the potential of improving R peak detection when the ECG is noisy or missing. The Physionet/CinC 2014 challenge provided a multimodal dataset of 100 recordings for this task.

**Methods:** An R peak detector was developed based upon the energy of the ECG. The R peak detector included compensation for the refractory period and a search back algorithm for missing beats. A second detector based upon the length transform (LT) was also applied to the ECG. Additionally, similar detectors based upon energy and LT were applied to the blood pressure (BP) signal when available. The final positions of R peaks were then chosen based upon signal quality of the ECG, as defined by agreement between the energy and LT detectors. If the ECG was of poor quality, the R peaks were determined using the BP signal, if available. We submitted entries that comprised of only R-peak detection or fusing estimates from both the ECG and BP based upon SQI evaluation. The methods were scored using the average of the sensitivity and positive predictive value calculated record wise and annotation wise on a distinct set of 100 recordings.

**Results:** Our entry attained an overall score of 89.85% in phase one of the challenge. This is higher than the 89.83% sample entry and ranks 11th out of 48 participants.

**Conclusion:** While the technique improved upon the sample entry, there is still room for improvement. Potential avenues include fusing estimates from other signals and improving the estimation of signal quality.

# Robust Detection of Heart Beats in Multimodal Data Using Integer Multiplier Digital Filters and Morphological Algorithms

Urska Pangerc and Franc Jager*

Faculty of Computer and Information Science
Ljubljana, Slovenia

**Aims:** We aim to develop a new, robust, fast, gain independent and efficient heart beat detector in multimodal data using an ECG signal, and one of the pulsatile signals such as blood pressure (BP) if present.

**Methods:** To calculate the detection functions, simple and fast integer multiplier non-recursive digital filters implemented recursively were developed. To derive an ECG detection function, a module with a slope- and peak-sensitive, sampling-frequency adjustable band-pass filters, both approx. 10-24 Hz, was designed. Similar module was used to derive an ECG noise detection function containing filters with pass bands approx. 24-60 Hz. To derive a BP detection function, a slope-sensitive band-pass filter 1.1-3.6 Hz was designed. To further improve the shapes of the detection functions morphological signal processing with flat structuring elements was used. Using the top-hat transformation, fluctuations of the base of the ECG and BP detection functions are subtracted. Similarly, the morphological smoothing is producing a smooth stepwise envelope over the peaks of the ECG noise detection function but in the noisy intervals only. During the learning phase, the detector is adaptively seeking for four consecutive heart beats of which detection pulses and beat-by-beat intervals do not differ much (initially 20%). After that, the link between the ECG and BP signal (if present) and the gain-independent and adjustable detection thresholds are established. The detected heart beats are those being detected in the ECG or in the BP detection function. The positions of the heart beats within the noisy intervals are set according to their positions in the BP detection function or according to current heart-rate pattern.

**Results:** At the end of Phase I of the Challenge, the detector showed good performance. The total average score was 89.24%.

**Conclusion:** Further improvements of the performance is possible and expected. Real time implementation is possible.

# Respiratory Rate Effect in the Power of Pulse Photoplethysmogram Derived Respiration Signals

Jesús Lázaro, Raquel Bailón, Pablo Laguna,
Yunyoung Nam, Ki Chon, Eduardo Gil

BSICoS Group, Aragón Institute for Engineering Research (I3A), IIS,
University of Zaragoza
Zaragoza, Spain

S52

Parameters derived from the pulse photoplethysmographic (PPG) signal, such as pulse rate, amplitude, and width variability (PRV, PAV and PWV) have been previously proposed for deriving respiratory rate, obtaining less accurate estimates for higher respiratory rates (0.5-0.6 Hz). In this work we analyze the power of respiration related oscillations in PRV, PAV and PWV as a function of respiratory rate in controlled respiration experiments.

Smartphone-camera-acquired-PPG signals from 10 subjects breathing at constant rates from 0.2 to 0.6 Hz (with an increment of 0.1 Hz) during 2 minutes, using three different devices (iPhone 4S, iPod 5 and Samsung Galaxy S3) were analyzed. Powers of PRV, PAV and PWV respiration-related oscillations were estimated by integrating their Welch periodogram within a band of 0.05 Hz centred on the respiratory rate. The Friedman statistical test was used in order to study whether there are significant differences (defined as $p$-value$<$0.05) for different respiratory rates for each device.

Statistical differences were found between following groups: iPhone: 0.2 and 0.4 Hz, and 0.2 and 0.5 Hz for PWV, and 0.2 and 0.4 Hz for PRV; Galaxy S3: 0.2 and 0.6 Hz for PWV). Tendencies of decrease when respiratory rate increases were observed for powers from PRV and PWV for all devices:

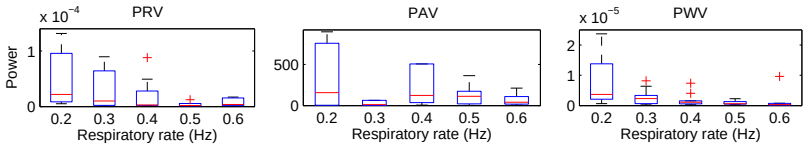


Estimated powers of PRV, PAV and PWV respiration-related oscillations for the Galaxy S3 device.

These results suggest that the strength of respiration-related modulations in PRV, PAV and PWV depends on respiratory rate. In case of PRV and PWV, this modulation has more power at lower respiratory rates than at higher rates. Therefore, obtaining accurate respiratory information based on these methods is more challenging in those situations at which the respiratory rate is high and could explain the performance degradation observed in previous works.

# Performance of the Low-frequency Power of the Maximal Value of the First Derivative of Arterial Pressure Waveform as a Sympathetic Activity Index

Salvador Carrasco-Sosa and Alejandra Guillén-Mandujano*

División de Ciencias Biológicas y de la Salud, Universidad Autónoma Metropolitana-I, DF, México
Mexico City, Mexico



The maximal value of the first derivative of the arterial pressure waveform (dAPmax) has been employed as a non-invasive measure of left ventricular contractile function. To document the possible autonomic influence on dAPmax beat-to-beat variability, we assessed the time-frequency spectra of dAPmax series during four maneuvers that produce different levels of autonomic activity, and examined the relations between dAPmax spectral measures and those obtained from RR intervals (RR), systolic pressure (SP), and respiration (Res) series. ECG, arterial pressure (AP), first derivative of AP and Res were recorded from 30 healthy volunteers during 5-min supposedly steady-state maneuvers: lying position (L), standing (S), controlled breathing (CB) and dynamic exercise (E). From RR, SP, dAPmax and Res series, auto- and cross-spectra were estimated using the smoothed pseudo-Wigner-Ville distribution to compute their low-frequency power (LFSP, LFdAPmax), high-frequency power (HFRR, HFdAPmax, HFRes), and the time-frequency coherence between HFdAPmax and HFRes. With respect to L condition, while LFSP and LFdAPmax increased progressively in S and E ($p<0.001$), HFRR and mean of RR decreased gradually ($p<0.001$). Correlations of LFdAPmax with HFRR and mean of RR were $-0.90\pm0.09$ and $-0.94\pm0.06$ respectively, and were greater ($p<0.001$) than the correlations with LFSP. HFdAPmax was greater in E ($p<0.001$) than in CB, during which HFRR was maximal ($p<0.001$). Coherence of HFdAPmax with HFRes was greater than 0.80 in all maneuvers. As indicated by heart rate variability spectral measures, the level of sympathetic activation was larger in E than in S. These indexes presented very strong correlations with LFdAPmax power, greater than with LFSP, which has been reported as a suitable sympathetic index. These results support that LFdAPmax performs better than LFSP as non-invasive sympathetic activity index. The striking increase of HFdAPmax in E condition, much greater than in CB, and its significant coherence with HFRes, document its mechanical respiratory origin.

# Sleep Stage Classification in Children Using Photoplethysmogram Pulse Rate Variability

Parastoo Dehkordi, Ainara Garde, Walter Karlen, David Wensley, J. Mark Ansermino and Guy A. Dumont

Electric and Computer Engineering in Medicine &
Department of Pediatrics
the University of British Columbia, Vancouver, Canada

S52

**Aim**- Human sleep is classified into Rapid Eye Movement (REM) and non-REM sleep. In non-REM sleep, the heart rate and respiratory rate decrease whereas during REM sleep, breathing and heart rate become more irregular. As such, identification of sleep stages by monitoring the autonomic regulation of heart rate is a promising approach. In this study, we extracted the variation of heart rate from the pulse oximeter photoplethysmogram (so-called Pulse Rate Variability (PRV)) to identify different sleep stages.

**Database**- The photoplethysmogram (PPG) was recorded from 142 children by the Phone Oximeter® in addition to overnight polysomnography. The children were suspected of having sleep disordered breathing and referred to the British Columbia Children's Hospital for standard sleep test.

**Method**- The recordings were divided into 1-min segments and labelled as wakefulness, sleep (REM or non-REM), non-REM and REM. For each segment, six standard time and frequency domain features of PRV were estimated. Two support vector machine classifiers were trained over two separate training data sets to classify wakefulness from sleep and non-REM from REM.

**Result**- When sleep progressed from awake to non-REM, the mean heart rate decreased reflecting the reduced sympathetic activity during non-REM. The spectral analysis of PRV showed the low frequency components of PRV to be diminished in non-REM sleep relative to wakefulness and REM sleep; the high frequency components of PRV was more pronounced in non-REM than in wake or REM sleep.

Wake and sleep were classified with an accuracy of 77% (sensitivity = 79%, specificity = 72%) and REM and non-REM were classified with an accuracy of 80% (sensitivity = 82%, specificity = 78%).

**Conclusion**- This study proposed a method to automatically classify sleep stages in children using PPG obtained from the Phone Oximeter®. This method would offer lower cost and higher portability with the potential of being used at home.

# Characterization of Pulse Transit Time and Photoplethysmogram Amplitude Dynamics in Sleep Apnea

Aziz El-Tatar*, Delphine Feuerstein, Laurence Graindorge, Amel Amblard, Jean-Louis Pépin, Alfredo Hernández

INSERM, U1099, Rennes, F-35000, France
Université de Rennes 1, LTSI, Rennes, F-35000, France

**Aims:** The purpose of this work is to characterize the dynamics of the photoplethysmogram (PPG) amplitude (PPGa) and the pulse transit time (PTT) during episodes of obstructive (OSA) and central sleep apnea (CSA), on adults suffering from severe Sleep Apnea Syndrome (SAS).

**Methods:** Ten overweight to obese adult male patients (age: 33 – 68, BMI: 26.28 – 47.02 $kg/m^2$) diagnosed with severe SAS (Apnea Hypopnea Index > 30 $h^{-1}$) were included in this study. They all suffered from both OSAs (OSA Index: 12 – 30 $h^{-1}$) and CSAs (CSA Index: 1 – 12 $h^{-1}$). PPG and PTT were extracted from polysomnography (PSG) records, acquired and manually analyzed at the Grenoble University Hospital, Grenoble, France. Signals were segmented into 60-second epochs, aligned around each annotated apnea event. Epochs including corrupted signals were rejected. PPGa and PTT were calculated from ECG and PPG signals for each epoch, and a mean response was calculated for each variable, according to the type of apnea. Paired signed-rank tests were performed to characterize the dynamics of the average PPG and PTT responses before and during apnea episodes.

**Results:** Significant differences ($p < 0.05$) were found in the PPG signal before and during apnea for all apnea types ($p_{PPG_OSA_before} = 0.625$, $p_{PPG_OSA_during} = 0.006$*, $p_{PPG_CSA_before} = 0.375$, $p_{PPG_CSA_during} = 0.002$*). On the other hand, the averaged PTT waveform did not show the same behavior as PPG for OSA, and presented a higher inter-patient variability ($p_{PTT_OSA_before} = 0.232$, $p_{PPG_OSA_during} = 0.131$, $p_{PPG_CSA_before} = 0.375$, $p_{PPG_CSA_during} = 0.037$*).

**Conclusion:** The findings suggest that PPGa seems to be a more robust indicator of cardio-respiratory changes during apnea than PTT. The analysis of the dynamics of PPGa may provide additional information for the automatic differentiation between OSA and CSA on patients with cardio-respiratory ambulatory monitors.

# Changes in Short-Term Blood Pressure Regulation in Adolescents with Type-I Diabetes Mellitus and Essential Hypertension

Eva Zavodna*, Zuzana Novakova, Magdalena Rohanova, Jana Stastna, Natasa Honzikova, Ludmila Brazdova and Hana Hrstkova

St. Anne´s University Hospital Brno
Brno, Czech Republic

S52

The aim of the study was to determine the relationship between the variability in systolic blood pressure (SBP) and RR-intervals (RRI) with respect to the baroreflex sensitivity (BRS) in adolescents with diabetes mellitus type-I (DM-I) and essential hypertension (EH). Blood pressure was recorded in 171 adolescents (130 healthy, 25 DM-I, 16 EH; 16-20 years) for 5-min (Finapres, metronome controlled breathing at a frequency of 0.33 Hz). The power spectra of SBP [mmHg2/Hz] and RRI [ms2/Hz] were calculated. BRS was determined by cross-spectral method. Adolescents were divided into groups according to the spectral power around the frequency of 0.1 Hz. The limits of power were estimated as percentils (33.3% and 66.6%) in group of healthy adolescents: high – hSBP≥103, hRRI≥10600; middle - 103≥mSBP≥50, 10600≥mRRI≥6200; low – lSBP<50, lRRI<6200. We analysed the relationships between the subgroups A(hSBP, hRRI), B(mSBP, hRRI), C(lSBP, hRRI), D(hSBP, mRRI), E (mSBP, mRRI), F(lSBP, mRRI), G(hSBP, lRRI), H(mSBP, lRRI), I(lSBP, lRRI). Group of DM-I has significantly higher SBP and RRI variability but no changes in BRS in comparison to healthy, however DM-I have in comparison with EH significantly higher BRS and RRI variability but there were no significant changes in SBP variability. We found significant changes in distribution of hypertensive and diabetic adolescents: DM-I and EH have significantly higher concentration in subgroup A than healthy controls ($p<0.05$), there is no significant difference in subgroup A between DM-I and EH; subgroup G contains significantly higher number of adolescents with EH ($p<0.01$) than healthy or adolescents with DM-I. Adolescents with DM-I are concentrated in area with high SBP and RRI variability which corresponds to the mean values of BRS. On the other hand, EH adolescents concentrate to the areas only with high SBP variability which corresponds to the low values of BRS.
Supported by European Regional Development Found (No.CZ.1.05/1.1.00/02.0123).

# Dynamics of Arterial Blood Pressure Components in a Conscious Sheep Model of Hemorrhage

Christopher G Scully, George C Kramer, David G Strauss

US Food and Drug Administration, Silver Spring, MD, USA



**Aims:** The aim of this study was to identify arterial blood pressure waveform variability measures that are potential markers of impending cardiovascular collapse in a conscious sheep model of hemorrhage.

**Methods:** Arterial blood pressure of adult sheep (7 sheep, N=14 experiments) was sampled continuously at 1,000 Hz for 5 min before and throughout a 25 ml/kg hemorrhage over ~15 min. Pulse-pulse interval, systolic blood pressure, and pulse pressure were determined for each beat and resampled to 20 Hz. The continuous wavelet transform (Morlet mother wavelet) was applied to each component and the spectral area over 1 min periods before and after the peak pulse rate was computed in 4 frequency domains: total 0.025-1 Hz, high frequency (HF) 0.15-1.0 Hz, low frequency (LF) 0.06-0.15 Hz, and very low frequency (VLF) 0.025-0.06 Hz. Dunnett's multiple comparison method was used for testing significance from baseline.

**Results:** The median time till the peak pulse rate was 10 min (range: 5-22 min) with a pulse rate increase from baseline of 80±27 BPM (mean ± SD). Pulse-pulse interval variability decreased in all frequency ranges around the peak pulse rate ($P<0.05$) with HF and LF decreasing up to 3 min and 1 min respectively prior to peak. Systolic blood pressure total power increased 1 min before peak pulse rate due to an increase in the contribution of VLF and LF ($P<0.05$). Systolic blood pressure VLF continued to rise while LF retreated to baseline levels after the peak pulse rate. Pulse pressure variability in each frequency region was stable before and after the peak pulse rate.

**Conclusion:** Pulse-pulse interval and systolic blood pressure variability measures changed distinctively during hemorrhage. Combining measures from both may be useful to understand and monitor compensation mechanisms.

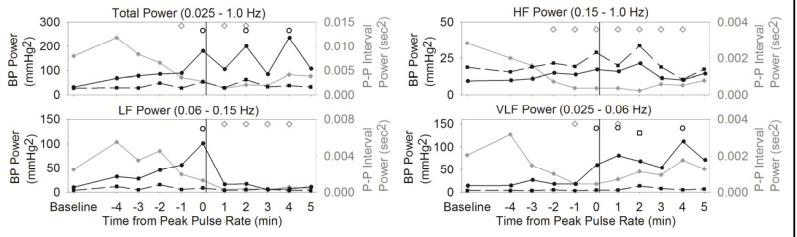


Wavelet powers before and after peak pulse rate (0 min) for systolic blood pressure (solid black), pulse pressure (dashed black) and pulse-pulse interval (gray). Open markers indicate significance from baseline ($P<0.05$).

# Automatic Detection of Left Ventricular Cardiac Aneurysms in Echocardiograms

Raziuddin Mahmood, Quan Wang and Tanveer Syeda-Mahmood*

IBM Almaden Research Center
San Jose, United States

S53

In this paper we address the problem of automatic detection of left ventricular cardiac aneurysms from 4-chamber views in cardiac ultrasound videos. Left ventricular cardiac aneurysms often manifest as bulgings in the myocardium causing an irregular distortion of the left ventricular shape from its normal bullet-like appearance. The method first locates the left ventricle using multi-level Otsu thresholding and selecting the dark region closest to the apex in a 4-chamber view. The apex of the heart is estimated from the point of intersection of the bounding lines of the viewing sector. By averaging the detection across the heart cycle using successive frames of the video, we obtain a mean thresholded shape. Using the apex as the reference point, the left ventricular boundary is regularly sampled into 100 points and a 5-dimensional scale-invariant feature vector formed by noting the curve position, angle of curvature, orientation of the normal, and the orientation of the two incident lines at a point along the curve. These feature vectors from labeled training videos of normal and left ventricular cardiac aneurysms were then used to train a support vector machine classifier using radial basis function kernels and unlabeled sequences were then classified. The method was evaluated on 400 normal and 254 cardiac aneurysms cases from the 123sonography ultrasound collection and the classification accuracy performance varied between 78%-92% using 20%-80% of the data for training thus demonstrating the validity of the approach for automatic classification of left ventricular cardiac aneurysms.

# CAPSU: a Completely Automated Method for Carotid Plaques Segmentation in Ultrasound Images

Francesca Galluzzo*, Cristiana Corsi, Carmela Morizzo, Luca De Marchi, Nicola Testoni, Nicolò Speciale and Guido Masetti

University of Bologna
Bologna, Italy

Carotid atherosclerosis (CA) diagnosis, usually guided by ultrasound imaging, is based on the assessment of the stenosis degree due to the presence of carotid plaques (CPs) and on plaques composition study. CPs segmentation (CPs-S) is a prerequisite for these evaluations. However ultrasound data characteristics make this task complicated and extremely operator-dependent. We propose CAPSU: a completely automated method for CPs-S in ultrasound images. It is based on level-set segmentation (LS-S) with an innovative initialization procedure that makes this approach completely user-independent. The initialization procedure focuses on a motion analysis whose results, combined with intensity distribution information, are used to produce a binary mask that constitutes the LS-S initialization. Particularly, a block matching algorithm is used to estimate motion between pairs of frames. The resulting displacement vector maps are then post-processed and used to differentiate image blocks belonging to CPs from ones belonging to blood or carotid walls. In addition, accumulated strain measurements have been computed to improve the differentiation between CPs and the carotid wall. Ultrasound sequences from 10 patients were acquired using a novel ultrasound advanced open platform for experimental research (ULA-OP). Selected frames were manually segmented by an expert sonographer. CAPSU performance were assessed by comparing manual and automated contours. Strain induced performance improvement was also evaluated. Average kappa index equal to 80% and 70% was achieved respectively with and without the strain computation. Average sensitivity and specificity values, respectively equal to 80% and 85% with the strain computation, were also improved in the range of 5% by exploiting the strain analysis. These results demonstrate the CAPSU effectiveness at achieving accurate CPs-S as well as a significant performance improvement obtained by introducing the strain analysis. CAPSU is shown to be an accurate and reliable tool for fully automated CPs-S in ultrasound images.

# Near-Automated Quantification of Prenatal Aortic Intima-Media Thickness from Ultrasound Images

G Tarroni[1], S Visentin[2], E Cosmi[2], and E Grisan[1]
[1] University of Padova, Italy; [2] University Hospital of Padova, Italy

S53

**Background.** Prenatal events such as intrauterine growth restriction (IUGR) and prenatal birth have been shown to correlate with increased rates of cardiovascular diseases (eg atherosclerosis) and metabolic disorders (eg diabetes) in adult life. Recent studies indicate that IUGR is associated with an increase in the abdominal aortic intima-media thickness (aIMT), which is thus considered an early biomarker for this condition. Unfortunately, the estimation of aIMT through ultrasound images (US) currently relies on error-prone and tedious manual tracing. The aims of this study were to develop and test a near-automated technique for aIMT quantification from US images.

**Methods.** After the manual selection of a region-of-interest containing the abdominal aorta (figure, left), the lumen is automatically segmented using adaptive thresholding and image components labeling based on shape metrics. Narrow-band statistical level-set methods are applied in the regions above and below the aortic lumen to segment the portions between the blood-intima and media-adventitia interfaces (figure, right, solid lines), allowing aIMT estimation on both walls through shape-based measurements. The technique was tested on 44 images acquired from 11 patients (4 images each). For performance evaluation, an experienced interpreter traced blood-intima and media-adventitia interfaces on all images (figure, right, dashed lines). Automatically and manually computed aIMT values were compared (on a patient-by-patient basis, separately for upper and lower aortic wall) by means of Bland-Altman, linear regression and correlation analyses.

**Results.** Excluding one outlier, automatically estimated aIMT values were in good correlation with manually extracted ones, especially for the upper wall (upper wall: R=0.92, lower wall: R=0.79). Bland-Altman analysis showed small biases (upper wall: -0.03mm; lower wall: 0.03mm) and narrow limits of agreement (upper wall: std=0.09mm; lower wall: std=0.10mm) compared to mean values (0.75mm).

**Conclusion.** Near-automated quantification of aIMT from US images using narrow-band statistical level-sets is feasible, and thus a potential alternative to manual analysis.

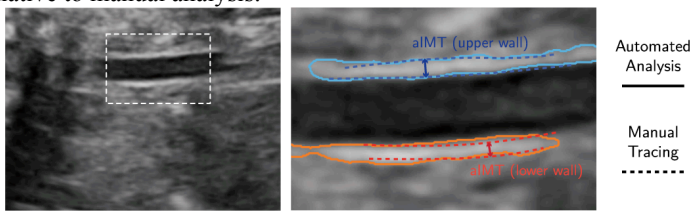

# Anatomical Structure Labeling in Apical Four-Chamber View Echocardiogram Images

Yu Cao*, Colin Compas, Hongzhi Wang and Tanveer Syeda-Mahmood

IBM
San Jose, United States

**Aims:** This work proposes a new method for anatomically labeling cardiac structures in echocardiography images. Echocardiography is a popular screening tool for many cardiac diseases and labeling anatomical structures in the images can assist in cardiac disease diagnosis by providing a framework for calculating geometrical statistics. General labeling algorithms often focus on stationary body structures and do not perform well in echocardiography due to cardiac motion, low signal to noise ratio, and structural deformation caused by diseases. In order to assess the proposed labeling algorithm the four cardiac chambers were automatically labeled in a single image from 50 patients, with 14 having normal cardiac anatomy and 36 being abnormal, with diseases including amalyoidosis, ventricular/atrial hypertrophy, and rheumatic heart disease.

**Methods:** We propose a new method for anatomical structure labeling that works on mid-level primitives (segments). The method defines a constellation model that has a score function that is designed to measure the consistency between a testing candidate configuration and the constellation model. The parameters of the score function are learned through a discriminative training framework. Given a test image and its corresponding multi-level segmentation, we use an MCMC-based sampling algorithm to infer a configuration that best fits the constellation model.

**Results:** The four cardiac chambers were manually segmented by an expert in the apical four chamber view of the echocardiogram. The proposed method was used to segment and label the chambers and the mean dice coefficient was found for each chamber compared to the manual segmentation. Left Ventricle: 0.702, Left Atrium: 0.673, Right Atrium: 0.678, and Right Ventricle: 0.542.

**Conclusion:** The proposed method for automatic segmentation and labeling of the cardiac chambers in echocardiography is an important first step for any automated analysis to be performed for detection of disease.

# Necrotic Tissue Distribution Analysis: Preliminary Investigation for Reducing Necrosis Overestimation in Intravascular Ultrasound Virtual Histology Images

Fernando J R Sales*, Breno A A Falcao, Joao L A A Falcao, Sergio S Furuie and Pedro A Lemos

Universidade Federal de Pernambuco
Recife, Brazil

S53

**Background:** The intravascular ultrasound (IVUS) Virtual Histology (VH) classifies the atherosclerotic plaque components, according to four classes – fibrous (FT), fibrofatty (FF), dense calcium (DC), and necrotic tissue (NC). Past works have proven a possible overestimation of necrotic content in VH images, particularly when NC is confluent to DC. Additionally, NC has been used as a severity marker for atherosclerotic plaque. Aiming to observe a possible correction rule for overestimation problem, an experiment was designed.

**Methods:** Eight patients have been submitted to stent implantation (PCI). VH examinations have been performed before (PRE) and after (POS) PCI, totalizing more them 300 frames. NC content was divided into two classes: RW and RP, which corresponds, respectively, to NC confluent to DC and not confluent. Grayscale IVUS images were processed to extract normalized intensity histograms according to NC classification. To compare these distributions, four metrics were selected: Earth Mover Distance (EMD), Bhattacharrya Distance (BHA), Symmetrised Kullback-Leibler Divergence (KLD) and Jensen-Shannon Divergence (JSD).

**Results:** Firstly, distances between RW and RP histograms were directly compared, according to PCI status: PRE or POS. The obtained results (mean +/- std) were: EMD_RW_RP = (24.66 +/- 4.84); BHA_RW_RP = (0.29 +/- 0.06); KLD_RW_RP = (1,87 +/- 1,37); JSD_RW_RP = (0.11 +/- 0.04). Additionally, distance between histograms for same classes in different moments (PRE and POS) was calculated. Obtained results were: EMD_PRE_POS = (8.46 +/- 6.66); BHA_RW_RP = (0.14 +/- 0.07); KLD_RW_RP = (0,37 +/- 0.07); JSD_RW_RP = (0.03 +/- 0.03). Between-classes distances were superior inner distances for every metric analyzed, as observed in visual analysis of distribuitions.

**Conclusion:** There are differences between intensity distributions RW and RP necrotic tissue, which may be useful to be considered to minimize overestimation of necrosis in VH images. These preliminary results encourage further investigation with larger sample sizes for proposing correction-imaging methods.

# Optimized Modelling of Maternal ECG Beats Using the Stationary Wavelet Transform

Fernando Andreotti, Hagen Malberg, Sebastian Zaunseder

Institute for Biomedical Engineering, TU Dresden
Dresden, Germany

P61

**Introduction:** Non-invasive fetal electrocardiogram (FECG) offers new diagnostic possibilities for prenatal medicine. Difficulties in separating maternal and fetal components from the abdominal signal mixture have hampered its use in clinical praxis. The Extended Kalman Filter (EKF) is a promising method to extract the FECG. However, EKF requires a dynamic model to estimate the maternal component. This model approximates an average maternal ECG beat through Gaussian kernels. Such approximation results in a non-linear optimization problem (finding ideal positions, width and height for these kernels). This contribution proposes a novel scheme that aims at improving the modelling by incorporating stationary wavelet transform (SWT).

**Methods:** In the literature, fixed positions are used to initialize the optimization procedure. We propose to use a quadratic spline wavelet and calculate a SWT by applying the algorithme à trous. The Gaussians are positioned at the low-pass scales' absolute maxima, which can be interpreted as correlation between the signal and the scaling function which is similar to a Gaussian. We apply the SWT model alone and, alternatively, use the found position as initialization for the non-linear optimization. For validating the proposed method, 23 five-minute abdominal recordings were used. Average beats were created every 30 seconds. The goodness of the fit was measured using the normalized mean square error.

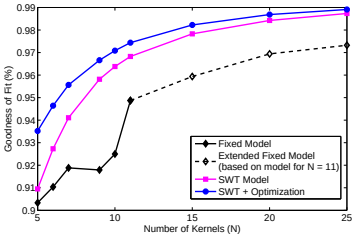


Figure 1. Comparison between fitting models in literature and proposed methods.

**Results:** Both approaches outperformed the models described in literature (see Figure 1). Average computational times for fixed model and SWT with optimization were similar, while SWT alone requires only 35.2% of the time.

**Conclusion:** The proposed methods are able to produce better beat approximations, while reducing the computational time. Such findings render the proposed method a promising tool for other applications (e.g. compression).

# Estimation of Atrial Fibrillatory Frequency by Spectral Subtraction of Wavelet Denoised ECG in Patients with Atrial Fibrillation

Jonathan Goodfellow*, Omar J Escalona, Philip R Walsh, Vivek Kodoth and Ganesh Manoharan

University of Ulster
Newtownabbey, United Kingdom

P61

**Introduction:** Dominant atrial fibrillatory frequency (DAFF) is a parameter which is useful in clinical decision making for patients with atrial fibrillation (AF). This study aimed to assess the estimation of DAFF by spectral subtraction after extracting ventricular activity (VA) in the AF-ECG by applying wavelet filtering.

**Methods :** Body surface ECG recordings from 20 patients with persistent AF who underwent internal DC-cardioversion were retrospectively analysed. A 20-second segment of baseline AF-ECG was isolated in each case. After Butterworth-bandpass and notch pre-filtering, QRST cancelation was implemented to resolve DAFF conventionally as the method for comparison. A different method for estimating DAFF incorporates 10-level decomposition via Daubechie's wavelet, wherein the AF activity was treated as noise and removed by selectively thresholding coefficients to obtain the VA signal. Denoising performance of wavelet filtering was assessed via 200ms noise-measuring windows placed within the TQ-intervals. Relative denoising performance was quantified with respect to noise level prior to pre-filtering (%). Denoising ability in TQ-intervals whilst preserving the QRST waveform was assessed by computing correlation coefficients between individual QRST-waveform segments and the corresponding average template. Using a similar method the wavelet filtering performance was quantified. The power density spectrum (PDS) of wavelet denoised AF-ECG was subtracted from the PDS of the original signal. DAFF was identified as the dominant peak in the 3-15Hz range and percentage similarity ratio of estimated DAFF values using both methods was quantified.

**Results:** The wavelet denoising performance was 90.50%±7.38% compared to 82.97%±15.25% for pre-filtering. A higher correlation in QRST-waveform segments was achieved via wavelet, 0.9840 vs. 0.9807 for the conventional technique. Estimated DAFF values presented 97.41%±2.93% similarity between the two methods.

**Conclusions:** Wavelet denoising provides improved performance, suitable for spectral-subtraction DAFF estimation, with high similarity to conventionally estimated DAFF values, avoiding the complexity of conventional QRST-cancelation due to the required time alignment process.

# Morphology-based QT Interval Measurement Using Frame-based Representation of ECG Signal

Alireza Ghodrati* and Abbas Babajani-Feremi

Biomedian LLC
United States

Acute increases in the QT interval can be observed in multiple clinical situations and are associated with an increased risk of syncope and sudden death from Torsades de pointes (Tdp) ventricular tachycardia. Current measurement techniques rely on sporadic manual methods by health care professionals with calipers on a printed ECG strip. Therefore, continuous and automatic measurement of the QT interval is highly valuable to complement the manual measurements. We propose a new method for QT interval measurement which first detects the morphology of the T-wave and then finds the T-end according to the detected morphology. The proposed method has more emphasis on detection of the T-wave morphology which helps more accurate detection of the T-end and better lead selection for QT interval measurement. To detect the morphology, we first find the characteristic points of the ECG signal between two consecutive QRS complexes and then represent the signal with primitive patterns connecting the characteristic points. Six types of T-wave morphologies(normal, invert, biphase +-, biphase -+, only upward and only downward) have been considered and a rule-based algorithm employed to detect the T-wave morphology by examining the primitive components. Followed by the detection of the morphology, the T-end is determined as the point on the signal that has maximum distance to the line representing the last segment of the T-wave. The proposed method has been tested against the QT database available on Physionet. The mean difference between the T-end in the reference annotation and the calculated one by our method is 0.9 ms and the standard deviation is 18.9 ms. The preliminary results are quite promising and future improvements of the method, especially incorporation of a multi-lead QT analysis algorithm, could considerably improve automatic and continuous monitoring of the QT interval.

P61

# Wave Sequence Based Identification of Sinus Rhythm Beats on a Microcontroller

Alexander Noack*, Rüdiger Poll and Wolf-Joachim Fischer

Fraunhofer IPMS Dresden,Germany
Dresden, Germany

P61

**Aims:** In the last years Holter recorders improved significantly in terms of battery lifetime, signal quality and computational capabilities. With these new resources the classic focus on ventricular arrhythmia detection slowly augments towards other long term applications like: atrial fibrillation detection, ST-T-segment evaluation, heart rate variability observation or calculation of heart rate turbulence. However, these methods prerequisite an accurate identification of physiological excited sinus rhythm beats to work properly.

**Methods:** For each detected beat an individual sequence of characteristic wave points is extracted (P-wave, iso-level and T-wave). The relative distance to the R-trigger of these sequence points as well as a morphology similarity value of the QRS-complex is then used to compare the current beat under inspection to neighboured beats. If these 4 values resemble sufficiently within the surrounding beats the morphology is considered to be a referenceable normal. Once labelled to be referencable a beat morphology can be identified as the dominant one, allowing to classify a beat as sinus even if the chronological sequence may be disturbed due to noise. However, in any other case the beat is labelled to be deviant.

**Results:** A sinus beat is considered to be true positive if it is labelled as normal in the reference annotation. Any other annotation (even fusion, atrial or supraventricular) is considered to be false positive . For BIH-MIT Arrhythmia Database the algorithm reached a sensitivity (Se) of 93,52% and a positive predictive value (+P) of 90,24%. Normal Sinus Rhythm database results are Se=98,56% and +P=99,65% respectively. The procedure was implemented on an Cortex M3 microprocessor and is running in real time.

**Conclusion:** A real time applicable high accuracy normal beat classification approach was developed. It allows an active beat by beat identification of sinus rhythm excitations to continue with comprehensive evaluations which rely on physiological conduction properties.

# A Signal Decomposition Approach to Morphological Modeling of P-wave

Ebadollah Kheirati Roonizi and Roberto Sassi*

Università degli Studi di Milano
Crema, Italy

**Aims:** Parameters derived from morphological modelling of P-waves, in electrocardiographical (ECG) recordings of patients suffering from paroxysmal atrial fibrillation, were shown to improve arrhythmic risk stratification. In this work, we compared different approaches for morphological modeling of P waves, based on signal decomposition.

**Methods:** Several basis functions including; discrete cosine transform (DCT) based models, Bézier, B-spline, and Gaussian functions were used for morphological modeling of signal-averaged P waves. The performances of the approximations were evaluated using compression efficiency measures, like the percentage of root-mean-square differences (PRD). The comparison between models was performed at a common fixed number of parameters (ranging between C=3 to 21).Nonlinear iterative parameter identification was employed for Gaussian models, while the parameters of the other basis functions were calculated through a closed formula. We tested the effectiveness of the several methods on the PhysioNet PTB diagnostic ECG database (386 subjects, 10 s each, 12 leads).

**Results:** DCT-based and B-spline models proved to be the most effective in following the details of the morphology (PRD: 0.51%±0.62%, 0.99%±0.96%, respectively, on lead V1 at C=21), possibly as they form an orthogonal basis for the specific signal. This property is not shared by Bézier curves and Gaussian basis functions (PRD: 2.47%±2.17% and 3.57%±6.83%). Correspondingly, the number of free parameters necessary to have a PRD<5% in lead II, increased: C=10 for DCT, 11 for B-splines, 15 for Bézier polynomials and 18 for Gaussian functions.

**Conclusion:** The four methods were able to follow the P-wave morphology in details and they could be successfully employed for subsequent ST analysis as well as wave amplitude assessment and model-based filtering (given the fact that the P-wave frequency content is mainly located in the low frequencies). When compactness of the model is an advantage, DCT-based and B-spline were found to be preferable.

# Reducing ECG Alarm Fatigue Based on SQI Analysis

Zehui Sun*, Jianwei Su, Chaocheng Xie, Jiao Yu, Wenyu Ye and Shen Luo

Mindray
Shenzhen, China

P61

**Background** Contaminated ECG signals may bring about an increased incidence of false positive monitor alarms causing alarm fatigue, which in turn can lead to missed or delayed alarm response. Some research aims to enhance the value of heart rate (HR) and reduce the false positive arrhythmia (ARR) alarms related to HR (sinus tachycardia, sinus bradycardia, asystole, etc). However, this approach cannot reliably reduce common false alarms if ventricular premature beats (VPBs), are involved.

**Objectives:** To reduce alarm fatigue, especially for the false alarms related to VPBs.

**Methods:** ECG signals are divided into five signal quality index levels (SQI): 0~4, where level 0 represents a noise free signal and level 4 indicates the worst signal quality. The key of the method is to judge the noise level by recognizing P, QRS, and T waves effectively. If the SQI value is found to be high, some strategies can be implemented to reduce alarm fatigue, including improvement of QRS classification of VPB-like QRS complexes, correction of some false ARR alarms, and standstill of HR value for a few seconds.

**Results:** The AHA and MIT-BIH database (DB1: consisting of 122 cases with less severe noise) and Mindray's monitoring database (DB2: consisting of 304 cases with significant severe noise) were used to evaluate SQI performance. Compared with the new method, QRS and VPB detection accuracies were almost the same based on DB1; however, the false ARR alarms of DB2 reduced from 17% to 3%.

**Conclusions:** The SQI analysis can reduce alarm fatigue effectively, not only for the false alarms without VPBs involved, but also for false alarms arising from ECGs with VPBs.

# Classification of Supraventricular and Ventricular Beats by QRS Template Matching and Decision Tree

V Krasteva[1], R Leber[2], I Jekova[1], R Schmid[2], R Abächerli[2]*

[1]Institute of Biophysics and Biomedical Engineering, Sofia, Bulgaria
[2]Schiller AG, Baar, Switzerland

P61

Automatic detection and classification of heartbeats is an important computerized diagnostic tool applied in monitoring applications and for assisting cardiologists in the task of long-term electrocardiogram inspection by marking the presence of sustained, transient or casual arrhythmias.

This study presents a system for heartbeat classification based on a real-time processing concept by a two-stage platform. The first stage is dedicated to initial assignment of beats towards continuously updated beat templates of the predominant rhythm, and to calculation of robust to noise features extracted from averaged templates rather than only considering single beat features. A set of 20 features is computed related to: matching a predominant, other or none beat template; presence of P-wave in beat and predominant template; correlation coefficient of the current, previous and next beats against the predominant template; QRS duration, relative QRS activity, QRS mobility (high/low frequency ratio) of the beat, the predominant template and the difference between both; duration of current/next RR-interval; RR-interval variability during the last 10 s. The second stage implements a classification tree for categorizing beats according to their supraventricular (SVB) or ventricular (VB) origin, applied only to those heartbeats, which are not matched to the predominant beat templates and assigned to SVB-class by the first stage. The training of the classification tree aims at selection of the optimal feature space by iterative minimization of the number of errors – both false positives in SVB-class and false negatives in VB-class considered at equal weight, which are particularly assessed by maximizing the mean value of sensitivity (Se) and positive predictivity (P+).

Independent datasets are used for training and test-validation – EDB, AHA, SVDB databases are involved in the training process, test-validation is done with MIT-BIH database. The performance of the two-stage beat classifier in terms of specificity (Sp), Se, P+ is shown in the table.

| **ECG database** | **Sample size** | | **Accuracy (%)** | | |
|---|---|---|---|---|---|
| | **SVB-class** | **VB-class** | **Sp** | **Se** | **P+** |
| AHA database | 164992 | 16488 | 99.8 | 94.7 | 98.0 |
| EDB: European ST-T database | 785992 | 4467 | 99.9 | 97.0 | 86.6 |
| SVDB: Supraventricular Arrhythmia database | 174553 | 9934 | 99.7 | 90.5 | 95.2 |
| MIT-BIH Arrhythmia database | 102205 | 7235 | 99.7 | 95.9 | 95.1 |

# Respiratory Rate Estimation from Multi-Lead ECGs using an Adaptive Frequency Tracking Algorithm

Leila Mirmohamadsadeghi*, Jean-Marc Vesin

Swiss Federal Institute of Technology
Lausanne, Switzerland

P61

**Purpose:** Estimating the respiratory rate (RR) from an electrocardiogram (ECG) is of interest, as its direct measurement involves uncomfortable and expensive equipment. The RR has already been estimated from the R-peak amplitude modulation (RPA). However, this estimate is not always accurate. In this study, the RR is estimated from multi-lead ECGs by using an adaptive frequency estimation algorithm to track the common respiratory frequency present in the RPA of several ECG leads.

**Methods:** The RPA waveforms from three leads were independently derived. A weighted multi-signal oscillator-based algorithm (W-OSC) was used to adaptively track the common frequency of two or three RPA waveforms. It was also applied to each RPA separately. This tracking algorithm is based on a band pass filter whose central frequency is updated using signal-to-noise ratio weighting from the inputs. A classical Fourier maximum-frequency estimate from each lead was computed as well for control. The algorithm was evaluated on a subset of 20 records from the Physionet MGH/MF dataset. This dataset contains leads I, II, an unidentified V lead and the respiratory impedance, digitized at a rate of 360 Hz.

**Results:** Table 1 reports that the RR estimates using the W-OSC algorithm with two or three RPA waveforms are more accurate than the Fourier-based estimates by an average of 2.0 breaths-per-minute. They are also more accurate than the RR estimates from each lead individually by an average of 1.73 breaths-per-minute.

**Conclusions:** Using the W-OSC algorithm with the RPA waveforms from two or three leads is beneficial compared to using it with one lead alone. In both cases, the estimates are more accurate than a Fourier-based estimate. This method provides an inexpensive RR estimate when a multi-lead ECG is available.

*Table 1: Absolute errors in breaths-per-minute of W-OSC and Fourier-based RR estimates.*

| W-OSC | | | | | | | Fourier-based | | |
|---|---|---|---|---|---|---|---|---|---|
| I & II | II & V | I & V | all | I | II | V | I | II | V |
| 3.28 | 3.10 | 3.18 | 3.00 | 4.99 | 4.67 | 4.95 | 5.58 | 4.99 | 4.87 |
| **3.14** | | | | **4.87** | | | **5.14** | | |

# QRS Detectors Performance Comparison in Public Databases

Mariano Llamedo, Juan Pablo Martínez

BSICoS, Aragon Inst of Eng Research, IIS Aragón, Univ of Zaragoza, Aragon, Spain
CIBER of Bioengineering, Biomaterials and Nanomedicine (CIBER-BBN), Spain

*Introduction*: The detection of heartbeats is an important step for several automatic analysis performed in the ECG signal. The objective of this work is to perform a thorough performance evaluation of QRS detectors in public databases.

*Materials and Methods*: We evaluated the performance of five QRS detectors, three of them freely available at Physionet, other was developed in our group (*wavedet*) and the last is *aristotle*, a commercial software. The five single-lead detectors were evaluated in 13 databases, grouped in four types: arrhythmia, long-term and stress. The performance evaluation was performed in terms of sensitivity ($S$) and positive predictive value($P^+$).



*Results*: Results show that detector *gqrs* achieved the best performance in 11 public databases, and our detector in other 2 databases. The median results presented as ($S$, $P^+$) are summarized in the following table for the best performing lead:

| ($S$, $P^+$) | Sinus | Arrhythmia | Stress | Long-term |
|---|---|---|---|---|
| *gqrs* | (100, 100) | (100, 100) | ( 75, 100) | (100, 100) |
| *wavedet* | ( 83, 100) | ( 99, 100) | ( 99, 100) | ( 99, 100) |
| *aristotle* | (100, 100) | (100, 98) | ( 79, 88) | (100, 100) |
| Pan-Tom | (100, 100) | (100, 100) | (100, 100) | (100, 75) |
| *sqrs* | ( 21, 21) | ( 40, 40) | ( 70, 20) | ( 21, 20) |

*Discussion*: The best performing detector achieved median performances above 75% in both $S$ and $P^+$, assuming that the best performing lead can be selected for each recording. Otherwise this performance decrease considerably depending on the database. The performance of *wavedet* was slightly lower to the performance of gqrs in general, but better in stress databases. In conclusion, *gqrs* and *wavedet* are the best overall detectors. *Wavedet* has the advantage of providing the delineation of ECG waves while *gqrs* is freely available on Physionet.

# An Algorithm for the Detection of ST Segment Elevation Relating to Induced Ischemia in Body Surface Potential Maps

Dewar Finlay*, Daniel Guldenring, Raymond Bond and Michael Daly

University of Ulster
Belfast, United Kingdom

P61

Criteria for the detection of ST segment elevation myocardial infarction (STEMI) in the 12-lead ECG are widely published. Such criteria allow highly specific detection of STEMI however sensitivity is low. Body surface potential maps have the potential to improve diagnostic performance by sampling information from areas of the torso not interrogated by the 12 lead ECG. In this study we investigate a BSPM STEMI detection algorithm that is based upon an extension of published 12-lead ECG STEMI criteria. The algorithm detects STEMI when J-Point potentials exceed predefined thresholds in two contiguous leads. Thresholds were set at 0.05 mV for posterior leads, 0.05 mV for right ventricular leads and 0.1 mV for remaining anterior leads with the exception of leads in close proximity to V2 and V3. Thresholds for leads in close proximity to V2 and V3 were set at 0.15 mV for females and 0.2 mV for males >= 40 years of age and 0.25 mV in males < 40 years of age. Our algorithm was applied to 45 subjects who had 120 lead BSPMs recorded during percutaneous transluminal coronary angioplasty (PTCA). A total of 90 BSPMs (j-point iso-potential maps) were studied representing the 45 subjects at baseline and the same 45 subjects during peak balloon inflation (15 left anterior descending, 15 left circumflex and 15 right coronary artery). When our algorithm was applied to BSPM leads STEMI, corresponding with peak balloon inflation, was detected with a sensitivity of 84.4% and specificity of 75.6%. Standard STEMI criteria, applied to 12-lead ECGs extracted from the same data, resulted in a sensitivity of 46.7% and a specificity of 95.6%. These results illustrate how applying current criteria, developed for the detection of STEMI in the 12-lead ECG, to BSPMs has the potential to increase sensitivity. This does however result in a reduced specificity.

## Trend Strips: a New Tool to Analyze RR Time Series

Antônio Carlos Silva Filho, Fátima Maria Helena Simões Pereira da Silva*, Júlio Cesar Crescêncio and Lourenço Gallo Júnior

Uni-FACEF - Centro Universitário de Franca
Ribeirão Preto, Brazil

There are many different tools and parameter that can be used to analyze RR time series, as the Correlation Dimension, the Lyapunov Exponents, the Higher Reconstruction Step and so on. Here we address the problem of discriminating between two populations: one with some cardiac disease and another with healthy people, in a no invasive way, through RR time series. The mathematical tool used to analyze the series is called Trend Strips (TS) and was proposed recently in the scientific literature. TS are a sequence of "0" and "1", where "1" means that the value in some position is greater than the value in a previous position in the series, while "0" means the opposite. We can use TS of any size, where the size is the amount of "0" and "1" considered. If we choose TS of size 4 we will have 16 different sequences at our disposal, from "1111" to "0000". What we do, then, is to compute the relative frequency of occurrence of each of them in a particular time series and to compare the frequencies in both groups. We collected RR time series from two groups of men at rest: one group with a cardiac chagasic disease (24 individuals) and a second one of healthy people (21 individuals). We analyzed TS of sizes from 2 to 5 and found significant TS that discriminate the two groups at all sizes. The statistical test used was a ttest and some of the TS useful, with a $p < 0.01$ were: (a) for n=2, TS "00" (p=0.0009); (b) n=3, TS "101" (p=0.0055) and TS "000" (p=0.0061); (c) for n=4, TS "1011" (p=0.0059), TS "1000" (p=0.0071) and TS "0001" (p=0.0073), etc. The set of significant TS can be useful, than, for diagnostic purposes. SUPPORT OF FAEPA-HC-FMRP-USP AND FAPESP AND CNPq

P61

# Morphological Analysis on Single Lead Contactless ECG Monitoring based on Beat-template

Jesús Hernández-Ortega*, Francisco-Javier Gimeno-Blanes, Jose-Luis Rojo-Álvarez, Rafael Maestre-Ferriz, Jose-María López-Ayala, Juan-Ramón Gimeno-Blanes, Arcadi García-Alberola, Andrés-Lorenzo Bleda-Tomás and Jose-Antonio Flores-Yepes

Universidad Miguel Hernández
Elche, Spain

P61

Introduction and Objective. In an attempt to implement a ECG model that does not require active participation from the individual himself, contactless sensors are playing a relevant role in recent research. Up to now, the extremely high contribution of the noise, only allowed to analyze heart rate information. In this work we propose a viable method to pre-process single lead raw contactless ECG records, without any pre-emphasizing, or amplification, to allow their morphological analysis. Method and Signals. Signals were obtained using Plessey contactless sensors in clinical environments, without any special noise restriction, by using a single lead sensor and following the instruction defined by the manufacturer. Sensors were placed in three different positions for obtaining the signals, namely, wrist, forearm, and back. In all cases, clothing was not removed, and sensor never had direct contact with the body. Processing. An initial segmentation based on statistical parameters was developed to discard invalid sections. Artifact removal filter was later applied on the previously selected valid segments. An effective RR detection method based on discrete derivative was applied. For each supposed QRS complex, considered as a window surrounding the detected R-peak, correlation analysis was performed, excluding for this process the ectopic beats and subsequent. Finally a smoothing statistical filter was applied to create a noise-less beat template where morphological analysis was then possible.

**Results:** The best configuration proved to be sensoring in the back (84% beats detected), while for the forearm and wrist it was 80% and 70%, respectively. Conversely, the best correlations among QRS complexes were obtained with wrist signals (71%), while forearm and back presented 63% and 62%, respectively. A higher number of beats are required for beat-template development, and so for morphological analysis.

**Conclusions:** Morphological analysis can be achieved in single-lead long contact-less ECG registers (>1 min).

# Internet based ST Map Software: A Web Service, a Decision Support System and an Educational Tool

Raymond Bond*, Dewar Finlay and Daniel Guldenring

Univeristy of Ulster
Newtownabbey, United Kingdom

ST segment values from a 12-lead electrocardiogram (ECG) are used to assess patients with suspected myocardial ischemia. The ST segment is assessed through interpretation of ECG complexes either presented on a computerised display or on paper printouts. Given ST segment changes can be missed in busy clinical environments, researchers have proposed alternative methods for visualising ST segment data. One such method is the ST Map and given this has recently been integrated into the clinical environment, we investigated the feasibility of a Web based system that could be used to further the acceptance and understanding of this approach.

**Methods:** An ST Map system was developed using ActionScript 3.0 (a programming language for Adobe Flash). The software uses ST values to display two ST Maps to represent the horizontal and frontal planes respectively. Each ST Map consists of 1mm concentric circles. The user can choose to visualise ST values as vectors or as polygons, which are both generated using simple trigonometric functions.

**Discussion:** The software is available online (http://tinyurl.com/a7dsvp9) and can be accessed on any device that supports the Adobe Flash Player. This tool can potentially be used as a decision support system where a user can input ST segment values and use the resulting visualisation to assist in making a diagnosis. This software can also be used as an educational tool for learning the relationship between the ST vector and the ischemic regions. Thirdly, the tool can be used as a Web service by other ECG machines/applications, i.e. an ST Map can be automatically generated by transmitting ST0 values through a REST (HTTP/GET) Web service. ST Maps can then be saved as image files (.PNG).

**Conclusion:** The authors developed ST Map software that can potentially be used as a Web service, a decision support system and as an educational tool.

# Normal Ventricular Repolarization Dispersion Range with Abrupt Heart Rate Changes

Pablo Daniel Cruces, María Paula Bonomini, Marcos Javier Teperino, Ana Mincholé, Pablo Laguna and Pedro David Arini*

CONICET
Ciudad Autonoma de Buenos Aires, Argentina

P62

Ventricular repolarization dispersion (VRD) constitutes a substrate for arrhythmias. We characterized the range of normal variations of different electrocardiographic indices of VRD responding to changes in heart rate (HR) induced by a tilt-test in healthy subjects as a criterion for lower bound risk stratification. The study group consisted of 17 healthy subjects (28.5±2.8 yrs), who underwent a head-up tilt-test trial according to the following protocol: 4-min in the supine position and 5-min in the standing position tilted head-up to an angle of 70°. We computed, using a multilead criterion to determine T-wave boundaries in the I, III, V1-V6 leads, the following ECG indices: T-wave onset-to-peak interval (TOP), T-wave peak-to-end interval (TPE), T-wave amplitude (TA), the ratio of the second to the first eigenvalues of the ascending (λ21A) and descending (λ21D) limb of the T-wave. The statistical analysis was realized by comparing the ECG indices in Supine position (Sp) versus Tilt position (Tp) using a two-sided Mann-Whitney U-test, being (*)$p<0.01$, (†)$p<0.0005$ and (NS)$p>0.05$. The results, Mean±SD, were: TOP(Sp)=147.75±1.84ms vs. TOP(Tp)=115.82±1.62ms(†); TPE(Sp)=120.79±4.86ms vs. TPE(Tp)=120.42±4.20ms(NS); TA(Sp)=2.13±1.05mV vs. TA(Tp)=1.54±0.76mV(NS); λ21A(Sp)=3.28±2.08% vs. λ21A(Tp)=1.85±3.14%(*) and λ21D(Sp)=2.38±3.61% vs. λ21D(Tp)=5.38±6.69%(NS). Results indicate that under abrupt HR increases, the ECG indices of the first half of the T-wave, TOP and λ21A, decrease significantly during Tp with respect to Sp, while ECG indices of the second half of the T-wave, TPE and λ21D did not change significantly with respect to Sp. Also, the TA decreased in Tp without statistically significant differences with respect to Sp. It was inferred that in healthy subjects, the duration dependency with HR of the action potentials is responsible for the inscription of the first half of the T-wave and are significantly modified by abrupt increases of HR while the second half of the T-wave, associated to the transmural VRD, remained unaltered.

## Repolarization Effects of Sertindole Manifest as T-wave Flatness on the ECG

Tanveer A Bhuiyan*, Claus Graff, Jørgen K Kanters, Jimmi Nielsen and Johannes J Struijk

PhD student
Aalborg, Denmark

**Introduction:** Sertindole's propensity to alter repolarization has been verified in both preclinical and clinical studies. Preclinical studies with dogs have shown prominent triangulation of the monophasic action potential, which has been found to correlate with flattening of the electrocardiographic T-wave. We have previously shown that the ratio of T-wave area to the area of a rectangle connecting the ascending and descending parts of the T-wave (relative T-wave area – RTA) is correlated to triangulation. RTA also attains maximum value just before onset of TdP arrhythmia in dogs. In this study, we sought to determine if RTA can also be used to assess the repolarization effects of sertindole in a clinical setting.

**Methods:** 12-lead ECGs from 37 patients were obtained at baseline and after switching to 16 mg sertindole. We also obtained recordings on baseline and treatment days for 55 moxifloxacin subjects - a safe and commonly used positive control in drug studies, and 57 placebo subjects. The effect on repolarization in each study arm was assessed by change from baseline in the RTA measurement of T-wave flatness.

**Results:** The sertindole-induced change in RTA was significantly greater than the change in RTA after moxifloxacin (0.05 vs 0.02, $p<0.001$). In contrast, there was no difference between the two drugs when changes from baseline were assessed by the Fridericia corrected QT interval (QTcF) - (13 vs 10 ms, $p=0.23$).

**Discussion:** The relative T-wave area (RTA) is a new measure of T-wave flatness that can be used to indicate abnormal repolarization in both preclinical and clinical studies of drug effects on cardiac repolarization.

P62

# Changes in the ST- and Ventricular Gradient Vectors over a Period of 20 Years

Marjolein De Jongh, C Cato Ter Haar, Sumche Man, Maurits Van der Heide, Roderick Treskes*, Arie C Maan, Martin J Schalij and Cees A Swenne

Leiden University Medical Center
Leiden, Netherlands

P62

**Background:** Ischemia detection in the ECG is essential for adequate triage at first medical contact in acute coronary syndrome. The current ST threshold of 100 μV has low sensitivity; however, a lower threshold of 50 μV requires intra-individual serial comparison with a previous non-ischemic ECG, to correct for preexisting nonzero ST amplitudes. Additionally, serial comparison of the spatial QRST area (ventricular gradient, VG; threshold 16.2 mV·ms) is useful for ischemia detection (Ter Haar, Comput Cardiol 2013;40:9-12). With serial analysis, the question emerges how long a previously-recorded non-ischemic ECG remains valid as reference ECG. We attempted to answer this question for the longest time interval that we could practically address.

**Methods:** We studied 114 patients (67/47 male/female, mean±SD age at baseline 41±12 years) of whom there were two non-ischemic digital ECGs >20 years apart in the hospital ECG database (created 1986 and comprising >800,000 ECGs). We analyzed the ECGs with our vectorcardiogram-oriented LEADS program, determined the ST and VG vectors and computed the magnitudes of baseline-follow-up differences, ΔST and ΔVG.

**Results:** At baseline, 85 (74%) patients had one or more cardiovascular diagnoses. At follow up, several new diagnoses had emerged. The ΔST value was >50 μV in 49% of the patients, and 90% had a ΔVG>16.2 mV·ms. As VG is known to depend on heart rate, we looked for a relation between ΔVG and the difference in heart rate between the baseline and follow-up ECG, but no correlation was found.

**Discussion:** The first results of our study suggest that ECG changes over 20 years due to emerging/developing disease, medication changes and ageing are considerable. More frequent sampling of the ECG than once per 20 years is required to obtain reference ECGs that are useful for serial ECG analysis intended to detect acute ischemia.

# Valuation of an Index Which Estimate the Heterogeneity of Ventricular Repolarization (V-index) by BSPM and Application to Patients with Early Repolarization Syndrome

Paola De Marco* and Irene Rossi

Politecnico di Milano/UPV
Italy

Spatial dispersion of ventricular repolarization is a property of the human heart and it's responsible for the genesis of the T-wave on the ECG. An amplification of such dispersion favours the development of ventricular tachycardia andfibrillation. Therefore, being able to assess repolarization heterogeneity from the ECG would be of clinical value for the prognosis of ventricular life-threatening arrhythmia and cardiovascular side effects of drugs. This is possible by using a biophysical model of the phenomenon, that approximates the standard deviations of cardiac repolarization time and links them to observable changes on the ECG. In order to obtain this we used an index, developed by Mainardi et al., that estimates the dispersion of ventricular repolarization, calculated through the ratio of the standard deviations of the lead factors measured across successive beats on the lead: v-index=std[w2(i)]/std[w1(i)] The aim of this work is to evaluate the clinical utility of the V-index and to understand how to use it for assessed cardiac risk. The first clinical trial was lead on Chagas disease. Here the index was applied to the Early Repolarization Syndrome that was considered a benign disease till now, but is proved that it causes arrhythmias that can take to sudden death. Moreover it's known that although a lower number of leads cause a lower error on the evaluation, this is simply due to a mathematical factor; on the contrary a larger number of leads is an advantage, since it converges to the actual value of the estimator. For this reason we decided to apply the V-index to BSPM signals (64-leads) compared to the results obtained with 3-12 leads. We expect to observe an high variation in the V-index, comparing the data collected from pathological and control subjects. The increase of the index implies that there is an increased risk of arrhythmias.

P62

# Lack of Specificity of the Moving Average Method for Detecting Alternans

David Mortara*

Mortara Instrument and UCSF School of Nursing
Milwaukee, United States

P62

The moving average method of detecting alternans, as originally described by Nearing and Verrier, does not address several factors that may impact its specificity. Omitted factors include the influences of RR interval irregularity and the harmonics of 4:1 processes like respiration. Also missing is a test for statistical significance. The relevance of these factors has been tested in a database of 383 recordings from a large trial on chronic heart failure patients (the GISSI-HF study). This database consists of 12-lead 24-hour Holter recordings with a sampling rate of 1000 Hertz. Non-overlapping 128-beat segments were analyzed to obtain the average odd minus even beat difference of normal beat pairs. The database provided 284,000 such segments, each with at least 36 odd/even pairs of normal beats. Only lead V5 was evaluated for alternans. 28,000 distinct 128-beat segments exhibited an alternans amplitude > 20 microvolts in at least one 20ms part of the average ST-T window odd/even differences. However, requiring this 20 microvolt amplitude to have three standard deviation significance reduced the number of alternans segments to 2759/28000. A non-zero mean difference (<DD>) of successive odd/even pair differences is a potential expression of a 4:1 process (an ECG modulation with a period of 4 beats). In this dataset, <DD> values were at least ½ of the alternans amplitude in 936/2759 segments cited above, leaving 1823 candidate alternans segments. Subjecting the RR interval sequence to a similar alternans analysis, and requiring that the RR sequence not exhibit 3 standard deviations of RR alternans further reduced the 1823 events above to 1008 segments. Finally, only 438 events remain if the ST-T is divided into only two windows of equal length, and these are tested for alternans in the same manner.

# The Accuracy of the EASI Derived Spatial QRS-T Angle

Daniel Guldenring*, Dewar Finlay, Raymond Bond, Alan Kennedy and James McLaughlin

University of Ulster
Newtownabbey, United Kingdom

There has been recent interest in whether the spatial QRS-T angle (SA) can be used in Thorough QT studies to serve as a marker for increased risk of torsades de pointes. The determination of the SA requires vectorcardiographic data. Such data is however seldom recorded in monitoring applications. Specifically the number and the location of the electrodes, that are required when recording the Frank VCG, complicates the recording of vectorcardiographic data in monitoring applications. An alternative and more practical way for obtaining vectorcardiographic data in monitoring applications is the utilisation of the EASI lead system. A previously published set of linear lead transformations allows for the derivation of the Frank VCG from the EASI lead system. This EASI derived VCG can be used for the determination of an EASI derived SA (ESA). The accuracy of the ESA has, however, not been reported in the literature. The aim of this research was the quantification of the differences between the ESA and the SA. This was achieved using electrocardiographic data recorded from 229 healthy subjects. To this end, the difference (ESA-SA) between the ESA and the SA was calculated for all 229 subjects. This difference was subsequently analysed in order to determine the systematic error (mean difference) and the random error (Bland-Altman 95% limits of agreement) that is made when determining the ESA. The systematic error (mean; p-value of the one sample t-test) between the SA and the ESA was found to be (4.30°; $p<0.001$). The random error (Bland-Altman lower limit of agreement; Bland-Altman upper limit of agreement) was found to be (-27.05°; 35.74°). The findings of this research suggest that both systematic and random error can not be overlooked when using the ESA as a substitute for the SA.

P62

## Electrocardiographic Abnormalities in Hypertrophic Cardiomyopathy

Ana Mincholé*, Rina Ariga, Stefan Neubauer, Hugh Watkins and Blanca Rodriguez

United Kingdom

P63

Hypertrophic cardiomyopathy (HCM) is a genetic disorder affecting 1/500 individuals and is the main cause of sudden cardiac death in young adults. HCM phenotype is characterized by localized thickening of the ventricular myocardium, myocardial-fiber disarray and electrophysiological and calcium subsystem remodeling. The manifestation of HCM-induced structural and electrophysiological remodeling in the ECG is still unknown but may potentially improve methods for risk stratification. In this study, we aim at quantifying ECG-based biomarkers in Holter recordings obtained in HCM patients and compared to those obtained in healthy volunteers. QRS complexes are analyzed to investigate the potential impact of abnormalities in activation sequence caused by structural-fiber disarray and wall thickening. ECG-based biomarkers such as T-peak to T-end interval (Tpe) and the QTc are also quantified to assess potential abnormalities in repolarization caused by mutations in sarcomeric genes, commonly found in HCM patients. Furthermore, biomarkers quantified during changes in heart rate are also investigated to identify potential changes in rate dependence in repolarization caused by HCM. In particular, we quantify a novel arrhythmic risk biomarker that accounts for spatial heterogeneity in the repolarization restitution dynamics, DRest. 50 12-lead Holter recordings (36 HCM patients and 14 controls) are analyzed and biomarkers computed in the lead with higher signal-to-noise ratio. DRest was computed in 19 HCM and 10 controls where significant heart rate changes were obtained. HCM patients display prolonged QTc intervals (HCM/Controls: 440/414ms, p-value<0.04), and higher values of DRest (0.065±0.03/0.035±0.02, p-value<0.02). Recordings also show a trend towards wider QRS intervals (92ms±13/87±13ms and longer Tpe intervals (98ms±14/93±7ms) in HCM, but the differences weren't found to be statistically significant. Biomarkers including a combination of conduction/repolarization (QTc) or rate dependence/repolarization (DRest) may be more specific to identify HCM than those accounting for repolarization or conduction individually. Higher DRest values in HCM patients are in agreement with in vivo studies suggesting a correlation between increased restitution dispersion and arrhythmic risk.

# Low Level and High Frequency Fragmentation of the QRS Changes During Acute Myocardial Ischemia in Patients with and without Prior Myocardial Infarction

Pedro Gomis* and Pere Caminal

Universitat Politecnica de Catalunya
Barcelona, Spain

**Introduction:** High frequency QRS (HFQRS) fragmentation and very-low amplitude abnormal intra-QRS potential (uAIQP) analyses have been used to track ischemic changes during coronary artery occlusions. The aim of this study is to assess the relationship between these two techniques in detecting acute myocardial ischemia and the effects of a previous myocardial infarction (MI).

**Methods:** Fifty-six patients who underwent elective percutaneous coronary intervention (PCI) procedures were selected. Patients were classified into 2 groups according to the presence of prior healed MI (old-MI) (n=18) or not (no_MI) (n=38). Continuous ECG before and during the PCI were recorded and signal averaged. uAIQPs were obtained using a signal modeling approach. HFQRS was obtained by filtering the ECGs through a 150 to 250 Hz band-pass filter. uAIQP and HFQRS indices were obtained from a baseline ECG and an occlusion-PCI ECG episode.

**Results:** uAIQP and HFQRS values decreased ($p<0.05$) for each of the 12 leads at the PCI event respect to baseline in all patients and the no-MI group. Old-MI group presented decreased values during ischemia in the limb leads in both indices. Changes in uAIQP or HFQRS did not separate the groups. uAIQP values at baseline were lower in all leads, except V1-V2, in the old-MI groups compared to no-MI ($p<0.05$). However, HFQRS values at baseline were similar in both groups. Pearson's correlation showed week relationship between uAIQP and HFQRS indices in most of leads. They were correlated in V2-V4 and V6 leads ($p<0.05$).

**Conclusions:** Very-low level fragmentation and HFQRS were reduced during acute myocardial ischemia mainly in patients without previous MI. uAIQP and HFQRS indices could add diagnostic value to ST analysis for diagnosing ischemia. Patients with old-MI presented lower uAIQP amplitudes compared to no-MI, however further studies are needed to elucidate the effects of old MI on very-low level fragmentation of the QRS.

P63

# Assessing the Accuracy of Limited Lead Recordings for the Detection of Atrial Fibrillation

Kerri Griffiths, Elaine Clark, Brian Devine* and Peter Macfarlane

University of Glasgow
Glasgow, United Kingdom

P63

**Introduction:** Atrial Fibrillation (AF) is a common cardiac arrhythmia which, if left untreated, can lead to ischaemic stroke. A number of small, low cost hand held devices which use a single lead I ECG to facilitate detection of a cardiac arrhythmia have recently appeared on the market. These devices could provide a valuable approach to community screening for AF but might be enhanced by the addition of an automated ECG interpretation.

**Aim:** To assess the accuracy of using limited lead ECG recordings for the detection of AF using the University of Glasgow (Uni-G) ECG analysis program.

**Methods:** A dataset comprising 210 12-lead resting ECGs was extracted from an existing database. Five ECGs were excluded from the study for various reasons. The final dataset consisted of 98 confirmed cases of AF and 98 confirmed cases of Sinus rhythm, 49 with PVCs and 49 with PACs, all of which were correctly reported by the Uni-G program and a further 9 cases of confirmed AF which had not been correctly reported by the Uni-G program. To simulate recordings made with a reduced number of electrodes, each 12-lead ECG was processed to generate two separate ECGs, one with only lead I available and another with only leads I and II available. A series of lead transformations was then applied to these limited lead recordings to construct 12-lead ECG data files for analysis using the Uni-G program.

**Results:** The sensitivity of reporting AF using a single lead ECG and a 2-lead ECG was identical at 93.8%. However, specificity was greater in the 2-lead ECG at 94.8% compared to 83.6% in the single lead ECG.

**Conclusion:** The results show that a single lead ECG or a 2-lead ECG recording could be effective in screening populations for cardiac arrhythmias.

# QRS and T Loops Area Changes During Haemodialysis

Iana Simova, Ivaylo Christov, Liliana Kambova, Giovanni Bortolan*, Tzvetana Katova

Institute of Biomedical Engineering ISIB - CNR, Padova, Italy

P63

**Background and objective:** Haemodialysis (HD) induces changes of the electrical activity of the heart which can be successfully analyzed by vectorcardiography (VCG). In the current study we are paying special attention to the QRS and T loops area – parameters that have not been used so far.

**Methods:** We studied 58 patients, age 59±13 years, 52% males, with renal disease duration 9.7±6.7 years and HD duration 5.2±4.4 years. We performed 1-minute ECG recording before and after HD session with determination of QRS and T loops area, maximal vector and QRS-T angle. Serum electrolytes (potassium-K, sodium-Na, phosphorus-Ph and calcium-Ca), urea and creatinine levels were evaluated before and after HD. Percentage change of the above mentioned parameters during HD was estimated.

**Results:** QRS loop area increased (see the figure) after HD (from 34.9 to 50.4 $mV^2/1000$, $p<0.001$), while T loop area did not change significantly. Maximal QRS vector increased (from 0.48 to 0.54 mV, $p<0.001$), maximal T-wave vector decreased (from 0.14 to 0.12 mV, $p<0.001$) and QRS-T angle remained relatively the same.

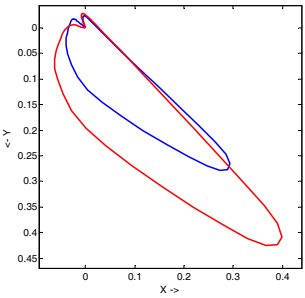
0
0.05
0.1
0.15
0.2
0.25
0.3
0.35
0.4
0.45
<- Y
0
0.1
0.2
0.3
0.4
X ->
Y ->
X ->
Z ->
Y ->
Z ->
X ->
Z ->
Y ->
Z ->
X ->
Y ->
Z ->
X ->
Y ->
Z ->
X

# Left Ventricular Hypertrophy Index based on a Combination of Frontal and Horizontal Planes in the ECG and VCG: Diagnostic Utility of Cardiac Vectors

María Paula Bonomini, Fernando Ingallina, Valeria Barone, Max Valentinuzzi and Pedro David Arini*

Facultad de Ingeniería, Universidad de Buenos Aires
Ciudad Autónoma de Buenos Aires, Argentina

P63

The changes that left ventricular hypertrophy (LVH) induce in depolarization and repolarization vectors are well known. We analyzed the performance of the electrocardiographic and vectorcardiographic horizontal planes (HP in ECG and XZ in VCG) and frontal planes (FP in ECG and XY in VCG) trying to separate out LVH patients from healthy subjects. In an age-balanced set of 51 patients (LVH: 26 patients, 68.6±11.4 yrs vs Control: 25 patients, 62.4±12.2 yrs), the directions and amplitudes of QRS-complexes and T-wave vectors in both planes were studied. Among several changes, we have used the most important results for the construction of a new LVH index (RT-ratio). The repolarization vector significantly decreased in modulus from Controls to LVH in the horizontal planes (HP: 0.45±0.17mV vs 0.25±0.13mV, $p<0.0005$; XZ: 0.43±0.17mV vs 0.28±0.11mV, $p<0.005$). Besides, the depolarization vector significantly decreased in angle in the electrocardiographic frontal plane (Controls vs LVH, FP: 50.33±33.66º vs 45.77±38.04º, $p<0.005$, XY: 19.13±39.76º vs 19.53±13.14º, NS). The RT-ratio combined information from the horizontal and frontal planes as the ratio of the depolarization vector angle in the frontal plane and the modulus of the repolarization vector in the horizontal plane. The performance of the RT-ratio was compared in both electrocardiographic and vectorcardiographic spaces. Notice that the information required for the computation of the RT-ratio can be easily obtained in the ECG space. The RT-ratio produced a better ROC curve in the ECG space (area under the curve AUC: 0.76, Sensitivity: 0.84, Specificity: 0.70) than in the VCG space (AUC: 0.50, Sensitivity: 0.53, Specificity: 0.50), providing an easy-to-obtain, efficient and clinically available ECG-based LVH index.

# The Loss of Multifractality as Evidence of Impaired Left Ventricular Ejection Fraction in Patients after Acute Myocardial Infarction

Fátima Maria Helena Simões Pereira da Silva*, Antonio Carlos da Silva Filho, Julio Cesar Crescencio, Valéria Papa and Lourenço Gallo Júnior

University of São Paulo/School of Pharmaceutical Sciences of Ribeirão Preto
Ribeirão Preto, Brazil

Multifractal analysis of heart rate variability (HRV) has been used to discriminate healthy subjects from patients with severe health conditions. We analyzed the fractal structures of the ECG recording of 11 patients who suffered acute myocardial infarction in order to identify those with impaired Left Ventricular Ejection Fraction (LVEF). We estimated the multifractal spectrum computed in Matlab code from the series of RR intervals,in supine rest. We noted that for 4 patients the parables representing the multifractal spectrum will be closing in small arcs, as a monofractal structure. The change in shape of multifractal spectrum curve for this group can provide information on changes in cardiac dynamics of patients with greater impairment of the muscles of the heart. We also compared the degree of multifractality defined as the width of multifractal spectrum. Moreover, all patients had undergone Doppler echocardiography and a quantification of left ventricular function was done by the Simpson technique (for LVEF less than 50% the patient was classified as belonging to the group with depressed LVEF). The Mann-Whitney test (p-value<0.01) revealed that the degree of multifractality for the group with impaired LVEF is very significantly lower than for the group with preserved LVEF. We concluded that the loss of multifractality may indicate an impairment of left ventricular ejection fraction in patients after acute myocardial infarction, but we could not measure the extent of this loss as an indication of greater or lesser severity.

## Extended Parabolic Phase Space Mapping (EPPSM): The Novel Quadratic Function for Representation of Heart Rate Variability Signal

Sadaf Moharreri[1]*, Nader Jafarnia Dabanloo[1], Saman Parvaneh[1,2]

[1]Islamic Azad University, Science and Research Branch, Department of Biomedical Engineering, Tehran, Iran

[2]University of Arizona, College of Medicine, Department of Surgery

P64

Poincare plot of RR time series demonstrate patterns of heart rate dynamics resulting from nonlinear processes.

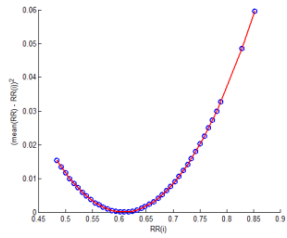


Estimation of a quadratic equation for point's distribution in HRV phase space.

In this paper, we have introduced Extended Parabolic Phase space mapping (EPPSM), a novel method for representation of heart rate which is obtained using RR interval time series signal consist of all the ordered pairs: $(RR_i, (\overline{RR} - RR_i)^2)$, $i = 1, \dots, N-1$ where $\overline{RR}$ is the mean of RR intervals. By analyzing the point's distribution in this map, we could estimate a two degree polynomial equation in the form of y = $Ax^2 + Bx + C$ in which y is $(\overline{RR} - RR_i)^2$ and x is $RR_i$. The useful features obtaining of this map are the coefficients *A*, *B*, and *C*.

These features were evaluated in distinguishing four groups of subjects (Arrhythmia, Congestive Heart Failure (CHF), Atrial Fibrillation (AF) and Normal Sinus Rhythm (NSR)) obtained of Physionet database. Kruskal-Wallis test was used to define the level of significance of each feature. The results show that these features discriminate CHF from NSR subjects by *p<E-5;* arrhythmia from NSR by *p<E*-7; and AF from NSR by *p<E*-6.

Advantage of this mapping is that the points overlapped with each other as a kind of compaction and so this map deletes the extra and useless information and just keeps the useful ones. Moreover, the resulted quadratic equation has the capability of being used as a prediction method for some kinds of cardiac arrhythmia.

# HRV Spectral and Fractal Analysis in Heart Failure Patients with Different Aetiologies

Elisa Fornasa*, Agostino Accardo, Martino Cinquetti, Marco Merlo and Gianfranco Sinagra

University of Trieste
Trieste, Italy

**Aims:** The purpose of the study was to evaluate how spectral and fractal HRV characteristics change in patients with heart failure caused by either dilated cardiomyopathy (DCM) or ischemic heart disease compared to normal subjects, so that these parameters, easily obtained from Holter recordings, can be used to discriminate between different aetiologies.

**Methods**: RR time series extracted from 24-hours Holter monitoring of 20 DCM and 20 ischemic patients, matched by age and sex with 20 normal control subjects, were retrospectively analysed. In order to minimize the effect of artefacts on the analysis, the RR time series were divided into intervals of 15min considering only those which had less than 5% of artefacts. Parameters calculated on these intervals were then averaged considering two different periods of six hours each, corresponding to day-time and night-time. The analysis considered the power spectra in the very low, low (LF) and high (HF) frequency range, the LF/HF ratio and Higuchi's fractal dimension (FD). Nonparametric tests were used to compare the results among the three groups.

**Results:** In the day-time all the proposed parameters showed significantly different ($p<0.009$) values for normal subjects and ischemic patients, while changes between all the three groups were significant ($p<0.02$) only for HF, LF/HF and FD measures. LF, LF/HF and FD values changed ($p<0.04$) between normal and ischemic group also in the night-time, but none of the proposed parameters showed differences between the DCM group and both the others, with DCM values intermediate between normal and ischemic ones.

**Conclusion:** Some of the examined spectral and fractal HRV measures present significantly different values among the considered groups, especially during the day-time epoch, and they may be profitably used in HRV feature identification of ischemic and DCM patients.

P64

# The analysis of human heart rate for healthy and ill patients using the recently published method Multiscale Multifractal Analysis

Dorota Kokosińska*, Jan Gierałtowski, Jan Żebrowski, Rafał Baranowski and Ewa Orłowska - Baranowska

Poland

P64

The subject of our research was the analysis of human heart rate, using the recently published method Multiscale Multifractal Analysis - MMA. The main goal was an attempt to obtain a correct diagnosis, based mainly on the results of MMA, which we used as a screening examination method. We analyzed 38 heart rate variability night-time recordings of healthy patients and 226 recordings of ill patients in four groups: 103 patients with aortic valve stenosis, 36 patients with hypertrophic cardiomyopathy, 15 patients with atrial fibrillation and 82 patients with cardiac arrest. We applied MMA - method developed at our lab, describing the scaling properties of fluctuations as a function of the multifractal parameter q and the scale s. The end result of the MMA is the Hurst surface h(q,s), where h is the local Hurst exponent, q is value of fluctuation and s is series length. We prepared 6 criteria quantifying mainly the local shape of the surface. The criteria were intended as a screening examination method and allow us to classify patients as healthy, when all of the criteria are fulfilled or ill, when at least one criterion was negative. In order to check reliability of applied method and defined criteria, we calculated measures of diagnostic test as sensitivity, specificity, positive predictive value and negative predictive value were respectively as follows: for patients with aortic valve stenosis: 81%, 74%, 89%, 58% , hypertrophic cardiomyopathy: 47%, 74%, 63%, 60% , atrial fibrillation: 100%, 74%, 60%, 100% and for patients with cardiac arrest: 69%, 74%, 85%, 53%. These results show that analysis of human heart rate based on MMA is promising. However, we believe that this method still requires improvement and a lot of tests in order to obtain higher values of measures of diagnosis accuracy.

# Time-domain, Frequency Domain and Non-linear Measurements in Infant's Heart Rate Variability with Clinical Sepsis

E Godoy, J Lopez, L Bermudez, A Ferrer, N Garcia, C Garcia Vicent, EF Lurbe and J Saiz*

Universidad Politècnica of Valencia
Valencia, Spain

**Aims:** Sepsis, a critical bacterial infection of the bloodstream, is a frequent cause of illness and death. It is important to look for parameters that can help to identify sepsis in the new born. Previous studies have shown that Heart Rate Variability is reduced when associated with sepsis and that pathological conditions diminish the adaptive capacity of the individual degrading the information transported by their signals. This study aims to evaluate the diagnostic value of parameters derived from Heart Rate Variability analysis in patients with clinical diagnosis of sepsis. Methods and

**Results:** To test for the statistical significance in discriminating between healthy neonates and sepsis diagnosed neonates we analysed the Inter-Beat-Interval derived from 90 minutes electrocardiographic recordings obtained from 14 sepsis diagnosed infants and 35 healthy infants at the Hospital General Universitario of Valencia. Statistically significant time-domain measures ($p<0.05$) of the time series (mean value and standard deviation of the normal-to-normal interval) or the geometric measures (triangular interpolation of the normal-to-normal interval histogram) produced paradoxical results comparing sepsis with healthy subjects. In the case of frequency-domain analysis of Heart Rate Variability, separating sympathetic and parasympathetic activity, the low-frequency power ($p<0.05$) and low / high frequency ratio ($p<0.05$) were reduced in subjects with sepsis (3.9 vs 2.9); conversely high-frequency power was significantly ($p<0.05$) higher in the sepsis group. Non-linear measures such as Detrended-Fluctuation-Analysis technique showed no significant differences between the two groups; and Sample-Entropy measurements showed significant difference between groups ($p<0.01$) and lower values in subjects clinically diagnosed with sepsis (1.3 vs 0.84) suggesting lower Inter-Beat-Interval signal complexity.

**Conclusions:** Heart Rate Variability analysis shows differences between neonates with clinical sepsis and healthy neonates. Although these differences are present, no single technique would be capable of characterising and differentiating sepsis from healthy time series; rather a set of techniques would be necessary.

P64

## Nonlinear Features of Neonatal Heart Rate Dynamics

Barbora Czippelova*, Lenka Chladekova, Zuzana Turianikova, Ingrid Tonhajzerova, Kamil Javorka, Zuzana Uhrikova, Mirko Zibolen and Michal Javorka

Jessenius Faculty of Medicine, Comenius University, Slovak Republik, Martin, Slovakia

P64

Purpose The aim of this study was to investigate the short-term heart rate variability (HRV) as an index of the cardiac autonomic control development in healthy full-term neonates compared to the adults using various new complexity and irreversibility measures. Methods HRV in 20 healthy full-term neonates was compared to HRV recorded in healthy young adults. Besides traditional time (meanRR, SDRR, rMSSD) and frequency domain (LF, HF) measures, we assessed HRV complexity measures including normalized complexity index (NCI), normalized unpredictability index (NUPI), pattern classification (0V%, 1V%, 2LV%, 2UV%) and multiscale irreversibility indices (P%, G%, E). All measures were derived from data segments of 1000 RR intervals. The multiscale analysis was performed on four time scales and the presence of irreversibility was assessed by surrogate data analysis. Results HRV magnitude was significantly reduced in the neonatal group compared to the adults. HRV complexity measures, i.e. indices NCI, NUPI and pattern indices 1V%, 2LV%, were also significantly reduced. Pattern classification parameter 0V% and Porta's irreversibility index P% showed significant increase in newborns compared to adults suggesting an increase in sympathetic activity. Surrogate data analysis revealed asymmetrical nature of the HRV series present already in the neonatal age and no between-group differences of the irreversible series percentage for all irreversibility indices and for all time scales. Conclusions Novel HRV measures showed between-groups differences in the complexity and irreversibility of the HR suggesting the shift in the sympathovagal balance of neonates towards sympathetic predominance. Supported by grant VEGA 1/0059/13, VEGA 1/0223/12, APVV-0235-12 and Project ESF IV "The increasing of opportunities for career growth in research and development in the medical sciences", ITMS: 26110230067

# Continuous Information Extraction from Blood Pressure Data Using Reconstruction of Attractors

Philip J Aston, Manasi Nandi, Mark I Christie, Ying H Huang

University of Surrey
Guildford, UK

P64

**Aims:** This work aimed to extract continuous information from a blood pressure signal which could be used for the early detection of sepsis.

**Methods:** Cardiovascular data are usually viewed as a time trace in which only the increase or decrease of the blood pressure can be readily observed. Our method extracts information from the blood pressure signal by viewing it in a reconstructed phase space, factoring out the vertical motion, and extracting less obvious changes in the signal.

A window of blood pressure data is used to reconstruct an attractor in a three-dimensional phase space using time delay coordinates. The time delay parameter $\tau$ is chosen to be the average of the cycle lengths in the data. This attractor is projected onto a plane in order to factor out the vertical motion in the signal and a density is generated from the attractor (see Fig. 1).

From this density, a variety of scalar measures can be extracted. The window is moved through the data and a time trace of the scalar measures is generated. A mathematical analysis of a periodic signal provides a means of relating the scalar measures derived from the density back to particular features of the (aperiodic) blood pressure signal. A strength of this method is that it analyses all of the data, taking account of the shape of the waveform, not just a sample or beat-to-beat intervals.

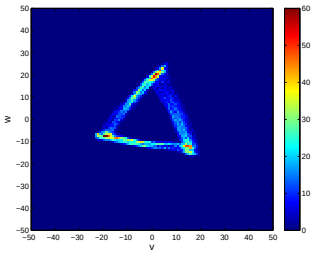


Figure 1. Density from a reconstructed attractor.

**Results:** Clear changes in the time traces of the scalar measures are observed where there is no obvious change in the blood pressure signal. Data from a healthy mouse and a mouse with sepsis were analysed. Some of the time traces showed clear differences when comparing healthy and early stage sepsis data.

**Conclusion:** This new approach of analysing blood pressure data can detect the early onset of sepsis in a mouse.

## Analysis of Maternal-Fetal Heart Rate Coupling with High Resolution Joint Symbolic Dynamics

Ahsan Khandoker, Andreas Voss*, Steffen Schulz, Miyuki Endo, Yoshitaka Kimura and Marimuthu Palaniswami

Khalifa University
United Arab Emirates

P64

Maternal psycho-physiological activities affect the fetal heart rate and heart rate variability. However, origins and patterns of maternal and fetal heartbeat coupling are still poorly understood. The aim of this study was to quantify short-term maternal-fetal cardiac couplings in early, mid and late gestation fetuses by using the high resolution joint symbolic dynamics (HRJSD) analysis approach. The analysis was based on foetal electrocardiograms (FECGs) of 66 healthy fetuses [22 from 16~25 weeks (GA1), 22 from 26-30 weeks (GA2) and 22 from 32-41 weeks (GA3)]. Results demonstrate that HRJSD revealed eight significant pattern families that were able to differentiate patterns of heart rate coupling among three gestational groups. In conclusion, the application of HRJSD revealed detailed information about short-term nonlinear maternal-fetal cardiac couplings and regulatory mechanisms (patterns) of developing autonomic nervous system function.

# Recurrence Quantification Analysis of Heart Rate and Blood Pressure Variability in Obese Children and Adolescents

Zuzana Turianikova*, Ingrid Tonhajzerova, Barbora Czippelova, Kamil Javorka, Zuzana Lazarova and Michal Javorka

Jessenius Faculty of Medicine in Martin, Commenius University in Bratislava
Martin, Slovakia

P64

**Introduction:** Obesity is a rapidly growing complex medical problem having a pandemic characteristics nowadays. Obesity now increasingly occurs already in childhood. The large importance of negative influence of pediatric obesity is evidenced by the linear dependence between the severity of overweight/obesity and cardiovascular complications risk in adulthood. The change in the autonomic nervous system activity is an important factor contributing to initiation and progression of various cardiovascular complications of obesity. We propose that novel nonlinear dynamics based measures of heart rate and blood pressure dynamics will be more sensitive for detection of cardiovascular autonomic dysregulation in otherwise healthy obese children and adolescents.

**Aim:** The aim of this study was to detect the presence of cardiovascular dysregulation using various nonlinear measures and compare their performance with linear heart rate and blood pressure variability (HRV and BPV) analysis.

**Methods:** We examined 40 obese children and adolescents, mean age 14.7±0.3 (SEM) years and 40 age and gender matched control subjects. Continuous finger arterial blood pressure was measured in supine position by photoplethysmographic volume-clamp method (FinometerPro, FMS, Netherlands). ECG signal was recorded from bipolar thoracic lead (Cardiofax ECG-9620, NihonKohden, Japan). Resulting HRV and BPV time series (2000 heart beats length) were analysed using linear (time and frequency domain) and nonlinear analysis, including symbolic dynamics, multiscale entropy analysis and recurrence quantification analysis (RQA).

**Results:** No significant between groups differences in BPV dynamics were detected. In HRV analysis, only RQA measures were able to detect a reduction in cardiovascular control complexity associated with obesity.

**Conclusion:** We conclude that RQA is the most sensitive method to detect subtle abnormalities in heart rate dynamics associated with obesity. Supported by grants VEGA no. 1/0059/13 and APVV-0235-12.

## Multiscale Cardiovascular Autonomic Modulation Following Treatment in Patients with Anorexia Nervosa

Herbert F Jelinek*, David J Cornforth, Sera P Lam, Janice Russell and Ian Spence

Australia

P64

Alteration in sympathovagal balance may be a mechanism of increased cardiovascular mortality and sudden death of patients with eating disorders. This study investigated multiscale HRV analysis of 5-minute short-term R-R interval recordings, in order to identify possible changes in the autonomic control of the cardiovascular system in subjects with anorexia nervosa. We investigated HRV in a group of patients with anorexia nervosa at admission and following a 6-weeks treatment program. HRV was assessed from a standard 3-lead electrocardiogram which was digitized and analysed using Chart® software. HRV analysis included time and frequency domain measures as well as multiscale Renyi entropy of 5-minute R-R interval tachograms recorded during supine and standing position. Preliminary analysis suggests that anorexia nervosa has altered cardiovascular sympathovagal balance and loss of complexity with emergence of more regular ECG patterns. HRV and Multiscale Renyi entropy in particular may prove as useful diagnostic and prognostic tool in anorexia nervosa, particularly in clinical monitoring of patients with increased risk of cardiovascular complications and sudden death.

# An Android Application for ECG Processing

Rene Ivan Gonzalez-Fernandez* and Margarita Mulet-Cartaya

IFMBE/Central Institute of Digital Research
Havana, Cuba

**Aims:** This paper is focused on the discussion of the main features implemented in an Android application for ECG processing.

**Methods:** The software was designed to use a mobile phone, connected to a battery-powered ECG device, as a signal acquisition layer in a Telemedicine platform oriented to implement several health services. The ECG device is able to acquire and transmit, via Bluetooth, the ECG continuously. The Android application receives the ECG data according to a simple protocol. The Bluetooth pairing process is made by the proposed software following the traditional procedure. ECG data is filtered using a FIR moving average filter. QRS complexes are detected and classified, as premature or not, RR intervals are measured and heart rate is computed. An energy collector, combined with heuristic rules, was implemented to detect QRS complexes. The classification process is made taking in count RR interval duration and QRS complex width. All these information is uploading to a web site using GSM/GPRS network and HTTP protocol. Also, all the data is store in a database implemented in the phone; this feature allows downloading that information into a personal computer to make other studies. The software was programming in Java language using Eclipse SDK and SQLite database engine. Results: The proposed software has been tested with five models of Android mobile phones, working without problems. Errors have not been reported in communications when the distance between the ECG device and the phone is less than ten meters. QRS complex detection algorithm was tested with MIT-BIH database and the QRS detection sensitivity was 98,77%.

**Conclusions:** The developed software seems a powerful tool to convert a mobile phone, combined with the appropriated ECG device, in a medical device for several Telecardiology services. Also, an event recorder or a medium-term Holter can be implemented.

P65

# Design and Optimization of an ECG Holter Hybrid System for Mobile Systems based on DSPIC

Flavio Pineda-López*, Andrés Martínez-Fernández, José Luis Rojo-Álvarez and Manuel Blanco-Velasco

Universidad de Rey Juan Carlos
Fuenlabrada, Spain

P65

This paper presents the architecture of a portable system that enables the acquisition, processing, storage and transmission in real-time of a 12-lead standard ECG, the system can also be used as long-term Holter. The prototype was designed using a DSPic 33FJ256GP710 module to achieve efficient local processing such as compression with filter banks based on Nearly Perfect Recontruction Cosine Modulated Filter Bank, ECG data acquisition with the new ADS1198 (Low-Power, 8-Channel,16-Bit Analog Front-End for Biopotential Measurements) and memory management for local storage when working in offline mode. The system was connected to a smartphone through a Bluetooth module, which allows two working modes: Display, storage of the ECG signal in the smartphone and Display, transmition ECG signal for remote diagnosis and patient history storage. The system has a flexible design allowing recording of ECG Data either locally in the cell phone or in the cloud. Additionally, either lossless or lossy compression can be chosen during transmission. The preliminary analysis of the system was carried out with data taken from the Physionet dataset in order to determine its correct performance in three modalities: In local mode, a recording time of over 120 hours has been achieved, 10 days data was stored on the phone and an unlimited time was stored on a remote server. The storage capacity can be increased by a factor of six, if the compression process of the ECG signal is performed before saving. For remote signal visualization, the average delay of the packets is less than 1.73 ms with a mean power consumption of 0.48 w/h. In these conditions, the data acquisition time achieved was higher than 12 hours using a battery of 2 A/h such as that of a cellular phone.

# Analysis of Heart Rate Changes in Newborns to Investigate the Effectiveness of Bag-Mask Ventilation

Huyen Vu*, Trygve Eftestøl, Kjersti Engan, Jørgen Linde

University of Stavanger, Stavanger, Norway

P65

**Objectives**: The increasing in heart rate could be the indication of successful manual bag-mask ventilation. ECG and ventilation signals were detected and parameterized into relevant information to explore the relationship between those therapeutic parameters and the changing in heart rate to identify the determinant factors of the effective ventilation.

**Methods**: The dataset contains 172 cases. To characterize resuscitation performance, six parameters detected from bag-mask ventilation sequences by using pressure and flow signals were defined: average bag-squeezing frequency, average peak inspiratory pressure (PIP), initial pressure, ratio between total time of bag-squeezing events and total resuscitation time, average inspired volume and average expired volume.

The RR intervals longer than a threshold were considered as ectopic beats and replaced by linearly interpolated beats. RR interval at a specific point of time was calculated by using piecewise cubic interpolation of 4 RR intervals surrounding that point. The instantaneous heart rates measured at the beginning and at the end of each ventilation sequence were the inverse of corresponding RR intervals.

P-value method was used to test the statistical significance among groups of babies with a specific outcome to investigate if any of these ventilation parameters could be significant. The criteria for grouping patients was the delta heart rate (DHR) defined as the last measured heart rate - the first measured heart rate of an episode. Group 1 had DHR $<=$ threshold and group 2 had DHR $>$ threshold.

**Results**: P-values below significance level (5%) were found for some of the ventilation parameters: average bag-squeezing frequency (1.85%), average PIP (0.10%), initial pressure (0.001%), ratio between total bag-squeezing time and total resuscitation time (0.03%).

Significant p-values of ventilation parameters

| Ventilation parameters | P-values (%) |
|---|---|
| Average squeezing frequency | 1.85 |
| Average PIP | 0.10 |
| Initial pressure | 0.001 |
| Ratio squeezing/total resuscitation time | 0.03 |
| Average inspired volume | 10.88 |
| Average expired volume | 7.38 |

**Conclusion**: This data analysis framework indicates a promising approach to discriminate groups of patients and generate hypotheses about the determinant ventilation variables to improve treatment on asphyxiated newborns.

# Proof of Concept for an International Long-time Preservation ECG format

Roberto Sassi*, Luca Sparagino, Norman L Stockbridge, Juan Guadiana and Fabio Badilini

Università degli Studi di Milano
Crema, Italy

P65

ECG systems by most manufacturers provide the possibility of exporting traditional 12-lead printouts in common formats (e.g., ISO 32000-1:2008 Portable Document Format). These printouts permit some interpretation; however, often only a portion of the data are included and, even worse, any analysis from the picture is limited by printing resolution. Raw digital ECG data would facilitate subsequent quantitative assessments, with a clear advantage in diagnosis. In fact, more than 10 years ago, the need for fully reviewable ECGs led the US Food and Drug Administration (FDA) to require digital submission of ECG waveforms and annotations employed in the cardiac evaluations of new drugs. A specific Health Level Seven (HL7) XML-based annotated ECG standard (aECG) was designed by several partners, leading to a format that ANSI adopted. While digitally is the right way to store and preserve records, standard paper printouts remain a preferred and frequent choice of clinicians, because of portability. We present a proof of concept that combines a digital ECG and a standard graphical report. Our solution is based on the very recent PDF/A ISO 19005-3:2012 standard, which dictates an electronic document format for long-term preservation. The proof of concept designed is a PDF/A-3u (Unicode) envelope containing the ECG graphic (with no predefined layout), the ECG digital data in HL7 XML format, and a digital signature, assuring that the two contents match. The new PDF/A-3u + HL7 XML document can be redistributed and opened with most available PDF readers. Moreover, analysis software could be adapted to accept the file as input for subsequent analysis which could be overlaid on the printout itself.

# Encoding the Electrocardiogram Details in the Host Record's Bandgap for Authorization-Dependent ECG Quality

Piotr Augustyniak

AGH-University of Science and Technology
Krakow, Poland

P65

Time-scale decomposition of the electrocardiogram shows large areas where cardiac component are not expected. In this bandgap located roughly between T-onset and P-onset in two upper scales data containers of considerable size can be defined without altering the record diagnostability. In this paper we propose using this extra storage area for high frequency details of the signal. Authorization-dependent access to these details allows privileged users for high precision analysis, while regular users with an access to standard resolution signal are still able to correctly calculate essential parameters.

The proposed method consists in recognition of P-QRS-T wave borders and rhythm type for each heartbeat. For each normal beat a reversible time-frequency transform is then performed allowing for revealing the bandgap size and selecting the details to be encoded. The length and the noise level of the T-onset to P-onset section is determining the maximum capacity of each data container. The encoding itself is based on changing the order and not the value of existing time-frequency atoms. Consequently the statistics of the signal are unchanged, and a regular user doesn't suppose the existence of extra data. Finally, the inverse time-frequency transform is applied to restore a regular time representation of the ECG.

ECG distortions from coded data

| coding bits | Δ QRS length | PRD |
|---|---|---|
| 1 (250bps) | 0.73 ms | 0.10 |
| 3 (750bps) | 1.57 ms | 0.15 |
| 5 (1250bps) | 6.14 ms | 0.57 |

The proposed method was tested with ECG files from CSE Multilead Dataset 3 recommended by IEC60601-2-51 as a reference for measurement of repeatability of wavelength calculation. We tried encoding of 1 (i.e. c.a. 250bps @ 500Hz, 16 bit) to 3 bits of supplementary data per time-frequency atom, and the inaccuracy of measurements doesn't overpass the required limits of 10ms (30ms in case of T-end). Higher encoding densities (5 bits) led to changes in signal statistics (making more evident the existence of encoded data) and degrade the cardiac components outside of the bandgap.

The proposed methods allows for embedding any hidden data (e.g. personal information, diagnostic results or extra samples) into a standard ECG. The storage space is sufficient for accommodate oversampling details enhancing the signal in selected area (e.g. QRS-end for VLP). The precision of selected measurements is then significantly improved for privileged users.

# A Low-Cost Solution to Follow the Evolution of Arrhythmic Patients

Rene Gonzalez-Fernandez*, Margarita Mulet-Cartaya, Juan Dayron Lopez-Cardona, Alejandro Lopez-Reyez, Rolando Lopez-Rodriguez and Rolando Lopez-Creagh

IFMBE/Central Institute of Digital Research
Havana, Cuba

P65

**Aims:** This paper is focused on discussing the main features of a system designed to study the evolution of arrhythmic patients doing their daily activities.

**Methods:** The proposed system is composed by three parts: a small battery-powered device designed to acquire and transmit, via Bluetooth, an ECG channel; a mobile application based on Android operating system to process the ECG and a web application. The ECG device is able to acquire and transmit the ECG continuously since it is turn on; pacemaker spikes and electrode status are detected and transmitted too. The Android application receives the ECG data; QRS complexes are detected and classified and RR intervals are measured to compute heart rate. All these information is uploading to a web application using GSM/GPRS network and HTTP protocol. The web application stores each ECG file in a MySQL database; cardiologists can check ECG strips and analyze trend charts associated to each patient. Also, cardiologist can call any patient in order to adjust his drug treatment. The ECG device is easy to use, patient only have to attach three electrodes to his skin and press the ON/OFF button. Results: Two ECG device´s prototypes have been tested according to the IEC 60601-2-47 standard and all the tests were passed successfully. The Android application has been tested with two hundred three-minute ECG strips; Bluetooth communication was without errors. QRS complex detection algorithm was tested with MIT-BIH database and the sensitivity was 98,77%. Web application provides several graphical tools to analyze the electrocardiographic information captured. The MySQL database has been tested without any problem to store or recover information.

**Conclusions:** The proposed system seems easy to use by arrhythmic patients and cardiologists; it could be an important tool to follow the cardiac arrhythmias evolution with limited material resources and minimal discomfort for patients.

# Telemedicine Network for Collaborative Diagnosis and Care of Heart Malformations

Alessandro Taddei*, Andrea Gori, Tiziano Carducci, Giuseppe Augiero, Alessio Ciregia, Emiliano Rocca, Giacomo Piccini, Nadia Assanta, Giorgio Ricci and Bruno Murzi

Monasterio CNR Tuscany Foundation
Massa, Italy

Health cooperation with Balkan Countries in diagnosis and care of congenital heart malformations was the objective of the project involving pediatric division and medical informatics department at Heart Hospital in Massa (HHM)(Monasterio Tuscany Foundation). Since 2008 the Association "Un Cuore un Mondo" with Tuscany region supported this initiative, developing a telemedicine network interconnecting HHM with selected pediatric and gynecology centers in Croatia, Bosnia-Herzegovina, Albania and Romania. While echography equipment allows recognizing cardiac abnormalities, in neonate or even in fetus, often sonographers are not skilled and live guidance during patient examination is demanded to reach an expert-enlightened joint diagnosis. Thus the synchronous approach is preferred for tele-echocardiography. Videoconferencing equipment was used for streaming echocardiograms by standard encryption allowing interaction between specialists and remote staff. Tele-consultation service was provided on demand: while a part of patients resulted not complex or normal, the others were transported to Massa for cardiac surgery intervention or adequate care. Even pregnant women, in case of critical fetal abnormalities, were transferred before delivery to allow prompt intervention on newborns. After the service was made available, a total of 82 patients were transferred from Balkan countries. Further extension of Balkan telemedicine network was allowed in the frame of European IPA programme by AdriHealthMob project, aimed at better planning or possibly reducing cross-border mobility of citizen for health and care in the Adriatic area. The telemedicine network has been recently experimented in Tuscany to drive implementation at health sites, beginning with those hard to reach areas. Even if high diagnostic accuracy was reported in clinical practice by live tele-echocardiography , using efficient lossy image compression, DICOM images are later forwarded for allowing confirmation or revision of diagnosis to respect the legislation. Web-based facilities are added for patient data exchange and reporting as well as for scheduling the tele-consultation service.

P65

## Telemedical Human Activity Monitoring System based on a Wearable Sensors Network

Eliasz Kańtoch*

AGH University of Science and Technology
Kraków, Poland

P65

Recent advances in microprocessor chip technology, wireless communication, and biomedical engineering it is possible to develop miniaturized ubiquitous health monitoring devices that are capable of monitoring physiological and movement signals during daily life activities. The aim of the research is to implement and test a telemedical system to monitor and analyze physiological and movements signals from human. The system consists of the body central unit with Bluetooth module and wearable sensors: the dedicated ECG sensor, the temperature sensor, the skin humidity sensor and accelerometers placed on the human body or integrated with clothes and a network gateway to forward data to a remote medical server. The system includes specially designed transmission protocol and remote web-based graphical user interface for real time data analysis. The system was tested on 20 healthy volunteers (15 male, 5 female) during activities of daily living (ADL). Experimental results showed maximum 4% absolute error compared to certified medical devices and demonstrated the possibility of delivering the telemedical service using data from a remote wearable sensor network. The results are promising and indicate that the developed wireless wearable monitoring system faces challenges of multi-sensor human health monitoring during performing daily activities and open new opportunities in developing novel healthcare services.

# Effect of Telehealth on Self-Care Behavior of Heart Failure Patients

Carolina Varon*, Jan Minter, Michelle Stapleton, Stuart Thomson, Siegfried Jaecques, Hans-Peter Brunner-La Rocca, Sabine Van Huffel

KU Leuven, iMinds Medical IT, Leuven, Belgium

**Aims:** Telehealth systems to monitor heart failure patients have become a very important tool in the last decade. However, little is known about the effect that such monitoring systems have on the self-care behavior of these patients. In this respect, this study aims to investigate this effect, and determine whether Telehealth helps improving patients' compliance.

**Methods:** Daily measurements of blood pressure, pulse, $SpO_2$ and weight were collected from 49 patients suffering from heart failure. These patients were monitored during 42 days, using the Motiva telehealth platform offered by Philips. In addition, they were asked to fill out the *European heart failure self-care behavior scale* questionnaire before and after the monitoring period. In order to determine the effect of the monitoring program on self-care behavior, the evolution of each physiological parameter is quantified. This evolution is then compared against the answers to the questionnaires, and differences are evaluated with a confidence interval of 95%, using the Kruskal-Wallis test.

**Results:** Significant differences were found between the self-care behavior scale before and after the monitoring program. More specifically, the questions concerning weight and fluid intake per day, show a significant ($p<<0.05$) improvement in the compliance of the patients to the program (top panel of the figure). These improvements were validated using the evolution of the physiological parameters. Patients whose blood pressure and weight tend to decrease, also appear to cope better with their condition. This is indicated in the middle and bottom panels of the figure. The lower the score, the better. The scores are indicated before (light grey) and after (dark grey) the monitoring period.

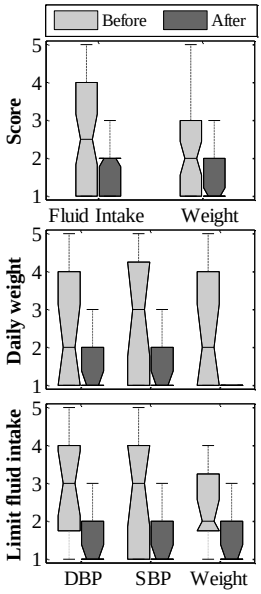


**Conclusions:** Telehealth systems have a direct, positive effect on the self-care behavior of patients suffering from heart failure. These findings will be validated further on a bigger dataset, and using a quality of life questionnaire.

P65

# Optimization of Shifts and On-Call Coverage of Cardiologists Working in a Hospital Complex Structure by Using Free Software

Eugenio Cervesato*, Giovanni Righini, Gian L Rellini, Matteo Cassin, Rita Piazza and Gian L Nicolosi

Cardiology Dept.-ARC , "Santa Maria degli Angeli" Hospital, Pordenone, Italy
Pordenone, Italy

P65

**Background:** The organization of shifts and on-call coverage of Cardiologists working in a hospital complex structure must ensure the availability 24h, full year, complying with laws and contractual, social and professional obligations. To overcome manual handling, an automation project was started through an Hospital / University collaboration.

**Materials and Methods:** The team consists of 15 Cardiologists to ensure a daytime and a nighttime guards, on-call service for full day on weekends and holidays and a 24h hemodynamic on-call coverage (this assigned to the same specialist weekly). For weekends and public holidays, it was agreed to combine guards and on-call coverage in a way to reduce the number of Cardiologists involved. Special situations and exceptions are taken into account: one Cardiologist works 30 daytime guards per year (on Tuesdays or Thursdays); one Cardiologist performs 60%; the four hemodynamists contribute at the cardiology guard and on-call coverage pooled. An original software was developed in Java to input data, generate the mathematical model and read back the solution, relying on a SQL database. The solution is obtained by GUSEK, an open tool to the linear programming solver GLPK, freely downloadable from Internet, minimizing the sum of the deviations from individual quotas.

**Results:** The system generates the shifts monthly. To harmonize contiguous months, usually the operator sets absent in the early days people working the last days of the previous period. Typical computation time is few minutes to ensure that a solution exists (if not the constrains must be changed) and several hours to obtain the optimized solution. The system is in use for 22 months and continuously improved to handle specific situations. It provides equal assignment of Cardiologists to each type of shift with uniform like distribution, avoiding immediate repetition of the same shift. The software is open source available for download: www.arc.fvg.it.

# European Patient Summary Guideline and Continuity of Care Document: A Comparison

Ana Estelrich, Harold Solbrig, Marcello Melgara, Giorgio Cangioli and Catherine Chronaki*

HL7 Foundation
Brussels, Belgium

The HL7 Consolidated CDA (CCDA) Implementation guide has harmonized seven document types including the Continuity of Care Document that is referenced by MU2 as the standard to document a clinical summary after a medical appointment. The eHealth Network of EU Member State (MS) representatives established under Art14 of the EU Directive on CrossBorder Care, endorsed the European Patient Summary (EU PS) Guideline for the exchange of patient summaries among MS in the context of unplanned care. This paper compares clinical summaries in the US with patient summaries in the EU and presents an architecture for their communication in unplanned care settings. The EU PS Guideline specifications and HL7 CCDA/CCD were compared. Starting with the patient summaries of two fictitious patients crossing the Atlantic, Martha and Paolo, we compared them with the corresponding clinical summaries in the US and reflected on ability to map one to the other. Although clinical and patient summaries are based on the same base standard, HL7 CDA, there are differences that have important implications for the development of an international standard or implementation guide for patient summarie. Firstly, while CCD is an open template and sections can be added from the full CCD specification, the EU PS is a closed template eventhough MS may choose to implement a subset of the EU PS. There are 12 clinically equivalent sections, but the structure and underlying terminologies differ. 40+ value sets are referenced in the EU PS specification that is the smaller of the two specifications. Most challenging were the problem list (ICD10/SNOMED-CT) and the medication (ATC/RxNORM).

**Conclusions:** Structural and terminology differences challenge the exchange of EHR among systems even when the same base standard is used. Strategies need to be developed that allow sharing of interoperability assets that are quality assured, can be combined, and elaborated upon.

P65

# Automated Measurement of Fetal Isovolumic Contraction Time from Doppler Ultrasound Signal without Using Fetal Electrocardiography

Faezeh Marzbanrad*, Yoshitaka Kimura, Miyuki Endo, Marimuthu Palaniswami and Ahsan H Khandoker

The University of Melbourne
Parkville, Australia

P65

Isovolumic Contraction Time (ICT) is the interval from mitral valve closure (Mc) to aortic valve opening (Ao). It is a reliable index of fetal cardiac contractility and can sensitively detect impaired cardiac function. Fetal ICT can be noninvasively measured from Doppler Ultrasound (DUS) signal. Previous studies proposed to use band-pass filtering, wavelet analysis or Empirical Mode Decomposition (EMD) to decompose the DUS signal into a high frequency component linked to the valve motions. Differentiation of mitral and aorta opening and closing events were performed manually in earlier studies and automatically in recent studies. Simultaneously recorded fetal electrocardiogram (fECG) has a crucial role, particularly in automated methods; by specifying the beginning of cardiac cycle segments. However recording of abdominal ECG simultaneous with DUS and separation of fECG from a noisy mixture of maternal ECG and other interfering signals and artifacts complicate this technique. In this study automated identification of valve motions from DUS signal without using fECG was investigated. To this aim the DUS signal was decomposed by EMD to Intrinsic Mode Functions (IMF). The first IMF was linked to valve motions and the fourth IMF was related to wall motions. The peaks of the latter represented the cardiac wall contractions which were used for segmentation of the first IMF into cardiac cycles as a substitute for fECG. The mitral and aortic valve motions were automatically identified by hybrid Support Vector Machine (SVM)-Hidden Markov Model (HMM). This method was tested on 1 minute recordings of DUS from 21 fetuses. A significant positive linear correlation was found between average ICT obtained with fECG (previous method) and without using fECG (new method) ($r=0.90$, $p<0.0001$) and mean absolute difference was 1.4 msec. Larger differences were found for beat to beat ICA measured with and without using fECG ($6.1 \pm 3.8$ msec).

## Assessment of Dynamic Autonomic Changes with Posture using Instantaneous Entropy Measures

Gaetano Valenza*, Luca Citi, Enzo Pasquale Scilingo and Riccardo Barbieri

University of Pisa
Italy

Dynamic analysis provides a powerful methodological framework for characterizing physiological systems. In particular, complex heartbeat dynamics related to autonomic control mechanisms are known to change at each moment in time, and complexity measures have been proven to have prognostic value in both health and disease. Nevertheless, an instantaneous measure of complexity for cardiovascular time series (or any other series of stochastic physiological "events") is still missing. In this study we introduce a mathematical framework serving instantaneous complex estimates of heartbeat dynamics to characterize different activities, tasks, and/or pathological states. In particular we propose new definitions of inhomogeneous point-process approximate and sample entropy where the discrete events are modeled by probability density functions characterizing and predicting the time until the next event occurs as a function of past history. These definitions are built on our previous work employing Laguerre expansions of the Wiener-Volterra autoregressive terms to account for long-term memory. We demonstrate an exemplary study on heartbeat data gathered from healthy subjects undergoing postural changes such as stand-up, slow tilt, and fast tilt. Results show that instantaneous complexity is able to effectively track the complex autonomic changes as they are affected by different postural changes.

P65

# Heart Murmur Detection Using Ensemble Empirical Mode Decomposition and Derivations of the Mel-Frequency Cepstral Coefficients on 4-Area Phonocardiographic Signals

Joe A Jimenez, Miguel A Becerra* and Edilson Delgado-Trejos

Instituto Tecnologico Metropolitano ITM
Medellín, Colombia

P65

Procedures based on the 4 standard auscultation areas yield a better clinical decision support system for heart murmur diagnosis, as it is possible that a disturbance due to a murmur is not always recorded in all the auscultation areas. This paper presents an automatic detection system for the classification of normal and pathological phonocardiographic (PCG) signals using 4 standard auscultation areas (one of each cardiac valve) for heart murmur diagnosis. The database of 4-area PCG records used in this study belongs to the National University of Colombia. A set of 50 individuals were labeled as normal, while 98 were labeled as exhibiting cardiac murmurs, caused by valve disorders. With the help of medical experts, 400 representative beats were chosen, 200 normal and 200 with evidence of cardiac murmur from 4 different areas of auscultation. First, the PCG signals were preprocessed; next, four different derivations of Mel Frequency Cepstral Coefficients (MFCC) were extracted, where statistical moments of Hilbert Huang Transform (HHT) were estimated using different combinations of the signal components, with the aim of focusing the heart murmur dynamics. In component extraction, Empirical Mode Decomposition (EMD) was compared to Ensemble Empirical Mode Decomposition (EEMD), in terms of computational complexity and effects derived from adding white noise to the original signal to solve the mode-mixing problem. Finally, stochastic analysis of the feature space was carried out by an ergodic-HMM trained using the expectation maximization algorithm. The global classification result for the 4 auscultation areas was around 98% with acceptable sensitivity and specificity scores, using a 30-fold cross-validation procedure (70/30 split).

# Towards Semantic Interoperability for Cardiovascular Risk Stratification into the Electronic Health Records Using Archetypes and SNOMED-CT

Alfonso Sanchez-Cano, Cristina Soguero-Ruiz, Inmaculada Mora-Jiménez, Luis Lechuga, Javier Ramos-Lopez, Arcadi García-Alberola, Pablo Serrano-Balazote and José Luis Rojo-Álvarez*

Rey Juan Carlos University
Fuenlabrada, Spain

**Background:** Clinical data exchange among different organizations could be of great value in the field of Cardiovascular Risk Stratification (CVRS) research. Semantic interoperability is an essential key in order to integrate and exchange medical records and to automate the clinician workflow. Objective. We present a proposal to pave the way towards the exchange of CVRS data, prototyped and focused on Heart Rate Turbulence (HRT), by using archetypes, SNOMED-CT and web technologies.

**Materials and Methods:** Archetypes are considered to achieve semantic interoperability when representing and storing data in Electronic Health Record (EHR). Starting from a previously developed prototype of HRT ontology, based on the conceptual model of SNOMED-CT in the EHR, an HRT archetype is created, yielding an agreed, formal, and interoperable specification for representing a given clinical entity within the EHR. This archetype compiles the ECG signal processing information of 24h Holter recordings, in order to have a standard data structure to infer the CVRS in terms of HRT values. Furthermore, the archetype supports the recording of risk factors such as hypertension, diabetes, age, sex or smoking to provide with a complete CVRS research repository.

**Results:** The built archetype achieves: (1) a standardized HRT data structure, involving domain specialists; (2) interoperability into EHR for HRT data exchange; (3) structured HRT recordings for a simple follow up by medical societies, and with statistical, research and educational purposes. The system enables clinical research and the continuous improvement of the signal processing methods used in CVRS.

**Conclusions:** Interoperability between heterogeneous systems in Holter recordings for HRT analysis can be obtained by designing a HRT data structure, where specialists from different fields work together. Structured data from EHR following formal model for recording clinical information improves CVRS decision support.

P65

# Clinical Decision Support System for Post-Procedure Management of Transcatheter Aortic Valve Replacement

Stefan Nelwan*, Mark Ronkes, Jeroen van den Berg and Teus van Dam

Erasmus MC
Rotterdam, Netherlands

P65

**Introduction and aim:** In recent years, transcatheter aortic valve replacement (TAVR) has become a procedure for patients with symptomatic aortic stenosis and who are considered at high risk for valve replacement surgery. However, TAVR is associated with several complications, including stroke, vascular complications, valvular leaks and rhythm disturbances such as complete atrioventricular blocks. The aim of this study was to design, build and clinically validate a clinical decision support system (CDSS) for post-procedure clinical management of TAVR patients at the intensive coronary care unit (ICCU).

**Methods:** The CDSS has been designed to record, store and monitor vital signs, including heart rate, invasive blood pressures, pulse oximetry, 12-lead ECGs and lab results and to assist the clinician with an up-to-date overview screen with relevant information such as the PR width as a marker for PR prolongation. The system monitors and informs clinicians near the bed based on the vital signs and a digitized nursing protocol as used on paper by the clinicians.

**Results:** The CDSS has been integrated with the patient monitoring equipment used at the ICCU. We have used the open source NoSQL database MongoDB to store and integrate the various incoming data from the patient monitors, lab system and user input. The underlying decision support system is Drools. The graphical user interface is web-based Javascript application and accesses patient data and clinical notifications by using a RESTful web service.

**Discussion and conclusion:** We have developed a clinical decision support system that has been developed for assisting clinicians with patient who underwent a TAVR procedure. The system combines several data sources in a single screen and provides notifications for early detection of complications and timely intervention during patient care and treatment.

# New Algorithm to Identify Focus of Atrial Ectopic Activity from Multi-lead ECG Systems – Insights from 3D Virtual Human Atria and Torso

Erick Andres Perez Alday, Michael A Colman*, Philip Langley and Henggui Zhang

University of Manchester
Manchester, United Kingdom

Ectopic atrial activity, associated with atrial tachycardia and atrial fibrillation (AF), may predispose to cardiac arrhythmias, death and stroke. The abnormal atrial excitation patterns which result from such activity may be reflected in changes to the P-wave morphology (PWM). Compared to the standard 12-lead ECG, more detailed ECG configurations may provide further information necessary for precisely locating the origin of atrial excitation without the need for invasive methods. In this study, we use a biophysically detailed model of the human atria and torso to develop a new algorithm for correlating the origin of atrial excitation with PWM. We implement a recently developed 3D human atrial model to simulate normal (sinus rhythm) and ectopic electrical activity. Activation patterns from the atrial model are placed inside a newly segmented torso model taken from the visible human dataset with consideration for the lungs, liver, spinal cord and blood masses. A boundary element method is used to determinate the body surface potential resulting from atrial excitation. Elements of the torso mesh in agreement with the location of the placement of electrodes in 12 and 64 lead ECG systems were selected to produce ECG P-waves. The torso model was validated using experimental data in control, comparing the spatio-temporal evolution of the atrial dipole and PWM in 12 and 64 lead ECG systems. The atrial model was then excited from various regions throughout the atria to stimulate ectopic activity. Correlation of 64-lead ECG PWM with the focus of ectopic activity al-lowed the development of a focus-location algorithm, by dividing the atria and torso into two sets of quadrants and analyzing P-wave polarity within the torso quadrants. In simulation tests, the new algorithm had a higher success rate than those based on the 12-lead ECG (93% vs 72%), demonstrating the advantage of using such systems.

# Huge reduction of defibrillation thresholds using four electrode defibrillators

Ana Simic*, Inma R. Cantalapiedra+, Jorge Elorza, Jean Bragard

University of Navarra
Pamplona, Spain

+Polytechnic University of Catalonia
Barcelona, Spain

P66

**Aims:** Defibrillation is the standard clinical treatment used to terminate ventricular fibrillation. In order for the shock to be successful it is necessary to apply high-energy shocks, typically around 150J for transthoracic defibrillation. There have been different attempts to reduce the defibrillation thresholds by reversing the shock polarity during the defibrillation and optimizing the reversal time, waveform and duration of the shock. In this paper we propose a new procedure that is based on a four-electrode system instead of the standard two-electrode system.

**Methods:** The model is tested using a one-dimensional ring with bidomain properties and with the Beeler-Reuter model for the active properties of the membrane. Three different shock protocol are tested: monophasic, symmetric biphasic (both phases of equal duration) and asymmetric biphasic (second phase is shorter than the first). The results are compared with those obtained with standard two-electrode protocol. Defibrillation efficacy is evaluated by comparing the dose-response curves for each protocol. The resulting defibrillation thresholds corresponding to 50% success (E50) and 90% (E90) success rate show a clear improvement for the four-electrode system as compared to the two-electrode system. As in the case of the two-electrode system, we have found that successful defibrillation outcomes can be classified into four mechanisms: direct block, annihilation, delayed block and direct activation.

**Conclusions:** Analysis of defibrillation mechanisms of four-electrode system reveals that E90 success rate is achieved with direct block, annihilation or delayed block. The same defibrillation threshold for two-electrode defibrillation is achieved primarily with direct activation. The lowest E90 success is achieved with asymmetric biphasic; confidence interval is: (2.31—2.33) V/cm (alpha=0.01). This must be compared with two-electrode confidence interval: (5.83—5.85) V/cm (alpha=0.01). We also found that the supremacy of asymmetric biphasic shocks lies behind the interplay of the duration of the cathodal and anodal phases.

# Quantitative Insights into the Closed-loop Cardiovascular System Using an Electrical Lumped Element Physiological Model

Athanasios Tsanas*, Gari Clifford, Vassiliki Vartela and Petros Sfirakis

University of Oxford
United Kingdom

**Introduction:** We extended our closed-loop physiological model of the human cardiovascular system, where all major vascular regions were modelled using lumped electrical equivalent components. These components were linked to subject-specific factors such as age, gender, smoking, fitness, and cardiovascular medical history records. Data: 289 participants were referred to Onassis Cardiac Surgery Centre for an Exercise Treadmill Test (ETT). Approximately 15% of the participants were without any known cardiovascular pathology or risk factor of cardiovascular disease. Systemic arterial pressure and heart rate were recorded at rest and during ETT using standard clinical protocols. In most cases, detailed medical history for the participants was also available.

**Methods**: Compared to our previous model we (a) solved mathematically more rigorously the resulting systems of differential equations, (b) expressed heart rate as a function of the subject-specific factors as a critical aspect of the model, and (c) proposed quadratic polynomial relationships associating each lumped component with the subject-specific factors. We optimized the model's parameter values using robust multi-objective constrained optimization tools and evaluated its generalization performance using cross-validation tests.

**Results:** We demonstrated that the model provides accurate values of systemic arterial blood pressure (4.3% deviation from the clinicians' measurements), realistic heart-related characteristics (ejection fraction, cardiac output, valve behaviour), and realistic values of pressures and blood volumes for the other major vascular parts of the cardiovascular system.

**Conclusion:** The proposed physiological model offers valuable, clinically interpretable, quantitative insight into the properties of the cardiovascular system at rest and during exercise, offering a convenient framework for associating subject-specific factors with cardiovascular characteristics. Moreover, the model implicitly explains important phenomena such as feedback and interaction of the major vascular parts in the cardiovascular system, and can tentatively indicate cardiovascular-related pathologies due to the causative model parameters in the respective parts of the circulation.

# Modeling of the Human Heart Rate Variability Enhanced Using Stochastic Sleep Architecture Properties

Mateusz Solinski*, Jan Gieraltowski and Jan Zebrowski

Faculty of Physics, Warsaw University of Technology
Warsaw, Poland

P66

Human sleep consists of four characteristic phases: light (L), deep (D), REM sleep and almost-awake state (W) with additional arousal episodes. All of these elements create a nontrivial, complex structure, the statistical properties of which were studied here carefully. We observed a different behaviour of heart rate variability for each phase. Thus, we should take these specific properties of sleep architecture into consideration while modeling heart rate variability. We analyzed 34 simultaneous heart rate variability and 30 EEG nighttime recordings from healthy adults. EEG provides accurate information about sleep phases. The main idea behind our sleep architecture reconstruction is to consider two properties: probabilities of transitions between all possible pairs of phases and probability distribution of phase durations. We calculated the probabilities of transition between each pair of phases and we aggregated them into two probability matrices (separately for each half of the sleep period because the character of the inter-phase transitions is different in early and late sleep). We found also that the probability distribution of L, D and REM sleep duration are described by a gamma distribution and that of the W phase - by a Pareto distribution. To generate the RR intervals for every sleep phase, we use the model described in [1]. We consider three variants: (a) periodic sleep cycles with the sequences of phases: L, D, REM, W in each cycle, (b) a randomized distribution of phases, (c) the architecture based on our model. The results show that variant (c) gives 50% of the time series indistinguishable from real data using all standard linear and nonlinear HRV assessment methods while for variants (a) and (b) we obtain 41% and 3% accordingly. [1] J.W. Kantelhardt, S.Havlin and P.Ch. Ivanov, Modeling transient correlations in heartbeat dynamics during sleep, Europhys. Lett., 62 (2), pp. 147-153 (2003)

# A simple 2D Whole Heart Model for simulating Electrocardiogram

B.Minimol, V S Chakravarthy,Soma Guhathakurta

Indian Institute of Technology Madras, Chennai, India.

A simplified whole heart model which simulates the Electrocardiogram (ECG) accurately is presented. Extremely detailed whole heart 3D models are available, but they are computationally expensive. On the other hand most of the 2D cardiac models are homogeneous models aiming at modeling activation propagation in a small patch of cardiac tissue; they are not meant to be whole heart models. A two-dimensional heterogeneous "whole heart" model consisting of an array of specialized cardiac cells, with appropriate anatomical distribution, interacting via gap junction communication (GJC) is envisioned to be a midway solution to this problem.

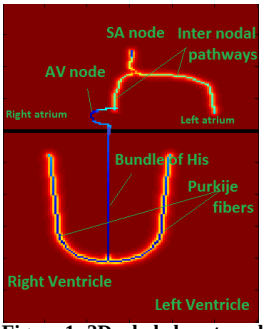


**Figure 1: 2D whole heart model**

The proposed 2D whole heart model includes various key components of the electrical conduction system of the heart including the SA (Sino atrial) node, fast conducting inter-atrial pathways, slow conducting AV (atrio-ventricular) node, Bundle of His, Purkinje network, and atrial and ventricular myocardial cells as shown in figure (1). Atrial and ventricular myocardial cells are modeled by Aliev-Panfilov (AP) two-variable model proposed for cardiac excitation. The autorhythmic cells are modeled by Fitzhugh-Nagumo (FN) model operated in the oscillatory mode. The frequency of SA node is highest at 80BPM, varying continuously along the cardiac conduction system with AV node and Purkinje cells firing at60 BPM and 40BPM respectively. Action potential duration of the ventricular myocardial cells decreases in the medial-lateral direction. In addition to normal ECG, the model also reproduces AV second degree conduction abnormalities like supraventricular tachycardia and Wenckebach phenomenon as shown in figure (2).

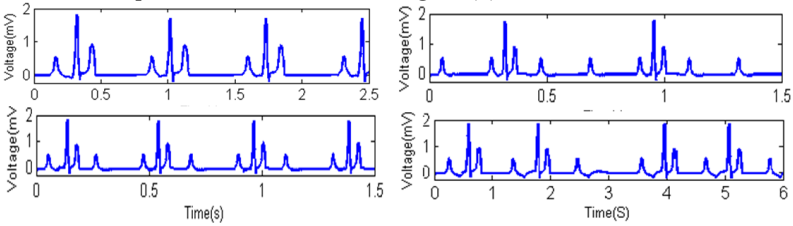


**Figure 2: (a) Normal ECG (b)SupraVentricular tachycardia (c) Wenckebach (2:1) (d) 3:2**

P66

# Parameter Sensitivity Analysis of a Human Atrial Cell Model using Multivariate Regression

Eugene TY Chang* and Richard H Clayton

University of Sheffield
Sheffield, United Kingdom

P66

**Motivation:** Mechanisms of atrial fibrillation (AF) initiation and maintenance are poorly understood and may be addressed by computational models. Atrial cell models form the building blocks of complex multicellular models and contain many input parameters within a large parameter space. A rapid systematic way of quantifying changes in model outputs due to input parameter variability would enhance mechanistic understanding.

**Methods**: A parameter sensitivity study on input model conductances within the Courtemanche-Ramirez-Nattel (CRN) human atrial cell model was performed, following Sobie (2009). Input maximal ionic conductances (p=13) were varied by randomly scaling baseline model values, and used in single cell action potential (AP) simulations. From input value matrix X (p x n), m=10 model outputs per simulation were extracted to output matrix Y (n x m), and multivariable regression performed to find a m x p regression matrix B which minimised differences between output Y and predicted Y* = XB. Regression values were mean-centred and normalized to standard deviation (SD). A +0.5 value implied parameter input 1SD above mean increased output by 0.5SD. Simulations were performed in Matlab (Mathworks).

**Results:** AP determinants – action potential duration (APD), AP amplitude (Vamp), time from activation to peak (tpeak) and dV/dtmax – were compared (n=100). dV/dtmax and Vamp showed strong sensitivity only to maximal sodium conductance G¬Na (0.98 and 0.94 respectively), whilst APD and tpeak were weakly sensitive to multiple conductances: GK1, Gto, GKr, GbCa, for APD (±0.3-0.6), GK1, INaKmax, GbCa for tpeak (±0.3-0.6). Predicted outputs showed strong correlation to measured values: APD (R2=0.966), Vamp (R2=0.998), tpeak (R2=0.880), dV/dtmax (R2=0.961).

**Conclusions:** Multivariable regression is a novel tool for examining parameter sensitivity of the CRN AP model and offers rapid insight to the relative importance of input parameters to specific outputs. Further work is required to fully characterise cellular parameter sensitivities in multicellular cardiac tissue.

# Detection of Abnormal Cardiac Activity using Principal Component Analysis

Ariel Greisas, Sharon Zlochiver
Tel Aviv University
Tel Aviv, Israel

P66

**Background**: Electrogram-guided ablation has been recently developed for allowing better detection and localization of abnormal atrial activity that may be the source of arrhythmogeneity. Nevertheless, no clear indication for the benefit of using electrogram guided ablation over empirical ablation was established thus far, and there is a clear need of improving the localization of cardiac arrhythmogenic targets for ablation. In this work we propose a new approach for detection and localization of irregular cardiac activity during ablation procedures that is based on dimension reduction algorithms and principal component analysis (PCA).

**Methods**: Using an extended bi-domain mathematical modeling and computer simulations of the cardiac electrical conduction, the effect of two sources of abnormal activity - fibrotic patches and spiral waves - on the electrical conduction was studies in 2D ventricular tissues. A dimension reduction algorithm and PCA were employed on extra-cellular data collected on an 8x8 electrode-array and a manifold of the primary component locus was built that allowed easy visualization and detection of possible arrhythmogenic ablation targets characterized by the irregular conduction.

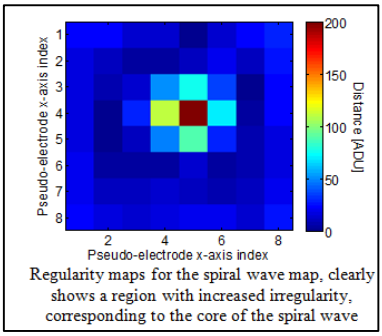

Regularity maps for the spiral wave map, clearly shows a region with increased irregularity, corresponding to the core of the spiral wave

**Results**: Our results show that the PCA method can differentiate between focal ectopic activity and spiral wave activity, as these two types of activity produce substantially different manifold shapes. Moreover, the technique allows the detection of spiral wave cores and their general meandering and drifting pattern. Fibrotic patches larger than 2 mm2 could also be visualized using the PCA method, both for quiescent atrial tissue and for tissue exhibiting spiral wave activity. We envision that this method, contingent to further numerical and experimental validation studies in more complex, realistic geometrical configurations and with clinical data, can improve existing atrial ablation mapping capabilities, thus increasing success rates and optimizing arrhythmia management.

# Quantifying Tikhonov Regularization Uncertainty in the Inverse Problem of Electrocardiography

Jessie J France*, Yaniv Gur, Robert M Kirby and Chris R Johnson

University of Utah
Salt Lake City, United States

P66

**Aims:** This study aimed to quantify differences in uncertainty from zeroth, first, and second order Tikhonov solutions (ZOT, FOT, and SOT, respectively) for the inverse problem of electrocardiography. We developed a new method for analyzing the uncertainty in Tikhonov solutions that quantifies the 95% confidence intervals (CIs) for a given optimal Tikhonov solution. Methods: We used a Bayesian approach to reformulate the optimal Tikhonov solution in terms of a maximum a posteriori (MAP) estimate. Through reverse application of Morozov's discrepancy principle, we modeled the unknown torso voltage noise variance as an inverse gamma distribution, and used a block-wise Gibbs sampler to indirectly analyze the uncertainty in the Tikhonov solution for different choices of regularizers on both hybrid and non-hybrid meshes, with and without conductivity information. A total of 4,000 Gibbs samples were collected for each simulation, using the same random number stream for all meshes and regularizers. Using functional band depth analysis, we calculated the percentage of the true heart voltages that fell between the 95% CIs. We ran a total of 50 simulations comparing each regularizer and mesh combination (150 total) with Gaussian noise added to the torso potentials at 1%, 3%, or 5% of the 2-norm of the true torso voltages.

**Results:** Out of all trials, the posterior conditional mean variance from our algorithm accurately predicted the true noise variance 82% of the time to within 8% absolute error. For all noise levels, the 95% mean CIs for FOT and SOT always captured 11% to 42% more of the true heart voltages than ZOT.

**Conclusion:** We propose a novel method for torso voltage noise estimation for a given Tikhonov solution, and use it to demonstrate the impact of different Tikhonov regularizers and mesh choices on uncertainty levels.

# How Accurately Can Cardiac Conductivity Values Be Determined From Heart Potential Measurements?

Barbara M. Johnston, Peter R. Johnston

Griffith University
Nathan, Queensland, Australia

**Aims:** This focus of this study was to compare analysis methods and obtain results for determining six cardiac bidomain conductivity values and fibre rotation from realistically large sets of simulated heart potential measurements.

**Methods:** The simulated measurements of potential were found using a bidomain model of cardiac tissue that included conductivity values in three different directions (longitudinal, transverse and normal) in each of the intracellular and extracellular domains. It also allowed for a linear variation of the direction of the cardiac fibres through the tissue, via the fibre rotation angle. A two-pass inversion method, based on Tikhonov regularisation, was then used to retrieve the conductivities from the potentials. Sets of one hundred measurements of potential were used to mimic a realistic experimental scenario, something that has become possible because of the speedup in the inversion routine due to its recent implementation on GPUs. From the above-mentioned measurements, one hundred sets of parameters (each containing seven values, the six conductivities mentioned above, as well as fibre rotation) were determined via the inversion method. A number of different analysis methods were compared for this process and the best methods were identified.

**Results:** It was found that the three extracellular conductivities could be retrieved extremely accurately, with relative errors of less than 5%, even with noise of up to 40% added to the potential measurements. In addition, both the intracellular longitudinal conductivity and the fibre rotation could be retrieved accurately, with relative errors at worst around the added noise and generally less than that, especially for higher values of noise. The intracellular transverse and normal conductivities were often more difficult to retrieve, with relative errors less than four times the added noise.

**Conclusions:** It is possible to determine cardiac bidomain conductivity values accurately from large sets of simulated measurements of heart potentials.

# Accuracy of inverse solution computation of dominant frequencies and phases during atrial fibrillation

J Pedrón-Torrecilla, AM Climent, A Liberos, M Rodrigo*, E Pérez-David, J Millet, F Fernández-Avilés, F Atienza, O Berenfeld, MS Guillem.

Bio-ITACA, Universitat Politècnica de València, Valencia, Spain.

P66

**Aim:** Ablation of sources identified by dominant frequency (DF) or phase analyses in patients with atrial fibrillation (AF) is proposed as a therapy to terminate the arrhythmia. The aim of this study was to evaluate non-invasive identification of atrial sources by solving the inverse problem (InvP).

**Method:** Simultaneous atrial electrograms (EGMs) and 67-lead surface recordings were obtained in two AF patients with right-to-left and left-to-right DF gradients. The torso and both left and right atria were reconstructed by CT segmentation for each patient and their InvP was solved via the Tikhonov's method. For better evaluation we also computed the forward problem on a realistic torso and atria computer model, and solved its InvP with and without 10 dBs noise. Original and inversely computed EGMs were compared in terms of the relative error of their DFs and instantaneous phases (representing activation).

**Results:** In patients, inversely computed DF maps (panels C, D) were consistent with the recorded EGMs (panels A, B). In models without noise, atrial DFs were estimated with lower relative errors than phases (7±16 vs 41±17 % respectively, $p<0.01$). Differences between relative errors of DFs and phases were more pronounced after noise addition (10±18 vs 48±14 %, respectively, $p<0.01$).

**Conclusion:** Solving the InvP in AF is more accurate in the frequency than in the phase domain, which implies that during AF the atrial DFs may be preferred over the activation patterns for identification of sources prior to ablation.

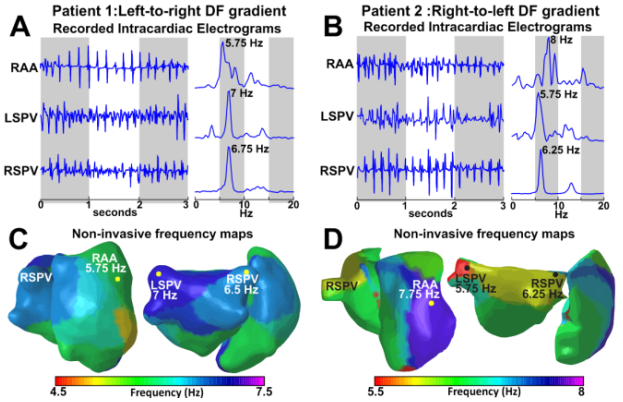

# Fecgsyn: A Graphical User Interface for the Simulation of Maternal-Foetal Activity Mixtures on Abdominal Electrocardiogram Recordings

Mohsan Alvi[1], Joachim Behar[1], Fernando Andreotti[2], Julien Oster[1], Gari D. Clifford[1,3]

[1] University of Oxford, Oxford, United Kingdom
[2] Institute for Biomedical Engineering, TU Dresden, Germany
[3] Department of Biomedical Informatics, Emory University, USA

P66

Accurate extraction of foetal electrocardiogram (FECG) morphology using non-invasive measurement remains an open problem. This is in part due to the lack of available public databases with expert-labeled FECG QRS complexes and other morphological parameters making the creation of robust FECG signal-extraction algorithms difficult.

In this paper, we present a graphical user interface (GUI) based on the *fecgsyn* ECG model, which was used for producing a subset of data of the Physionet/ Computing in Cardiology Challenge 2013.

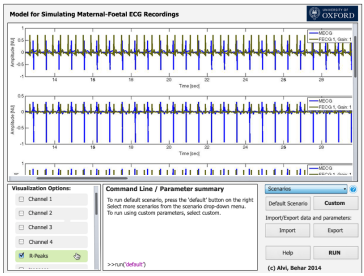


Figure 1: Channel View

The intuitive graphical user interface allows user-defined generation of abdominal ECG mixtures, for a range of clinically relevant scenarios. ECG mixtures can be generated with realistic beat-to-beat variability, morphology, amplitude modulation due to respiration, and foetal movement. The GUI allows the user to generate a set of realistic scenarios to stress test any analysis algorithm. Electrodes can be placed on the mother's abdomen using an interactive geometric representation. Simulation parameters and generated signals can be exported to scripts for running batch tests.

Using the underlying model code, noise sources can be defined, ectopic beats, and multiple foetuses can be added. A series of pathological situations, for which data collection is problematic in reality are included (e.g. umbilical cord compression).

The MATLAB-GUI is available as a free download on Physionet.org together with the underlying toolbox which can run stand-alone, and is released under the GNU General Public License.

## Correlation Dimension as a Measure of the AF Capture during Atrial Septal Pacing

Adrian Luca* and Jean-Marc Vesin

Swiss Federal Institute of Technology, Lausanne, Switzerland
Lausanne, Switzerland

P66

Purpose. In the present model-based study, the correlation dimension (D2) was used as a measure of the effectiveness of atrial septal pacing (ASP) during atrial fibrillation (AF). We analysed the complexity level of the electrical activity during pacing in order to assess the pacing cycle length (PCL) of ASP leading to appropriate AF capture. Methods. Sustained AF was generated by using a biophysical model based on a homogenous tissue in which the Luo-Rudy model was adjusted to mimic electrical remodelling as observed in patients with permanent AF. A database of simulated AF was created by selecting 10 instantaneous transmembrane potential maps during ongoing AF and keeping them as initial conditions for the subsequent simulation of ASP. For each initial condition, a rapid pacing from the septum area with PCL in the range 60-100% of the AF cycle length (AFCL) was applied. Transmembrane potentials time series at four sites on the right/left atrial (RA/LA) walls were recorded and D2 was separately computed (Grassberger-Procaccia algorithm).

**Results:** The results indicated a low D2 value (mean +/- SD: 2.17±0.42) for PCL in the range 85-95% of AFCL. This represented a significant decrease ($p<10\text{-}7$, K-S test) compared with the value of D2 (3.53±0.31) obtained for the other PCL values (i.e., a more organized atrial activity for PCL in the range 85-95% of AFCL). Moreover, for PCL in the range 85-95% of AFCL the results indicated a better AF capture in the RA than in the LA ($p<0.005$).

**Conclusions:** D2 can discriminate between different levels of atrial activity organization during AF pacing therapies. A better capture within the RA may be due to the influence of LA anatomical obstacles on AF perpetuation. The results motivate further application of D2 to specific clinical problems in the context of AF treatment.

# Robust Detection of Heart Beats in Multimodal Data: The PhysioNet/Computing in Cardiology Challenge 2014 (II)

George B Moody, Benjamin E Moody and Ikaro Silva*

MIT
United States

The 15th annual PhysioNet/CinC Challenge aims to encourage the exploration of robust methods for locating heart beats in continuous long-term data from bedside monitors and similar devices that record not only ECG but usually other physiologic signals as well, including pulsatile signals that directly reflect cardiac activity, and other signals that may have few or no observable markers of heart beats. Our goal is to accelerate development of open-source research tools that can reliably, efficiently, and automatically analyze data such as that contained in the MIMIC II Waveform Database, making use of all relevant information. Data for this Challenge are 10-minute (or occasionally shorter) excerpts ("records") of longer multiparameter recordings of human adults, including patients with a wide range of problems as well as healthy volunteers. Each record contains four to eight signals; the first is an ECG signal in each case, but the others are a variety of simultaneously recorded physiologic signals that may be useful for robust beat detection. We prepared and posted 100 training records, and retained 300 hidden test records for evaluation of Challenge entries.

## PhysioNet/CinC Challenge

Abid K and Deepu Vijayasenan*

NITK
Malappuram, India

Robust Detection of Heart Beats in Multimodal Data Abid K., Deepu Vijayasenan National Institute of Technology Karnataka, India

**Aim:** This study aimed at the robust detection of heart beats in multimodal data

**Methods:** Our method used a separate peak detection algorithms for ECG and BP signals (if present). Wavelet transform is applied on the raw ECG signal to remove baseline wandering and other high frequency noises. Peaks are detected from fourth detail to avoid false positives and corresponding peaks are found in higher details. Several conditions like minimum QRS width, minimum inter-beat gap etc. are applied to these peaks to remove false positives. Peak pairs with opposite maximum amplitudes are found in the first detail whose zero crossing points are the desired ECG peaks. A similar wavelet-based method is applied for BP signal also to find BP peaks. Delay in the two signals is adjust to match each other. Both the set of peaks are compared to each other over a span of short window and window with minimum variance is considered as the best peaks. Sensitivity (Se) and Predictivity (+P) are calculated for the result. An overall accuracy is calculated as average of gross sensitivity, gross productivity, average sensitivity and average predictivity.

**Results:** The ECG peak detection algorithm alone gave overall accuracy of 99.4% for the training database provided with CinC 2014 challenge and the same gave 91.07% on the challenge test database (Phase 1).

**Conclusion:** The current system based on only ECG input has a performance of 91.07%. The system will be augmented with BP signal input in Phase-2.

# Fusion of multimodal physiological signals using cepstrum analysis for robust heart beat detection

Yongwei Zhu, Haihong Zhang

Institute for Infocomm Research, Singapore

This study aimed for robust heart beat detection based on fusion of the results of single modality methods.

Our cepstrum analysis method could estimate beat-to-beat interval from pulsatile signals. A novel step of windowing of the logarithm spectrum in the calculation of cepstrum was introduced. A dominant cepstral peak would present if two beat patterns repeated in the time analysis window, regardless of the morphology of the waveform pattern. The cepstral peak is robust against noise in the signal, and in this study, it served as an indicator of the correctness of detected beats. Our method consists of 2 major steps: first, the filtering step operated in each individual modality, where a detected beat is filtered out if both of the 2 intervals involved with this beat are erroneous when compared with the cepstrum; second, the fusion step, where the gaps in the major modality (ECG) after filtering is filled with filtered beats from other modality (BP).



We considered ECG and BP in the experiment, and WFDB functions in Octave were used for ECG/BP beat detection. The evaluation scores were: gross and average statistics of sensitivity (Se) and positive predictivity (+P), and mean of the 4 statistics.

Results for test data set and training set is shown in the Table. The methods in comparison included Sample entry in Octave, our sole submitted entry and our un-submitted entry with bug-fix.

Our method improves the overall accuracy, and particularly the positive predictivity, compared with single modality methods. We expect further improvement when PPG is also included in experiment.

Results of the Challenge in Phase I

| Data Set | Method | Gross Se (%) | Gross +P (%) | Average Se (%) | Average +P (%) | Overall |
|---|---|---|---|---|---|---|
| Test Data Set | Sample entry | - | - | - | - | 88.89 |
| | Entry 1 | 85.68 | 93.03 | 85.55 | 91.65 | 88.97 |
| Training Data Set | Sample entry | 99.92 | 99.89 | 99.92 | 99.89 | 99.91 |
| | Entry 1 | 99.77 | 99.99 | 99.76 | 99.99 | 99.88 |
| | Entry bug-fix | 99.91 | 99.98 | 99.91 | 99.99 | 99.95 |

# Robust ECG beat detection in Multimodal data

Ahmad Marofkhani*, Ruhallah Amandi, Mohammad Farhadi*

Zanjan University of Medical Sciences, Zanjan, Iran

Beat detection is the first step on every computer based ECG diagnosis and sleep processing applications. As we have data from different sources we have more information's than usual processing systems, large and multimodal data needs more complex decision structures. Detect important parameters of signal is trivial task if ECG signal quality have high signal to noise ratio, these assumption in some cases not accessible so we must use information's from other available sources. Blood pressure influenced by stroke changes in ECG signal other leads have similar effects. Combination of knowledge from multisource may lead to severe deviations in the final beat detection result. Two main questions about beat detection in such cases are; how we can know ECG signal is not enough for beat detection in current processing window and how to combine information's from different sources to get better final detection result. Proposed algorithm consists of four steps: QRS Detection, estimate the QRS detection Quality, get the ICA features of Other leads, and finally if the Quality measure which was obtained in second step is below the threshold we use the Bayesian approach to get the final beat detection result. QRS detection done by using Coiflet wavelet and threshold its output by some rules which sample output shows in Fig.1. To process ECG lead information's we divide signal into multiple windows where each of them has common intervals with its successive window. Filtering done by using QRS detection quality measure which determined by studying on database signals. At Phase 1 we only use the QRS detection methods and process the ECG signal. Results shows the 91.93% as overall accuracy.

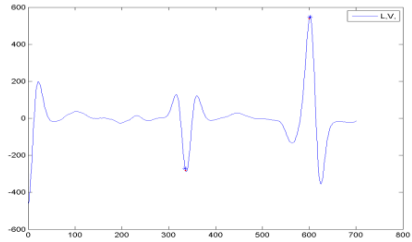


Fig1. Wavelet transformed signal, red dot point shows the human annotation and blue asterisk shows the R wave detection results.

S71

# PhysioNet/CinC Challenge 2014: The Noise Robust Method for Beat Detection in Continuous long-term Electrocardiogram Signal and Blood Pressure Signal

Hamid Ebrahimi Orimi*

Department of Mechanical Engineering at K.N.Toosi University of Technology, Tehran, Iran
Iran (Islamic Republic of)

The aim of this study is presenting a robust method for locating heart beats in continuous long-term data such as electrocardiogram signal (ECG) and blood pressure signal (BP). Most of the methods for heart rate calculation are based only on ECG signals. Since the ECG signal quality varies considerably over time, even the best beat detection methods in noisy areas of ECG signal or the areas with low quality do not have the necessary performance. In these cases, the simultaneous use of ECG signals and other pulsatile signals such as BP and photoplethysmograms (PPGs) can help significantly. In this paper, a method is proposed that simultaneous use of blood pressure signal (BP) and electrocardiogram signal (ECG) helps to detecting the final beats. An initial analysis of heart beats in both signals is done by wavelet transform and using the function of Daubecheis 6 wavelet in the second level, and all the beats in noisy areas or in areas without noise are recorded. In noisy areas, the initial recorded beats do not have discipline and the variance of first derivative derived from the beats (RR-interval) increases. In the proposed algorithm, in a window length of 5 seconds all the initial recorded beats of ECG and BP signal within the window are founded. Then, with using the variance of the first derivative of the beats the algorithm decides use the ECG or BP signal. If the blood pressure signal is used a delay of 0.2 seconds is also considered. The accuracy of this method is 89.01% compared with 88.89% of the sample entry in octave which shows the better performance.

# Hidden Semi-Markov Model-based Heartbeat Detection using Multimodal data and Signal Quality Indices

Marco Pimentel, Mauro Santos, David Springer* and Gari Clifford

United Kingdom

Automatic heartbeat detection using data from patients connected to bedside monitors is an important task as it allows the detection of pathological conditions. Heartbeat detection is traditionally performed using the ECG. However, current ECG-based heartbeat detectors rarely handle missing data and incorporate data from other cardiac signals, such as the arterial blood pressure (ABP) or photoplethysmogram waveforms. This paper discusses the development of an automatic heartbeat detector using multimodal data from bedside monitors for the Physionet Challenge 2014. The algorithm employs an extended hidden Markov model (HMM) to identify beat locations from multimodal data. An HMM is advantageous, as it allows the fusion of features from various data sources in a probabilistic framework. The model was extended to include signal quality indices (SQI) for each data source when deriving the probability of a beat being present at a given location. Furthermore, the incorporation of explicit duration distributions into the model, termed a hidden semi-Markov model (HSMM), allows the modelling of the expected time between heartbeats. Features from ECG and ABP waveforms were extracted using the wavelet transform. F1-scores based on the agreement of two ECG peak detectors (Pan-Tompkins and a simpler energy-based algorithm), and two ABP onset detectors (Physionet's wabp, and an ABP delineator from Bing Nan Li et al.), were used as SQI to identify noisy periods in these signals. The duration of a heartbeat, taken as the duration of the QRS complex in the ECG, was derived from the literature and incorporated into the HSMM. Preliminary results of this method were found from the first phase of the Challenge, with a gross sensitivity (Se) of 91.31% and positive predictivity (P+) of 93.10%. The average Se and P+ were 90.55% and 89.19% respectively, resulting in an overall score of 91.03%.

## Robust Multichannel QRS Detection

Filip Plesinger*, Juraj Jurco, Josef Halamek and Pavel Jurak

Institute of Scientific Instruments of the ASCR
Brno, Czech Republic

The task was to develop an algorithm for robust detection of QRS complex throughout different measurement data. Sampling frequency varied from 120 Hz to 1000 Hz and each record consisted of 4-8 channels. Type of recorded data was not defined except the first ECG channel. Other channels contained additional data such as blood pressure, EMG, OEG, respiration, etc. Maximum processing time of each record was limited to 40 seconds on dedicated hardware. Our proposed approach starts with detection of QRS complex in ECG channel using standard deviation and defines preliminary QRS annotations. Averaged shape (size of 480 ms) for each channel is found by accumulating data around preliminary annotations through the whole record (max. 10 minutes). Weight of each averaged shape is computed by average correlation of the shape with its original signal through all preliminary QRS annotations. Correlation of each averaged shape to corresponding channel is multiplied by its weight and forms a new channel, containing total correlation response. Resulting QRS annotations are found by tresholding this total correlation response. This approach leads to results of SE = 99.86 and +P = 99.92 with Challenge „Training Data Set“, containing 100 records. The average results of SE =88.28 and +P = 90.39 were achieved with „Hidden Test Data Set“ from Challenge Phase I. The best overall score was 73.85 in the end of the Phase I.

# Heuristic Algorithm for Multiparametric Beat Detection

Jesús Presedo[1], Constantino A. García[1], Daniel Castro[1], Tomás Teijeiro[1], Abraham Otero[2], Paulo Félix[1]

[1]CITIUS, University of Santiago de Compostela, Santiago de Compostela, SPAIN
[2]Department of Information and Communications Systems Engineering, University San Pablo CEU, Madrid, SPAIN.

**Aims:** This study aims to locate accurately the position of all beats in a multiparametric recording, so the information redundancy provided by the different signals on the recording could help us to better solve the problem.

**Methods:** We have designed algorithms to detect beats on different signals. At this moment, we process ECG, blood pressure (BP), stroke volume (SV) and photoplethysmogram (PPG) signals. For ECG and BP we have used, respectively, `gqrs` and `wabp` programs (distributed within the wfdb library).

We detect beats on SV signal by using a signal filter based on a daubechies 4 wavelet transform and then looking for local minima. We have observed that filtered SV signal has always a prominent minimum after the occurrence of each beat.



Beat detection based on the plethysmography is performed by first transforming the signal with a windowed slope sum function. Adaptive thresholding is used to detect pulses in the resulting signal. A local search strategy is used to mark the heart beat occurrence in the pulse onset.

We have made the assumption that the distance between the occurrence of the beat on the ECG signal and on the rest of the signals is constant and only depends on the patient and the type of signal considered. For this reason, we have searched for the mode of this distance, which will be used to correct the position given by the different algorithms.

Finally, we have grouped all temporal marks, taking into account that it is not possible to have replicated ones (distance between marks must be greater than refractory period) and suppressing marks that are not reasonably in time with regard to previous rhythm and that at the same time are only present on one signal.

**Results:** We have tested our approach on the phase I test set of the *Computers in Cardiology Challenge 2014*, obtaining the following results.

Results of the Challenge

| | Se(%) | +P(%) |
|---|---|---|
| Gross | 86.67 | 95.08 |
| Average | 85.93 | 94.95 |
| Overall | 90.65 | |

# Heart Beat Detection Method with Estimation of Regular Intervals between ECG and Blood Pressure

Jongmin Yu*, Taegyun Jeon, and Moongu Jeon

Gwangju Institute of Science and Technology
Gwangju, Republic of Korea

QRS detection is known to be very useful in assessing heart beat detection method. However, A noise with similar amplitude on QRS complex is one of the major causes of accuracy degradation in the heart beat detection method based on QRS complex. Thus, we need a robust heart beat detection method for complex and noisy environment.

In this work, we propose a framework for heart beat detection using combination of signals which are associated with cardiac activity directly or indirectly. The framework is designed as following: First, signal analysis on time domain, second, signals analysis on frequency domain, and finally data fusion using heterogeneous signals.

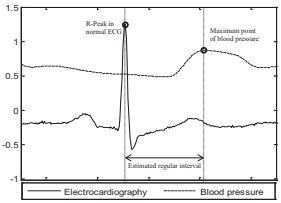


Figure 1. Estimate regular intervals between two characteristic points.

For the phase one, We propose heart beat detection method with estimation of regular intervals between ECG and blood pressure. In the normal signals, the two characteristic points are detected by window template matching for each heartbeat as shown in figure 1. The regular intervals between the two characteristic points are estimated from the cumulative detection results in the normal signals as follow:

$$Interval_i = MaxBP_i - ECG_{max(ECG[MaxBP_{i-1}, MaxBP_i])},$$

$$Interval_{regular} = \frac{1}{k} \cdot \sum_{i=1}^{k} Interval_i.$$

The extracted regular intervals are considered as an estimator for searching R-Peak in noisy sections. For the simple combination of ECG and BP, we selected the better detection results by comparing the number of estimated R-Peaks using the proposed method and WQRS algorithm.

The proposed method was applied to a testing data set of the CinC Challenge 2014 at phase one which achieved an overall score of 87.14%. For the next phase, we will improve it by using statistical multi-cue detectors and signal analysis for the direct and indirect groups associated with heart activities.

# Robust Detection of Heart Beats Using ECG, BP and EEG Signals

Soo-Kng Teo[1], Bo Yang[1], Dong Huang[1], Monterola Christopher[1], Yi Su[1],*

[1]Institute of High Performance Computing, A*STAR, Singapore

**Aims:** This study assessed the feasibility of using multimodal data, namely ECG, BP and EEG for the robust detection of heart beats in continuous long-term data in the PhysioNet/Computing in Cardiology Challenge.

**Methods:** When the ECG is clean, the location of the QRS can be determined accurately with the gqrs routine in the WFDB library. In the case when the ECG is noisy, we depend on the BP and EEG (if they are available) to locate the QRS signal in the following steps:

(i) Preprocess the signals to remove the baseline wandering for the three channels using the Butterworth low-pass filter. The EEG signal is also pretreated with the removal of the power-line noise.

(ii) Identify the clean part of the ECG and BP signal to determine the average and standard deviation of the delays between the QRS signal and the BP peaks. These data are used to define the search window relative to each QRS and BP peak identified by the gqrs and wabp routines respectively.

(iii) An error-correction code is implemented to check the interval where the BP may be missing or noisy. The error-correction code ensures that within any time window, if either ECG or BP channels is not noisy, the QRS is uniquely identified.

(iv) When both ECG and BP are noisy, the EEG signal is used. The peaks in the EEG coincide with the peaks in the QRS signal if the EEG signal is clean.

(v) In the rare case where all three signals (ECG, BP and EEG) are noisy or missing, the location of the QRS is inferred by the moving average intervals between consecutive QRS signals, obtained immediately before and after these "noisy" time windows.

**Results (Phase I):**

| | Se (%) | +P (%) |
|---|---|---|
| Gross | 85.53 | 92.63 |
| Average | 85.38 | 91.31 |
| Overall | 88.71 | |

## PhysioNet/CinC Challenge

Sachin Vernekar and Deepu Vijayasenan*

NITK
Kundapur, India

This work is part of the 2014 Physionet challenge that proposes a R peak detection program based on the ECG data using logistic regression. Wavelet decomposition of the raw ECG signal was performed to eliminate baseline drifting problem as well as high frequency noise. Three levels of wavelet decomposition are performed and the detail signals obtained from the third and fourth level are used as input to the algorithm. Coefficients from a context of 200 ms is joined together to make a fixed input feature. The samples is considered as a positive example if there is a R peak at the center. Similarly windows without a peak are considered as negative samples. Samples generated from the challenge's are used to train a logistic regression function. At the classification stage, a continuous stream of wavelet coefficients is considered, and a classification is performed every 4 ms. A ECG peak results in predicting a high value at the output of the trained logistic regression function. The local peaks of the logistic regression are then considered as the R peaks. Also temporal constraints such as the distance between the peaks are used to eliminate noisy outputs. In addition, simple windowing techniques are used to eliminate false positives using P peaks. The accuracy obtained on the challenge's development data was 96.27%. The result on the challenge data set evaluation data set is 92.85% after the post processing.

# Robust Detection of Heart Beats using Dynamic Thresholds and Moving Windows

Marcus Vollmer

University of Greifswald
Greifswald, Germany

**Background:** This contribution relates to the *PhysioNet/CinC Challenge 2014* on Robust Detection of Heart Beats in Multimodal Data. The aim is to locate heart beats in continuous long-term data.

**Methods:** The beat detection system consists of several parts. The preprocessing consists of a non-linear trimmed moving average filter for high pass filtering and standardization. Extrema of a moving window were used to capture the heart beat impulse. A windowed approach led to dynamic thresholds. Valid parts of the channels were determined and the location of beats were extracted. Followed by a dynamic delay correction for other channels than ECG, the beat locations of various channels were compared during the multichannel fusion procedure. Doubtful locations were checked using RR distances.

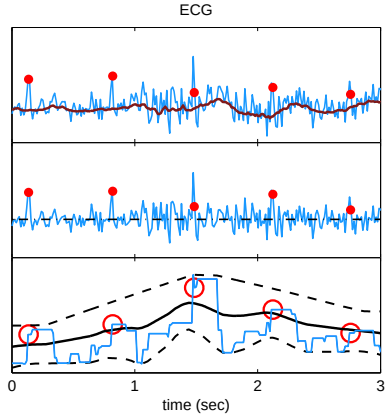


Exemplary beat extraction process.

**Results:** The preliminary algorithm was tested on the training data set for this challenge (composed of one hundred 10-minute recordings with various numbers of channels) and on the freely available MIT-BIH arrhythmia database (forty eight 30-minute excerpts of two-channel ambulatory ECG recordings). The preliminary algorithm scored 93.20 applied to the hidden Phase I dataset of the 2014 PhysioNet challenge.

Performance of the preliminary algorithm

| Division | Se | PPV | Overall |
|---|---|---|---|
| Training | 99.94% | 99.73% | 99.84% |
| MIT-BIH | 99.06% | 99.68% | 99.37% |
| Phase I | 93.44% | 93.76% | 93.20% |

**Conclusion:** The developed algorithm presents a promising approach to detect heart beats in multivariate records.

# Heart Beat Detection in Multimodal Data via Information Synthesis

Henian Xia*, Raj Baljepally and Xiaopeng Zhao

Zywie Inc.
Johns Creek, United States

Heart beat detection is usually conducted by detecting QRS in ECG. Many QRS detectors have been developed and show great robustness on clean signals. However, noise, artifacts, and missing data may frequently occur and severely corrupt ECG signals, leading to large errors in QRS detections. In many clinical and research settings, ECG is simultaneously recorded with other physiological signals, such as pulsatile signals that directly reflect cardiac activity, and others that may have few or no observable markers of heart beats. In this work, in response to the Physionet 2014 Challenge "Robust Detection of Heart Beats in Multimodal Data: the PhysioNet/Computing in Cardiology Challenge 2014", we develop a robust heart beat detection algorithm, which consists of three steps. After dividing an ECG signal to a series of ECG segments, the first step quantifies each segment's signal quality. In the second step, beats in segments with good signal qualities are detected using a robust QRS detector based on wavelet transformation; then relationships between heart rate and other physiological signals are learnt. In the third step, beat locations in segments with poor signal qualities are predicted using observed relationships between heart rate and other signals. A preliminary algorithm gives a score of 88.49.

# Lead Quality Monitoring for Detection of the Optimal Snapshot Time to Record Resting ECG

I Jekova[1], R Leber[2], V Krasteva[1], R Schmid[2], R Abächerli[2]*

[1]Institute of Biophysics and Biomedical Engineering, Sofia, Bulgaria
[2]Schiller AG, Baar, Switzerland

The earlier starting of the ECG recording with sufficient ECG quality is essential for the prompt reliable diagnosis. This study presents a lead quality monitoring system, which continuously scans the multi-lead ECG quality and automatically takes a decision to record 10s resting ECG. The system tracks the signal status (lead-off/valid) and the quality of every lead as percentage (0-100%). The ECG is analyzed within sliding 4s intervals and is divided into high, medium, low frequency parts that allow the estimation of spike noises, signal and in-band noises, offset and baseline noises, respectively. The lead quality is estimated as the ratio between the signal level and the sum of signal and all noise levels. Global ECG quality is calculated as the median quality for all leads. The minimal global quality within 10s, named 'Snapshot Quality' (SQ), is used for threshold based detection of the optimal snapshot time to record resting ECG.

Own ECG database (542 standard 12-leads ECGs, 5 minute duration, 1000Hz sampling rate, 1uV resolution), collected from chest pain patients at the emergency department in the University Hospital Basel is used. It is annotated in terms of maximal SQ and its time of occurrence observed in the recording. The threshold based detector is trained over 375 ECGs and tested with the remaining 267 ECGs. A fixed quality threshold (FQT) for starting automated ECG recording is applied over the training dataset. The detection accuracy is assessed by the percentage of ECGs that would be recorded at their best SQ (RecBestSQ). Maximal RecBestSQ=65% is achieved for FQT=75%. The time dependence of SQ level observed over the training dataset (see figure) suggests application of adaptive quality threshold (AQT) with initial level of 85%, decreasing to 65% within the 1st minute of ECG acquisition. The achieved accuracy is RecBestSQ>87% for training and test datasets.

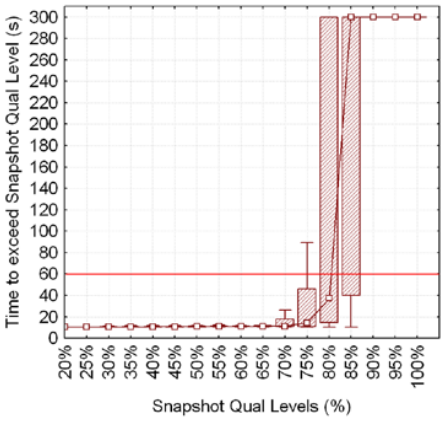

## Study of ECG Quality using Self Learning Techniques

Gianfranco Toninelli*, Alfonso Gerevini, Martino Vaglio and Fabio Badilini

Italy

**Aims:** The aim of this study is to introduce a method able to automatically evaluate the quality of ECG recordings. Since there is not a consensus on how define and quantify ECG quality, we applied self learning techniques starting from a set (N=1000) of randomly selected ECGs (12 leads and 10 second in length) from AMPS internal repository.

**Methods:** The full set of ECGs was blindly flagged by an expert cardiologist and subsequently analyzed by AMPS software (CalECG) which automatically computes a set of quality metrics which mainly include: -Low frequency and high frequency noise (LFNoise and HFNoise). -Complexity of the repolarization morphology (Tcomplexity). -A reliability index correlated with QRS detection of the embedded ECG measuring algorithm. These quality parameters were used to train a neural network and build a decision tree.

**Results:** 80% of the ECGs was involved in the training process of the neural network and the construction of the decision tree, while the remaining 20% was used only during the test phase. The performance of the proposed solutions were evaluated using the mean square error (MSE) between expected results (from the flags of the the ECGs set) and obtained results (from neural network and decision tree). The MSE resulting from the neural network and the decision tree were 0.005 and 0.004, respectively.

**Conclusions:** The proposed approach can be useful to assess the quality of ECGs in contexts of data analysis of large number of ECGs, for example within multi department clinical organizations and ultimately contribute to better care.

# ECG Recording Sites for Improving Signal to Noise Ratio during Atrial Depolarisation

Alan Kennedy*, Dewar Finlay, Daniel Guldenring and James McLaughlin

University of Ulster
Belfast, United Kingdom

P-wave indices have been associated with the onset of atrial arrhythmias, in particular atrial fibrillation; however, low signal amplitude and low signal to noise ratio (SNR) have prevented these parameters from being utilised from electrocardiogram systems. The aim of this study was to analyse atrial depolarisation patterns from 120-lead 352-node body surface potential map (BSPM) data to determine the location of the maximum and minimum p-wave amplitude. This in turn would allow identification of recording sites between which a bipolar lead, capable of maximising SNR, could be measured. BSPMs were recorded from 45 healthy subjects. The absolute median of each sample of the p-wave, across all 352 nodes for each individual subject, was analysed to determine the point in time where the greatest p-wave amplitudes occurred. Normalised p-wave values across all 352 nodes, at this point in time, were then extracted for each individual subject. The median of the normalised p-wave amplitude on each node was then calculated across all subjects to determine a population based optimal electrode position. The p-wave amplitude from the patient specific optimal electrode position was then compared to the population based optimal electrode position. The optimal bipolar electrode placement for recording of atrial depolarisation was just above the medial third of the right clavicle (minimum amplitude) and one intercostal space below precordial lead V4 (maximum amplitude). When comparing the p-wave amplitude recorded at the population based optimal lead position to the patient specific optimal lead position, a median of 83.53% of each subject's maximum p-wave amplitude was achieved. In this study we have analysed BSPM data to establish where bipolar electrodes could be positioned to capture the maximum amplitude signal during atrial depolarisation. Leads chosen in this way have the potential to improve SNR and allow for better application of algorithms that rely on p-wave analysis.

## New method for J-point Location in Subjects with Electrocardiographic Early Repolarization

Jacob Melgaard*, Johannes J Struijk, Jørgen K Kanters, Samuel E Schmidt, Ask S Jensen, John Hansen, Tanveer A Bhuiyan and Claus Graff

Aalborg University
Aalborg E, Denmark

**Introduction:** Early repolarization (ER) in the inferior/lateral leads of 12-lead ECG increases the risk of arrhythmic death. The ER pattern associated with highest arrhythmic risk is terminal QRS notching or slurring ≥0.1mV with a horizontal/downsloping ST-segment. Methods are needed to robustly locate the J-point in ER positive ECGs so large databases with electrocardiographic ER patterns can be analyzed. We developed and tested a new algorithm for J-point location in subjects with and without ER.

**Methods:** Electrocardiographic ER patterns from 50 healthy subjects with ER and 50 healthy subjects without ER were analyzed. ECGs were visually inspected and defined as positive for ER if there was terminal QRS notching or slurring of at least 0.1 mV in two contiguous inferior (II, III, aVF) or lateral (I, aVL, V4-V6) leads. Manual measurements of QRS duration (Q-onset to J-point) were com-pared to QRS durations obtained computationally between the manual Q-onset and the point with minimum standard deviation across all 12 leads between R-peak and T-peak (computerized J-point).

**Results:** The new algorithm for computerized J-point location found similar QRS durations in the ER+ and ER- groups (99±11 vs 101±15 ms, p=0.43). Manual QRS measurements were also similar in the ER+ and ER- groups (94±11 vs 96±14 ms, p=0.29). Computerized measurements of QRS duration were consistently longer than manual measurements in both the ER+ group (5.2 ms, CI: 2.2 to 8.3 ms, p<0.01) and the ER- group (4.6 ms, CI: 1.2 to 8.1 ms, p<0.01). There was no difference in heart rate between ER+ and ER- groups (65 vs 63 bpm, p=0.57).

**Conclusion:** Computerized measurements of J-point location were consistent with manual measurements of the J-point in subjects with and without early repolarization. The impact of varying terminal QRS patterns on J-point location is unclear and will be studied further.

# Automatic Real-Time Quality Assessment of a 12-Lead ECG Recording

R Firoozabadi*, RE Gregg, B Zengo, S Babaeizadeh

Advanced Algorithm Research Center, Philips Healthcare
Andover, MA, USA

**Background:** To obtain a diagnostically useful ECG recording, automatic real-time quality assessment of ECG signal can provide critical feedback to the person acquiring the ECG if there is a need to retake the signal while the patient is still present. Such automated analysis can also assist a clinician scanning hours of retrospective ECG to quickly find a high quality sample within a given time interval, for example, in hours before the patient reports chest pain. This study reports the performance of our quality assessment technique to identify if a 12-lead ECG recording is diagnostically acceptable.

**Method:** We used the CinC/Physionet 2011 challenge 12-lead 10-second ECG recordings with standard diagnostic bandwidth, collected at 500 samples-per-second, and 5μV amplitude resolution. The database is manually annotated by 23 experts and is divided into training (n=1000) and test (n=500) sets. Our algorithm calculates a noise score as the weighted sum of the inter-lead averages of the high-frequency noise (muscle artifact) and low-frequency noise (baseline wander) measures on 1-second ECG segments. Calculating the noise measures does not require beat detection or QRS segmentation. The recording is identified as acceptable if all its segments have noise score lower than a reference threshold which was selected for maximum accuracy on the training dataset. Using the same reference threshold we calculated the algorithm performance on the test dataset.

**Results:** A positive event being identifying a recording as unacceptable, ROC curve for the training dataset was plotted. Our method achieved maximum accuracy of 93.9% (with 84.9% sensitivity and 96.5% specificity). On the test dataset the accuracy was 90.2% which is among the top 10 scores achieved in the challenge.

**Conclusion:** Our automatic real-time signal quality assessment technique is highly accurate and can help with ensuring that the ECG recorded at the point of care is of diagnostically acceptable quality.

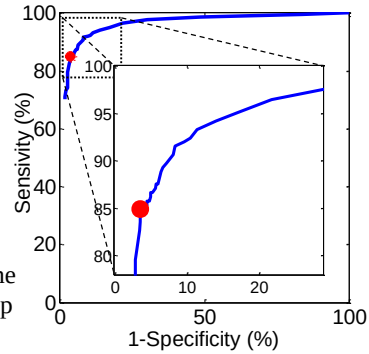


The ROC curve for the training dataset. The point of maximum accuracy, 93.9%, is marked by a dot. The area under curve (AUC) is 95.6%.

# Serial ECG Analysis: Can we Detect Faulty ECG Recordings?

Arie C Maan*, C Cato Ter Haar, Sumche Man, Roderick Treskes, Marjolein De Jongh, Maurits Van der Heide, Martin J Schalij and Cees A Swenne

Leiden University Medical Center
Leiden, Netherlands

**Background:** Ischemia detection in the ECG is essential for adequate triage at first medical contact in acute coronary syndrome. Serial comparison with an earlier non-ischemic ECG increases sensitivity (Ter Haar, Comput Cardiol 2013;40:9-12) but specificity may be corrupted by faulty ECGs, caused by, e.g., misplaced or interchanged electrodes. Methods. In each of 96 patients we studied four 12-lead ECGs recorded within 2 years. In each ECG the reconstruction index, RI, was computed, defined as the correlation of the original 12-lead ECG and a reconstructed 12-lead ECG, obtained after transformation of the original into a vectorcardiogram, using the Kors matrix, and back, using an optimized inversion matrix (Maan, Comput Cardiol 2011;38:289−292). Basically, with perfect electrode placement, RI expresses how well the conduction properties of the thorax of the individual resemble those of the thorax as assumed in the statistical models from which the transformation matrices were derived. Within subjects, the RI of repeat ECGs should be nearly the same, and a lower RI is likely due to faulty electrode placement. In each patient we identified the 3 ECGs with the best RI values, computed the range of these values, A, and the difference between the lowest of these values and the worst RI value, B. Finally we computed the relative distance, RD, of the worst measurement as RD = B/A.

**Results:** Average of the best 3 RI values was 0.94, average of the worst RI was 0.84. RD was 2.95±5.05 and significantly larger than 1. Discussion. In many cases one of the 4 ECGs had a low RI compared to the other 3 ECGs. This suggests that RI can be used to detecting faulty ECGs in serial ECG comparison, and thus help to reduce false positive diagnoses. We are currently determining the causes of these faulty ECGs.

# Analysis of non-linear respiratory influences on sleep apnea classification

Alexander Caicedo*, Carolina Varon, Sabine Van Huffel

KU Leuven, and iMinds Medical IT, Leuven, Belgium

**Aims:** In this work we aim at quantifying the non-linear coupling between heart rate and respiration. For this particular study, a novel methodology is proposed and applied to apnea classification.

**Methods:** We use concomitant measurements of ECG and Nasal breathing, obtained from 8 recordings from the Physionet Sleep Apnea Database. The tachogram was obtained from the ECG, and it was resampled, together with the respiratory signal, to 5Hz. We decomposed the respiratory signal using a $5^{th}$ level stationary wavelet transform. From this decomposition we used the approximations as a reference for the low-frequency band, and the $5^{th}$-$3^{rd}$ level details as a base for the high-frequency band. We construct a non-linear model based on kernel principal component regression between HR and the respiration. Furthermore, inside the nonlinear model we imposed a mean average structure of order 15. Additionally, from the obtained model we decomposed the HR in the components related to the low- and high-frequency bands. These components can be seen like a projection of the HR on the subspace spanned by the nonlinear transformation of the low- and high- frequency components of the respiration. Hence, the magnitude of these projections indicates the strength of the cardiopulmonary coupling in both frequency bands. We normalize the magnitude of these projections and used them as input for an apnea classifier. These results were compared with results obtained from a linear method, based on wavelet decomposition and orthogonal subspace projections that we previously developed.



**Results:** After evaluating the linear coupling an AUC of 88.29% was obtained, while using the novel non-linear method, the results were improved, obtaining an AUC of 92.36%. See ROC figure.

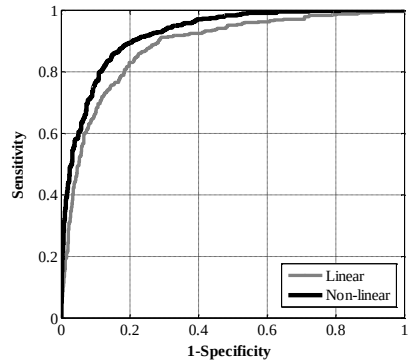


**Conclusions:** These findings indicate that this novel, non-linear methodology outperforms linear methodologies, currently used to quantify the cardiorespiratory coupling.

# Rank-based Multi-Scale Entropy analysis of Heart Rate Variability

Luca Citi*, Giulia Guffanti and Luca Mainardi

University of Essex
United Kingdom

The method of MultiScale Entropy (MSE) is an invaluable tool to quantify and compare the complexity of physiological time series at different time scales. MSE works by constructing coarse-grained versions of the original signal and computing the entropy measure corresponding to each scale factor. Although MSE traditionally employs sample entropy to measure the unpredictability of each coarse-grained series, the same framework can be applied to other entropy metrics. Here we investigate the use of a family of rank-based entropy measures within the MSE framework. Like in the traditional method, the series are studied in an embedding space of dimension m. The novel entropies assess the unpredictability of the series using the ranks of the mutual distances between the vectors representing each point in the m and m+1 dimensional embedding space. Being based on ranks rather than a hard threshold , these measures can extract useful information even from very short time series (as few as 300 samples). Analysis of simulated signals with known properties highlights the ability of each entropy measure of extracting a specific type of information and to distinguish series with different characteristics. We tested our novel method on tachograms extracted from the Fantasia database. After splitting each record in 15 short 300-samples non-overlapping windows, the method was able to find statistically-significant differences between young and healthy elderly subjects in: a) 5 windows at scale 1; b) 12 windows at scale 2; c) 9 windows at scale 3. Furthermore, the multi-scale plots computed on each window are representative of the one computed on the whole series which, in turn, is qualitatively similar to that computed by the traditional sample-entropy-based MSE. These encouraging results suggest the possibility of using these measures to perform a time-varying assessment of complexity with an increased accuracy and temporal resolution.

# A Methodological Assessment of Phase-Rectified Signal Averaging through Simulated Beat-to-Beat Interval Time Series

Massimo W Rivolta, Tamara Stampalija, Daniela Casati, Enrico Ferrazzi, Axel Bauer and Roberto Sassi*

Università degli Studi di Milano, Italy
Italy

S73

Aims. Phase-Rectified Signal Averaging is a methodology capable of extracting quasi-periodic oscillations out of noisy and non-stationary signals. Typically employed on heartbeat interval time series, it provides two measures that quantify the average cardiac acceleration (AC) and deceleration (DC) capacity. Calculation of AC and DC depends on three parameters (T, L and S). Aims of the study were to: 1) further clarify the influence of these parameters on AC/DC; 2) evaluate the inter-correlation between AC and DC; and 3) explore the relation between AC/DC and traditional spectral parameters, as high (HF) and low (LF) frequency power contents. Methods. An extensive set of simulations was performed, and AC/DC were computed: 1) while varying magnitude and phase of the poles of a second-order autoregressive (AR) model; 2) on sawtooth-like heart rate trends (i.e. intervals training in sports medicine or umbilical cord occlusion in fetal animal models); 3) on synthetic data generated by AR models fitted on real RR series.

**Results:** When computed on series generated by AR models, AC and DC were quantitatively equivalent ($p<0.05$). The parameter S, more than T, affected the results, while values of L>S were equivalent. In fact, S selected the oscillations to which AC/DC resulted maximally sensitive (at 75 beats-per-minute, HF oscillations for S=2 and 3 and LF oscillations for S=4 to 12). On the contrary, sawtooth-like series, with different growth and decrease rates, showed a marked difference between AC and DC.

**Conclusions:** AC and DC are not simply related to the HF and LF contents, as obtained with spectral analysis. In fact, AC/DC assume identical values for any S when the series is symmetrical under time-reversal, as in AR models. Instead, AC and DC are also linked to the asymmetries between the rates of growth and decrease of HRV, and might quantify differently underlying regulatory mechanisms.

# QT-Interval Adaptation to Changes in Autonomic Balance

Ehimwenma Nosakhare*, George Verghese, Robert Tasker and Thomas Heldt

MIT
United States

The role of the autonomic system in regulating cardiac function, and the prospect of inferring the state of the autonomic system through examination of cardiac behavior, are important subjects. Here, we assess variability of the QT-interval during changes in autonomic balance. To assess the QT-interval, we developed a pair of detection algorithms based on the curve-length transform. A forward curve-length transform was used to detect the Q-onset, and a backward curve-length transform with maximum distance search was used to detect the T-offset. These were tested against cardiologists' annotations of 105 records in the PhysioNet QT database. The Q-onset and T-offset algorithms achieved a mean error (± standard deviation) of −0.8 (±13) ms and −7.0 (±17) ms respectively. The archived PhysioNet annotations associated with these records, as detected using the differentiated threshold algorithm, achieved a mean error of −1.8 (±30) ms and −7.6 (±46) ms for the Q-onset and T-offset, respectively. These algorithms were applied to archived ECG records of ten subjects undergoing tilt-table experiments. Both the QT-interval and RR-intervals were extracted. The interventions included passive rapid tilt-up, passive slow tilt-up and actively standing up. Each subject underwent each change in posture twice, for a total of 20 maneuvers. The RR-intervals responded quickly to each change in posture, while the QT-intervals showed a distinctly slower response with characteristics of a first-order exponential. An exponential model was fitted to the QT-interval adaptations, and time constants in the range of 70-95 s were obtained. Our results demonstrate slower adaptation of the QT-interval than the RR-interval to changes in autonomic balance induced by changes in posture. This slower adaptation might be primarily due to sympathetic modulation of the QT-interval (as opposed to sympathetic and parasympathetic control of RR-interval), or due to slower intracellular mechanisms. Further studies are required to tease these mechanisms apart.

# Separating Respiratory Influences from the Tachogram: Methods and their Sensitivity to the Type of Respiratory Signal

Devy Widjaja*, Carolina Varon, Dries Testelmans, Bertien Buyse, Luca Faes and Sabine Van Huffel

KU Leuven
Leuven, Belgium

**Aim:** Respiration is one of the main modulators causing heart rate variability (HRV). However, when interpreting studies of HRV, the effect of respiration is largely ignored. We, therefore, previously proposed to take respiratory influences into account by separating the tachogram into a component that is related to respiration and one that contains all residual variations. In this study, we aim to investigate the sensitivity of two of such separation methods, i.e. one based on an ARMAX model and another one based on orthogonal subspace projection (OSP), towards different respiratory signal types, such as nasal airflow (the reference), thoracic and abdominal efforts, and three ECG-derived respiratory (EDR) signals.

**Methods:** The sensitivity of both separation methods to the type of respiratory signal is evaluated by assessing the information transfer, as measured by the cross entropy, from the reference respiratory signal to the residual tachogram, where the latter is obtained using each time a different type of respiratory signal. The lack of information transfer serves as proof that the residual tachogram does not contain any respiratory-related heart rate variations, and thus demonstrates the efficiency and robustness of the separation method.

**Results:** The results show that OSP is the least sensitive to the different types of respiratory signals; 16 (15) out of 18 recordings show no significant information transfer when OSP (ARMAX) is used in combination with recordings of the abdominal and thoracic efforts. Even when an EDR signal obtained using kernel principal component analysis is used, OSP yields a correct separation in 13 out of 18 recordings.

**Conclusion:** OSP is less sensitive than ARMAX to the different morphologies of several respiratory signal types. Additionally, preliminary results based on EDR signals suggest that the separation of the tachogram could be feasible even if only the ECG signal is available.

## Dynamic Network Interactions of the Cardiac System

Ronny P Bartsch, Amir Bashan, Kang KL Liu, Chunhua Bian, Gustavo Zampier dos Santos Lima and Plamen CH Ivanov*

Boston University
Boston, United States

The human organism is an integrated network, where organ systems, each with its own regulatory mechanism, continuously interact to optimize and coordinate their function. Organ-to-organ interactions occur at multiple levels and spatiotemporal scales to produce distinct physiologic states: wake and sleep; light and deep sleep. The nature of these interactions and their collective role in maintaining health is not understood. We investigate how the cardiac system dynamically interacts with other organ systems: brain, respiration, eye-movement, leg and chin muscle tone. We propose an approach based on the concept of time delay stability --- the delay with which bursts in cardiac dynamics are consistently followed by corresponding modulations in other systems. Periods with constant time delay indicate a stable interaction. To probe the network of interactions between the cardiac and other systems, we analyze 8-hour multi-channel recordings during sleep, obtained from 36 healthy subjects (18 female, 18 male, ages 20-40): heart rate, respiratory rate, variance of the electrooculogram and electromyogram signals, EEG from six scalp positions (frontal, central, occipital) in physiologically-relevant frequency bands. We uncover a strong relationship between network connectivity, patterns in link strength and physiologic function. Specifically, the number of heart-brain links and their strength varies for different brain areas and dramatically changes with transitions across sleep stages: higher connectivity and link strength during light sleep and wake compared to REM and deep sleep. Remarkably, we observe the same type of phase transitions in network interactions between the cardiac system and the other systems. This sleep-stage stratification pattern in network organization is in contrast to earlier findings of higher degree of heart rate auto-correlation and nonlinearity during wake and REM compared to non-REM (light and deep) sleep, and indicates a very different neuroautonomic regulation of the cardiac system itself compared to the regulation of its interactions with other systems.

# Robust Heart Rate Estimation from Noisy Phonocardiograms

David Springer*, Thomas Brennan, Jens Hitzeroth, Bongani Mayosi, Lionel Tarassenko and Gari Clifford

United Kingdom

Accurate heart rate estimation is a fundamental process when analysing phonocardiograms (PCGs), as it allows more accurate segmentation of the fundamental heart sounds, and hence, more accurate classification of pathologies. While heart rate estimation is trivial in noise-free recordings, it becomes a difficult task in PCGs corrupted by various in-band noise sources, such as speech, pathological sounds and motion artefacts. Numerous heart rate estimation techniques have been explored in the literature the majority involving analysis of the autocorrelation function. However, no comparison between these various techniques has been performed to identify the optimal method in noisy recordings. This paper evaluates various denoising, normalisation, envelope extraction and heart rate estimation techniques on three datasets, which used six different devices for PCG recordings. The detection of the first significant peak in the autocorrelation function, following Hilbert envelope extraction, was found to be the optimal method across all but one of the training data sets. Wavelet denoising and normalisation parameters varied between recording devices. The optimal algorithm, found on the combination of all 585 PCGs in the training set, correctly estimated the heart rate in 471 (80.5%) of these PCGs, while correctly estimating the heart rate in 86% of the PCGS from a separate (publicly available) test dataset. Therefore, it can be concluded that the optimal algorithm on the entire training set, using single peak detection in the autocorrelation waveform after extracting the Hilbert envelope with 95% normalisation threshold and using the Biorthogonal 2.8 wavelet for denoising yields the most accurate HR estimates across a variety of PCGs.

# A Novel Technique for Analyzing Noisy Noninvasive Fetal Electrocardiogram Signals

Mohammad Javad Mollakazemi, Seyyed Abbas Atyabi* and Ali Ghaffari

CardioVascular Research Group (CVRG), Department of Mechanical Engineering at K.N.Toosi University of Technology, Tehran, Iran
Iran (Islamic Republic of)

In this study, a new method is presented to identify fetal QRS complexes (fQRS) in noisy data which completely is noise robust. This method can be used both in adults electrocardiogram signal (ECG) and fetus electrocardiogram signal (fECG). The existence of noise is one of the fundamental problems in the study of fECG signal. The amplitude and the energy of the fQRS complex depending on age of fetus or other factors, is different and sometimes fetal complexes can barely be seen. In this case, even little amount of noise will make problems for finding the exact location of fetal beats and measuring the fetal heart rate accurately. To solve this problem, a new method is presented that can detect the presence of noise accurately and if a range of the signal has noise, another channel will be used in that specific noisy range. If the noise exists in all available channels, the fetal heart beats in that noisy range are predicted according to the former fetal RR intervals (FRR). The Wavelet based analysis is used for detecting noise, and the wavelet function of ' Symlets6' in first level is used for decomposing the signal and then with estimation of the detail coefficients' standard deviation, the noisy intervals are recognized. In this paper there are some significant characteristics. The first one is recognition of noise. Secondly, in presented method extraction of mECG or fECG of abdominal signal is not the case and both maternal and fetal ECGs are analyzed together in all the stages of processing. Finally, the simultaneous combinational use of the available channels has improved the algorithm performance. This method was applied on the fetal electrocardiogram database of physioNet and resulted average Sensitivity of 93.08% and average positive predictivity of 94.1% which shows the promising performance of the algorithm.

# Subject-Optimized Feature Selection for Accurate Classification of Cardiac Beats

Piotr Augustyniak

AGH-University of Science and Technology
Krakow, Poland

Beat classification is a difficult task due to high subject-related variability of the features. While numerous approaches in the past aimed at discovering a universal most-discriminative parameter (or set of parameters), we propose to use genetic algorithm to select a very small patient-dependent feature sets of high discrimination capabilities.

The method starts with applying a conventional kNN-based classification to several ECG strips randomly selected in a 24h record. The classification results are presented for the operator for confirmation of correctness, and used as a patient specific learning set. If the features determined as optimal varies from strip to strip, the algorithm is run again for concatenated strips. Finally, the optimal set of features is attributed to the patient and used in whole present and future records.

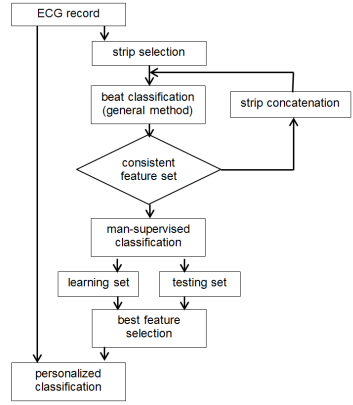


Optimization block diagram

The proposed method was tested on MIT-BIH Arrhythmia database providing reference beat types for each record. We implemented algorithms calculating 57 different parameters of the beat (mainly focused at the QRS), based on shape, acceleration, area, length etc. and used kNN and SVM as classification methods. We built the learning set out of 15 strips of 10s length and assume that a feature set contains maximum of 5 elements.

Percentage of misclassified heart beats

| classification | reference | optimized |
|---|---|---|
| kNN | 3.11 | 1.15 |
| SVM | 2.73 | 0.69 |

Comparing to the classification based on reference minimum correlation-based selection of features we observe significant reduction of misclassified beats ratio (for SVM from 2.73% to 0.69% in average).

Reduction of the feature set size reveals that the 3-elements optimized set is still more distinctive than the 5-elements reference. Since the optimization stage is performed once (unless the patient has significant progress of cardiac disease), the algorithms calculating the optimal features may accompany the personal data or embedded in reprogrammable personal ECG recorders.

## Evaluation of FHR Recordings based on Clustering

Václav Chudáček*, Jiří Spilka and Tereza Janíčková

Czech Technical University in Prague
Czech Republic

Fetal heart rate (FHR) recorded within the cardiotocography (CTG) measurement is currently the main method to evaluate fetal health state during delivery. The CTG provides valuable information about fetal behavior as a reaction to stressful events (hypoxic episodes). The presented paper proposes to use data driven analysis of FHR – the clustering analysis. Even though the clustering is well grounded in signal processing tasks in the FHR research it is used sparingly due to high inter-individual variability of fetuses and difficulties to link different temporal events. Data from the open access CTU-UHB database (552 CTG records) available at the Physionet are used in this work. The 30 minutes segments at the end of the first stage of labor are analyzed. Different sets of features were extracted: Classical time and frequency domain features, features based on SAX, and piecewise linear interpolation. K-means algorithm was used for clustering. The presented contribution confirms the conclusions of Keogh&Lin that clustering of the time series subsequences is meaningless. The subsequences hinder the global picture of FHR and yields to misleading results. Second, the clustering suggests four different classes of FHR. This is in contrast with objective evaluation (two classes usually determined with pH threshold) and three classes (used by clinicians for evaluation). However, four classes revealed by FHR clustering independently confirms our previous results on latent class modeling of clinicians' annotations that were shown to lead to four classes as well. The classification based on clustering achieved sensitivity of 58.7% and specificity of 69.4% for the two class classification – well comparable to other pH based studies. Sensitivity was improved to 71.4% for four cluster settings, nevertheless to properly describe the link between these clusters and clinical evaluation robust interpretation is still necessary.

# Support Vector Machine Hidden Semi-Markov Model-based Heart Sound Segmentation

David Springer*, Lionel Tarassenko and Gari Clifford

University of Oxford, Oxford, UK
United Kingdom

The segmentation of the primary heart sounds within a phonocardiogram (PCG) is an essential step in the automatic analysis of heart sound recordings, allowing for the classification of pathological cardiac events. While segmentation is trivial in noise-free recordings, it becomes a difficult task when PCGs are corrupted by in-band noise. Common noise sources include talking, motion artefacts, background noise from machinery and physiological sounds. While threshold-based segmentation methods have shown moderate success, probabilistic models, such as hidden Markov models, have recently been shown to surpass the capabilities of previous methods. Segmentation performance is further improved when a priori information about the expected duration of the states is incorporated into the model, such as in a hidden semi-Markov model (HSMM). This paper addresses the problem of the accurate segmentation of the primary heart sounds within noisy, real-world PCG recordings using a HSMM, extended with the use of support vector machines (SVMs) for emission probability estimation. A database of 123 patients with over 20,000 labelled heart sounds were used to train and test the algorithm. Best reported alternatives in the literature were also implemented and tested on the same data. On out-of-sample test data, our method outperforms previously reported methods with sensitivities of 94.9% and 91.0% and positive predictivities of 95.2% and 90.9% for the first and second heart sounds respectively, as compared to 92.6% and 89.0% sensitivities and 92.3% and 88.3% positive predictivities using previous state-of-the-art methods. The greater discrimination between states afforded by the non-linear kernel of the SVM as opposed to the previous Gaussian distribution-based emission probability estimation allows this method to significantly outperform previous methods based on a one-sided, paired t-test.

# Acute Ischemia Detection using a QRS Angle-based Method

Daniel Romero*, Juan Pablo Martínez, Pablo Laguna and Esther Pueyo

Université de Rennes 1
France

**Background** Ischemia detectors represent a useful diagnostic tool to assess patients with suspected or known coronary artery disease. Currently, most ischemia detectors are based on evaluation of ST segment deviation rather than on QRS changes. However, distinction between ischemic and non-ischemic ST deviation episodes remains a challenge.

**Methods:** In this work we present and evaluate an ischemia detector based on the analysis of changes in the angles of the QRS complex, for which a model of gradual transitions contaminated by Laplacian noise is assumed. ECG recordings of 79 patients undergoing prolonged coronary occlusion in one of their major coronary arteries (LAD=25, RCA=16 and LCX=38 patients) were investigated. Individual ECG leads were independently considered for ischemia detection. Results were evaluated in terms of sensitivity (Se) and specificity (Sp).

**Results:** In the LAD subgroup, leads V1, V2, V3 and V4 showed the best detection performance, with maximum Se=67% and Sp=93% (lead V3). In the RCA subgroup, optimum leads were aVR, II and aVF, with associated maximum Se=56% and Sp=94% (lead II). In the LCX subgroup, the best performance was achieved for leads V4, V5, V6 and aVL, with maximum Se=33% and Sp=84% (lead V5).

**Conclusion:** Evaluation of ECG depolarization by analysis of QRS angles, as proposed in this study, shows capability for detection of acute myocardial ischemia. Optimum leads for detection are highly dependent on the occluded artery suggesting using combinations of leads for a better detection performance. The proposed method could be used as an adjunct tool to ST segment deviation to improve the performance of current ischemia detectors.

## Serial ECG Analysis for Ischemia Detection: How Representative Is a Reference ECG?

Roderick Treskes*, C Cato Ter Haar, Sumche Man, Marjolein De Jongh, Maurits van der Heide, Arie C Maan, Martin J Schalij and Cees A Swenne

Leiden University Medical Center
Leiden, Netherlands

**Background:** Ischemia detection in the ECG is essential for adequate triage at first medical contact in acute coronary syndrome. The current ST threshold of 100 μV has low sensitivity; however, a lower threshold of 50 μV requires intra-individual serial comparison with a previous non-ischemic reference ECG, to correct for preexisting nonzero ST amplitudes. Additionally, serial comparison of the spatial QRST area (ventricular gradient, VG; threshold 16.2 mVms) is useful for ischemia detection (Ter Haar, Comput Cardiol 2013;40:9-12). For serial analysis it is important that a reference ECG remains representative. It is, however, not known how clinical events and medication changes influence ST and VG. Methods. From the hospital database we selected patients with 3 ECGs, A-B-C, taking care that ECGs A-B and B-C randomly differed either 1-2 weeks / 1-2 years, or 1-2 years / 1-2 weeks, respectively. This selection ensured presence as well as absence of intervening clinical events and medication changes. Patients with acute ischemia were excluded. We analyzed the ECGs with our vectorcardiogram-oriented LEADS program, determined the ST and VG vectors and computed the magnitudes of the differences, ΔST and ΔVG, between ECGs A-B, A-C and B-C.

**Results:** The study group comprised 106 patients (74,5% male) with a mean age of 57.8 years. In 40,5% of the ECG comparisons made, ΔST was >50 μV. Additionally, 68.2% had a ΔVG >16,2 mVms. Discussion. Our results show that serial comparison of clinical but non-ischemic ECGs would yield a substantial amount of false positive ischemia detections. We are currently investigating till what extent intervening clinical events and medication changes have contributed to these ECG changes. If they are the major cause of changes in the reference ECG, new reference ECGs should be recorded after alterations of the medication or after intervening clinical events.

# Improving Automatic Detection of Acute Myocardial Infarction in the Presence of Confounders

Richard E. Gregg, Saeed Babaeizadeh

Advanced Algorithm Research Center, Philips Healthcare
Andover, MA, USA

**Background:** Several ECG features are common electrocardiographic markers for manual interpretation of early repolarization (ER) and acute pericarditis (PCARD), confounders for acute myocardial infarction (AMI). However, these features are not often used in automated ECG interpretation. We studied if these features could improve automated AMI detection in the presence of ER and PCARD.

**Method:** The training set of ECGs included cardiologist reading of ER (n=147), PCARD (n=114), normal (n=239) and AMI (n=380). AMI was confirmed by reading infarct evolution in serial ECGs. ECGs not meeting STEMI criteria by algorithm were excluded. The test set came from emergency department chest pain patients (n=832). The reference was discharge diagnosis of AMI. Positive ECGs (n=261)were both STEMI and NSTEMI. Two logistic regression AMI classifiers were compared, one using traditional features, another using traditional plus additional features to help with detecting ER and PCARD. Traditional features were Selvester QRS score, standard ST-segment, and T-wave amplitudes. Additional features included J-waves, notches, slurs, PQ segment depression, upward ST-T concavity, spatial QRS-T angle, T-wave complexity, and J point ST to T-wave amplitude ratio. Both classifiers used forward step-wise feature selection on the training set to choose the ten best representative parameters of the ECG features.

**Results:** The table below shows the classifiers performance on the test set where ECGs not meeting STEMI criteria were classified AMI negative.

| Features | Sensitivity | Specificity | Pos. Predictive Value | Neg. Predictive Value |
|---|---|---|---|---|
| traditional | 38 | 98 | 89 | 78 |
| traditional + additional | 47 | 97 | 88 | 80 |

As expected, the traditional features had the most discrimination power. However, the automatically-selected best features included the number of anterior leads with concave up ST-to-T-peak segments and the mean anterior PQ segment depression.

**Conclusion:** Additional ECG features aimed at ER and PCARD may improve automatic AMI classification when STEMI criteria are met.

# A Real-time ST-segment Monitoring Algorithm based on a Multi-channel Waveform-length-transformation Method for Q-onset and J-point Setection

Wei Zong*, Scott Kresge, Haisheng Lu and John Wang

Philips Healthcare
Andover, United States

**Introduction:** Real-time ST-segment monitoring, which allows for continuous detection and tracking of cardiac ischemia, is a valuable clinical tool for patient management. To measure the ST, Q-onset (Q), used for locating isoelectric point (Iso), and J-point (J) must be determined reliably. In this paper, we describe a new method for determining the Iso and J used in a real-time ST measurement algorithm.

**Methods:** For each ST measurement interval, a representative ECG waveform is generated by averaging the selected dominant normal beats. After excluding leads with low signal quality, the remaining leads are used in a multi-lead waveform-length-transformation (WLT) to form a single-channel detection function for Q and J determination. From Q, the Iso is determined and used with the J to measure the ST-segment level at J or J plus an offset for all available leads. A dataset of 158-patient ECG records with cardiologists' beat-by-beat Q, J annotations was used in developing the Q, J detection algorithm.

**Results:** Using a 60-patient annotated test dataset, the accuracy results for Q and J, measured as the mean difference (MD) ± standard deviation of difference (SDD), are -2.5±7.7ms, and 0.5±10.5ms, respectively. The algorithm's ST performance at J+80ms, tested using the 90-record ESC ST-T database, measured as MD, mean absolute difference (MAD), correlation coefficient (CC), and linear regression slope (LRS), are 1.8uV, 49.1uV, 96.3, and 0.98, respectively. These results are as good as the results obtained by manually setting the optimal Iso and J points. In addition, using an annotated 60-patient 12-lead PTCA dataset, the ST measurements at J-point measured as MD, MAD, CC, and LRS, are -1.3uV, 24.9uV, 97.1, and 0.97, respectively.

**Conclusion:** The test results using a variety of annotated databases have demonstrated the performance of the ST-segment measurement algorithm based on the Q-onset and J-point determined by the multi-lead waveform-length-transformation method.

# Wavelet Based Method For Localization Of Myocardial Infarction Using Vector Electrocardiogram

Nader Jafarnia Dabanloo, Azadeh Nooriyan and Saman Parvaneh*

Department of Biomedical Engineering, Science and Research Branch, Islamic Azad University, Tehran, Iran
Tehran, Iran (Islamic Republic of)

Detection of MI aims to classify healthy and who having MI and Localization aims to specify the infracted region of the heart. Electrocardiogram is a classical diagnosis to detect heart malfunctioning and heart muscle damage. It is also safe and fast method for diagnosis . In this paper we presented a method for detection and localization of myocardial infarction (MI) using RBF neural networks classifier with wavelet coefficient as features extracted from Frank leads. We used the electrocardiogram (ECG) source used in the PTB database available on physio-bank. We use 50 records of 12-lead standard ECG to train and test the proposed algorithm in about 3611 beats extract from these records. The collected ECG traces contain different kinds of MI (Inferior –lateral, Inferior-posterior-lateral, Inferior, Antero-septal, Antero-lateral ,Anterior, Posterior-lateral, Lateral, Posterior) and healthy cases. All the ECG records had been diagnosed by cardiologist. Frank lead vx,vy,vz was extracted from 12 lead ECG using Dower transformation. Then we calculated wavelet coefficients in three level 3, 4, 5 from three wavelet haar,db4,db10 to evaluate the different kinds of wavelet . We used PCA to reduce the number of features. Then we used 70% data (about 2504 beat) for training the neural network and 30% data (about 1099 ECG beat) for test. First we classified the data into 2 classes: healthy and having MI. Here it was found that the sensitivity and specificity is about 99% and 96% . For localization in the best re3sults the error was less than 10%. The proposed method due to its simplicity and high accuracy over the PTB database can be helpful in correct diagnosis of MI localization.

# A Platform to guide Catheter Ablation of Persistent Atrial Fibrillation using Dominant Frequency Mapping

Xin Li*, João L. Salinet, Tiago P. Almeida, Frederique J. Vanheusden, Gavin S. Chu, G. André Ng, Fernando S. Schlindwein

University of Leicester,
Leicester, UK

**Introduction:** Dominant frequency (DF) mapping has been widely used to study the pathophysiology of atrial fibrillation (AF). In this study, a DF mapping system was developed to guide catheter ablation on electrophysiology (EP) procedures of persistent AF patients.

**Methods:** 5 persistent AF patients undergoing left atrium (LA) catheter ablation were enrolled. A non-contact balloon array (St. Jude Ensite Velocity System) was introduced transeptally in the LA. 2048 channels of virtual unipolar electrograms (EGMs) were simultaneously acquired for 30 s. During the EP procedure, data were exported and investigated on the DF mapping platform hosted by a user-oriented graphic interface (GUI) developed in Matlab. The DF mapping platform was divided in the following modules: 1) read the .csv files containing the data; 2) QRST subtraction on all EGMs; 3) Fast Fourier transform of EGMS segmented in 4-s windows (50% overlap) to calculate DF, organization index (OI), regularity index (RI); 4) phase map for all EGM samples; 5) save the data. DF, OI and RI of each window were colour-coded and plotted on a 3-D LA mesh. High DF areas and the trajectory of their centres of gravity were also projected on the 3-D LA mesh. 3-D videos of the phase can be observed using a slider. EGMs of interest can be assessed in any atrial region.

**Results:** The overall platform processing time (mean ± SD) per module for the 5 patients is shown on Figure A (total processing time 10.4 ± 1.5 min).

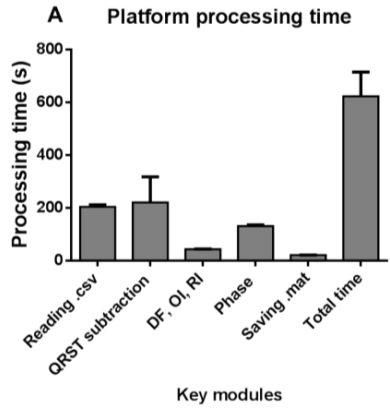


**Conclusion:** The proposed DF mapping platform is a fully automated GUI that provides 3-D representation of the left atrium with the DF behaviour. This platform was used to guide catheter ablation on EP procedures in 5 persistent AF patients and the clinical outcomes are currently being assessed.

# Spatiotemporal Behaviour of High Dominant Frequency during Persistent Atrial Fibrillation

Nawshin Dastagir*, Joao L Salinet, Frederique J Vanheusden, Tiago P Almeida, Xin Li, Gavin S Chu, Andre G Ng and Fernando S Schlindwein

University of Leicester
Leicester, United Kingdom

Introduction- Atrial electrograms (EGMs) with high dominant frequency (DF) are believed to represent atrial substrates with periodic activation responsible for the maintenance of persistent atrial fibrillation (persAF). This study aimed to assess the DF spatiotemporal behaviour using high density noncontact mapping in persAF. Methods- For 8 patients undergoing left atrial (LA) persAF ablation, 2048 noncontact virtual unipolar EGMs were simultaneously collected using a balloon array (Ensite 3000, St. Jude Medical, 1200 Hz). After QRST subtraction, fast Fourier transform was used to detect the DF on each EGM (range 4 Hz-10 Hz; 4 s time window; 50% overlap; up to 38 s per patient). Atrial areas with highest DF (HDF, DF ± 0.25 Hz) were delimited in each frame for all 2048 EGMs, creating HDF clouds. Cumulative HDF clouds found at each frame were counted in the 3-D LA representation. To further assess the temporal stability of the cloud, the number of EGMs not hosting any HDF was determined for each window over time. Results- Figure 1 shows cumulative HDF clouds on the 3-D representation of the atrium for 1 patient. The number of occurrences of HDF clouds in the atrium is represented by the colorbar. In this case, the maximum recurrence of HDF cloud in the same atrial region (darkest region) was 16 times. Figure 2 shows the number of positions on the 3-D representation of the atrium (total, 2048) not visited by HDF. Logarithmic curves were fitted for each patient. In this case, the time constant ($\tau$) of the log best fit is 5.31 s. The average for all patients (±SD) was 6.45 ± 3.59 s. Conclusion- Our results suggest DF in persAF is not temporally stable. Some atrial regions are more prone to host HDF clouds and mapping the cumulative HDF might be an interesting strategy for ablation.

# Distinctive Patterns of Dominant Frequency Trajectory Behaviour in Persistent Atrial Fibrillation: Spatio-temporal Characterisation

Joao Salinet*, Jiun Tuan, Angela Salinet, Xin Li, Peter Stafford, G Andre Ng and Fernando Schlindwein

University of Leicester, UK
São Paulo, Brazil

**Introduction:** Though the use of dominant frequency (DF) mapping to guide catheter ablation during persistent atrial fibrillation (persAF) has been proposed as a potential strategy, the characteristics of high DF sites have not been extensively studied. This study aimed to assess the spatiotemporal stability of DF using simultaneous, high density, non-contact mapping (NCM) of persAF.

**Methods:** 8 persAF patients were studied using NCM. Ventricular far-field cancellation was performed followed by the calculation of DF using Fast Fourier Transform. 3D DF maps with 2048 non-contact unipolar atrial electrograms (EGMs) were generated over consecutive frames of up to 1min (windows of 4s with 50% overlap). Stability of DF activity and analysis of spatiotemporal behaviour of DF were investigated including characteristics of the highest DF area (HDFA). The electrograms' DF organisation of sites localised on the HDFAs core (OICG) and its periphery (OIPer) were also analysed.

**Results:** A lack of DF spatiotemporal stability was observed demonstrating that AF mapping would be preferable performed using simultaneous multipolar recordings. Although DF is not stable, a certain degree of DF reappearance was observed, mostly within 10 s. Tracking of the centre of gravity (CG) of HDFAs revealed 3 types of propagation behaviour, namely i) local, ii) cyclical and iii) chaotic activity, with the former 2 patterns accounting for most of the observed events. Sites at the HDFAs' core presented higher DF organisation than areas by the HDFAs' periphery ($p=0.0061$). Real-time implementation was shown feasible in reducing the processing time from $2.46\pm0.05$s (single core) to $0.27\pm0.01$s (480 Graphic Processing Units).

**Conclusion:** The research has demonstrated the importance of real-time DF mapping as an auxiliary tool providing further mechanistic insights into the maintenance of persAF. A tailored ablation approach should therefore be considered for each individual case, provided that effective real-time, high resolution DF mapping can be performed.

# Detection of Atrial Fibrillation Using Contactless Facial Video Monitoring

Jean-Philippe Couderc*, Survi Kyal, Lalit Mestha, Beilei Xu, Derick Peterson, Xiaojuan Xia and Burr Hall

University of Rochester
United States

It is estimated that 33.5 million people in the world have developed atrial fibrillation (AF) and an estimated 30% of patients with AF are unaware of their diagnosis (silent AF). We tested a new technology for contactless detection of AF based on facial video recordings and the extraction of beat-to-beat blood pulse in patients undergoing electrical cardioversion for AF. The proposed technique called videoplethysmography (VPG) uses a webcam to record an individual's face and extract the subtle beat-to-beat variations of the skin color reflecting the cardiac pulsatile signal. In adults referred for electrical cardioversion, we simultaneously recorded the body surface ECG and the video of the subjects' face prior and after the procedure. We extracted the beat-to-beat pulse rates expressed as pulses per minute (ppm). The ECG recordings were used as a reference. We quantified the variability of the heart rate and pulse rate (pulse peak intervals) using the standard deviation (SD) of intervals, root means square of successive differences of intervals, SD of the minor axis and of the major axis of the Lorentz plots of these intervals. A novel quantifier of pulse variability called the Pulse Harmonic Strength (PHS) is proposed to detect the presence of AF. In 11 subjects (65±6 years, 8 males), the VPG and ECG-based rates were statistically different between the AF and sinus rhythm periods: 72±9 vs. 57±7 ppm ($p<0.0001$) for the VPG, and 80±17 vs. 56±7 bpm ($p<0.0001$) for the ECG signals. Among the 407 epochs of 15 sec. of synchronized ECG and VPG signals, PHS was associated with a 20% detection error rate, the error rates of the automatic ECG-based measurements ranged between 17% and 29%. Our preliminary results support the concept that contactless video-based monitoring of human face for the detection of abnormal pulse variability due to AF is feasible.

## Towards Impedance Optimised Transcutaneous Atrial Defibrillation

Philip R Walsh*, Paola A Rodrigues, Niall Watermann, David McEneaney and Omar J Escalona

Centre for Advanced Cardiovascular Research, University of Ulster, Newtownabbey, UK.
Waterford City,, Ireland

Introduction Atrial fibrillation is responsible for 30-40% of all cardiac arrhythmia related hospital admissions and the need for improved therapeutic options remains self evident. In this work, an impedance compensated transcutaneous atrial defibrillator is reported. Methods The system employs near field coupling at 180kHz for transcutaneous power transfer from an external portable hand-held unit to a battery free implantable device. On the implant side, a low-power microcontroller (FRDM-KL25ZARM) coordinates between two distinct operational modes: cardiac sense mode (wake-up, measure and communicate) and shock mode (defibrillation). In sense mode, low-power measurement circuitry non-destructively determines the impedance of the cardiac substrate by injecting a small sinusoidal current of fixed magnitude and measuring the response across frequency (1-100kHz). Measurement data communicated to the hand-held unit via a low-power data communications link (433Mhz) can then be used to adjust the defibrillation impulse to an optimum therapeutic value for delivery in shock mode. Results A prototype system was built and characterised. In sense mode, >5W of sustained dc power was delivered across a 2.5cm air-skin barrier with approximately 40% dc-to-dc power transfer efficiency at a transmission frequency of 180kHz; thereby providing a 16Vdc/300mA supply to the implant side. Full functionality of the microcontroller and RF communications link was demonstrated. In shock delivery mode, >150W (rectilinear monophasic shock pulse: 100V@1.9A for 12ms) was reliably delivered transcutaneously to a 50Ω cardiac load. Further testing in ten porcine models verified in-vivo operation of the impedance measurement circuitry; with a measurement repeatability of approximately 3% achieved. Conclusions A novel impedance compensated transcutaneous atrial defibrillator system was implemented and assessed. The in-vivo tests demonstrated reliable intracardiac impedance measurement for optimisation of the defibrillation waveform. The proposed architecture opens the possibility of more effective therapeutic options for AF sufferers. Further work towards acute pre-clinical trials remains on-going.

# Specific Patterns of Premature Beats Tend to Initiate Ventricular Tachyarrhythmias in Human Patients

Anna RM Gelzer, Robert F Gilmour Jr and Niels F Otani*

Rochester Institute of Technology
Rochester, United States

Introduction. The partial block of a propagating action potential is known to be one way to initiate ventricular fibrillation (VF), through its tendency to create a self-sustaining rotating wave formed by the surviving portion of the action potential. Previously, we demonstrated that certain patterns of abnormal rapid beats, notably "short-long-short-short" (SLSS) patterns, tend to produce action potential block in computer models, and tend to initiate VF in in vivo canine experiments. Here we present evidence that these same patterns often precede VF in human ECG recordings. Methods. Thirty-four ECG recordings showing activity just prior to and during tachyarrhythmic events were obtained from ICDs implanted in several human patients. The RR intervals of the first four abnormal beats preceding the arrhythmia were determined manually. The distributions of the RR intervals for each of these beats were individually fit to single-gaussian and dual-gaussian distributions, using an expectation-maximization method. The presence of a specific number of gaussians "bumps" was assumed when the fit was better than 5% of distributions generated randomly using the corresponding fitted distribution.

**Results:** Dual-gaussian distributions were obtained for the second and third abnormal beats, while single gaussian distributions were obtained for the first and fourth. These distributions were found to be consistent with the tendency of the SLSS pattern of premature beats, as well as SLLS and SSSS patterns, to precede the tachyarrhythmic event. All are consistent with our existing theory.

**Conclusions:** The results provide further evidence that electrical restitution theory, the basis for both our theory and computer model, although imperfect, is sufficient to both predict and understand the manner in which premature beats initiate VF. This understanding may, in the future, lead to new methods for preventing VF, through the imposition of stimuli designed to avoid the dangerous premature beat patterns revealed in this study.

# A Computational Investigation into the Effect of Infarction on Clinical Human Electrophysiology Biomarkers

Louie Cardone-Noott, Alfonso Bueno-Orovio, Ana Mincholé, Kevin Burrage, Mikael Wallman, Nejib Zemzemi, Erica Dall'Armellina, Blanca Rodriguez

University of Oxford
Oxford, UK

P83

The ECG is a first-line tool to diagnose myocardial infarction. However, the initial ECG has low sensitivity to acute MI and provides limited information on location, extent, and severity of injury.

Here we present our computational framework for solving the bidomain equations over an image-based human geometry with a biophysically-detailed human ventricular model, and results on the effect of infarction on the ECG.

First, we use our approach to solve several cases with heterogeneously distributed repolarisation of local action potential duration. We examine the effect of transmural, apicobasal, and interventricular heterogeneities/gradients in the delayed rectifier potassium channel. We report that transmural dispersion of APD is needed to generate a positive T wave.

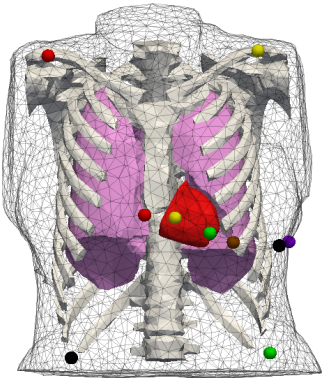

Our heart and torso mesh with standard electrode locations.

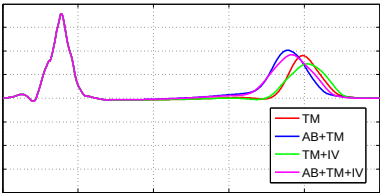


Four of the simulations generated a positive T wave in lead V5.

Second, we present early results of a simulation with an irregular anterior infarction. The ECG displays ST segment elevation typical of STEMI (ST segment elevation myocardial infarction), an altered QS complex, prolongation of the QT interval, and a longer $T_{peak}$ to $T_{end}$ interval.

Further studies will integrate this framework with clinical data to investigate the biophysical interpretation of ECG biomarkers and the signature of disease.

# Inverse estimation of left ventricular Purkinje network pathways from sequence of depolarization

Ruben Cardenes, *Rafael Sebastian, Oscar Camara

University of Valencia
Valencia, Spain

**Aims:** The electrical activation of the heart is a complex process that is essential for the understanding of several cardiac dysfunctions, such as ventricular tachycardia. Patient-specific local activation times (LAT) on the left ventricular endocardium can be estimated from electro-anatomical maps, however unveiling the underlying fast pathways formed by the Purkinje network remains a complex problem. This study presents a method to estimate regions on the endocardium with a potential number of Purkinje myocardial junctions (PMJs), and the corresponding Purkinje network structure from a set of endocardium LATs.

**Methods:** Five different Purkinje networks, following an L-system model fed by ex-vivo anatomical data were built on a segmented 3D human ventricular model. Electrical simulations were performed using specific ionic models for Purkinje and for the working myocytes. From LAT maps critical points (sink and source) were estimated from propagation gradients. Following minimal cost paths were obtained from critical points using a function of the LAT as weight functions to reconstruct the Purkinje networks.

**Results:** Simulations with simplified Purkinje trees and uniformly distributed PMJs were faithfully reconstructed (see Fig. 1), showing the main branch architecture and an average PMJ distance error of 0.08mm to 0.16mm as a function of the number of LAT endocardial samples used. In complex Purkinje structures main features were properly estimated, although redundant branches were often missed. PMJs detection distance error ranged from 3.6mm to 2.2mm for sets with 400 to 1600 sample LATs, correspondingly.

**Conclusion:** Using dense electrical activation maps regions with PMJs can be detected with accuracy, and main structure of the Purkinje tree reconstructed. This information could be useful to better plan ablation paths with complex arrhythmias.

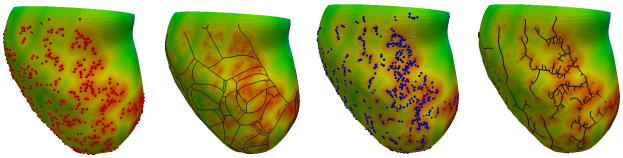

(a) (b) (c) (d)

**Figure 1**. (a)-(b) original PMJs (red points) and Purkinje network, and (c)-(d) the corresponding estimated version

P83

# Sensitivity Study of Fiber Orientation on Stroke Volume in the Human Left Ventricle

Lukas Baron*, Thomas Fritz, Gunnar Seemann and Olaf Dössel

Karlsruhe Institute of Technology (KIT)
Germany

Orientations of myocytes play an important role for electrical activation and mechanical contractions in the human heart. Their contraction is responsible for the deformation of the ventricles and the blood circulation in the cardiovascular system. In experiments, fiber orientation angles were measured at species (rat, canine, dog, human) with a large range of partly inconsistent results by various reasons. These angles however still are often used for setting of fiber orientations by so-called rule-based methods (RBM). It is unclear to what extent non-exact fiber angles impact the quality of computational simulations. A sensitivity study clears the question how much differing fiber angles contribute to important measures in mechanical simulations of the human heart. In this paper, mechanical simulations of a human heart were initalized with an RBM, performed and compared. Six different sets of of ventricular angles were computed, with helix angles between 20° and 70° on endocardium and −70° and −20° on epicardium. The simulations covered the complete heart with both ventricles, both atria and the pericardium and were performed using a finite element method. Results are evaluated by means of ventricular pressure difference, atrioventricular plane displacement (AVPD), stroke volume, ejection fraction and pV-work. Simulations showed a continuous dependency of all measures on orientation angles. Stroke volume and ejection fraction changed over all simulations by 34.0%, respectively compared to the lowest values. The maximal AVPD values spread over a range of 0.54 cm to 1.30 cm (factor of 241 %). Pressure difference between endsystolic and enddiastolic states changed in the left ventricle over all simulations by 8.3 %. However, it could not be observed that a higher AVPD yields a higher stroke volume. Concludingly, fiber orientations are important for reliable computational simulations of human hearts and should be incorporated with great care.

P83

## Modeling the Takeoff Voltage of the Action Potential during Fast Pacing

Diandian Chen*, Richard Gray and Flavio Fenton

georgia tech
United States

To date over 50 models for cardiac action potential have been developed, and while they vary widely in their complexity and the physiological characteristics that they reproduce, most of them fail to accurately replicate the takeoff potential during fast pacing. A specific aspect we focus is on is the take off potential for anS2 stimulation following a steady S1 action potential. In micro-electrodes and optical mapping experiment, the take-off voltage of an S2 action potential has been shown to be relatively high while most cardiac cell models do not reflect this feature, as the voltage needs to return close to the resting membrane potential before it can be reactivated. Since this difference can have great effects in electrical waves and their dynamics during tachycardia and fibrillation, we developed a framework that can be incorporated into the models so they can reproduce the experimentally observed higher take off potential. Sodium current activation is key to the activation from an S2 stimulus. Therefore, we focused on the sodium current inactivation gates, h and j. We hypothesized that the j gate is the source of the low take off potential because it opens more slowly. Our procedure is to model the dynamics of both gates via a single one with an adjustable time constant tau. We model tau with a lorentzian equation for the left side from its maximum value and a Gaussian from the right. Using this two equation form, we can manipulate the width, height, and asymptotic values of tau. The features that change the take off potential significantly are the midpoint and asymptotic value of tau. By shifting the midpoint value of tau to a higher value, the take off potential increase, while rest of the sodium dynamics remains unaltered.

P83

## Verification of a Defibrillation Simulation Using Internal Electric Fields in a Human Shaped Phantom.

Jess Tate*, Thomas Pilcher, Kedar Aras, Brett Burton and Rob MacLeod

University of Utah
Salt Lake City, United States

We have developed a computer simulation to evaluate the success of Implantable Cardioverter Defibrillators (ICDs) in a patient specific manner. We have used this system to guide optimization of ICD placement, evaluate the consequences of residual metallic devices in the torso, and to predict the interactions between ICDs and other implantable devices. Though we have validated the simulations by means of surface recordings of shock potentials in humans, recordings of potentials within the heart and torso are needed to further verify the model for use in a clinical setting. To carry out such verification, we suspended an explanted porcine heart in a torso shaped electrolytic tank and recorded potentials on the tank surface, the epicardial surface, and within the myocardium with customized multielectrode arrays and acquisition system. The corresponding torso and heart shapes and electrode and ICD positions were then used in an finite element methods simulation of the ICD. Potentials recorded from the surface and within the volume of the torso tank agreed well with the simulated potentials. Quantitative comparison between recorded and simulated potentials showed a correlation of 0.82 and a relative RMS error of 15.3%. Ongoing improvements in the experiments studies and analysis of the results seek to identify the sources of remaining error, however, these results suggest that our simulation model can guide the optimization of ICD design and use.

P83

# Quantitative Analysis of Rate Dependent of Human Heart Failure Action Potential Model on Alternans Onset and Arrhythmias

Mohamed Elshrif*, Elizabeth Cherry and Pengcheng Shi

Rochester Institute of Technology
Rochester, United States

Abstract: It is known that at the living organism level, Heart Failure (HF) increases the susceptibility incidence of cardiac alternans, both of which are strongly associated with Sudden Cardiac Death (SCD). It is important to build a multi-scale system that links the sub-cellular, cellular, tissue, organ, and liv- ing organism levels. Once we build this framework and validate it at each level, we can systematically study the effect of blocking Na+ or Ca2+ channels on a living organism and facilitates new therapeutic avenues to alleviate SCD. We investigate quantitatively how the HF human ventricular cellular model affects the rate-dependency action potential alternans onset and its mechanism, differ- ently from the normal cellular model. Also, characterizing how the restitution curves dynamics and short-term memory are altered during alternans in both cases, normal and HF, at different scales. We validate our results with available experimental observations.

**Methods:** We conduct computer simulations of isolated single cells, one-dimensional cable, and two-dimensional tissue domains of cardiac tissue using the epi-, endo-, and midmyocardial cell type of the modified HF O'Hara (OVVR) model that can reproduce alternans with time resolution 0.02ms and space resolution 0.015cm.

**Results:** For single epicardial cell, we found that the range of alternans cycle lengths in HF increases, 320.0-460.0ms, compared with normal, 165.0ms, which is close to the measured value in experiments CL≤240ms for control and CL≤500ms for HF in tissue, as well a s the alternans magnitude (HF: 8.0ms, N: 1.5ms), in a single cell. The threshold of alternans increased in 1D cable in both cases. In a 2D homogeneous tissue, the dynamics of spiral waves behave differently and have distinct tip trajectory patterns.

**Conclusion:** We have found that our simulations in single cell, and 1D are capable of producing alternans that are in agreement with experimental observations on control and HF.

P83

# Automatic Extraction of Arterial Centerline from Whole-body Computed Tomography Angiography

Xinpei Gao[1]*, Shengxian Tu[1], Michiel A. de Graaf[1], Liang Xu[2], Pieter Kitslaar[1], Arthur J. H. A. Scholte[1], Bo Xu[2], Johan H. C. Reiber[1]
1 Department of Radiology, Leiden University Medical Center, Leiden, The Netherlands.
2 Catheterization Lab, National Center for Cardiovascular Diseases of China and Fu Wai Hospital, Beijing, China.

Automatically extracted centerline superimposed on 3D rendering view.



Aims: The aim of this study was to develop a new, fully-automated approach for the extraction of arterial centerlines from whole-body computed tomography angiography (CTA) data sets for the planning of transcatheter aortic valve replacement (TAVR) procedures by the transfemoral approach.

Methods: The method starts with an image preprocessing step to correct contrast inhomogeneities in different image slices, followed by the detection of anatomical landmarks and subsequent wave propagation, generating a cost matrix that represents the wave traveling time. Finally, the arterial centerlines are extracted from the aortic root to the femoral arteries using the conventional Dijkstra algorithm.

Materials: 36 patients who underwent TAVR procedures with whole body CTA scans were included in this study. 15 were used for training and the remaining 21 for testing. 2 analysts delineated the centerline and used it as reference, i.e., the "true", centerline. The extraction error was defined as the distance between the reference centerline point and the closest point in the automatically extracted centerline.

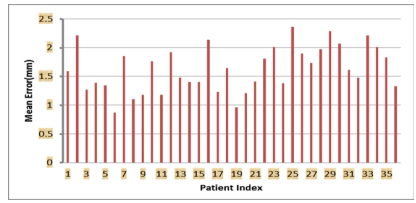


Results: In 1 training case and 2 testing cases, interaction was needed by the user to correct the centerline (in the femoral artery). In the remaining 33 cases (91.7%), a fully-automated centerline was obtained with excellent results. In all cases, the average root mean square error was 2.55±0.70mm (training 2.26±0.48mm versus testing 2.77±0.77mm, $p$ = 0.03) and the average mean error was 1.63±0.40mm (training 1.46±0.35mm versus testing 1.74±0.39mm, $p$ = 0.02).

Conclusions: This method is robust and effective to extract arterial centerline automatically from whole body CTA data sets. This is a first and important step towards efficient planning of TAVR procedures.

# Fusion Imaging of Computed Tomography and 3D Echocardiography: Combined Assessment of Coronary Anatomy and Myocardial Function

Francesco Maffessanti, Karima Addetia, Gillian Murtagh, Lynn Weinert, Amit R. Patel, Roberto M. Lang, Victor Mor-Avi

University of Chicago
Chicago, IL

**Background.** Cardiac multimodality imaging offers new opportunities for novel ways to display composite information not available with any of the imaging modalities alone. We tested the feasibility of fusion of coronary anatomy and left ventricular (LV) function obtained from computed tomography (CT) and 3D echocardiography (3DE).

**Methods.** 24 patients underwent CT coronary angiography and transthoracic 3DE imaging on the same day. CT images were acquired according to standard clinical protocol at 78% of the cardiac cycle. Apical full-volume 3DE images were analyzed offline to derive a dynamic LV endocardial surface (TomTec). Custom software was used to extract the coronary tree and calculate LV radial shortening fraction (RSF). Dynamic LV surface, color-encoded with RSF and CT coronary tree were co-registered using a rigid spatial transformation between corresponding anatomic landmarks.

**Results.** Three patients (12%) were excluded because of suboptimal quality of CT images. The composite display of coronary arteries and parametric images depicting RSF allowed visual appreciation of the functional significance of stenosis when present. While patients with normal coronary arteries had uniform RSF, those with significant stenosis (N=3/21) had wall motion abnormality in the area supplied by the stenosed artery (Figure).

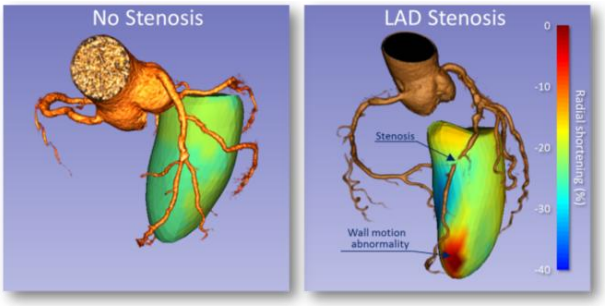


**Discussion.** Fusion of CT coronary angiography and parametric imaging of RSF derived from 3DE is feasible, potentially providing physiologically meaningful and easy-to-interpret combined display of coronary abnormalities and their functional impact. This approach is versatile, as it may be applied to a variety of parameters of cardiac mechanics.

# Automatic Correction of Motion Artifacts in 4D Left Ventricle Model Reconstructed from MRI

Yi Su*, May-Ling Tan, Chi-Wan Lim, Soo-Kng Teo, Senthil Kumar Selvaraj, Liang Zhong, Ru-San Tan

Institute of High Performance Computing, A*STAR, Singapore

**Aim:** Respiration and patient movement often contribute to misalignments in data acquired through breath-hold cine Magnetic Resonance Imaging (MRI). In this work, we aim to develop an automatic algorithm to restore the shape of such 4D (i.e., spatial + time) left ventricular (LV) models created from MRI data.

**Method:** A time-series model of the LV endocardial and epicardial surfaces are created from border-delineated MRI data at every time frame of the cardiac cycle. A geometrically-based approach is used to achieve smooth epicardial shapes by iterative in-plane translation of vertices in the LV model. The principle curvatures ($\kappa_1$, $\kappa_2$) of the LV epicardial surfaces across multiple time frames are used to construct a shape-based optimization objective function to restore the shape of a motion-affected LV via a dual-resolution semi-rigid deformation process and a free-form deformation process. A limited memory quasi-Newton algorithm, L-BFGS-B, is then used to solve the optimization problem.

**Result:** We tested our algorithm on 9 *in vivo* patient-specific models affected by motion or respiration during MRI scanning. The results show that our method is able to correct motion artifacts without altering the general shape of the heart, such as its asymmetrical shape. The magnitudes of in-plane translations ($\Delta x$ = 0.972±0.857 mm and $\Delta y$ =1.306±1.290 mm in the *x*- and *y*-directions, respectively) are also within the range of published experimental findings. The average computational time to correct each 4D model is 6 min 34 sec.

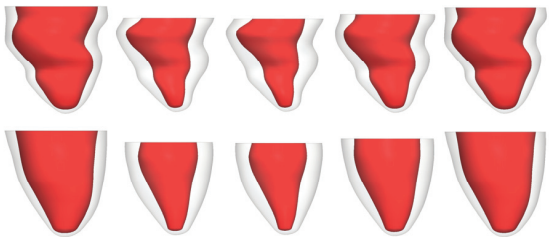

Top Row: 3D mesh models of left ventricle affected by motion artifact; Bottom Row: Corresponding 3D mesh models of left ventricle after restoration.

**Conclusion:** The proposed solution is a viable software-based alternative to correct MRI data affected by patient motion without the need of addition hardware-based motion registration tools. It is sufficiently efficient for real clinical utilization.

# 3D Echocardiographic Quantification of Ejection Fraction and Cardio-toxicity Onset

Cinzia Lorenzini, Michele Aquilina, Claudio Lamberti, Cristiana Corsi

DEI, Cesena Campus, University of Bologna
Bologna, Italy

Ejection fraction (EF) estimate is crucial in diagnostic and therapeutic decision making in different clinical pathways, including definition of cardio-toxicity onset in oncologic patients. Three dimensional echocardiography (3DE) has already proved its superiority with respect to two-dimensional echocardiography (2DE) for left ventricular (LV) function assessment. Several 3DE analyzing software are available and can be used to compute EF. The aim of this study was to evaluate how variability in EF estimate could affect cardio-toxicity assessment. We analyzed 2DE and 3DE datasets in 94 patients treated for breast cancer with anthracycline and trastuzumab. EF was computed from 2DE and 3DE data using two software packages (EchoPAC, GE Healthcare (A) and TomTec 4D LV analysis (B)). Corresponding estimates were compared. In addition, in a subgroup of 20 patients 3DE data were re-analyzed and intra- and inter-observer variability by three investigators were computed, using both software packages. Results are reported in the table. As expected 2DE-based estimates significantly underestimated 3DE-based estimates. Intra-observer and inter-observer variability for both packages showed a huge variability, due to significant differences in ESV and EF. Following clinical definition of cardio-toxicity onset (EF decrease >5% with symptoms of heart failure or asymptomatic EF decrease >10%), the variability results could be a confounding factor since variation in EF measurements are in the range of EF decrease due to cardiac adverse effects from cancer therapeutic drugs. In addition, different 3DE software packages for EF assessment should not be used interchangeably.



Results of EDV, ESV and EF estimates and variability analysis from 2DE and 3DE using software packages A and B

| | EDV | ESV | EF |
|---|---|---|---|
| 2DE | 70±18 ml | 25±9 ml | 64±8 % |
| 3DE using A | 85±19 ml | 35±10 ml | 59±6 % |
| 3DE using B | 85±24 ml | 34±13 ml | 59±7 % |
| Intra-obs using A | 3.4±5.3 % | 5.5±6.2 % | 2.2±1.8 % |
| Intra-obs using B | 6.5±5.5 % | 11.5±6.9 % | 4.6±3.3 % |
| Inter-obs using A | 3.1±3.6 % | 6.4±4.9 % | 3.6±2.7 % |
| Inter-obs using B | 6.4±4.0 % | 11.9±5.3 % | 6.3±4.3 % |

# Temporal Sparse Promoting Three Dimensional Imaging of Cardiac Activation

Long Yu*, Zhaoye Zhou and Bin He

BME dept, U of Minnesota
St Paul, United States

Introduction Non-invasive cardiac electrical imaging, as an alternative approach of the invasive mapping techniques, can provide important information regarding the arrhythmogenesis which is crucial for the success of the ablative procedures. We in this study propose and computationally evaluate a new Cardiac Electrical Sparse Imaging (CESI) technique to image cardiac activation throughout the three-dimensional (3D) ventricular myocardium from body surface electrocardiogram (ECG) with the aid of individualized heart-torso geometry. Methods The sparse property of cardiac electrical activity in the temporal domain is utilized in the temporal sparse promoting inverse problem. Computer simulations were carried out to evaluate the performance of this imaging method in various circumstances. Artificial noise of various levels (0-80 □V), hospital recorded sensor noise and different modeling errors are employed to test CESI's accuracy, stability and robustness in noninvasive imaging. Results The results show that CESI can image with improved accuracy, stability and stronger robustness in both simulated and experimental circumstances. The Correlation Coefficient (CC) between CESI imaged results and the simulated activation sequence is in average 0.95 against artificial noise and 0.91 against hospital recorded sensor noise. In simulation with various modeling errors, CESI also achieved a CC as high as 0.93 in average. In all simulations, the Relative Temporal Shrinkage (RTS) was smaller than 2%, showing CESI is able to image in full temporal resolution. The comparisons showed that CESI in general outperformed conventional Weighted Minimum Norn method. Conclusions We have proposed a novel method for cardiac activation imaging, and our results suggest that CESI has enhanced performance, and offers the potential to image the ventricular activation and to assist in the clinical management of ventricular arrhythmias.

# An Iterative method for solving the inverse problem in Electrocardiography imaging : From body surface to heart potential

Nejib Zemzemi*, Hamed Bourenane and Hubert Cochet

INRIA Bordeaux Sud-Ouest
Talence, France

**Aims:** Solving the inverse problem in electrocardiography imaging (ECGI) is a challenging problem. In this work, we present an ECGI solver based on an efficient iterative method Kozlov-Maz'ya-Fomin (KMF) approach. Because of the lack of gold standards data for this problem, we propose to test this method on synthetical data generated on a real women torso.

**Methods:** We segmented a CT-scan of a 43 years old women torso. In order to take into account the conductivity heterogeneity in the torso, we distinguished the lungs the bones and the remaining tissue. We then produced a finite element mesh that will be used for computation. In order to generate the synthetical data we use our electrophysiolgy forward problem solver. We generated a normal heart beat and a reentry heart wave using the S1S2 protocol. We extract the heart surface elctrical potential and on the body surface potentials (BSPs). We consider this data as our "Gold standard". We then add different levels of noise to the BSPs and we solve the inverse problem using the KMF method. We compare the obtained solution to the gold standard electrograms.

**Results:** Adding 5% (respectively 10%) of noise to the BSP and computing the inverse solution on the heart surface, we obtain a relative error of 110% (respectively 142%). Although, the relative error is too hight, the wave front is well captured in both cases for a normal heart case (panel A) and reentry case (panel B). This is reflected in the correlation coefficient varying between 0.64 and 0.78 (respectively between 0.61 and 0.78) in time.

**Conclusion:** We presented an iterative approach based on the KMF algorithm. The method was tested on synthetical data generated using our ECG simulator and a real 3D torso. The results are promising and need to be tested on real life recordings.

# A Pattern-Recognition Approach for Lead-Selection in Heartbeat Detection

Mariano Llamedo, Juan Pablo Martínez, Pablo Laguna

BSICoS, Aragon Inst of Eng Research, IIS Aragón, Univ of Zaragoza, Aragon, Spain
CIBER of Bioengineering, Biomaterials and Nanomedicine (CIBER-BBN), Spain

*Introduction*: In this work we developed and evaluated an algorithm for selecting the most suitable lead for performing heartbeat detection in cardiovascular signals. The objective of this work is to quantify the quality of the fiducial points produced by heartbeats detection algorithms. The objective of this quality metric is 1) to rank the leads in order to select the best performing lead in an unassisted operation, and 2) to serve as input to subsequent semiautomatic correction algorithm in an assisted mode.

*Materials and Methods*: For the development and evaluation we used public dataset of 927 multilead stress-test recordings, with manually reviewed heartbeat locations. The algorithm consists of a pattern-recognition block based on features calculated from the RR interval sequence, and a mixture of Gaussian classifier. This block estimates whether the heartbeat is correctly or incorrectly detected, in order to calculate a final estimate of the detections quality.

*Results*: Results show that the correct lead has been selected 70% of the times, and 93% of the time the best lead was among the top 3 leads with higher detection quality. This decision produces a gross median sensitivity of 100%, ranging from percentiles 5 to 95 at 99.6 to 100%, and a gross median positive predictive value of 98.9%, with percentiles from 89.2 to 100%.

*Discussion*: The work presented can be extended to other class of ECG recordings and CV signals, such as BP and PPG, and also for shorter time windows in order to deal with transient signal loss. The results presented suggest that the algorithm performance is adequate for ECG stress-test recordings.

| lead selected | $S$ | | $P^+$ | |
|---|---|---|---|---|
| best | 100 | (99.7 – 100) | 99 | (89.5 – 100) |
| this algorithm | 100 | (99.6 – 100) | 98.9 | (89.2 – 100) |
| worst | 93.2 | (76.4 – 99.9) | 89.1 | (69.5 – 98.9) |

# Adaptive Beat-to-Beat Mathematical Morphology Approach for QRS detection in the ECG

Sasan Yazdani*, Jean-Marc Vesin

EPFL, Swiss Federal Institute of Technology
Lausanne, Switzerland

**Purpose**: Fixed structure Mathematical Morphology (MM) operators have been used to detect QRS complexes in the ECG. These schemes are limited by the arbitrary setting of threshold values. Our study aims at extracting the fiducial points of the QRS complexes using an adaptive structuring element on a beat-to-beat basis.

**Methods**: Using MM filtering, impulsive noise is removed and QRS complexes are detected by computing the top and bottom hat average with predefined structuring element for a limited time window. The structuring element is updated using a learning coefficient, set close to one at the start and continuously adapted based on the characteristics of the previously detected QRS complexes and RR intervals. The MIT-BIH arrhythmia and Physionet QT databases were respectively used for assessing the performance of R-waves and other fiducial points detection.

**Results**: For the 116137 existing R-waves in MIT-BIH database, our proposed method achieved a 99.79% detection rate with 108 false positives beats and 137 false negatives beats in total. Other fiducial points such as QRS onset and offset, Q- and S-points, were detected respectively with 97.9%, 98.18%, 99.02% and 99.66% accuracies.

**Conclusions**: Our preliminary results suggest that the adaptive structuring element can efficiently estimate the QRS onset and offset, Q- and S-points as well as preventing false negative R-waves detection. Importantly, the low computational complexity and the absence of arbitrary threshold values of the proposed scheme make it suitable to be applied in Body Area Networks, in which computation costs plays a vital role.

# An Adaptive Heart-beat Classification System Based on Learning from Difficult Cases

Philip de Chazal

MARCS Institute, University of Western Sydney, Australia

An adaptive system for the automatic processing of the electrocardiogram for the classification of heartbeats into beat classes that preferentially learns from difficult cases is presented. A first set of beat annotations is produced by the system by processing an incoming recording with a global-classifier. The beat annotations are then ranked by a confidence measure calculated from the posterior probabilities estimates associated with each beat classification. An expert then validates and if necessary corrects a fraction of the least confident beats of the recording. The system adapts by first training a local-classifier using the newly annotated beats, and then combining the outputs with the global-classifier to produce an adapted classification system. The adapted system then updates the remaining beat annotations of the recording.

Data was obtained from the 44 non-pacemaker recordings of the MIT-BIH arrhythmia database. We investigated the problem identifying the following 13 beat types: normal, left bundle branch block, right bundle branch block, atrial escape, nodal escape, atrial premature, aberrated atrial premature, nodal premature, supraventricular premature, premature ventricular contraction, ventricular escape, fusion, and unclassified beats.

With no adaptation we achieved a classification accuracy of 49% for the 13 classes. By adapting the classifier using up to 100 beats from the recording under analysis, classification accuracy could be increased to over 92.5%. Our results show that a significant boost in classification performance of the system is achieved even when using a small number of beats for adaptation.



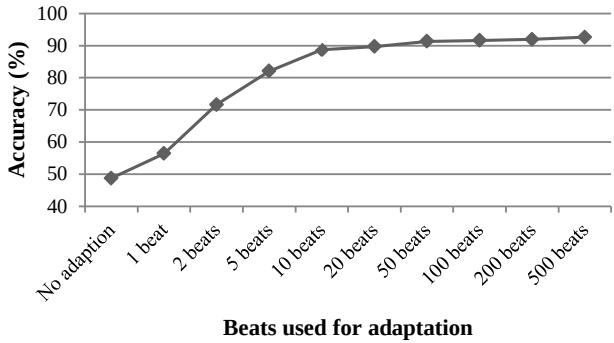


Figure 1: Classification accuracy as a function of beats used for adaptation

# A real-time QRS detector based on higher-order statistics for ECG gated cardiac MRI

Marcus Schmidt, Johannes W Krug, Andreas Gierstorfer, Georg Rose

Department of Medical Engineering, Otto-von-Guericke-University of Magdeburg, Magdeburg, Germany

INTRODUCTION: QRS detection for ECG-based gating in cardiovascular magnetic resonance (CMR) can be hampered by the magnetohydrodynamic (MHD) effect. To cope with this problem, a QRS detector based on higher order statistics is proposed.

METHODS: The algorithm was evaluated using two different databases. The first database ($ECG_{MRI}$) was recorded inside a 3T MR scanner using a 12-lead Holter ECG. A total of 9241 QRS complexes were acquired from 9 healthy subjects placed in head-first and feet-first positions. The 12-lead arrhythmia database from St.-Petersburg Institute of Cardiological Technics ($ECG_{InCarT}$) was used as a second database.

Before the QRS detection, the ECG signal was bandpass filtered by cascading a 30Hz low pass and a 2Hz high pass filter. The 4th order central moments were calculated from the filtered signal using a sliding window of length $L=0.02 \cdot f_s$ with a step width D=L/4. A threshold was required to distinguish between QRS complexes and peaks caused by the MHD effect. The threshold was calculated by the median of a reference vector which contained the 4th order central moments of the last 10 QRS complexes.

RESULTS: Best results were achieved using lead V4 and a threshold of 5% of the reference vector's median. For the presented method a sensitivity (Se) of 99.99% and a positive predictive value (+P) of 99.60% were achieved for the $ECG_{MRI}$ database. The average time delay between the annotated and the detected beats was 7.77ms with a jitter of 2.89ms. For the $ECG_{InCarT}$ database, the results were Se=99.43% and +P=99.91%. The mean time delay was 12.16ms with a jitter of 7.17ms.

CONCLUSION: The presented algorithm based on the 4th central moment enables a QRS detection with high Se and +P and a low time delay and jitter. Hence, this method could be used to trigger CMR imaging sequences.

# QRS Detection Optimization in Stress Test Recordings using Evolutionary Algorithms

David Hernando*, Raquel Bailón, Rute Almeida and Alfredo Hernández

Spain

**Aims:** QRS detection in exercise stress test recordings remains a challenging task because they are highly non-stationary and contaminated with noises, such as large baseline wander and muscular noise, among others. A wavelet-based QRS detector has been previously validated for a given set of parameter values in standard resting electrocardiogram (ECG) recordings. The aim of this work is to find the optimal set of parameters for QRS detection in stress testing ECGs.

**Methods:** Parameter optimization was addressed by an evolutionary algorithm. These optimization algorithms are particularly adapted to problems involving cost functions that are not differentiable and presenting multiple local minima. A training database was created using the MIT-BIH Arrhythmia Database, which contains 48 half-hour-length ECG recordings with manually-annotated QRS complexes. Each ECG recording is artificially contaminated with 3 types of real noise. These noises include baseline wander, muscle artifact and electrode motion artifact, with a signal to noise ratio as low as -6 dB. A cost function combining the detection error probability, the mean detection jitter, and its standard deviation was defined, in order to obtain a quantitative performance evaluation of the detector. Evaluation was performed on an exercise stress test database composed of 54 real ECG recordings, with annotated QRS. QRS complexes were detected by the wavelet-based detector configured with default parameter values, and also with the optimal values obtained from the evolutionary algorithm.

**Results:** The QRS detector with its optimized parameters showed a global improvement of 3.5% compared to its performance with the default parameters. Furthermore, the use of optimized parameters led to at least the same performance than the initial parameters for all records, and the improvement was higher (up to 10.46%) in noisy records, demonstrating the advantages of the optimized parameters in noisy environments.

# A Vector-based Pace Pulse Detection Algorithm for the surface ECG

Simon C Chien*, Po-Cheng Chang, Hong-Ta Wo, Eric Helfenbein, Chun-Chieh Wang and Ming-Shien Wen

California Institute of Technology
Pasadena, United States

**Background** The recent advancement of pacemaker technology has brought challenges for detection of pace pulses (PPs) in the surface ECG. Since pacemakers consume less power with lower pulse amplitudes, PPs are now less distinguishable from environmental impulse noise. Non-synchronous biventricular (biV) PPs are closely spaced in time, and provide challenges to detect both ventricular chamber PPs. Pacing rates can be adaptive, so the pacing interval can vary beat-to-beat. Undetected and unresolved PPs may consequently have a detrimental impact on a diagnostic ECG algorithm's rhythm or morphology interpretations.

**Method:** Our algorithm is designed to strengthen an existing PP detection algorithm using vector information to reject false positive PPs and detect the existence of a second biV ventricular pulse closely spaced in time. The vector angle of a PP from a specific pacemaker lead is not pacing interval dependent. PPs can be easily distinguished from impulsive noise, while the vector angle is utilized with the pulse-to-QRS interval for classification. Since the projection of biV pulses on a single lead may look like only one pulse, evaluating the vectors around a recognized ventricular pulse can reveal a possibly hidden second ventricular PP. Result: We collected 500sps continuous 12-lead ECGs from 8 patients with biV pacemakers of various manufacturers, while gradually changing RV-to-LV pacing intervals from 70msec to -70msec, to generate 658 total cases of 10sec biV paced ECGs. The biV ECGs were mixed with 907 cases of non-biV paced ECGs from different patients to make training and testing sets. After training on the development dataset, our algorithm showed a detection sensitivity of 94.3% with a detection specificity of 99.3%.

**Conclusion:** The results show that our algorithm's use of vector information can greatly improve detection of current pacemaker PPs and biV pulses in the surface ECG.

# Optimization of Pharmacotherapy for Familial Atrial Fibrillation in a Numerical Model of Human Atrial Electrophysiology

Axel Loewe[1], Yannick Lutz[1], Mathias Wilhelms[1], Eberhard P Scholz[2], Olaf Dössel[1], Gunnar Seemann[1]

[1] Institute of Biomedical Engineering, Karlsruhe Institute of Technology, Karlsruhe, Germany
[2] Department of Internal Medicine III, University Hospital Heidelberg, Heidelberg, Germany

Pharmacological therapy of atrial fibrillation (AF) is still a major clinical challenge. Particularly AF of early onset has a significant familiar component and was associated with various gene mutations. In this study, we designed and optimized antiarrhythmic agents for atrial substrates affected by human ether-à-go-go-related gene mutations L532P and N588K.

In a first step, a virtual multichannel blocker was designed aiming at a restoration of the wild-type (WT) action potential (AP) on the single cell and tissue level. Furthermore, the amiodarone and dronedarone concentrations yielding the smallest difference between WT and mutated APs were identified.

The WT AP course at a basic cycle length (BCL) of 1000 ms could be restored by significant block of $I_{Kr}$ and $I_{Kur}$ ($\geq$39%) and less pronounced block of $I_{Ks}$, $I_{Ca,L}$, $I_{b,Na}$, and $I_{b,Ca}$ ($\leq$17%) for both mutations. Effective dronedarone concentrations of 88 nM for L532P and 40 nM for N588K yielded matches almost as good while amiodarone could not sufficiently restore the WT AP. $APD_{90}$ restitution was effectively restored by the tuned N588K agent whereas differences of up to 34 ms were observed for low BCLs using the tuned L532P agent.

Our results show that combined reduction of ionic current conductances can counterbalance changes in $I_{Kr}$ kinetics due to e.g. genetic mutations. Moreover, the importance of the complex, non-linear interaction of different ionic currents was demonstrated and advises against solely considering the main effect (i.e. potassium channel blockage) when characterizing mode of action.

Concluding, this study provides insight into the pharmacodynamic response of mutated myocytes rendering patients vulnerable to AF and may aid in the design and optimization of patient group-specific therapeutic and preventive approaches.

# Atrial Rotor Drifting Using Induced Spatial Tissue Temperature Gradients

Guy Malki, Sharon Zlochiver

Tel Aviv University
Tel Aviv, Israel

**Introduction:** The existence of cardiac rotors and their spatial drifting are known indicators for cardiac arrhythmogenesis. The characterization of these rotors is key to successful ablation procedures. However, the mechanistic interpretation of existing mapping techniques is poorly established. We propose a new strategy that is based on controlled rotor meandering under spatial temperature gradients (STG). We hypothesize that rotor meandering under prescribed STG is due to induced excitability heterogeneity, such that drifting is established towards low excitability regions.

**Methods:** Cardiac electrical conduction was simulated in 2D atrial tissue, and stable spiral waves were established. Human atrial kinetics were employed using the CRN model, and temperature effect on the various gating rate variables was incorporated by inclusion of channel-specific $Q_{10}$ factors for $I_{Na}$, $I_{CaL}$, $I_{to}$, $I_{kur}$, $I_{kr}$ and $I_{ks}$. A linear temperature gradient between T1=37° C (y=0mm) and T2 (y=300mm) was employed. For each simulation the mean route trajectory was computed, according to the completion time of each spiral wave cycle. The maximum values of the sodium channel availability ($h \cdot j$) was calculated for each cell at the same activation phase.

**Results:** Linear STG consistently resulted in rotor drifting towards the colder region of the tissue, in a diagonal trajectory. The maximal drifting translation distance depended on the gradient magnitude. As the temperature difference within the tissue increased, the drifting occurred faster and along a longer distance. The drift in the vertical direction was due to the heterogeneity in tissue excitability, while the horizontal drift is due to the chirality of the rotating wave.

**Conclusion:** STGs can be employed to control rotor drifting. We envision that by measuring the Doppler shifts in the activation frequencies at few known locations, the drifting trajectory may be deciphered, thus contributing to the characterization and localization of rotors.

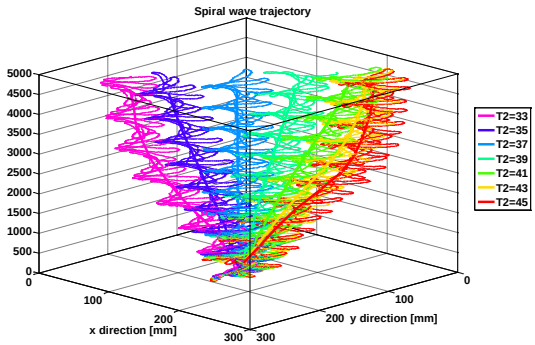

# A Simulation Study of Electrotonic Coupling between Human Atrial Myocytes and Mechanosensitive Fibroblasts

Honglian Su, Heqing Zhan, Yinglan Gong, Dingchang Zheng* and Ling Xia

Zhejiang University
China

**Aims:** Experimental studies have demonstrated that cardiac fibroblasts (Fbs) can transform mechanical compression into electrical signals. This study aimed to investigate the effect of Fbs with the incorporation of mechano-gated currents induced by mechanical compression (Ici) of cardiac Fbs on adjacent myocyte.

**Methods:** With two different experimentally observed Fbs compression (2 μm and 3 μm), Ici was numerically simulated as Icil and Icih. They were then incorporated into two types of electrophysiological models of human atrial Fbs: passive and active models, respectively. The human atrial myocyte (hAM) was modeled by the Courtemanche-Ramirez-Nattel (CRN) model.

**Results:** In both models, compression depolarized the membrane potential of cardiac Fbs. When coupled with passive Fbs, the action potential duration at 90% (APD90) was increased to 382 ms (in comparison with 304 ms for uncoupled hAM). With the incorporation of Icil into passive Fbs, APD90 was further increased to 403 ms, and with Icih, the membrane potential of hAM did not return to -70.6 mv required for APD90 at 500 ms. When coupled with active Fbs, similar increases were obtained with the incorporation of both Ici. The corresponding APD90 was 326 ms (without Ici), 340 ms (with Icil), and 390 ms (with Icih). Furthermore, the resting potential and the maximum value of the action potential of hAM were also increased for both models and with both Ici. In terms of the action potential duration of hAM at 50% (APD50), it was prolonged slightly when coupled with passive Fbs, but decreased with active Fbs. After the incorporation of Ici, the APD50 difference between the two Fbs models decreased, indicating that Ici could effect electrical excitation of hAM.

**Conclusion:** The preliminary simulation study confirms that mechanosentitive currents in fibroblasts play an important role in mechano-electrical coupling and should be further investigated in future cardiac modelling studies.

# Accurate Characterization of Rotor Activity during Atrial Fibrillation Depends on the Properties of the Multi-electrode Grid

Laura Martinez, Lucia Romero, Catalina Tobon, Jose M Ferrero, Jose Jalife, Omer Berenfeld and Javier Saiz*

I3BH, Universitat Politècnica de València, Valencia, Spain
Valencia, Spain

**Background** Multi-electrode array systems are increasingly being used to study atrial electrical excitation in humans and are shining new light on the mechanisms of atrial fibrillation (AF). However the mapping systems that are currently being used to characterize the rotors that are postulated to drive AF have not been systematically analyzed for accuracy.

**Objective:** To quantify the effect of the multi-electrode grid configuration on the accuracy of detection of rotors and their pivoting point meandering.

**Methods:** Computer simulations of AF were carried out using a realistic 3D model of the atria. Extracellular electrical potentials were calculated on intra-atrial 22x22 electrode arrays placed at the driving rotor area. The array-to-endocardial wall distance was set at 0.2, 1, 2 and 5 mm and uniform interelectrode-distances were set at 1, 2 or 5 mm. The instantaneous location of the rotor tip and its meandering were analyzed on interpolated phase movies based on the Hilbert transform.

**Results:** Increasing the distance of the array from the endocardium decreased electrogram amplitude (26.4%-90.96%). At a spatial resolution of 1 mm and array-to-wall distance of $\leq$2 mm, the rotor tip location on the array was not significantly different from that in the wall, although meandering at the array was larger than in the atrium (0.4 vs 0.22 cm2). At a spatial resolution of 2 mm, increasing the array-to-wall distance further increased the detected meandering area (0.52-0.68 vs 0.22 cm2). Finally, when the spatial resolution was 5 mm, the array recognized the presence of the rotor, but not its tip trajectory regardless of the array-to-wall distance.

**Conclusion:** The use of interpolated phase analysis of AF dynamics using multi-electrode arrays should consider that increasing the inter-electrode distance or the array-to-wall distance to $\leq$5 mm, reduces precision in tracking the rotor's tip trajectory, but does not preclude rotor identification.

# Constructing Human Atrial Electrophysiological Models Mimicking a Patient-Specific Cell Group

Anna Muszkiewicz, Alfonso Bueno-Orovio, Xing Liu, Barbara Casadei, Blanca Rodriguez

University of Oxford, Oxford, UK

**Aims:** We aim to construct multiple human atrial electrophysiological models mimicking the action potential (AP) biomarkers obtained from experiments with single cells extracted from a homogeneous patient group.

**Experimental data:** We used AP biomarkers from 18 atrial myocytes of 8 elderly male patients in sinus rhythm, undergoing coronary artery bypass graft in Oxford, UK. AP biomarkers were collected over five frequencies (0.25, 0.5, 1, 2, 3Hz) and included resting membrane potential (RMP) and action potential duration (APD) at 20, 50, and 90% repolarization. APDs obtained in experiments were 2-3 times lower than in human atrial electrophysiological models (APD90 of 80-150ms vs. 300-350ms).

**Methods:** Based on the Maleckar model of human atrial electrophysiology, we generated 15000 models by varying ionic conductances of 11 most important currents underpinning AP. Conductances were varied simultaneously within $\pm 100\%$ range from their baseline model values using Latin Hypercube sampling. Models were paced at 5 frequencies and in different conditions, with varying ion concentrations and stimulus strength. If all AP biomarkers were in experimentally observed ranges, the model was accepted for further analysis.

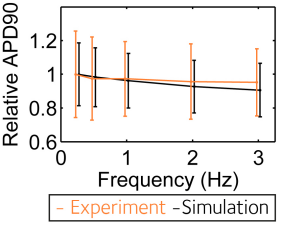


APD rate dependence. APDs are normalized to 0.25Hz.

**Results:** Ionic conductances significantly influence APD90, while external factors (ionic concentrations, stimulus strength) play a critical role in producing RMP and APD20 values consistent with experiments. By mimicking experimental conditions, we generated 604 models fully covering the experimental range of AP biomarker values. 3/4 of the conductances underpinning these 604 models are spread within 35% of their median values, indicating that most of the models with unusual parameters were rejected. APD rate dependence of the accepted models agrees with experiment (see Figure).

**Conclusions:** Ionic conductances and external factors, such as ionic concentrations and stimulus strength, are vital in tailoring the single-cell electrophysiological models to a narrow patient group. This has implications in understanding the propensity of subgroups of the population to disease conditions.

# Evaluating Effects of Fibrosis on Atrial Re-entry Using 3D Computational Modelling

Ross Morgan*, Michael Colman, Martin Kruger, Gunnar Seemann, Kawal Rhode and Oleg Aslanidi

Kings College London
london, United Kingdom

**Aims:** This study investigates the effect of fibrosis on atrial fibrillation (AF) using three dimensional (3D) computational modelling. 3D modelling provides a quantitative framework for integrating realistic atrial geometry, regional electrophysiological variations and AF induced remodelling, as well as structural and functional aspects of fibrosis. Model simulations enable the understanding of the detailed interactions of fibrosis with electrophysiological factors of wave dynamics that sustain AF.

**Methods:** The electrophysiological cellular models were developed previously to describe human atrial action potential [Courtemanche et al., 2000] and myocyte-fibroblast electrotonic coupling [MacCannell et al., 2007]. The models were integrated into 3D atrial geometry derived from the Visible Human dataset with rule-based fibre orientation. Variable cell-to-cell coupling parameters, such as diffusion coefficients and anisotropy ratios, were used to account for AF related structural tissue changes. Regional electrophysiology and its ionic remodelling were included to model the respective functional changes. A simpler 1D cable model was applied to accurately measure conduction velocity and action potential duration (APD). The 3D atria model was paced 10 times at 300ms, and afterwards a cross-field protocol was applied to generate re-entrant waves.

**Results:** In the 1D cable, conduction velocity was reduced from 0.85 to 0.82 and 0.49m/s and APD was reduced from 285 to 135 and 225ms for ionic remodelling and fibrosis, respectively. This resulted in the respective reduction in the wavelength from 250mm to 109mm (ionic remodelling) and 120mm (fibrosis). Combined fibrosis and ionic remodelling showed reductions in conduction velocity, APD and wavelength to 0.58m/s, 125ms and 73mm. In the entire 3D atria geometry, the likelihood of re-entry initiation (quantified as the vulnerability window) and the duration of re-entry sustenance was higher for both fibrosis and ionic remodelling compared to control.

**Conclusion:** Fibrosis can significantly reduce the wavelength, increasing the likelihood of re-entry initiation and sustenance.

# Age- and Gender-related Shift in Cardiovascular Variability in Healthy Volunteers

Hagen Malberg*, Hendrik Bonnemeier, Andreas Müller, Sebastian Zaunseder and Niels Wessel

TU Dresden
Germany

Analysis of cardiovascular variability, heart rate and blood pressure variability as well as baroreceptor sensitivity have become proven markers for diagnosis, monitoring and risk stratification of several cardiovascular diseases. In this background, the analysis of age- and gender related healthy volun-teers are essential. In this study, 309 investigated healthy voluntees (CON) had been investigated. The population contained the age-related distribution: 10-20 years: 15 CON, 21-30 years: 50 CON, 31-40 years: 81 CON, 41-50 years: 61 CON, 51-60 years: 40 CON, 61-70: 35 CON, 71-88: 26 CON. The time course of blood pressure was registered by noninvasive continuous blood pressure measurement device Finapres for 10 minutes under resting conditions. Baro-receptor sensitivity had been characterized by Dual Sequence Method; heart rate variability by several methods containing linear and non-linear approaches. The results show a gender and age-related time course of blood pressure regulation. The age related decrease of BR events seems to be more distincted in female than ($p<1$ E-6) in male ($p=0.001$). Baroreceptor sensitivity as a measure of regulatory sensitivity on changes in blood pressure showed in higher ages a decrease; in female ($p<1$ E-8) stronger than in male ($p<1$ E-4). While standard HRV-parameters showed no significant changes, the nonline-ar parameters „FORBWORD“ and „SHANNON“ showed alterations in the age ranges lower and higher 40 years. The results point to an age specific decrease of the healthy baroreflex regulation. In female, this reduction seems to be more extensive. Additionally, the results prove the sense of age- and gender related standards in healthy volunteers.

## Causality of Heart Rate – Blood Pressure Interactions during Mental and Orthostatic Stress

Michal Javorka*, Barbora Czippelova, Lenka Chladekova, Zuzana Turianikova, Zuzana Visnovcova, Zuzana Lazarova, Kamil Javorka and Ingrid Tonhajzerova

Comenius University, Jessenius Faculty of Medicine
Martin, Slovakia

Baroreflex sensitivity is frequently measured from spontaneous oscillations of blood pressure (BP) and heart rate (HR) assuming the unidirectional influence from BP to HR – the BP drop is sensed by baroreceptors and the response include the increased HR predominantly mediated by parasympathetic withdrawal. However, the interaction of BP and HR is bidirectional – HR also influences BP by changes in diastolic heart filling via Frank-Starling mechanism. The novel methods based on Granger causality concept for separate analysis of feedback (baroreflex) and feedforward (mechanical) interactions between HR (or its reciprocal value – RR interval from ECG) and BP were recently developed. The aim of our study was to analyze the changes in proportion of both causal directions between RR and systolic blood pressure (SBP) oscillations during supine rest and application of two different stressors. We have noninvasively recorded BP (Finometer Pro, FMS, Netherlands) and ECG (CardioFax ECG-9620, NihonKohden, Japan) signals in 16 healthy volunteers (7f / 9m; age 20.5 (20.1 – 21.1) years) during supine rest, mental arithmetics task and head-up tilt test. We have analyzed 500 heart beats long recordings. Linear analysis of RR/SBP causal interactions was performed by bivariate causal close-loop model and coherence in both causal directions was quantified separately. Alternatively, information domain approach was used to separately analyze coupling strength in both directions. In supine rest, RR oscillations cause SBP oscillations while the opposite direction (feedback influence) is less important. During mental stress, a tendency towards increased feedback influence was observed. The dominance of feedback interaction (SBP to RR) during head-up tilt was revealed by both linear and information domain analysis. The strength of feedforward influence did not change during protocol. We conclude that the proportion of causal interactions between SBP and RR changes during various conditions. Supported by grants VEGA 1/0059/13, VEGA 1/0087/14 and APVV-0235-12.

# Heart Rate Variability Associated with Different Modes of Lower Abdominal Muscle Tension during Zen Meditation

Masaki Hoshiyama* and Asagi Hoshiyama

Meisei University
Kamakura-shi, Japan

Zen is a traditional meditation method which utilizes unification of body, respiration and mind. Zen is spreading widely into western world today, realizing deeper meditation with minimum body movement and distraction. While heart rate variability (HRV) during controlled autonomic stimulation has been studied in the past, there remains a lack of consensus whether heart rate during Zen elicit consistent HRV differences for different modes of lower abdominal muscle (LAM) tension. To better understand the effect of LAM tension modes on hemodynamic events elicited by deep Zen meditation, we studied heart rate in 2 intermediate Zen meditators. The study took place over 9 sets of Zen meditations in a quiet, Zen practice hall. Each set of Zazen lasted at least for 25 minutes. The first sets were used for habituation, and the data obtained from the following eight sets were used for analysis, where 2 modes of LAM tension, i.e., intentional LAM contraction (LAMC) and LAM relaxation (LAMR), were allocated alternately. Power spectrum analysis showed distinctive change in frequency components. High frequency (HF) components increased for LAMC ($p=0.05$). Most notably, detrended fluctuations analysis (DFA) of HRV were around 1/2 for LAMC and 0.82 for LAMR. During Zen practice, we seat ourselves in a lotus posture with LAMC, practice lower abdominal (Tanden) breathing, and keep mind free from distraction. We attribute the increase of HF components and decrease of DFA exponent in LAMC to the parasympathetic stimulation, and to the minimal use of antigravity muscles in the optimal posture generated by LAMC, as contrasted with the active use of antigravity muscles in the unstable posture during LAMR, hence to the effective regulation of mind during meditation toward the edge of sleep, but not quite over it. This result suggests the possibility of HRV as a handy and quantitative evaluator for Zen meditation.

# Impacts of labour first and second stages on Hurst parameter based intrapartum fetal Heart Rate analysis

Jiří Spilka, Patrice Abry, Paulo Goncalves, Muriel Doret,

Physics Dept., ENS Lyon, France

**Objectives:** Intrapartum fetal heart rate (FHR), the main information channel about fetal health status during labour, is routinely monitored to enable obstetricians to perform early detection of fetal asphyxia and thus to prevent adverse outcomes. This study aims at quantifying the impacts of labour first and second stages on the characterization of intrapartum fetal heart rate variability temporal dynamics as well as on the discrimination of healthy from acidotic fetuses.
**Methods:** FHR temporal dynamics are quantified using Hurst paramater, $H$, practically estimated within a wavelet framework. Analyses are performed within 20-minute long sliding windows, with 5 minutes overlap (for respectively, 60 and 15 minutes within first and second stages of labour), over a large (3049 records) and well document database, collected at *Hôpital Femme-Mère-Enfant*, in Lyon, France.
**Results:** Change in $\hat{H}$ between first and second stages of labour is found statistically significant (increase of $\hat{H}$ from 0.46 (95% CI: 0.46-0.49) to 0.51 (95% CI: 0.50-0.52), $p < 0.05$). Further, it is observed that $\hat{H}$, for healthy fetuses, remains constant along first stage and then significantly increases during second stage ; while, for acidotic fetuses, $\hat{H}$ starts to increase to much larger values earlier within first stage. This may indicate that the defense mechanism classically at work during second stage as a reaction to excessive stress, is already in use during first stage for acidotic fetuses. ROC curves also show that second stage $\hat{H}$ permits to better discriminate healthy from acidotic fetuses, compared to first stage $\hat{H}$. Further, it will be illustrated how improper comparisons of $H$ estimated without splitting a priori first and second stages lead to biased classification performance evaluation.

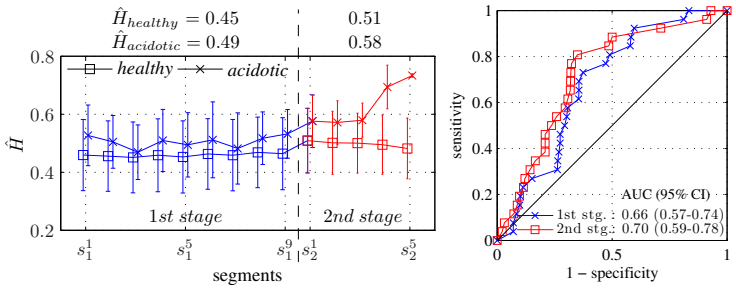


Left: Evolution along time of $\hat{H}$. Right: ROC curves from $H$ estimated in 1st and 2nd stages.

# Phase Transitions in Independent Forms of Cardio-Respiratory Coupling across Sleep Stages

Ronny P Bartsch, Kang KL Liu, Qianli DY Ma and Plamen CH Ivanov*

Boston University
Boston, United States

Physiologic organ systems exhibit complex nonlinear dynamics characterized by non-stationary, intermittent, scale invariant and multi-fractal behaviors. Moreover, nonlinear coupling and interactions between organ systems influence their output dynamics and coordinate their function, leading to another level of complexity. It is an open problem to adequately determine interactions between complex systems, where their coupling is not known a-priori, and where the only available information is contained in the output signals of the systems. Neuroautonomic regulation of the cardiac and the respiratory system changes with transition from one physiologic state to another. Thus we hypothesize that cardio-respiratory coupling also undergoes phase transitions in order to facilitate and optimize organ interactions during different physiologic states. We further hypothesize that the cardiac and the respiratory system can communicate through several independent mechanisms of interactions which operate at different time scales and can simultaneously coexist. We analyze ECG and respiratory recordings from 190 healthy subjects (100 female/90 male, ages 20-95) during sleep. To probe distinct forms of cardio-respiratory coupling, we apply three methods: (i) analysis of respiratory sinus arrhythmia, (ii) phase-synchronization analysis, and (iii) time delay stability analysis. We find pronounced phase transitions in these forms of cardio-respiratory coupling: each form exhibits significantly different strength during different sleep stages. Further, we find that each form of coupling is characterized by a distinct stratification pattern across sleep stages, indicating complex reorganization in physiological interaction. Our observations show that the cardiac and the respiratory system can interact through several independent forms of coupling, that are affected in a different way by changes in neuroautonomic control across physiologic states. We demonstrate that physiologic systems interactions are not of constant strength but are of transient and intermittent nature, with 'on' and 'off' periods, and that different forms of coupling, representing different aspects of physiologic regulation, can simultaneously coexist.

# Time-Domain and Spectral Analysis of Heart Rate Variability in Rats Challenged with Hypoxia

Stanislaw Zajaczkowski*, Maria Smolinska, Piotr Badtke and Tomasz Wierzba

Medical University of Gdansk
Gdansk, Poland

Different approaches based on spectral and time-domain analysis of heart rate variability (HRV) were used to evaluate cardiac rhythm regulatory response to hypoxia. Twenty male Wistar rats (300-350 g) with previously implanted subcutaneous ECG electrodes, were maintained unrestrained in originally designed experimental setup, during normobaric 60-min normoxia, followed by 60-min hypobaric hypoxia (-400 mmHg). RR intervals (RRi) were extracted from continuous ECG recording digitized with a 16-bit resolution at 4 kHz by Powerlab (AdInstruments,Australia). Time- and frequency-domain HRV estimates were computed (Kubios HRV Pro software;Finland) from time-series of 1024 consecutive RRi, recorded in possibly stationary conditions during normoxia and hypoxia. Power spectrum (very low frequency – VLF: 0.02-0.2 Hz; low frequency - LF: 0.2 – 0.75 Hz; high frequency - HF: 0.75 – 2.5 Hz, and total power - TP: 0.02 – 2.5 Hz) was obtained with a fast Fourier transform and autoregressive (AR) modeling (AR order – 40). Compared to normoxia, hypoxia resulted in a significant increase of mean RRi (188±17 ms, 203±28 ms, respectively, p=0.033), SDNN (standard deviation of all RRi; 4.31±1.36 ms; 6.07±2.85 ms; p=0.015), rMSSD (the root mean square value of successive differences between adjacent RRi; 4.02±0.5; 6.57±2.47 ms; p=0,0011), TINN (triangular interpolation of RRi; 28.68±11.16 ms; 58.84±30.88, p=0.0015), and asymmetry of RRi dispersion as shown by change in skewness (from -0.12±0.81 to 1.05±1.67; p=,0107). AR and FFT analysis provided concordant power spectra across all tested bands. TP, including VLF, HF and predominantly LF, was increased in hypoxia, whereas LF/HF index of the sympatho-vagal balance remained unchanged. Changes in spectral power (TP, VLF, LF, HF) and skewness evoked by hypoxia correlated positively (r ranging from 0.46 to 0.94; p from 0.04 to <0.00001) with simultaneous changes in SDNN, rMSSD, TINN, and also LF/HF. Interestingly, correlation coefficients r obtained from AR and FFT were not significantly different.

# CrowdLabel: A Crowd-sourcing Platform for Electrophysiology

Tingting Zhu[1], Joachim Behar[1], Tasos Papastylianou[1], Gari D. Clifford[1, 2]

[1] Institute of Biomedical Engineering, Department of Engineering Science, University of Oxford, UK
[2] Department of Bioinformatics, Emory University, USA

**Introduction**: In foetal electrocardiographic monitoring, extraction of morphological measurement such as QT interval is particularly challenging due to its invasive nature and low amplitude foetal ECG (FECG) signal. Assessment of foetal QT (FQT) in identifying foetal hypoxia has been limited to date, partly due to the lack of available public databases with expert labels.

**Method**: Our proposed platform, CrowdLabel (see Figure 1), a web-based and open-source annotation system, was developed for crowd-sourcing medical labels from multiple expert and/or non-expert annotators. In this study, we describe the platform and an example of use; to improve FQT estimation, creating reference labels against which automated algorithms can be benchmarked. A total of 501, 30s segments were extracted from 15 FECG recordings from a private database.

Figure 1: The CrowdLabel interface: Labelling a feotal QT annotation

**Results:** Twenty-three volunteers participated in the study and provided a total of 7,307 FQT annotations, which were aggregated using a novel probabilistic label aggregator (PLA). The best annotator identified by the PLA had a variance of 1.3ms and 4.69ms in his annotations when labelling FECG with very good and poor signal quality. However, the PLA does not require any ground truth to identify the best annotator or annotations. Annotator accuracy was also show to be a function of objective signal quality measures.

**Conclusion**: This paper presents a proof-of-concept crowd-sourcing methodology to aggregate human annotations in FECGs. The feasibility of the CrowdLabel annotation system for ECG crowd-sourcing with an unknown ground truth, as well as the results of the first experiment conducted using such a platform have been demonstrated.

# Increasing the Dynamic Range of a Pulse Oximeter Using Heart Rate Characteristics

Chris J Brouse*, Ronald Gatzke, Daniel K Freeman and Yu Chen

Draeger Medical Systems, Inc.
Andover, United States

**Aims:** This theoretical investigation aimed to increase the dynamic range of a pulse oximeter by reducing electronic noise in the photoplethysmogram (PPG) using characteristics of the heart rate (HR) signal. The PPG is used to measure blood oxygen saturation (SpO2). Analog front end (AFE) circuitry introduces electronic noise into the PPG signal, which decreases the signal-to-noise ratio (SNR) and limits the dynamic range. We wish to increase the dynamic range to handle clinically challenging conditions such as thick/dark fingers (low signal DC level) and weak pulse/low perfusion (low signal AC level).

**Methods:** We developed a novel algorithm for dynamically tuning a band-pass filter in real-time to pass the SpO2 information while maximally rejecting the electronic noise. The SpO2 information exists in the PPG around the pulse frequency (i.e. the HR). The algorithm tunes the filter based on characteristics of the HR signal recorded from a separate source (e.g. ECG). We derived a theoretical model of the signal and noise levels in a Dräger M540 monitor. We derived the theoretical minimum required SNR to accurately measure SpO2. We simulated conditions across a range of PPG signal levels, and calculated the theoretical resulting SNR. Finally, we compared the SNR over a traditional bandwidth of 5 Hz to the new theoretical bandwidth of 0.2 Hz, and calculated the expected increase in SNR and thus dynamic range of the oximeter.

**Results:** The narrow-band filter increased the PPG SNR by 14 dB (5x). When the filter was applied to the Dräger M540 SpO2 AFE output, the device could theoretically measure signal levels 5x lower than without the filter.

**Conclusions:** A band-pass filter, tuned based on characteristics of the HR signal, can be used to reduce the electronic noise in the PPG signal, increasing SNR and thus increasing the dynamic range of a pulse oximeter.

# Noise and Spatial-resolution effect of Electrode Array on Rotor Tip Location during Atrial Fibrillation: A Simulation Study

Miguel A Becerra*, Juan P Murillo, Laura C Palacio and Catalina Tobón

Institución Universitaria Salazar y Herrera
Medellín, Colombia

Atrial fibrillation (AF) is the most common arrhythmia in clinical practice. Recently, a mechanism for maintaining the AF, which consists of one or more rotors activating the tissue at high frequency, has been proposed. Ablation is one of the treatments for AF whose effectiveness could depends on the localization of the rotor tip. Thus, we study the noise and the spatial resolution effect of electrode array on the information used to locate the rotor tip, which is determined from an analysis carried out by the algorithms based on approximate entropy (ApEn) and dominant frequency. In a previous research, the ApEn was proposed as an effective rotor tip detection system. However, this system was validated with an array of 22500 electrodes from which ideal noise-free simulated electrograms are originated, moving the system from reality in a significant way. Consequently, there are three analysis presented in this work; the first one is carried out with noise-free simulated electrograms, the second one is executed with simulated electrograms with noise of real electrograms (NoRE), and the third one is done by applying the Kalman filter on the simulated electrograms with NoRE. In each case, the effect of the dimension of electrodes array is analyzed with relationships of equidistant reduction rows-column from 2-2 to 6-6 on a 2D model of human atrial tissue under chronic AF conditions. So, this comparison showed that the noise has a greater negative effect than the one generated by the decrease of resolution in electrodes array, and despite of the acceptable Kalman filter's performance for increasing the SNR significantly, the localization of the rotor continues to be affected but to a lesser extent with respect to the obtained results with electrograms with NoRE, obtaining results adequate for locating the tip of rotor.

# Risk Assessment of Atrial Fibrillation: a Failure Prediction Approach

Jelena Milosevic[1], Andreas Dittrich[1], Alberto Ferrante[1], Miroslaw Malek[1], Camilo Rojas Quiros[2], Rubén Braojos[2], Giovanni Ansaloni[2], David Atienza [2]
[1]ALaRI, Università della Svizzera italiana, Lugano, Switzerland
[2]ESL, École Polytechnique Fédérale de Lausanne, Switzerland

We present a methodology for identifying individuals at risk of Paroxysmal Atrial Fibrillation (PAF) among a subjects population. Our work is focused on designing an unobtrusive system for concurrent detection and monitoring of chronic cardiac conditions by means of ECG. While effective methodologies for PAF prediction are proposed in literature, these works either employ computationally complex algorithms or use additional bio-signals, having a negative impact on the wearability of the system.

The proposed methodology comprises two stages: off-line training and on-line analysis. During training, relevant features are identified by using a statistical approach, without relying on a manual selection based on previous knowledge. The Local Outlier Factor (LOF) anomaly detection method is employed to identify abnormal features in the training set, which are then used to tune a classifier. Subjects are considered PAF-prone if the percentage of identified abnormal features is above a prespecified threshold. The analysis stage is based on two phases: feature extraction and detection of PAF patients. Low-complexity algorithms are employed for feature extraction, allowing the on-line implementation of this phase on wearable sensor nodes. The detection phase employs techniques borrowed from the field of failure prediction. While these methods have found an extensive application in diverse scenarios, their application to cardiac analysis has not been sufficiently investigated.

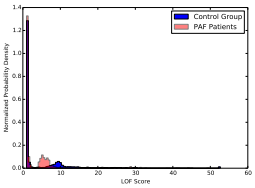

Histogram of anomalies in the subjects population.

Our framework is validated on the ECG data provided in the PAF Prediction Challenge. Precision obtained in classifying the subjects is 0.68, with a recall of 0.64 and of 0.71 for PAF patients and for control group, respectively. Obtained results, in terms of accuracy, are comparable to similar efforts in the field. However, the proposed method employs less complex algorithms, which are compatible with the computational constraints of state-of-the-art body sensor nodes.

# Multimodal Sensor Fusion of Cardiac Signals via Blind Deconvolution: A Source-Filter Approach

Christoph Hoog Antink, Christoph Brüser, Steffen Leonhardt

Philips Chair for Medical Information Technology,
RWTH Aachen University, Aachen, Germany

Sensor fusion is a growing field within the medical signal processing community. Traditionally, it is performed implicitly by the physician when diagnosing the state of a patient from various measurement modalities such as electrocardiography (ECG), arterial blood pressure (ABP), or photoplethysmography (PPG). These may represent different physical quantities like voltage, pressure, or scattering properties and are modulated by various physiological conditions and artifacts. Especially unobtrusive modalities are very sensitive to noise and motion, but even the classical modalities can be severely contaminated with artifacts. Still, they originate from a single source, the heart.

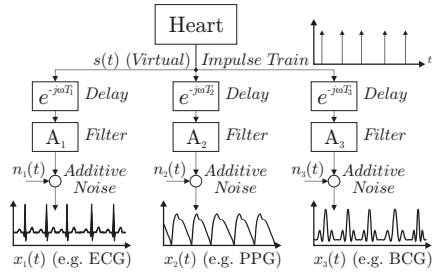


In signal processing, this is known as a single-input-multiple-output (SIMO) system. In our proposed approach, we model the heart as the source for a purely virtual signal representing the occurrence of each heart beat through an impulse-like response. Each measured signal is assumed to be derived from this source signal through delay and filtering operations as well as the addition of noise. Our aim is to solve the inverse problem, i.e., find the abstract source signal given the measured physiological signal. Thus, a blind deconvolution approach is chosen and adapted for physiological signals. The feasibility and robustness to outliers is shown using simulated data. Moreover, the approach is tested on real data recorded in a polysomnography setting, fusing PPG and ballistocardiography (BCG). Comparing the estimated source to an ECG reference, beat-to-beat accuracy could be shown. Interestingly, even the presence of a second common source (respiration) could be accurately estimated.

In the future, the proposed source-filter model could serve various purposes: If the sensor outputs can be predicted well using estimated source and filters, this could serve to perform data compression. On the other hand, large differences between model prediction and measurement could be used as "event indicators", indicating physiological changes or artifacts.

# A Data Driven Approach to Patient Cohort Identification

Thomas Brennan*, Marco Pimental, Mengling Feng, Li-Wei Lehman, Mohammad Ghassemi and Roger Mark

MIT
United States

Predicting mortality in intensive care units (ICU) remains a significant challenge. Common methods of predicting mortality, such as Severity of Acute Physiology Scure (SAPS) or the Acute Physiology and Chronic Health Evaluation (APACHE), use a combination of features to assess patient condition. However, both SAPS and APACHE tend to have poor predictivity across a population of patients. Our hypothesis is that in any given population, patient phenotypes can be clustered and that patient subgroups have different mortality profiles. To assess this hypothesis we propose a data-drive approach that uses principal component analysis (PCA) coupled with Gaussian mixture model (GMM) to identify different patient subgroups. We extracted 160 variables, representing both static and dynamic features, from the MIMIC-II database from the first 48 hours of an ICU stay for all adult patients admitted to the ICU (N=19,381). We represent each patient by feature vectors of lab values and vital sign measurements that reflect their admission status as well as trajectories of those variables over a 48-hour period. PCA was used for dimensionality reduction on this feature space, and the top 3 principal components, accounting for 85% of the information, were used as input to GMM to identify subgroup of patients with similar health status and trajectories during the first 24 hours in the ICU. Bayesian Information Criterion along with the Expectation-Maximization was used to identify the optimal number of patient subgroups (N=9). We demonstrate the clinical utility of the proposed framework in identifying subgroups of patients at high risk of hospital mortality.

# Altered Nonlinear Dynamics of Atrial Fibrillation Detected After Ablation

Kevin Sunderland*, Adam Berman and Autumn Schumacher

Georgia Regents University
Augusta, United States

**Introduction:** Atrial fibrillation (AF) is characterized by uncoordinated P and QRS waves on the electrocardiogram (ECG). Understanding this disorganized ECG activity is difficult since the QRS wave masks the P wave patterns. The purpose of this project was to eliminate the QRS wave and analyze the remaining atrial ECG signal with a nonlinear technique to better understand the underlying dynamics of this arrhythmia. METHODS: A continuous ECG signal (Lead II) was digitally recorded during a cardiac ablation procedure from 21 adult AF patients. Thirty-second segments of AF were selected before and after ablation from each patient's ECG recording. Each ECG segment underwent processing to remove the QRS wave using the adaptive singular value cancelation (ASVC) technique. ASVC uses the redundant QRS wave pattern to generate noise, which is then adapted to and subtracted from each QRS wave, leaving the atrial component of the ECG signal. Each atrial ECG segment was then analyzed with recurrence quantification analysis (RQA), which is an analysis technique using eight variables to quantify the nonlinear dynamics of each signal. Paired t-tests determined statistical group differences for each RQA variable at the .05 level of significance. RESULTS: The only RQA variable to show a statically significant group difference between before and after ablation was %determinism ($p = .042$). This finding shows that the nonlinear structure of AF diminished after ablation of the atrial myocardial tissue.

**CONCLUSION:** The results of this project demonstrated that the ASVC technique eliminated the QRS wave and RQA detected alterations in the nonlinear dynamics of the remaining atrial ECG signal after ablation. More research is needed with a larger sample size to determine the clinical benefit of analyzing the atrial signal to detect and better understand the underlying nonlinear dynamics of the AF arrhythmia.

SA1

# A Novel P-wave Duration Estimation Method to Assess the Impact of the Hybrid Procedure for Atrial Fibrillation Ablation

Pietro Bonizzi*, Narendra Kumar, Stef Zeemering, Ralf Peeters and Laurent Pison

Maastricht University
Maastricht, Netherlands

**Aims:** Changes in P wave duration (PWD) following atrial fibrillation (AF) ablation have been described and may have diagnostic value. Hybrid procedure (HP) involves epicardial isolation of pulmonary vein and posterior wall of left atrium, and endocardial checking of lesions and touchups (if needed). PWD is usually assessed manually from ECG. This study aimed at exploring a novel method for automated modeling of the P-wave and assessment of PWD. Moreover, it aimed at investigating the effect of HP on PWD.

**Methods:** P-waves were fitted with two half-Gaussian functions, to account for left-right asymmetries in P-wave morphology. PWD was assessed from the standard deviations of the Gaussian functions. Validation was based on the PTB Diagnostic ECG Database, including 51 recordings from healthy volunteers (mean age 44±16 years; male/female: 38/13). Two-minutes recording of X-Frank lead (sampled at 1000Hz) were used. P-waves were automatically segmented and visually inspected. The method was compared with a standard fitting based on one Gaussian function. Ability of the method to describe changes in PWD following HP was tested on 36 patients who underwent HP (58±10 years; males/females: 27/9; paroxysmal/persistent: 27/9). Method validation: The proposed method provided a better fit of the P-waves in terms of normalized root mean squared error (median±MAD; 0.14± 0.07 mV vs. 0.28±0.11 mV, $p<0.001$, Wilcoxon signed rank test). Effect of HP on PWD: Overall, PWD was significantly decreased after procedure (111.02±25.87 ms vs. 95.68± 31.98 ms, $p= 0.0319$). PWD pre-procedure was significantly higher in persistent patients than in paroxysmal patients (126.85±15.50 vs. 106.63± 27.10, $p= 0.0214$, Wilcoxon rank-sum test). Results were not significant for the single Gaussian model.

**Conclusions:** Pre-procedure PWD was higher for persistent than paroxysmal patients. HP reduced PWD significantly. The novel PWD estimation method may also enable automated assessment of patient-specific AF substrate complexity before procedure from the surface ECG.

# Atrial Fibrillation Substrate Characterization and Catheter Ablation Acute Outcome Prediction: Comparative Analysis of Spectral and Nonlinear Indices from Right Atrium Electrograms

Luigi Yuri Di Marco*, Daniel Raine, John P Bourke and Philip Langley

University of Sheffield
United Kingdom

**Background** Atrial fibrillation (AF) is the most common arrhythmia in clinical practice. Although catheter ablation (CA) is increasingly becoming the preferred treatment, not all patients respond well. Identifying predictors of CA outcome is important to assist clinical decision making. Previous studies have explored spectral and nonlinear indices. However, a comparative analysis of indices from preprocedural intracardiac recordings is currently lacking. AIM: To present a comparative analysis of spectral and nonlinear indices derived from a simple threshold-based segmentation of intracardiac electrograms (EGM) to characterize AF substrate (paroxysmal vs. persistent) and predict AF termination by CA. METHODS: Preprocedural 1 minute recordings of right atrium EGM from 54 AF patients (age 58±9 years, 37 male; 27 paroxysmal AF, 27 persistent) were used. EGM were band-pass filtered (F-EGM). f-wave activation fiducial points were identified using a threshold-based segmentation. The AF cycle length (AFCL) time series was built calculating the distance between consecutive fiducial points. The instantaneous fibrillatory rate (IFR) time series was calculated as AFCL inverse. Nonlinear indices were calculated: i) median AFCL (MAFCL); ii) localization index (LI) (concentration of IFR histogram around the mode); iii) sample entropy (SampEn); iv) root mean square error (RMSE) of IFR vs. Gaussian distribution fit. Standard spectral methods were used to calculate spectral indices: i) dominant frequency (fP); ii) organization index (OI) (ratio of area under fP and its harmonics to total power) of F-EGM. RESULTS: Persistent AF was associated with higher fP ($p<0.005$), lower MAFCL ($p<0.01$) and LI ($p<0.05$), higher SampEn ($p<0.05$) and RMSE ($p<0.01$). OI was not associated with AF substrate. Nonlinear indices: MAFCL($p<0.01$), LI($p<0.05$), RMSE($p<0.005$) predicted AF termination by CA, whereas spectral indices (fP, OI) did not.

**CONCLUSION:** Nonlinear indices outperform spectral indices in characterizing AF substrate and predicting AF termination by CA.

SA1

# Modification of Atrioventricular Node Conduction Increases RR Variability but not RR Irregularity nor Atrial Fibrillation Rate in Atrial Fibrillation Patients

Valentina DA Corino*, Sara R Ulimoen, Steve Enger, Luca T Mainardi, Arnljot Tveit and Pyotr G Platonov

Politecnico di Milano
Italy

Irregularity measures have been suggested as risk indicators in patients with atrial fibrillation (AF), however it is not known to what extent they are affected by commonly used rate-control drugs. The aim of the present study was to evaluate the effect of rate-control drugs on the variability and irregularity of the ventricular rate in patients with permanent AF. We analyzed data of 60 patients (age 71±9 years, 42 men) with permanent AF, from the RATAF (RATe control in Atrial Fibrillation) study, where Holter ECG were recorded at baseline and during treatment with rate-control drugs. For each patient, three 20-min segments were selected at baseline, during beta-blocker (carvedilol) and calcium channel blockers (diltiazem) administration. For every 20-min segment, heart rate (HR) was estimated as well as variability (SDNN, rMSSD, pNN50) and irregularity (regularity index, approximate (ApEn) and sample (SampEn) entropy) of RR intervals. A lower HR is obtained with both drugs, being the HR obtained during diltiazem administration lower than that with carvedilol (HR: baseline 110±18 bpm, carvedilol 88±14 bpm $p<0.05$ vs. baseline, diltiazem 79±16 bpm $p<0.05$ vs. baseline, $p<0.05$ vs. carvedilol). Both drugs increased the variability of ventricular response compared to baseline (as an example, rMSSD: baseline 171±47 ms, carvedilol 229±58 ms $p<0.05$ vs. baseline, diltiazem 256±87 ms $p<0.05$ vs. baseline, $p<0.05$ vs. carvedilol). Only carvedilol significantly increased the irregularity of the RR series (as an example, ApEn: baseline 1.86±0.13, carvedilol 1.92±0.09 $p<0.05$ vs. baseline, diltiazem 1.88±0.16 ns vs. baseline, ns vs. carvedilol). In conclusion, carvedilol and diltiazem influenced AV node conduction differently: both reduced HR and increased time-domain measures of heart rate variability, but only carvedilol increased the irregularity measures. The use of diltiazem does not necessitate adjustment of the model when assessing irregularity in AF patients, while carvedilol should be accounted for.

# Using a new Time-Independent Average Method for Non-Invasive Cardiac Potential Imaging of Endocardial Pacing with Imprecise Thorax Geometry

Jaume Coll-Font*, Burak Erem and Dana H Brooks

B-spiral group, ECE dept, Northeastern University
Boston, United States

Cardiac electrical imaging from body surface potentials is a technology with great potential for pre-procedure planning in the context of ventricular ablation. Two clinically desirable properties of such an imaging system are ability to localize endocardial as well as epicardial initation sites and limited dependence on anatomical imaging. Sensitivity to measurement noise makes increased signal SNR desireable when multiple beats with the same initiation are available. Standard ensemble averaging should increase SNR. However variability in timing or intra-beat wavefront velocity can introduce correlated noise that instead decreases SNR and increases solution error. Thus another approach is to reconstruct each beat separately and average the results. Here we report on study based on a combination of previous work on endocardial pacing site localization using limited torso imaging with our development of an averaging technique that is less insensitive to timing and velocity errors. For the geometric model we fit a generic torso and epicardial-endocardial ventricular heart surface geometries to limited axial X-Ray CT images of the volume containing the subject's heart. These geometries were then used to generate a mathematical forward model relating heart and body surface potentials. For a set of pacing site on the RV and LV endocardia of 3 subjects, we recorded multiple trials of 120 lead ECG. We reconstructed each beat and then reconstructed from ensemble averages and our new technique. The reconstructed heart potentials were then used to estimate the pacing sites that were then validated by comparison to previously recorded locations from a CARTO system. We report on solutions for using both all 120 leads and a standard 12 lead configuration. The solutions from our time insensitive averaging method show improvement in localization accuracy over the solutions obtained with ensemble averaging, although the average of single-beat reconstructions results in better precision for most pacing sites.

SA2

# Localization of Three-Dimensional Sources in Cardiac Tissue Using Optical Mapping

Gwladys Ravon, Yves Coudiere , Angelo Iollo, Olivier Bernus, Richard D Walton

Inria Carmen, LIRYC, Institut de Mathematiques de Bordeaux Bordeaux, France

**Aims**: Optical mapping allows the visualization of cardiac action potentials from cardiac tissue surfaces by fluorescence using voltage-sensitive dyes. So far, the surface measurements are directly related to surface action potentials. But as the incident light penetrates the tissue, the measurement contains three-dimensional information. Our aim is to exploit this information in order to reconstruct three-dimensional action potentials.

**Methods:** In this preliminary work, we tried to localize fixed electrical sources in a three-dimensional slab of tissue. We minimized the difference between the measure and a model, in a least squares sense. Our model assumed the existence of an unique, idealized, spherical or ellipsoidal source. Following the work of Khait *et al.*, we assumed that the incident light interacts with the tissue in a diffusive regime. We solved this photon diffusion equation with a finite elements numerical method in order to simulate *in-silico* measurements. We used a fixed-step gradient method combined to the BFGS (Broyden-Fletcher-Goldfarb-Shanno) algorithm to solve the least squares problem.

**Results:** We first used *in-silico* data to verify our method, and then experimental data obtained in cardiac optical phantoms to explore its practical possibilities and robustness. The *in-silico* data were more accurately and completely (both localization and diameters) reconstructed than in the work of Khait *et al.*, and could also be retrieved from data after the breakthrough of electrical activity on tissue surfaces and from sources closed to boundaries. From the experimental data we could determine the $x$ and $y$ coordinates of the center, the depth and the diameters of the sources with errors of 1%, 20% and 5% respectively.

**Conclusion:** Our technique provides complete localization, allows to use complex geometries, and to combine illuminations. The technique is promising on experimental data. We plan to use more complex parameterizations in order to identify more complex and dynamical sources.

# Noninvasive Identification of Three-dimensional Myocardial Infarctions from Inversely Reconstructed Equivalent Current Density

Zhaoye Zhou*, Chengzong Han and Bin He

United States

**Introduction:** Noninvasive characterization of the myocardial infarction (MI) is important for the clinical management of cardiac disorders, including lethal arrhythmias. In the study, we propose and evaluate a new method to non-invasively identify the 3-dimensional MI substrate from the equivalent current densities (ECDs) that's inversely reconstructed from body surface potential maps (BSPMs).

**Method:** The computer simulations were performed in a cellular automaton heart model embedded in a realistic-geometry piece-wise homogeneous heart-torso volume conductor. A total of 114 sites of transmural infarctions, 91 sites of epicardial infarctions, and 36 sites of endocardial infarctions were simulated. The ECDs are inversely reconstructed from the forward-computed BSPMs during S-T segment. The MI substrate was characterized using a threshold determined from the ECD magnitude. A series of computer simulations were performed to assess the performance in terms of: 1) transmural MI; 2) surface MI; 3) additive noise; 4) numbers of electrodes; 5) volume conductor modeling errors.

**Results:** With 205 BSPM electrodes and 10 μV Gaussian white noise, the averaged accuracies for estimating transmural MI are sensitivity = 83.4%, specificity = 82.2%, and the distance between the centers of gravity (DCG) = 6.5mm. For epicardial infarction, the averaged accuracies are sensitivity = 81.6%, specificity = 75.8%, and DCG = 7.5mm. For endocardial infarctions, the overall accuracies are comparable to the epicardial infarctions, with sensitivity = 80.0%, specificity = 77.0%, and DCG = 10.4 mm. The accuracy of estimating source depth for surface infarctions is around 2/3. A reasonably good imaging performance was obtained under a higher noise level, fewer BSPM electrodes, and mild volume conductor modeling error, respectively.

**Conclusion:** The results suggest that this method is capable of imaging the transmural and surface infarction, and offers the potential to assist in clinical identification of MI substrates.

SA2

# Local Regularization of Endocardial and Epicardial Surfaces for better Localization of Ectopic Beats in the Inverse Problem of ECG

Danila Potyagaylo, Walther HW Schulze, Olaf Dössel

Institute of Biomedical Engineering, Karlsruhe Institute of Technology, Karlsruhe, Germany

**Introduction:** In non-invasive imaging of cardiac sources from body surface potential maps (BSPM) a Tikhonov solution is biased toward the nodes located closer to the electrodes, i.e. in left ventricle the epicardial sources are favored over the endocardial ones.

**Methods**: To counterbalance this we proposed a local regularization method, consisting in different weighting of epicardial and endocardial surfaces in the penalty term. The method was evaluated with many simulated extrasystoles. As particular cases of this technique we compared Tikhonov regularization with endocardial and epicardial imaging of transmembrane voltages (TMV) for two pairs: epicardial/endocardial and right/left ventricular septal foci. **Results**: Tikhonov regularization tries to restore the true gradient of the TMV but 'pushes' the strong (in amplitude) sources to the epicardium. Therefore Tikhonov method and epicardial imaging delivered reasonable solutions for the epicardial extrasystole, but projected the septal sources to the epicardium as well. For the endocardial/septal foci endocardial imaging correctly located their origin, for the epicardial extrasystole it produced a source projected to the endocardial surface with inverted sign. The local regularization was able to correctly find the origin of all considered ectopic foci.

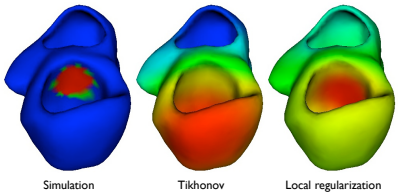


An endocardial ectopic beat simulation and reconstruction results

**Conclusion**: Based on three methods of reconstruction (Tikhonov, endocardial/epicardial imaging) one could identify the origin of an ectopic beat and thus eliminate the solution bias toward epicardial surface. In case the information about noise level is available a local regularization technique should be used.

SA2

# Validation of a Blood Pressure Simulator that Regenerates Oscillometric Cuff Pressure Waveforms

Dingchang Zheng*, Chengyu Liu, John Amoore, Stephan Mieke and Alan Murray

Newcastle University
Newcastle upon Tyne, United Kingdom

Blood pressure (BP) simulators that regenerate oscillometric waveforms provide an alternative for BP device validation. However, their ability to regenerate oscillometric waveforms recorded from unstable conditions has not been fully investigated. This study aimed to provide this information. BP measurements were performed on 30 healthy subjects under both resting and regular deep breathing conditions. Manual auscultatory systolic and diastolic blood pressures (SBP and DBP) were measured by a trained observer. During the measurement the oscillometric cuff pressure waveforms were recorded digitally at a cuff deflation rate of 2-3 mmHg/s. A specially designed BP simulator was then used to regenerate the oscillometric waveforms, which were presented to a clinically validated automatic oscillometric non-invasive BP (NIBP) device to obtain SBP and DBP from all the 60 waveforms. The effect of regular deep breathing on both manual and automated SBP and DBP was then quantified and compared. The SBP and DBP changes induced by deep breathing were finally compared with the measurement by the NIBP device and the manual auscultatory method. Deep breathing decreased both manual and automated SBPs significantly by 6.5 mmHg (mean±SD: 111.5±12.2 vs 118.1±13.0 mmHg) and 5.1 mmHg (112.9±11.6 vs 118.1±12.0 mmHg) respectively in comparison with those from the resting condition (both $P<0.001$). The corresponding decreases of manual and automated DBPs were 2.2 mmHg (75.7±8.5 vs 77.9±9.6 mmHg; $P<0.01$) and 4.4 mmHg (66.3±9.6 vs 70.8±9.5 mmHg; $P<0.001$). The auto BP decrease induced by deep breathing was not significantly different from that for manual BP ($P=0.5$ for SBP; $P=0.1$ for DBP), indicating that oscillometric waveforms recorded from non-resting condition were reliably regenerated by the BP simulator. Our results demonstrated that the BP simulator can regenerate unstable physiological oscillometric waveforms, confirming that it could be an alternative to clinical trials.

SA3

# Validation of a Smartphone-based Photoplethysmographic Beat Detection Algorithm for Normal and Ectopic Complexes

Lenn Drijkoningen, Frederic Lenaerts, Jo Van der Auwera, Christophe Smeets, Julie Vranken, Valerie Storms, Dieter Nuyens, Pieter Vandervoort and Lars Grieten*

Ziekenhuis Oost Limburg
Genk, Belgium

**Background** Smartphones and their applications are increasing in numbers and heart rate detection apps based on photoplethysmography (PPG) are plentiful. However, to date little or no applications exist to diagnose an irregular rhythm or differentiate between a normal heartbeat and a premature ectopic beat. In this work we developed and validated a smartphone based acquisition and processing algorithm based on PPG data collected in a controlled hospital environment.

**Methods:** A smartphone camera application was developed in order to acquire PPG data. Synchronization with a reference electrocardiogram allowed beat-to-beat comparison. In total ten subjects were recorded while undergoing an electrophysiological examination or ablation procedure. After signal analysis an algorithm was developed for irregular rhythms and ectopic beats. The data acquisition was validated by first introducing a sinus rhythm at different rates by applying a pacing train to the right atrium. To characterize arrhythmias in the PPG signal, supraventricular extrasystoles were induced every 20, 10, 5 or 3 beats. The coupling interval between a normal beat and the ventricular extrasystole was examined by altering the intermediary time by 400, 500 or 600 ms.

**Results:** After signal conditioning, an accurate beat detection was obtained from the PPG signal. Bland-Altman analysis indicated a nonsignificant difference in heart rate detection compared to the ECG reference system. Both supraventricular and ventricular complexes could be differentiated based on morphology or interval timings. If these premature complexes occurred on a frequent basis, they resulted in an irregular heart rhythm which could also be identified by the algorithm.

**Conclusion:** By acquiring a PPG signal, the smartphone is not only capable of determining a regular sinus rhythm but also has the power to detect irregular heart rates and identification of ectopic beats such as (supra)ventricular systoles with a high accuracy.

# Oscillometric Waveform Difference between Cuff Inflation and Deflation during Blood Pressure Measurement

Chengyu Liu*, Dingchang Zheng, Clive Griffiths and Alan Murray

Newcastle University
United Kingdom

The majority of automatic blood pressure (BP) measurement devices use the oscillometric method made during cuff inflation or deflation. However, there is currently little information available on the comparison of oscillometric waveform shape between cuff inflation and deflation. This study aimed to provide this information. Oscillometric cuff pressure waveforms were recorded digitally from 15 normotensive subjects during standard BP measurement at slow linear inflation and deflation rates of 2-3 mmHg/s. Three repeat sessions were performed for each subject. Four features were quantified for each oscillometric waveform: the maximum oscillometric pulse peak amplitude (Amax) and three cuff pressure widths corresponding to 70%, 50% and 30% of Amax (denoted as W70, W50 and W30 respectively). For all subjects, these oscillometric waveform features were then compared between cuff inflation and deflation. Analysis of variance showed that there was no significant difference between the three repeat measurements for all four waveform features (all $P>0.4$). Mean Amax from cuff inflation was 0.8 mmHg higher (mean±SD: 3.8±1.0 vs 3.0±0.8 mmHg, $P<0.001$) than that from cuff deflation. For the cuff pressure widths at the three thresholds, W70 was not significantly different between cuff inflation and deflation, but W50 and W30 were both significantly narrower for cuff inflation by 12 mmHg (67±10 vs 88±12 mmHg) and 21 mmHg narrower (67±10 vs 88±12 mmHg) respectively; both $P<0.001$. The oscillometric waveform differences during BP measurement suggest that arteries may behave differently during cuff inflation and deflation.

SA3

# Estimation of Respiratory Information from the Built-In Pressure Sensors of a Dialysis Machine

Frida Sandberg*, Mattias Holmer, Bo Olde and Kristian Solem

Lund University
Lund, Sweden

Sleep apnea is common in patients with chronic renal failure, but monitoring of respiratory information is not part of the clinical routine during hemodialysis. Introducing additional sensors to estimate respiratory information would cause patient discomfort and increased workload for the nursing staff. The purpose of the present study is to determine the feasibility of estimating respiratory information form the built-in pressure sensors of a dialysis machine. The main part of the pressure variations in the extracorporeal blood circuit are caused by the peristaltic pump, but variations caused by heart pressure pulses and respiratory induced pressure variations are also present. These biological pressure variations are of much smaller magnitude than the pressure variations caused by the peristaltic pump, making extraction of cardiac and respiratory information from the pressure signal challenging. The respiratory rate was estimated from the pressure signal using the respiration induced baseline variations and the peak-to-peak interval series of the cardiac component, respectively. The cardiac component was extracted using an alternating iterative technique, where successively better estimate of the pump-induced pressure variations are subtracted from the pressure signal. The short-time Fourier transform (60 s window, 1s overlap) was employed for time-frequency analysis. The study database consists of simultaneously recorded pressure signals and capnographic signals from 10 patients during hemodialysis treatment; the respiration rate estimated from the capnographic signal served as reference in the evaluation which was performed on 20-min excerpts of the signals. The root-mean-square error of the estimated respiration frequency from the baseline variations of the pressure signal was 0.042+-0.017 Hz (mean+-std); the corresponding error of the estimated respiration frequency from the peak-to-peak interval series of the cardiac component was 0.096+-0.025 Hz. These results suggest that it is possible to estimate respiratory information from the pressure sensors of a dialysis machine.

# Pro-arrhythmic Effects of Increased Late Sodium Current In Failing Human Heart

Jieyun Bai*, Kuanquan Wang, Xiangyun Bai, Yongfeng Yuan and Henggui Zhang

Harbin Institute of Technology
Harbin, China

**Introduction:** Patients with congestive heart failure (HF) are prone to develop complex ventricular tachyarrhythmias that may lead to sudden cardiac death. Experimental animal HF studies have shown that ventricular arrhythmias are mainly due to non-reentrant mechanisms, but most likely triggered activity arising from early af-terdepolarizations (EADs) that may result from an increased late so-dium current (INaL). However, how an increased INaL contributes to EADs genesis is unclear. The aim of this study was to investigate the effects of an augmented INaL on the rate-dependent electrical ac-tivity, excitation conduction and arrhythmia susceptibility in a com-puter model of human ventricular tissue.

**Methods:** The O'Hara et al. models of human endo-, mid- and epi- cardiac ventricular cell were modified to simulate HF ventricular action potentials based on experimental data. The cellular models were then incorporated into 1- and 2-dimensional reaction diffusion models. In simulations, the functional role of altered INaL on impairing the electrical activity of failing human ventricle were studied by char-acterizing its effects on the rate-dependence of [Na+]i, variability and dispersion of APD, and genesis of EADs. Using the 1-dimensional model, transmural ventricular APD dispersion and conduction veloci-ty restitution (CVr) of ventricular tissue were investigated. Using the 2-dimensional model, ventricular electrocardiograms (ECG) under normal and HF were simulated.

**Results:** Our simulation results showed that under the HF condi-tion, an enlarged INaL contributed to the reverse rate-dependent ef-fects, produced APD prolongation (268 ms vs. 383 ms) and genesis of EADs. In the tissue model, it was shown that it increased the transmural APD dispersion, and slowed down excitation wave con-duction. In 2D ECG simulations, an enlarged INaL produced an in-creased QT dispersion and the time interval between T wave's peak and end (54 ms vs. 94 ms).

**Conclusion:** An enlarged INaL plays an important role in increas-ing arrhythmia susceptibility in human HF.

SA4

# Late Sodium Current Inhibition Counteracts Pro-arrhythmic Mechanisms in Human Hypertrophic Cardiomyopathy

Elisa Passini*, Alfonso Bueno-Orovio, Ana Mincholé, Raffaele Coppini, Elisabetta Cerbai, Stefano Severi and Blanca Rodriguez

University of Bologna
Cesena, Italy

**Introduction and Aim:** Hypertrophic cardiomyopathy (HCM) is a genetic disorder characterised by increased arrhythmic risk. The causes are still unclear, but potential pro-arrhythmic mechanisms may include increased temporal and spatial variability in action potential duration (APD) and repolarisation abnormalities, such as early after-depolarisation (EADs) and alternans. We performed an in silico investigation of these pro-arrhythmic mechanisms in human HCM and of their modulation by late sodium current (INaL), significantly larger in HCM.

**Methods:** Two experimentally-calibrated populations of about 10000 healthy (CTRL) and HCM human action potential models were constructed, based on the O'Hara-Rudy human ventricular model and in vitro human recordings. Selective INaL inhibition was then simulated in both population, (based on 10 μM Ranolazine, 60% block).

**Results:** In agreement with experiments, APD was significantly longer in HCM than in CTRL, and exhibited higher variability (427±88 vs 278±49 ms, $p<0.001$). Moreover, the HCM population showed an increased Ca2+-transient duration and a smaller Ca2+-transient peak, both consistent with the HCM phenotype. APD and variability in HCM were reduced by INaL inhibition (367±67 ms), while only a minor effect was observed in CTRL. Spontaneous EADs were more common in HCM than in CTRL, and all of them were suppressed by INaL inhibition. At fast pacing rates (BCL=400 ms), about 15% of HCM models exhibited alternans (amplitude 16[6–44] ms, median[25th,75th]), and 65% of them were suppressed/reduced by INaL block. Within HCM population, alternans occurred in models with larger INaL conductance, suggesting the major role played by this currents and thus explaining both the higher incidence of alternans in HCM vs CTRL and their suppression by INaL inhibition.

**Conclusions:** Simulation results in populations of human action potential models show that HCM promotes EADs and alternans at rapid rates. Their occurrence is counteracted by INaL inhibition, suggesting this as a good therapeutic target in HCM.

# Theoretical Study of the Role of Funny Current (If) and the Background Inward Current (Ib) in Atrioventricular Nodal Conduction

Jue Li* and Mark R Boyett

United Kingdom

The atrioventricular node (AVN) is a part of the cardiac conduction system and is the only site where the action potential can pass from the atria to the ventricles. If is an inward current flowing during diastole. It is an important pacemaker current in the sinus node, but it is also present in the AVN. Surprisingly, there is functional evidence that If affects AVN conduction. This is of interest, because there is 'heart block' (slowing of AVN conduction) in heart failure and we have observed a downregulation of HCN4 (channel responsible for If) in the AVN in heart failure. The aim of the study is to explore the role of If in AVN conduction. The background current, Ib, is another inward current flowing during diastole and this was also investigated. We began with a model of the rabbit AVN action potential (N-type). A one-dimensional model made up of 100 elements, each 100 microM in length, was used. The diffusion coefficient, D, was set to 0.003 microSmm2. One end of the string (elements 1 to 3) was stimulated at 3 Hz. The conduction velocity was calculated from the times of arrival of the action potential at the 41th and 61th elements. In the normal configuration of the model, blocking If resulted in a 1% slowing of conduction, whereas blocking Ib had a greater effect (31% slowing). However, blocking If in the absence of Ib had a greater effect (11% slowing). There is uncertainty from experiments about the magnitude and properties of If and blocking If (in absence of Ib) resulted in a slowing of 15% when the conductance of If was increased 5 times and 16% when the If activation curve was shifted +20 mV. The results show that If can theoretically influence the conduction velocity of the AV node.

SA4

# Effect of Inter-Subject Variability in Determining Response to IKr Block in Human Ventricular Myocytes

Oliver J Britton*, Alfonso Bueno-Orovio, Laszlo Virag, Andras Varro and Blanca Rodriguez

University of Oxford
Oxford, United Kingdom

Causes of inter-subject variability in cellular electrophysiological behaviour are unknown. Understanding the effects of this variability is important, particularly as it can modulate response to drug application. Differences between individuals in response to drug action may be due to ionic-level differences, but the effects of these differences may be masked under normal physiological conditions. Therefore, investigating these differences is important to explain the effects of drug action on cells from different individuals. We performed investigations of the effects of variability and drug block using our population of models methodology. We used the O'Hara-Virag-Varro-Rudy human ventricular cell model as our baseline model, and varied by up to +/-100% nine conductances of the model's main ionic currents, to create an initial pool of 10,000 randomly generated models. We used recordings from human ventricular preparations in control conditions (n=85) to determine physiological ranges on 6 action potential (AP) biomarkers: AP Peak, APD40, APD50, APD90, AP triangulation and resting membrane potential. These ranges were used to calibrate a control population of 937 models that all displayed different but realistic biomarker behaviour under control conditions. We repeated the calibration process on this control population, using data from application of 50 nM dofetilide (n=13), which we simulated as 80% IKr block. This created a second population of 305 models, calibrated on control and dofetilide data. Analysing differences between the models in the two populations showed that the L-type calcium current was significantly lowered by 44% in the pop-ulation calibrated using control and dofetilide, compared to the control popu-lation. Models that were excluded from the dual calibrated population also displayed EADs during IKr block. These results indicate that in cells where L-type calcium current is elevated, there may be no indication under control conditions, but IKr block can reveal differences in susceptibility to repolari-sation abnormalities.

# Ischemia Alters Sensitivity of Action Potential to the Sodium-Potassium Pump

Sanjay Kharche[1,2], Edward Vigmond[3], Michael Coleman[1], Henggui Zhang[1]

[1]School of Physics and Astronomy, University of Manchester, Manchester, [2]CEMPS, University of Exeter, Exeter, Exeter. [3]Liryc Institute, University of Bordeaux

**Background:** Ischemia alters the sodium-potassium pump ($I_{NaK}$) and extracellular concentration of potassium, $[K^+]_o$. $I_{NaK}$ in cardiomyocytes maintains the ionic gradients across the cell membrane required to drive the action potential (AP). This study evaluated the sensitivity of $I_{NaK}$ parameters and of $[K^+]_o$ to AP in a human ventricle cell model using forward sensitivity analysis.

**Methods:** The O'Hara et al. (ORD) model for the undiseased human ventricle cell was adopted in this study. The cell model was paced at 1 Hz for 100 s and the results of the 100$^{th}$ AP excitation analysed. Simulations were carried out under healthy and ischemic conditions. Ischemia was defined as either a) altered extracellular potassium at values of 3 mM or 6 mM; b) a reduced MgATP; c) a combination of a and b. Forward sensitivity analysis (FSA) coefficients provide a temporal sensitivity of a state variable, e.g. AP, to a given parameter. FSA coefficients for $[K^+]_o$ and all $I_{NaK}$ parameters were computed using a difference quotient algorithm implemented in MATLAB. The coefficients were plotted as functions of time to examine their amplitudes (i.e. sensitivities) during an AP excitation.

**Results:** FSA coefficients for $[K^+]_o$ and $I_{NaK}$ parameters show a marked alteration of AP sensitivity to the modelling parameters (Figure).

**Conclusions:** Sensitivity analysis can be used to study the role of submechanisms governed by modelling parameters on systems behaviour. Ischemic conditions increased the AP sensitivity to the parameters.

SB1

Figure

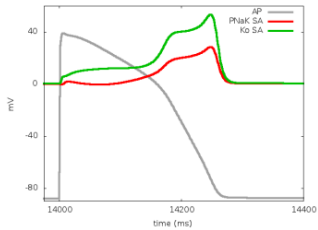


Figure. AP profile (gray), and sensitivities of AP to $I_{NaK}$ conductance (red) and $[K^+]_o$ (green).

# Dynamic Computational Simulations of Alternans in Acute Myocardial Ischemia

Antonio Felix de Castro, Adriano Giovanni and Jose M Ferrero*

Universitat Politecnica de Valencia
Spain

**Introduction:** Action potential (AP) changes occurring in acutely ischemic myocytes predispose the ventricular myocardium to develop ventricular fibrillation (VF) and sudden death. Because ischemia is a critical and unstable condition, experiments are very difficult to conduct at the cellular level in human. The aim of this work is to use computational models of the human cardiac AP to investigate the dynamic changes that occur dynamically in human ischemic myocardium. METHODS: An ischemia-adapted version of the ten-Tusscher model of the human AP was used to calculate the electrical activity of a ventricular myocyte under ischemic conditions. APs and ionic currents and concentrations were dynamically and continuously calculated during 20 minutes of simulated activity. During ischemia, pH and ATP, ADP and K+ concentrations where changed according to experimental values. An abrupt change of cardiac frequency (from 60 to 180 bpm) after 1 minute of ischemia was also introduced in the simulations. RESULTS: In the 3rd minute of ischemia, AP duration (APD) was reduced from 240 ms to 122 ms, as expected. Intriguingly, strong alternans (which are significantly more severe than typical non-ischemic alternans) begin to occur in the 3rd ischemic minute. APs with an APD of 120 ms and AP amplitude (APA) of +18 mV begin to alternate with depressed APs having an APD of 51 ms and an APA of -24 mV. The upstroke of the larger APs is divided into two phases, the first being maintained by Na+ current while the second is dependent on Ca2+ current. The shorter APs lack the Ca-dependent phase, suggesting that irregular Ca2+ cycling is responsible for the electrical alternans. Alternans are abolished from the 5th minute onwards. This severe alternation in APs could introduce a large degree of heterogeneity in the tissue which could become a substrate but also a trigger for VF.

SB1

# Effects of Acute Myocardial Ischemia in Mathematical Models of Heterogeneous Myocardium

Anastasia Vasilyeva[1,2], Nathalie Vikulova[1], Olga Solovyova[1,2], Dmitry Zamaraev[1], Vladimir S. Markhasin[1,2]

[1]Institute of Immunology and Physiology Ural Branch of Russian Academy of Sciences
[2]Ural Federal University, Yekaterinburg, Russia

**Motivation:** It has been shown that isolated sub-epicardial (EPI) and sub-endocardial (ENDO) myocytes have distinct electrical and mechanical properties in normal and pathological heart. ENDO regions are more vulnerable to metabolic changes during ischemia while decrease in the action potential (AP) duration and the conduction velocity are more prominent in EPI layers. The intracellular mechanisms of distinct ischemia-induced electrophysiological and mechanical responses of ENDO and EPI cardiomyocytes are still not clear.

**Methods:** We utilized our electromechanical EPI and ENDO models to simulate cardiomyocyte responses to the acute ischemia and to predict effects of cell electro-mechanical coupling within a heterogeneous 1D tissue model. Intracellular effects of acute ischemia were simulated via a combination of two hypoxic consequences – a time-dependent increase in $[K^+]_o$ and a reduction in $[ATP]_i$ which affected the activity of ATP-sensitive and other potassium channels.

**Results:** In cellular models, we showed that the higher sensitivity of ATP-sensitive potassium currents provided for a greater AP shortening and force decrease in EPI versus ENDO cells under hypoxia. In a 1D heterogeneous myocardial strand comprising segments of EPI, ENDO and intermediate cell type, the hypoxic consequences also resulted in a decrease in the force production, while the dispersion of repolarization between the coupled cells increased significantly above the difference in AP duration in uncoupled cells.

**Conclusion:** Our modeling results suggest significant increase in the transmural electrical and mechanical heterogeneity between isolated cells under hypoxia, which further increases due to cell interactions within the tissue creating substrate for arrhythmia.

This work was supported by RFBR (14-01-31134, 14-01-00885), UB RAS (12-M-14-2009, 12-П-4-1067), and by UrFU (Act 211 of RF Government #02.A03.21.0006).

SB1

# Metabolic but not Hypoxemic Stimuli are Related to the Apparent Recruitment of Capillaries in the Muscle

Vito Starc*

University of Ljubljana Faculty of Medicine
Ljubljana, Slovenia

Increased metabolic rate (MR) and arterial hypoxemia are independent stimuli to increase blood flow and delivery of oxygen (O2) into the active muscle tissue. Whereas both stimuli tend to reduce vascular resistance, they might differ in the location, either in the conduit arterioles or in the capillary network. As the later might be connected with the capillary recruitment, and hence the diffusion distance, we speculated that the blood gas analysis could provide the answer whether a given stimulus acts on the capillary resistance. We used data of Goodman et al. (1978) who studied effect of hindlimb MR on hindlimb hyperemia in anesthetized dogs, induced by graded levels of arterial hypoxia, changes in blood pressure, and/or by increasing MR by direct electrical stimulation of hindlimb muscles. A model of microvascular network was made in which the capillary resistance is proportional to the venous oxygen saturation (SVO2), the conduit arteriolar resistance exhibits flow-autoregulation properties, and both are inversely proportional to the accumulated O2 deficit. Diffusion of O2 into the tissue was treated using Krogh's model. The capillary oxygen saturation (SO2) falls linearly along the capillary, until reaching the critical SO2, just high enough for O2 to reach the Krogh's radius (rKrogh). Further on, the tissue close to rKrogh becomes increasingly anoxic, providing O2 deficit, and SO2 falls exponentially to reach SVO2. Finally, all unknown parameters were varied until providing the best fit simultaneously for all sets of data. Density of the recruited capillaries, inversely proportional to rKrogh, was calculated for each set of blood pressure, arterial SO2, MR, hindlimb blood flow, and O2 deficit. We found that it is nearly independent of the arterial SO2, but increases with the MR (Fig. 1, A – resting, B, C, and D – muscle electrical stimulation of 0.5, 1 and 1.5 pulses/s, respectively).

SB1

# Non-invasive Evaluation of the Effect of Metoprolol on the Atrioventricular node during Permanent Atrial Fibrillation

Valentina DA Corino*, Frida Sandberg, Luca T Mainardi, Sara R Ulimoen, Steve Enger, Arnljot Tveit, Pyotr G Platonov and Leif Sörnmo

Politecnico di Milano
Italy

During atrial fibrillation (AF), conventional electrophysiological techniques for evaluation of refractory period of the atrioventricular (AV) node cannot be used. The aim of this study was to evaluate changes in AV nodal properties during administration of metoprolol, using a novel ECG-based method for parameter estimation. The AV nodal parameters account for the probability of an impulse not taking the fast pathway, the absolute refractory periods of the slow and fast pathways (aRPs and aRPf), representing the functional refractory period, and related prolongation in the respective refractory periods. Twenty patients (age 71 ± 8 years, 14 men) with permanent AF from the RATe control in Atrial Fibrillation (RATAF) database were included in this study. For each patient, two 15-min ECG segments, recorded during baseline and metoprolol administration, were analyzed. Furthermore, simulated RR series were generated which mimic metoprolol administration through prolonged atrio–His conduction interval and AV node effective refractory period. In addition to the AV nodal parameters, atrial fibrillatory rate (AFR) and heart rate (HR) were also assessed. During metoprolol administration, AFR and HR decreased (AFR: 385 ± 52 fpm vs. 370 ± 68 fpm, ns; HR 106 ± 16 vs. 84 ± 12, $p<0.001$) and aRP was significantly prolonged in both pathways (aRPs: 350 ± 67 vs. 418 ± 99 ms, $p<0.01$; aRPf: 435 ± 88 vs. 542 ± 119 ms, $p<0.01$). Similar results were found for the simulated RR series: both aRPs and aRPf being prolonged with metoprolol (aRPs: 413 ± 33 vs. 437 ± 43 ms, $p=0.01$; aRPf: 465 ± 40 vs. 502 ± 69 ms, $p=0.02$). The AV nodal parameters reflect expected changes after metoprolol administration, i.e., a prolongation in functional refractory period. The simulations confirmed that aRPs and aRPf may serve as an estimate of the functional refractory period.

SB2

# Principal Component Analysis of Body Surface Potential Mapping in Atrial Fibrillation Patients Suggests Additional ECG Lead Locations

Stef Zeemering*, Theo Lankveld, Pietro Bonizzi, Harry Crijns, Ulrich Schotten

Maastricht University, Maastricht, The Netherlands

**Aims:** Atrial fibrillation (AF) is typically detected and analyzed in a non-invasive way using the standard 12-lead ECG. However, AF substrate complexity quantification may be suboptimal using conventional ECG locations. We analyzed high-density body surface potential maps (BSPM) of patients in persistent AF to locate regions where AF complexity was predominantly expressed and to search for potential additional lead locations.

**Methods:** BSPMs were recorded in 75 patients in persistent AF (120 anterior, 64 posterior electrodes). Principal component analysis (PCA) was applied to 1 minute of AF for each patient on 1) the original ECG, 2) a pseudo atrial activity (AA) signal of concatenated, detrended TQ segments and 3) extracted AA. Spatial AF complexity was expressed as the number of components needed to explain 95% of the variance in the signals ($k_{0.95}$). Average normalized PCA transfer matrix coefficient power maps were constructed to visualize the dominant regions for each component.

**Results:** Spatial AF complexity was higher when computed in AA or TQ segments than in ECG (median $k_{0.95}$ ±MAD, AA: 13±4.9, TQ: 7±2.6, ECG: 2±0.4, $p < 0.001$, Friedman test). The normalized variance described by the first three components was lower in AA (median %, AA: 82%, TQ: 87%, ECG: 99%, $p < 0.001$). Maps of averaged normalized component coefficient power showed expression of the first two ECG components concentrated in the region covered by V1-V6, while the first three TQ and AA components were more dispersed around the precordial leads. Only a minor contribution of the posterior leads was found.

**Conclusion:** The location of the leads that express the main components of atrial activity suggests that non-invasive assessment of AF complexity by the standard 12-lead ECG is suboptimal. Placing additional leads around the precordial leads may improve non-invasive characterization of the AF substrate.

SB2

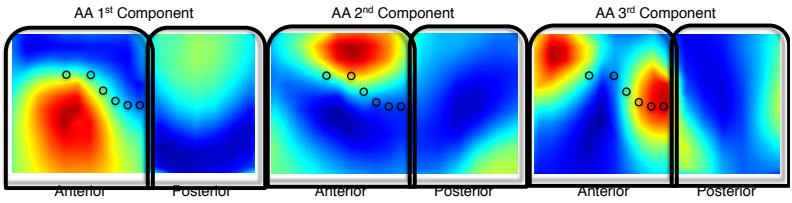

# Is it Possible to Detect Atrial Fibrillation by Simply Using RR Intervals?

Sándor Hargittai*

Hungary

**Aims:** Atrial fibrillation is the most common sustained arrhythmia in clinical practice worldwide. Several algorithms have been developed to detect atrial fibrillation which either rely on atrial activity analysis or are based on irregularity of RR intervals. This paper is addressed to study the latter type of algorithms. The main question is whether there is sufficient information in the sequence of RR intervals for reliable detection of atrial fibrillation and whether the atrial fibrillation can be differentiated from other ECG significant arrhythmias.

**Method:** The existing algorithms can be classified by several aspects. A part of the methods only uses the values of RR intervals, whilst others apply as well as its place in the sequence. Certain algorithms are based on differences between consecutive RR intervals, while others use only the values themselves. We have tested all these type of algorithms existing in the technical papers utilizing MIT-BIH ECG databases. We examined the following methods: Shannon and Sample entropy, Root Mean Square of Successive RR Differences, different run tests, turning point ratio, various scatter plots and statistical methods. Since the algorithm has to differentiate between atrial fibrillation and other irregular rhythms we have not used ectopic beat filtering before starting the algorithms. We tried to reveal the most characteristic features of different arrhythmias and compare them with the crucial steps of the algorithms. Result: Except the atrial fibrillation all other arrhythmias have some regularity, self-similarity and some degree of predictability. Therefore algorithms utilizing only the values of RR intervals without its order misclassify other irregular rhythms as atrial fibrillation. The best algorithm uses the scatter plot of successive RR differences. The overall precision was over 90 %.

**Conclusion:** It is possible to create a robust atrial fibrillation detection algorithm relying only on RR intervals utilizing its place in the sequence.

SB2

# Joint Entropy for Spatial Information Retrieval from Orthogonal Heart Planes Improves Catheter Ablation Outcome Prediction in Persistent Atrial Fibrillation

Meo Marianna*, Vicente Zarzoso, Olivier Meste, Decebal G Latcu and Nadir Saoudi

Brigham and Women's Hospital Harvard Medical School
Boston, United States

Predictability of catheter ablation (CA) outcome in persistent atrial fibrillation (AF) is still an open issue. Predictors in previous studies are mainly computed in only one ECG lead, and neglect relevant information from the other ones. In this study we investigate the role of interlead relationships on the 12-lead ECG in CA outcome prediction. Stepwise CA was performed in 36 AF patients. Standard ECG was acquired at the beginning of the procedure. Spatial relationships are assessed by joint entropy (JE) in each possible pair of leads on an ECG subset (I, II + V1-V6). JE quantifies the amount of information about AF patterns observed on two distinct leads. Clinical outcome prediction is assessed by area under curve (AUC). Our analysis reveals that the best prediction is obtained for pairs combining a frontal and a horizontal lead, as confirmed by the corresponding AUC values, e.g. leads I-V$_3$, AUC=$0.95$. Conversely, contributions from the same heart plane seem not to sufficiently characterize AF complexity content, thus yielding a less accurate prediction performance (e.g., leads V1-V5, AUC=0.63). Higher JE values denote a higher amount of interlead global information and render a more organized AF activity, which is more likely to be successfully treated by CA. Simultaneous analysis by JE of pairs of standard ECG leads from orthogonal heart planes enriches AF content characterization and enhances outcome prediction for CA.

# An approach to the enhacement of Sleep Apnea Detection by means of Detrended Fluctuation Analysis of RR intervals

Antonio Gabriel Ravelo García*, Ubay Casanova Blancas, Juan Luis Navarro Mesa, Sofía Martín González, Eduardo Hernández Pérez, Pedro Quintana Morales and Niels Wessel

University of Las Palmas de Gran Canaria
Spain

In this paper, Detrended Fluctuation analysis of Heart Rate Variability (HRV) is applied inorder to study the performance of a classification system of Obstructive Sleep Apnea (OSA), that integrates other variables as cepstrum coefficients and filter banks (FBANK) obtained from HRV. The database contains 70 records, divided into two equal-sized sets: a learning set and a test set. Each recording includes a continuous digitized single channel ECG signal and a set of apnea annotations, where a human expert classifies each minute indicating normal breathing or OSA, on the basis of a complete polysomnography (PSG). Detrended Fluctuation Analysis can analyze the scaling behavior and detect long range correlations. We will characterize the correlation behavior on short time scales between 10 and 40 beats, and longer time scales, between 70 and 198 beats. A FFT-based bank of equally spaced filters is applied to obtain the energy at each band. Cepstrum analysis is also applied due to its capacity to detect repeated patterns or periodicities. An automatic statistical classification method based on Logistic Regression (LR) is applied to the classification of sleep apnea epochs. LR presents an accuracy of 82.4% (sensitivity of 69.4% and specificity of 90.5%, auc=89.8) when FBANK and cepstrum coefficients are applied. The performance increases to 84.3% (sensitivity of 74.7% and specificity of 90.2%, auc=91.3) when DFA is added to the logistic regression model.

SB3

# Automated Detection of Obstructive Sleep Apnoea by Single-lead ECG through ELM Classification

Nadi Sadr*, Philip de Chazal

University of Western Sydney, MARCS Institute, Australia

**Aims:** This study aims to provide automated screening of obstructive sleep apnoea (OSA) by ECG signal processing. Sleep disorders are a prevalent health issue, which are currently costly and inconvenient to diagnose as they normally require an overnight hospital stay by the patient. Using ECG as an OSA diagnosis tool is an attractive alternative as it is low-cost and the diagnostic test can be performed at home.

**Methods:** Single-lead ECG recordings were used to detect apnoeic events through a minute-by-minute analysis. The MIT Physionet Apnea-ECG database was used. It contains 70 overnight ECG recordings from normal and obstructive sleep apnoea patients. Thirty-five recordings were used for training data and the other 35 for testing. Time and frequency domain features were obtained. Classification was achieved with an Extreme Learning Machine (ELM) as it provided a flexible non-linear classifier that was fast to train. The ELM is feed-forward network with one hidden layer. The input layer signals are connected to large number of non-linear hidden neurons, using randomly initialized connection weights. The output neurons are linear and the optimising values for the weights can be calculated in a single iteration.

**Results:** Classification accuracy was obtained with the hidden-layer neurons per input (fan-out) varying between 1 and 10. The highest accuracy was 87.7%, at a fan-out of 10, with specificity of 91.7% and sensitivity of 81.3%.

**Discussion and Conclusion:** Our results were comparable with other published systems using the Apnea-ECG database. OSA can be diagnosed from a single-lead ECG with a high degree of accuracy.

SB3

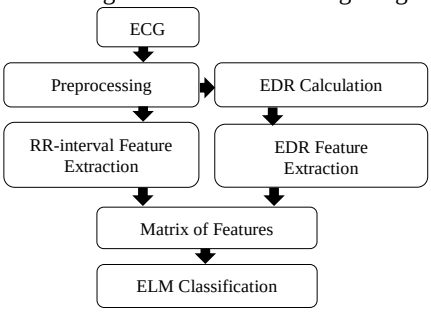


Figure 1. Schematic Representation of automatic OSA detection

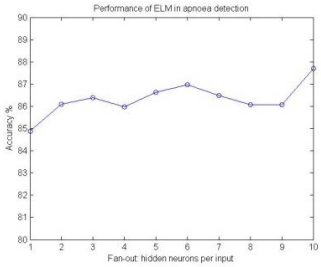


Figure 2. Performance results of ELM

# Development of Analytical Approach for an Automated Analysis of Continuous Long-Term Single Lead ECG for Diagnosis of Paroxysmal Atrioventricular Block

Muammar M. Kabir, Larisa G. Tereshchenko

Oregon Health and Science University,
Knight Cardiovascular Institute,
Portland, OR, USA

**Introduction**. Recent data shows a decline in primary ventricular tachyarrhythmias (VT) as a cause of the out-of-patient sudden cardiac arrest (SCA), while the rate of non-VT/VF causative arrhythmias of SCA remains unchanged. Paroxysmal atrioventricular block (PAVB) is one of such non-VT/VF causes of SCA. Therefore, prediction and early diagnosis of PAVB is crucial, which requires reliable detection of significant ECG features such as the P-wave, QRS-complex and T-wave. In this paper we introduce a new algorithm based on synchrosqueezing transform (SST) for detection of P-waves in long-term ECG recordings. SST is a powerful time-frequency analysis tool that provides precise frequency representation of a multicomponent signal through mode decomposition, and hence is hypothesized to be an efficient technique for characterization of ECG features.

**Methods**. One-lead surface ECG, digitized at 200 Hz, was recorded for up to 14 days using an ECG patch in study participants. Only one single ECG recording of 10 days duration was used in this study. The ECG recording was segmented into 24-hr periods for analysis. Baseline wandering and high frequency noise components were eliminated using median filter and SST respectively. Subsequently, the SST energy in the region 10-20 Hz was analyzed and characterized as P-wave if the energy was within a defined threshold.

SB3

**Results**. A fundamental issue in using SST is the choice of mother wavelet and the corresponding filter parameters; a poor selection can lead to a poor result. For the purpose of this study, four wavelet filters with different filter parameters was studied to identify the best specification for quantification of QRS and P-wave. Using morlet wavelet with a peak frequency of 5Hz and separation of 0.1Hz, our proposed algorithm was able to detect 99.5% of P-waves.

**Conclusion**. From this study, it appears that SST may provide a powerful robust technique for automated ECG analysis.

# Transient Behavior of Cardiorespiratory Interactions towards the Onset of Epileptic Seizures

Carolina Varon*, Katrien Jansen, Lieven Lagae, Luca Faes and Sabine Van Huffel

Belgium

**Aims:** Epileptic seizures are typically related to autonomic dysfunction. During seizures, the cardiac and respiratory mechanisms are deeply affected. This can also occur a few seconds before the seizure onset in the EEG. The interaction between respiration and heart rate is also expected to be affected. This study aims to determine whether the cardiorespiratory interactions change during seizures, and more importantly if they show a transient behavior towards the seizure onset.

**Methods:** Single-lead ECG signals were collected from 35 children suffering from epilepsy. In total, 87 seizures were recorded, of which 48 were of focal onset. The other 39 seizures were of generalized nature, with 10 absence seizures and 29 tonic or tonic/clonic. Measurements of respiratory effort are available for 18 seizures (8 focal, 10 absence), and two ECG-derived respiratory signals are computed from each ECG, namely one using principal component analysis (PCA) and another one using its non-linear version (kPCA). The cardiorespiratory interactions are estimated between the RR-interval time series computed from each ECG, and each respiratory signal. This is done by means of information dynamics estimation.

**Results:** Significant changes in the cardiorespiratory interactions are observed before and during the seizures. What is more important is that these changes show a transient behavior towards seizure onset. No significant differences are found between the respiratory signals. Storage measures like self entropy and conditional self entropy are significantly different around focal seizures. In addition, changes in transfer information between respiration and heart rate show a transient behavior for absence seizures. No differences were found for tonic and tonic-clonic seizures.

**Conclusions:** This study shows that the cardiorespiratory interactions allow for early detection of epileptic seizures, which can contribute to the improvement of closed-loop systems like vagus nerve stimulation, and to the development of alarm systems and more accurate drug delivery mechanisms.

SB3

# In Vivo $T_2$-mapping and Segmentation of Carotid Artery Plaque Components Using Magnetic Resonance Imaging at 1.5T

Bartosz Proniewski[1,2], Tomasz Miszalski-Jamka[1], Przemysław Jaźwiec[1]

[1]Department of Clinical Radiology and Imaging Diagnostics, 4th Military Hospital in Wrocław, Wrocław, Poland
[2]AGH University of Science and Technology, Krakow, Poland

**Aims:** Atherosclerosis is regarded as a lifestyle disease, where artery lumen is reduced due to deposition of calcium and fatty materials such as cholesterol and triglyceride. These plaques can become unstable and rupture, resulting in life threatening cardiovascular events. Multicontrast cardiovascular magnetic resonance (CMR) has been used on 1.5T and 3T scanners to identify carotid plaques and study their morphology in-vivo, however it does not provide quantitative information. The purpose of this study was to evaluate the use of in-vivo $T_2$-mapping at 1.5T for atherosclerosis plaque characterization.

**Methods:** The carotid arteries of healthy volunteers and patients with known atherosclerosis were imaged on a 1.5T Siemens Aera MRI scanner. Standard imaging protocol consisted of a TOF sequence to localize the carotid bifurcation, followed by the acquisition of $T_1$-, $T_2$- and PD-weighted images to assess the plaque qualitatively. Finally, $T_2$ relaxation time mapping was performed through the plaque center using a Multiple-Spin-Echo sequence. Variable echo times were chosen to sample the mono-exponential relaxation curve, assuming an expected $T_2 \sim 50$ ms for the normal carotid wall. Custom software was written in MATLAB to perform offline postprocessing: generation and segmentation of $T_2$ maps using a semi-automated method based on Bayes classifiers.

**Results:** Carotid artery plaques were segmented into 4 classes: calcification, lipid-rich necrotic core (LRNC), fibrous tissue and recent IPH. Plaque components identified with $T_2$ mapping were confirmed by multicontrast CMR. Mean ± SD of the $T_2$ values of voxels classified as LRNC (32±7 ms), fibrous tissue (51±10 ms) and recent IPH (102±31 ms) were calculated.

**Conclusion:** This study shows that $T_2$ mapping of atherosclerotic plaque is possible on a 1.5T scanner. Measurements demonstrate the ability to discriminate plaque components on $T_2$ maps, which are in good agreement with conventional multicontrast CMR.

PC1

# Fusion of Edge Enhancing Algorithms for Atherosclerotic Carotid Wall Contour Detection in CTA

Florentino Luciano Caetano dos Santos*, Atte Joutsen, Juha Salenius and Hannu Eskola

Tampere University of Technology
Tampere, Finland

The aim of this study is to assess the feasibility and performances of the fusion of edge enhancers in in-vivo computed tomography angiography (CTA) images for automatic segmentation of outer and inner vessel walls, in presence of atherosclerotic plaques. From 4 patient's CTA exams (stenosis degrees 70%–95%) 223 slices were hand segmented by a trained operator for the vessel walls. The analysed slices depict the common and internal carotid arteries and the carotid bifurcation. The automatic protocol exploits two different categories of image edge enhancers: 5 edge detectors (Sobel, Prewitt, Roberts, laplacian of gaussian (LOG) and Canny) and 5 filters/mapping functions (laplacian filter, gradient map (GM), Otsu thresholding (OT), local range map (LRM) and standard deviation (STD) map). Every algorithm was tested using a 3-pixel square window to produce an intermediate image (INT_IM) from each slice. The 10 INT_IMs were used to produce 10 binary masks as follows: (i) the OT INT_IM was directly used; (ii) LOG INT_IM was thresholded in 0 for closed contours; (iii) LRM INT_IM was binarized using the inclusion range [0–200]; (iv) the 7 remaining INT_IMs were thresholded using OT. Finally, for each slice, a unique binary mask was produced by fusing the 10 binary masks and the results of automatic and manual segmentations were compared. The mean correlation coefficient between the manual and the automatic masks was 48% [17%–63%]. By selecting the GM, LRM and STD algorithms only, the mean performance was improved up to 58%. This methodology was proven to be comparable to the manual one. The correct selection of the edge enhancers is critical for the performance optimization: GM, LRM and STD showed to be the most suitable for our purpose. This method will be used for further studies in plaque component characterization.

PC1

# Myocardium Segmentation Improvement with Anisotropic Anomalous Diffusion Filter Applied to Cardiac Magnetic Resonance Imaging

Antonio Carlos da S. Senra Filho, Gustavo C. Barizon, Luiz O. Murta Junior

University of São Paulo
Ribeirão Preto, Brazil

The magnetic resonance cardiology imaging (MRI) protocol has been a substantial improvements resulting from faster imaging acquisition and a higher spatial resolution. Thus, there is an emergent necessity for a suitable image processing for this type of image. The anomalous diffusion theory, through the use of the porous media equation, has been applied to digital image smoothing with the formulation of anisotropic anomalous diffusion (AAD) filtering. This new anomalous filtering method has been applied to medical image noise suavization. MRI miocardic imaging has a crucial role in cardiology studies, and it has been under increasing growth. However, some measurements usually are done with the manual approach, which implies in some practical problems such as the long measurement time and human error. Our study intends to apply the AAD filter on the cardiology MRI protocol to improve automatic miocardic area measurement.

Eleven MRI T1 weighted cardiology images were used here in which the AAD and Gaussian filter were used in the segmentation process in order to study the filtering application in an automatic segmentation algorithm (Geodesic Active Contour). The miocardic area (epicardic and endocardic tissue delimitation) and the root mean square error (compared with the manual measure) was used as quality index.

Area measurements

| Filter | Area (a.u.) | RMSE |
|---|---|---|
| Original | $1470.89 \pm 192.07$ | $17.26 \pm 4.70$ |
| AAD | $1264.22 \pm 164.44$ | $9.58 \pm 4.45$ |
| Gaussian | $1346.55 \pm 199.09$ | $13.19 \pm 4.76$ |

In comparison with the manual measurement ($a_{manual} = 1172.42 \pm 146.64$) the AAD filter show a significant segmentation accuracy enhancement ($p < 0.001$), which implies in a reduction for both the time necessary and the human error involved in this manual measurement.

Our preliminary experiment shown a promising results for the use of the AAD filter in the automatic myocardic area measurement, providing a better accuracy and robust and achievable miordiac segmentation.

PC1

# Automated Algorithm for Computing Left Ventricle Volume Changes from Cine-MR Images

Soo-Kng Teo[1], Wan Min[1], Chi-Wan Lim[1], Liang Zhong, Ru-San Tan, Yi Su[1],*

[1]Institute of High Performance Computing, A*STAR, Singapore

**Aims:** To determine the LV chamber volume from cine-MR images, it is necessary to locate the aortic/mitral valve plane with guidance from the long-axis images to isolate (or trim) the LV. However, manual identification of the trimming planes for all phases is tedious and does not guarantee that the LV myocardium volume is kept constant. This work aims to develop an automatic algorithm to compute the LV volumetric changes during the cardiac cycle while ensuring constant myocardium volume.

**Methods:** We reconstruct 4D (i.e., spatial + time) LV mesh models from border-delineated cine-MR images. The divergence theorem and Green's theorem are used to reduce the volume integral computation to a line integral equivalent so that the LV volume calculation can be performed efficiently from these meshes by utilizing only vertex and face topology information.

The trimming value at end-diastole (ED) is determined manually and the corresponding ED myocardium volume is computed and used as a reference. For the remaining frames, an iterative Newton-Raphson-like trimming procedure is used to find the trimming plane such that the resulting myocardium volume is the same as the reference. The end-systole (ES) frame is determined as the frame with the smallest LV chamber volume.

**Results:** ECG-gated cine-MR scans of 8 normal subjects were acquired and the LV chamber volumes over the whole cardiac cycle were computed based on our proposed algorithm. The results showed a mean ejection fraction (EF) of 62.4 ± 4.4%, which agreed with the normal range (EF > 50%) in clinical benchmark. We also observed LV shortening which is consistent with expectation, and the ES phase identified by our algorithm also matched those obtained from ECG gating.

**Conclusions:** We had developed an automatic and quantitative method of deriving LV chamber volumes and this can potentially reduce intra- and inter-observer variation in EF computation.

PC1

# A Local Phase-Based Algorithm for Registration of CMR Scans from Multiple Visits

Christopher Kelly*, Stefan Neubauer, Robin Choudhury, Erica Dall'Armellina, Vicente Grau

Institute of Biomedical Engineering, Department of Engineering Science, University of Oxford, Oxford, United Kingdom.

**Aims:** Longitudinal dynamic changes of myocardial tissue composition following ischemic injury determine left ventricular (LV) remodelling. Conventional manual 2D registration of clinical cardiovascular magnetic resonance (CMR) images acquired at different times aids the comparison of imaging findings, improving assessment of the effects on LV remodelling. However, we previously demonstrated that due to discrepancies in image plane selection on different hospital visits, significant displacements can exist between slices manually identified as corresponding. Additionally, intensity differences between MRI studies may preclude the use of conventional intensity-based registration methods. Here we propose a registration algorithm to overcome the challenges described above by a) performing a full 3D registration using a combination of short- and long-axis images, and b) using a similarity metric based on local phase to minimise dependence on intensity changes.

**Methods:** The proposed 3D registration method is based on the minimisation of local phase differences between two volumes, calculated using directional quadrature filters. A variational framework combining local and global regularisations is utilised for the minimisation. The method was validated on a) a simulated heart phantom, simulating intensity differences ranging from 0% to 40% between scans, and b) CMR data sets acquired from patients at 24 hrs and 6 months post primary percutaneous coronary intervention.

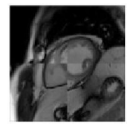
(a)
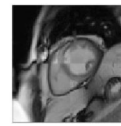
(b)

*Checkerboard pattern showing data alignment (a) before and (b) after registration using the proposed method*

**Results:** On the simulated heart phantom, our phase-based approach consistently outperformed an equivalent intensity-based implementation, obtaining a mean Dice coefficient of 0.96±0.02 for LV alignment. As expected, the improvement was larger as intensity differences increased. On real patient data, qualitative validation shows clear improvement in the alignment of the main cardiac structures. A quantitative analysis is currently under way.

**Conclusions:** The proposed phase-based 3D registration method outperformed the corresponding intensity-based approach in cases of intensity differences – a common occurrence in CMR images. Preliminary real data results were promising with visible improvement in contour alignment.

PC1

# Defining Angular and Radial Positions and Parameters for Myocaridial Pixels in Cardiac MR Images

Kjersti Engan, Leik Woie, Trygve Eftestøl

University of Stavanger, Stavanger, Norway

**Aims:** We aimed to automatically produce a measure for the angular and radial position of pixels within the myocardum in Late Gadolinium Enhanced Cardiac Magnetic Resconance (LGE-CMR) images, and use this in combination with scar segments from myocardial infarctions defining parameters of interest.

**Methods**: Primarily the myocardium must be segmented manually or automatically. The heart axis was defined from the centroid, *cm*, of the myocardial muscle through a manually marked point where the left and right ventricle coincides. For every pixel $x_{i,j}$ in the myocardium the radial axis is defined from *cm* through the pixel, and $\phi_{i,j}$ as the angle between the heart axis and the radial axis. $\lambda_{i,j} \in [0, 1]$, is given for the pixels inside the myocardium along the radial axis such that 0 always corresponds to the endocard and 1 to the epicardial border, independent of the changes in the thickness of the myocardial wall. Now all pixels in the myocardium can be regarded as a three dimensional vector $p_{i,j} = [x_{i,j}\ \lambda_{i,j}\ \phi_{i,j}]$. For all scar segments we define $\Delta\phi_k$ as the value in radians of the smallest angle (sector) containing all the pixels defined as scar segment $k$. $\lambda_{k_{min}}$, $\lambda_{k_{max}}$ and $\Delta\lambda_k$ for scar segment $k$ are other important parameters.

**Results and Conclusion:** The 3D vector $p_{i,j}$ gives an excellent foundation to define parameters of interests related to transmurality or position of scars etc. The position of scars and degree of scars in different heart sectors can easily (and automatically) be related to standardized model of CMR images. The defined parameters can also be used for exploring correlation with for example different arrhytmias.

Myocardial slice with marked heart axis and angular borders of two scar segments , corresponding angle ($\phi$) values and $\lambda$ values.

PC1

# Tissue characterization from myocardial perfusion and autonomic innervation using MRI and SPECT images in Chagas disease

Gustavo C. Barizon, Antonio Carlos da S. Senra Filho, Marcus Vinícius Simões, André Schmidt, Leonardo P. Gadioli, Luiz O. Murta Junior

University of São Paulo, Ribeirão Preto, Brazil

Chagas disease is a disease of major clinical relevance, with high incidence. Despite the knowledge of the clinical aspects of Chagas disease, relation between the myocardial tissue damage, myocardial perfusion and defects in the autonomic innervations is poorly understood. This project envisions the development and application of image analysis methods capable of providing an integrated visualization and analysis of tissue injuries through magnetic resonance imaging (MRI), and autonomic innervations and myocardial perfusion, available through photon emission tomography (SPECT). This paper describes and evaluate a method for tissue characterization and quantification. The proposed method is based on segmentation of MRI and registration between MRI images and SPECT images using MIBG and SPECT images using 99Tc (m)-MIBI. To perform the segmentation of the left ventricular myocardium, we used the technique of Geodesic Active Contour.

Segmentation of fibrosis in MRI images was performed based on the algorithm of maximum Tsallis entropy.

$$S_q = \frac{1 - \sum_{i=1}^{k} (pi)^q}{1 - q} \quad (1)$$

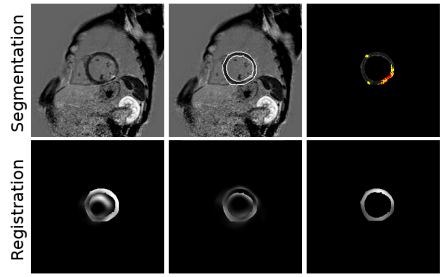

Segmentation of myocardium and fibrosis. NonRigid Registration of MRI and SPECT-MIBI(rest).

The nonrigid registration was performed based on B-Spline method. Initially, the registration was made between SPECT images using 99Tc (m)-MIBI and SPECT images using MIBG. Then was made the registration with MRI images. From the segmentation and registration between images, it is possible to observe regions of fibrosis and with absence or low synaptic activity comparatively to myocardial perfusion. Thus, the developed tool provides an integrated analysis of information contributing to a better understanding of the relationship between myocardial tissue damage and autonomic innervations injuries caused by Chagas disease, and propose new methods to evaluate the chagasic patient.

PC1

# Variance stabilizing transformations in the reduction of Poisson noise in 3D Nuclear Medicine images

FLÓREZ PACHECO Edward, FURUIE S Sergio

School of Engineering, São Paulo University, São Paulo – Brazil

Nuclear medicine is a modality of medical imaging that uses radioactive materials (radiopharmaceuticals) to provide information about the functioning of a person's specific organs, to generate accurate diagnosis and, to treat diseases. However, the Nuclear Medicine images are characterized by presenting poor signal to noise ratio, related to low counts and to Poisson noise because of the stochastic nature of the attenuation processes (absorption and scattering). These kinds of images depict regions with high counting photons (bright region) that are created by a group of cells that have a faster metabolism indicating physiological changes. This phenomenon could suggest the presence of a malignant neoplasia (tumor). Hence, before applying any technique for determining metabolic rates, first it is necessary to define the region of interest (ROI). For this purpose, segmentation techniques were used based on the Fuzzy Connectedness theory (using dynamic weights). It is possible to improve the efficiency of the segmentation stage by using appropriate filters for the treatment of Poisson noise. This study used anthropomorphic phantoms of the left ventricle of the heart inside the ribcage (Figure 1). A Nuclear Medicine exam was simulated using GATE platform with the volume coupled to the modeled PET scanner. Then, the projections obtained were reconstructed using the STIR platform. Several studies have shown the effectiveness of the Anscombe Transformation in the stabilization of the variance of nuclear medicine images. Nevertheless, in this paper other approaches (Table 1) were used and compared to that original method of transformation. Wiener filter was used in all cases. Table 1 shows that Freeman&Tukey/Wiener filter improve the efficiency of the segmentation stage compared to the other filters. This effect is represented graphically in Figure 2. In the near future, this procedure will be applied in real 3D images.

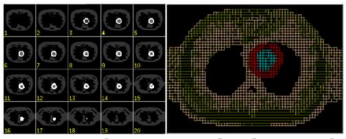

Figure 1. Phantom simulated using the NCAT-4D software.

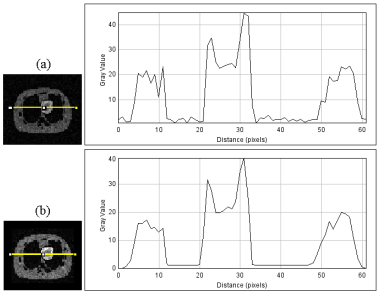


Figure 2. Profile (horizontal line) of (a) Image with Poisson noise and (b) Image after filtering.

Table 1. Results after the segmentation process using different filters.

| | Anscombe/ Wiener | | | Bartlett/ Wiener | | | Freeman&Tukey/ Wiener | | |
|---|---|---|---|---|---|---|---|---|---|
| **Image type** | TP (%) | FP (%) | $Max_{Dist}$ | TP (%) | FP (%) | $Max_{Dist}$ | TP (%) | FP (%) | $Max_{Dist}$ |
| **Images with Poisson noise** | 89.53 ± 4.71 | 6.34 ± 1.82 | 5 pixels | 89.53 ± 4.71 | 6.34 ± 1.82 | 5 pixels | 89.53 ± 4.71 | 6.34 ± 1.82 | 5 pixels |
| **Images after filtering** | 93.49 ± 1.31 | 2.25 ± 0.85 | 3 pixels | 92.07 ± 1.74 | 3.18 ± 0.94 | 3 pixels | 94.88 ± 1.12 | 1.34 ± 0.68 | 2 pixels |

PC1

# Optical ballistocardiography for gating and patient monitoring during MRI: an initial study

Johannes W Krug, Falk Lüsebrink, Oliver Speck, Georg Rose

Department of Medical Engineering,
Otto-von-Guericke University of Magdeburg, Magdeburg, Germany

INTRODUCTION: The ECG is required for patient monitoring or for acquiring motion insensitive data of the heart during magnetic resonance imaging (MRI) procedures. However, ECG analysis can be hampered by the effects of the static magnetic field and the switched gradient magnetic fields during imaging. Optical ballistocardiography (BCG) is a novel alternative approach for heart beat detection by measuring head movements caused by the ejection of blood. This work investigates the relation between these BCGs and ECGs.

METHODS: BCGs were acquired from four subjects inside a 3 T MR scanner using an MR-compatible camera system and a moiré phase tracking (MPT) marker. The MPT marker was placed on the subject's nasal bridge. Synchronised 12-lead ECGs were acquired using a Holter ECG. R-peaks in the ECG and corresponding J-peaks in the BCG were annotated manually (Fig. 1). Delay times $\Delta_{RJ}$ between R- and J-peaks were estimated. The mean heart rate and the Poincaré plot descriptors SD1 and SD2 were derived for patient monitoring purposes and HRV analysis.

RESULTS: Average delays $\Delta_{RJ}$ ranged from 237 ms to 275 ms in the different subjects. The same average heart rates were estimated from the BCG and the ECG signals. Differences of up to 17 ms occurred in the SD1 parameters.

CONCLUSIONS: Optical BCGs could constitute an alternative approach for retrospectively gated cardiac MRI sequences. Heart rate was correctly estimated using the BCG signal. Future studies will investigate the quality of BCG-gated CMR images and how cardiac arrhythmias affect the BCG signals.

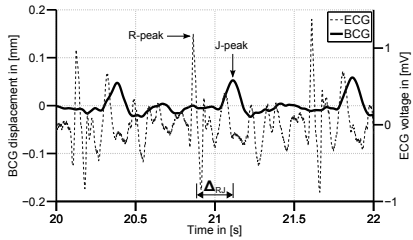


**Figure 1.** BCG and ECG signals acquired simultaneously at 3 T.

PC1

# Automatic Segmentation of Intravascular Ultrasound Images based on Temporal Texture Analysis

Chi Hau Chen* and Adithya G Gangidi

Univ. of Massachusetts Dartmouth
N. Dartmouth, United States

Abstract: Intravascular ultrasound (IVUS) continues to be an important technique for imaging of coronary arteries and the detection of atherosclerotic disease. Since its inception, much of the efforts towards IVUS image analysis have been done using spatial information of one single IVUS frame at a time. Accuracy of such approach is limited by the absence of clear boundary between lumen and arterial wall structure due to noise induced by catheter artifacts and speckle echo at high frequency. In our study we developed a novel automatic algorithm for the analysis and delineation of lumen and external elastic membrane (EEM) boundaries using both temporal and spatial variation of IVUS data. The pre-processing steps involve the construction of gradient image from neighboring images, and the use of discrete wavelet frame decompositions. The observation that Lumen is characterized by fine texture and that EEM is characterized by coarser texture is used to initialize the contours. A smooth Lumen and EEM contour is predicted by applying radial basis functions on contour initialization. This algorithm is evaluated on large datasets of multi-patient (15) IVUS images (~200 each) and pitted against the manually segmented contours by medical experts. It is observed that this algorithm reliably performs contour prediction with clinically appreciated limits of average prediction error equaling 0.1254 mm and 0.0762 mm for Lumen and EEM respectively. In an effort to provide direction to further improvements, a custom Lumen detection algorithm for stented images is proposed and tested with reported average prediction error of 0.048 mm.

PC1

# A New Method for Intraoperative Quantification of Mitral Leaflet Segment Prolapse

Sandy Engelhardt, Raffaele De Simone, Norbert Zimmermann, Matthias Karck, Hans-Peter Meinzer, Diana Nabers, Ivo Wolf

German Cancer Research Center (DKFZ)
Heidelberg, Germany

**Background**: During mitral valve reconstruction, intraoperative valve analysis is carried out by the cardiac surgeon for assessing location and extent of leaflet defects. The analysis of each leaflet segment is usually examined using two nerve hooks, as proposed by Carpentier. Traction perpendicular to the annulus plane is exerted on both nerve hooks to pull the free margin of the leaflet upwards. Qualitative comparison between the displacement is done in order to evaluate motion restriction or prolapse. However, this comparison depends on the subjective assessment and the experience of the surgeon.

**Methods:** We propose a new computer-based approach which allows for a quantitative measurement of the segment displacement in relation to the annulus plane. Infrared reflecting markers are attached to the instruments (nerve hooks and a pointing device) for optical tracking. The annular geometry is measured by pinpointing clockwise along the annulus. A plane is fitted onto the annulus points using orthogonal distance regression. Then, the segments are examined as proposed in the Carpentier method. Alternatively, our system allows quantifications using a single nerve hook. Distances between the segments are computed by projecting the points onto the normal of the annulus plane. Detailed visual feedback is provided during the measurements on a large screen.

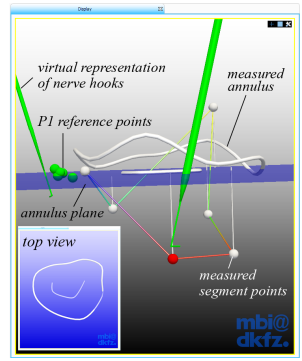

3D visualization of measurements.

**Results:** Evaluation was carried out by repeating measurements three times on a excised porcine heart. Mean chordae at the A2 segment were cut to induce a prolapse iatrogenically. The single-nerve-hook procedure has proven less time consuming and easy performable and showed a high reproducibility (mean standard deviation: 1.51 mm) in comparison to the two-nerve-hook approach (3.35mm).

**Conclusion:** Our method overcomes the limitations of actual subjective analysis, shows a unique ability to get quantitative and highly reproducible measurements of leaflet prolapse and provides valuable decision support.

PC1

# Ambulatory Impedance Pneumography Device for Quantitative Monitoring of Volumetric Parameters in Respiratory and Cardiac Applications

Marcel Młyńczak, Wiktor Niewiadomski, Marek Żyliński and Gerard Cybulski*

Department of Mechatronics, Warsaw University of Technology, Warsaw, Poland

**Aims:** The estimation of respiratory flow and volume parameters is hard to perform and not comfortable for patient during long-lasting monitoring outside the clinical environment. It is also difficult to perform during sleep due to the usage of facemask. Impedance pneumography (IP) device allows monitoring of breathing activity, estimating respiratory rate and providing the quantitative measurements of the static and dynamic respiratory parameters: tidal volume (TV) or peak expiratory flow (PEF). The miniaturized, Holter-type impedance pneumography device with analog output and intrinsic digital memory, was designed and constructed. The system allows the long-term evaluation of ventilation by measuring the changes in thoracic impedance, using tetrapolar method.

**Methods:** The Artificial Patient module was used to check stability of amplitude and frequency of application current (sinusoidal, 100kHz, 250μA) and to calibrate the measurements obtained by impedance pneumography device by finding the transfer function between voltage and impedance. Impedance values provided by IP device were compared with another bioimpedance measuring device in different electrode placement configurations (for cardiac and respiratory applications). Volume-related impedance signal was also compared with volume signal calculated from pneumotachometry (PNT). The measurements were conducted on the group of 12 young healthy volunteers (8 male).

**Results:** The comparison between impedance values from IP device and another bioimpedance measuring one showed high agreement in all tested electrode configurations. High value of determination coefficients (R2) describing fitting of linear regression model, individually achieved between IP and PNT signals varied within the range of 0.934 to 0.997 (average – 0.985).

**Conclusion:** Preliminary results show that our portable IP device provides impedance values related to respiratory activity according to the formula obtained individually for each subject. Impedance pneumography signal describing volumetric parameters could be used in analysis of respiratory and cardiac activities, e.g. might be helpful in autonomic nervous system testing or asthma monitoring.

PC1

# The Application of Different Metrics of Signal Shape for Automatic Identification of Artifacts in Impedance Cardiography Traces

Gerard Cybulski* and Piotr Piskulak

Department of Mechatronics, Warsaw University of Technology, Poland
Warsaw, Poland

**Aims:** Ambulatory Impedance Cardiography (AICG) monitoring allows estimation of cardiac haemodynamics during daily activity of the patients and transient events. However, some AICG recordings are noisy and their automatic analysis gives ambiguous results. It is important to find an easy and efficient method for automatic detection of abnormal evolutions in AICG signal. Form factors characterizing the shape of the trace were selected as a tool for identification of the artifacts due to simplicity of their implementation and low computational cost. The main objective of the study was to choose the most effective form factors.

**Methods:** It was created the pattern of AICG signal for single beat by averaging 50 consecutive evolutions synchronized by the Q wave in ECG. Several form factors were proposed and used to compare a single AICG evolution with a pattern and classify it as valid or artificial. The effectives of the form factors was determined using the area under the curve (AUC) in the receiver operating characteristic (ROC) analysis. The necessary data were obtained by analysis of absolute difference between value of the same form factor calculated for a single evolution and the pattern.

**Results:** We analyzed the cycles from 10-minute periods of AICG observation in 12 male subjects. The best efficiency was found for Malinowska's form factor, describing the ratio of surface area to circumference of AICG trace obtained during the period form Q-ECG to the end of the left ventricle ejection. For this ratio we obtained the following parameters: AUC= 0,8470, sensitivity= 75%., specifity = 81%, positive predictive value= 56%, negative predictive value = 91% and cost effective cut-off point =0,3863.

**Conclusion:** It seems that usage only one form factor as a classifier would not provide sufficient quality of artifact recognition.

PC1

# Antipsychotic Medication Influences Cardiovascular Coupling in Patients Suffering from Acute Schizophrenia

Steffen Schulz*, Karl-Juergen Baer and Andreas Voss

University of Applied Sciences Jena
Jena, Germany

Schizophrenia (SZO) is one of the most serious mental illnesses in the world with a lifetime prevalence rate of approximately 1% (US: 2.2 million, Germany: 800,000). Beyond univariate approaches bivariate coupling analyses reveal further information about the complex cardiovascular system in schizophrenia. Therefore the objective of this study was to quantify and characterize how different antipsychotics influence short-term nonlinear cardiovascular couplings in acute schizophrenia. In this study from 84 patients suffering from schizophrenia (42 unmedicated – UNMED and 42 medicated - MED) and 42 age and gender matched healthy controls (CON) heart rate variability and systolic blood pressure (30min) were recorded and analyzed. The coupling analysis was performed applying the recently published High Resolution Joint Symbolic Dynamics (HRJSD) where a coupling matrix of 8x8 pattern families was formed. Comparing CON vs. UNMED we found 6 significant different cardiovascular coupling patterns. Altered cardiovascular coupling in SZO was mainly dominated by a greater amount of slow increasing, slow decreasing, alternating and fluctuating systolic blood pressure in combination with invariable heart rate responses. Considering the groups UNMED and MED we could show a higher number of cardiovascular coupling patterns that were less predominant and more distributed in comparison to CON (decreased cardiovascular coupling in SZO). With HRJSD we could demonstrate altered cardiovascular coupling patterns in medicated patients that led to an increased impaired behavior of the cardiovascular regulation for the three different antipsychotic medications. In conclusion results from HRJSD might contribute to an optimal selection of therapy strategies in schizophrenia and thus to a more individual patient adapted therapy.

PC2

# Study of Induced Emotion by Color Stimuli: Power Spectrum Analysis of Heart Rate Variability

Sadaf Moharreri*, Nader Jafarnia Dabanloo and Saman Parvaneh

Islamic Azad University, Science and Research Branch
Iran (Islamic Republic of)

Every visual stimulus processed by the human perceptual system contains color information. Color has existed ever since life began, but its effect on humans has not been fully explored. In this paper, we analyzed Heart Rate Variability in frequency domain to study the effect of different colors and emotions (e.g. Calm, Energetic, Anxious, Happy, Sadness, Pleasure, Anger and Joy) on the autonomic nervous system (ANS). Sixteen female volunteers participated in this study. We used four main colors in psychology (e.g. blue, yellow, green and red) displayed on digital screen as a visual stimulus while the lead II of ECG was recorded. Data was also recorded while the participants closed their eyes (control state). For assessment of induced emotion by colors, validated Self-Assessment Manikin Test were used. Effects of colors on power spectrum of HRV were reported. The results showed that red and yellow in comparison to control state increased power in high frequency(HF) ($p<1E-4$). The value of low frequency power in response to yellow and green were less than control state. The peak of HF band increased during anxiety while it decreased in calmness ($p<2E-5$). In sadness, the power of VLF and HF band increased more than in other emotions ($p<1E-2$) while the power of LF has the highest value in pleasant and its lowest value in energetic ($p<3E-4$). The LF to HF ratio of the power increased in joy and calm in comparison to others ($p<E-3$). The results suggest that colors could be used to change the bahaviour of the ANS. Also, the change in emotion induced by colors could be captured by analysis of HRV in frequency domain . The finding of this research suggest that the colors could be utilized for HRV biofeedback training as well as method for changing emotion.

PC2

# In-vivo and Isolated Heart HRV Analysis by Hidden Markov Model

Oto Janoušek*, Marina Ronzhina, Peter Scheer, Jana Kolářová, Ivo Provazník and Marie Nováková

Brno University of Technology, Brno, Czech Republic
Brno, Czech Republic

**Introduction:** In in-vivo hearts, beat-to-beat variations of RR intervals display fluctuations over a number of different time scales. In case of isolated hearts, the RR intervals are prolonged; however, character of fluctuations remains almost the same. The only exception is occurrence of oscillation between consecutive RR intervals duration, resulting in saw-shaped curve of tachograms. In this study, consecutive RR intervals oscillation was investigated in in-vivo and isolated heart beat-to-beat series.

**Methods:** Five New Zealand rabbits and five isolated New Zealand rabbit hearts perfused at Langendorff setup were studied. The five minutes long tachograms were pre-processed by mapping of difference of tachograms's consecutive samples into three symbols: (↑) step-up, (↔) steady state, (↓) step-down. Series of symbols were used for training of two hidden Markov models (HMM) corresponding to in-vivo and isolated heart. Oscillation-related coefficients of HMM's transient matrixes were compared between in-vivo and isolated heart beat-to-beat series.

**Results:** All oscillation-related coefficients of HMM's transient matrix were significantly lower (Wilcoxon rank sum test, $\alpha = 0.05$) in isolated heart beat-to-beat series than in in-vivo ones. Probability of occurrence of RR-interval oscillation is 1.6-times higher in isolated hearts ($p = 0.85 \pm 0.19$) comparing with in-vivo ones ($p = 0.52 \pm 0.05$).

**Conclusion:** The significant tendency to compensate immediately changes in RR interval duration is characteristic for isolated heart model. Compensation process is very prompt, based on only one previous RR interval. Occurrence of oscillation in consecutive RR intervals may be used for intrinsic regulatory system behaviour assessment, however further studies are needed to understand the origin of oscillations.

PC2

# Detection of Electrocardiographic and Respiratory Signals Using a Wearable Transthoracic Bioimpedance Monitor for Improved Home-Based Disease Management in Congestive Heart Failure Patients

Silviu Dovancescu, Jarno Riistama

Philips Research
Eindhoven, The Netherlands

**Background:** The management of congestive heart failure (HF) patients at home requires robust, easy to use devices with the ability to assess patients' adherence to medication and to detect early signs of health deterioration. Such devices can facilitate early interventions and eventually prevent hospital admissions.

Pulmonary congestion is a typical sign of health deterioration in HF patients. A newly developed wearable transthoracic bioimpedance monitor (BIM) for daily self-measurements at home has been shown to detect accumulation of fluid in the lungs. Since HF is often also related to abnormal heart rhythms and respiratory patterns, the extraction of additional information related to cardiac activity and respiration from daily measurements might be advantageous for an improved home-based disease management.

**Aims:** In this study we evaluate the ability to detect the electrocardiographic and respiratory signals from spectroscopic bioimpedance measurements with the BIM.

**Methods:** Spectroscopic bioimpedance measurements are the underlying principle for the assessment of abnormal fluid buildup with the BIM. A safe alternating current is injected into the thorax by means of textile electrodes integrated into a vest. Sweeping the frequency of the current periodically enables the measurement of thoracic bioimpedance at multiple frequencies and a robust estimation of intracellular and extracellular fluid content. Using prior knowledge about the frequency sweep it is possible to also extract the electrocardiographic and respiratory signals from spectroscopic bioimpedance measurements.

20 healthy volunteers performed measurements with the BIM prior to and immediately after physical exercise. The ECG and respiration signals were recorded simultaneously with a portable reference device.

**Results:** The preliminary analysis on a subset of the data (1780 heartbeats and 288 breaths) supports the idea that the BIM enables an accurate assessment of both inter-beat (RMSE=2.27ms) and inter-breath (RMSE=0.43s) intervals. The paper presents the detailed quantitative analysis of all 20 datasets.

PC2

# Heart Rate Variability Analysis of Pre and Post-awakening of 10 Year Old Children

Taher Biala*, Syamil Muhammad, Fernando Schlindwein and Michael Wailoo

University of Leicester
leicester, United Kingdom

**Introduction:** Sudden cardiac death (SCD) has high occurrence around the wake up time. In this work the frequency domain heart rate variability (HRV) indices is computed before and after awaking and compared between normal and intrauterine growth restriction (IUGR) children. Males and females were compared to see if there are any significant differences.

**Methods:** The analysis consists of detecting the start of the day and night by specifying an RR threshold. When the threshold value is reached the algorithm marks the start of the day and night. The RR signal was subjected to cubic spline interpolation to produce a uniformly sampled time series and fast Fourier transform (FFT) was computed for every 5 min segment along the 1 hour before and 1 hour after awakening. Welch method was used to calculate low frequency LF , high frequency HF, and low over high frequency components of the signal LF/HF. Results One hour before and after awakening was selected to calculate the FFT of 5 min intervals. The frequency domain HRV measures, (LF=0.04-0.15 Hz, HF=0.15-0.4 Hz and LF/HF) for one hour duration were calculated for all the children and then normal, IUGR and gender results were compared. ANOVA test shows that there is significant difference in LF between normal and IUGR before and after wake up. LF is a marker of sympathetic activity of the Autonomic nervous system ANS.

**Conclusions:** Frequency domain measures for IUGR and normal (LF, HF and LF/HF) were found to be SD before and after wake up. This might suggest that IUGR have less developed ANS. It is well documented in research and clinical that Heart Rate Variability is low in subjects with diabetes and cardiac diseases. Females have higher LF/HF ratio than males. Higher values of LF/HF ratio were found to be associated with cardiac heart failure.

PC2

# Global Optimization Approaches for Parameter Tuning in Biomedical Signal Processing: A Focus of Multi-scale Entropy

Mohammad Ghassemi*, Li-Wei Lehman and Shamim Nemati

United States

**Introduction:** The existing literature suggest that Heart rate (HR) time series may exhibit pathological fluctuations that are predictive of physiological deterioration (e.g., onset of sepsis) in critical care patients. One of the most frequently used techniques for quantifying time series variability in the biomedical engineering community is Sample Entropy (SampEn). Multiscale Entropy (MSE) has been described as a more robust alternative to this method, due to its ability to quantify time series patterns at multiple time scales. MSE, however, has several hyper-parameters (including number of scales, template size, etc.) that must be selected by the investigator, prior to analysis. While recent work has suggested that tuning of these hyper-parameters can have drastic effects on the performance and accuracy of the MSE algorithm, there remains little consensus on how to meaningfully select these parameter values. To address this issue, we propose the use of recent advances in global optimization techniques for the identification of optimal MSE hyper-parameters.

**Methods:** This study utilized retrospective heart-rate time series from 118 (survived=73, expired=45) patients with sepsis and hypo-tension from the publicly available MIMIC-II database. The dataset was randomly partitioned into a training (70%) and testing (30%) set. We compared the efficacy of a logistic classifier with MSE-based features, whose model parameters were trained using the training set, for mortality prediction on the testing set. MSE hyper-parameters were selected by the Multi-start and Genetic Algorithm approaches to global optimization and compared against the default settings for MSE.

**Results:** Both SampEn and MSE with default settings made testing set predictions that were around the chance level (AUC=0.5). Application of global optimization with the Multi-Start method resulted in ~25% improvement in AUC (from 0.49 to 0.61). Our preliminary results suggest that several other widely used physiomarkers can benefit from hyper-parameter tuning via global optimization.

PC2

# Heart Rate Variability in Ultra-Trail Runners

Umberto Melia*, Montserrat Vallverdú, Emma Roca, Daniel Brotons, Alfredo Irurtia, Joan A Cadefau, Pere Caminal, Alexandre Perera

Centre for Biomedical Engineering Research, CIBER-BBN BarcelonaTech, Barcelona, Spain

**Aims:** To analyze the HRV in ultra-trail runners. It is known that in this kind of races the effort intensifies, and the work on the heart speeds up.

**Methods:** RR signals were obtained from heart rate monitor (POLAR Electro Oy, Oulu, Finland) during a 82 Km ultra-trail race in two groups of runners at different training regimes (ACTIVE/ELITE). Indexes from time and frequency domain, time-frequency representation (TFR) and auto-mutual-information function (AMIF) were calculated in RR windows of 5-minutes with step of 1 s. Indexes from the 1st, the 6th and the last hour of each runner were statistically compared using Wilcoxon's test for paired data.

**Results:** When comparing the 1st and the 6th hour of the ultra-trail race statistical significant differences were found in Instantaneous Frequency (*Instf*), first decay of AMIF (*AMIFdec*) and AMIF in LF (*AMIF_LF*) band (see Table). These indexes showed similar tendency when comparing the 1st (see Table) and the last hour (*Instf*: 0.093±0.036; *AMIFdec*: 0.306±0.112 and *AMIF_LF*: 0.199±0.086) with $p<0.002$. Standard deviation of RR (*SDRR*) obtained in ultra-trail runners was lower than the values of previous studies on healthy subjects. Furthermore, it was found that *SDRR* was lower in ELITE runners (1st hour: 12.4±6.5; 6th hour: 11.3±3.5) than in ACTIVE runners (1st hour: 23.9±10.9; 6th hour: 50.4±32.3). LF/HF showed increasing tendency in ACTIVE runners (1st hour: 3.50±0.36; 6th hour: 4.17±2.41), while showed decreasing tendency in ELITE runners (1st hour: 2.82±0.44; 6th: 2.27±0.92).

**Conclusions:** Indexes from TFR and AMIF present statistical significant differences when comparing the 1st and the 6th hour of the race. The *SDRR* values, within the pathological range, may be caused by the hard training of the ultra-trail runners. The extremely low values correspond to the ELITE runners that could confirm the previous hypothesis. When increasing the effort during the trial, from the 1st hour to the 6th, the *SDRR* increases tending to physiological values of healthy subjects.

HRV indexes during two time intervals of the race

| **indexes** | **1st hour** mean±SD | **6th hour** mean±SD | **p** |
|---|---|---|---|
| *SDRR (ms)* | 20.1 ±10.9 | 40.7 ±33.2 | 0.0547 |
| *Instf (Hz)* | 0.054 ±0.013 | 0.089 ±0.044 | 0.0234 |
| *AMIFdec* | 0.206 ±0.057 | 0.293 ±0.127 | 0.0391 |
| *AMIF_LF* | 0.283 ±0.041 | 0.184 ±0.079 | 0.0234 |

PC2

# Discrimination of Normal and At-Risk Populations from Fetal Heart Rate Variability

Philip A Warrick* and Emily F Hamilton

Perigen Inc.
Canada

Using clinically measured intrapartum cardiotocography (CTG) data, the objective of this study was to compare the discrimination of fetal heart rate variability in the low frequency (LF, 30-150mHz) and movement frequency (MF, 150-500mHz) bands for two at-risk groups: fetuses experiencing either neonatal depression or metabolic acidosis. We used CTG from singleton, term pregnancies having no known congenital malformations, with >=3 hours of tracing just prior to delivery. 3188 of the cases were normal while 10 experienced neonatal depression (Apgar 5 minute score <=4) and 12 had developed metabolic acidemia (umbilical cord base deficit <=12 mmol/L). We first estimated the fHRV using an autoregressive model of the CTG FHR signal to estimate the power spectral density (PSD), as described in \cite{Warrick2012b}. The PSD was integrated over LF and MF bands to obtain three instantaneous components of fHRV. Using overlapping 20 min epochs, the quiescent component of each band was computed from the 5$^{th}$ percentile of their probability distribution functions. We then compared these estimates for normal cases and the two indexed groups. Figure 1a shows that in both bands, the neonatal depression group had consistently lower fHRV over time compared to the normal group, with all epochs showing statistically significant differences in the LF band and 6 epochs doing so in the MF band. However, in Figure 1b the metabolic acidosis group had higher fHRV than normal, especially in the last 90min of labour with 2 LF epochs showing significant differences. These results are consistent with conventional clinical measures of variability. Our fHRV estimates have identified two at-risk fetal populations with very different characteristics: elevated (metabolic acidosis) or reduced (neonatal depression) fHRV. These sub-populations may have very different etiologies reflecting different neural mechanisms. These parameters are therefore useful discriminants of fetal state with promising potential for automated clinical decision-making.

PC2

# Investigation of Baroreflex Autonomic Control by Spectral Coherence of fMRI Independent Components and Neck Suction Stimulation Signal

Matteo Mancini*, Eugenio Mattei, Federica Censi, Barbara Basile, Marco Bozzali and Giovanni Calcagnini

Università degli Studi di Roma Tre
Italy

Functional Magnetic Resonance Imaging (fMRI) has proved to be a powerful technique for the analysis of the central autonomic control on the cardiovascular system. The carotid stimulation represents a viable non-invasive tool to investigate the brain areas involved in the central autonomic control. In this paper a resting-state fMRI protocol has been designed: carotid stimulation has been performed by neck suction with a custom MRI-compliant device, using rectangular pulses of 8 s, spaced by 4 s (repetition frequency=0.08 Hz). Two suction pressures were used: 60 mmHg (active stimulation) and 10 mmHg (dummy stimulation). Each recording session lasted 480 s (40 stimulation pulses). Whole brain fMRI signals were collected using a 3T Siemens Allegra scanner, with an echo-planar T2* sequence, with BOLD contrast, and a repetition time of 2.08 s. Twelve healthy volunteers were examined. fMRI data were preprocessed to realign and filter the images. To detect the brain region involved in processing the carotid baroreceptor efferent signals, a combined approach of independent component analysis (ICA) and spectral coherence (SC) has been used in each subject, as follows: 1) Twenty ICs data have been estimated from fMRI data using the GIFT toolbox; 2) the SC between each IC and the neck stimulation signal has been computed; 3) ICs having a SC > 0.5 at 0.08 Hz were considered as stimulus-related. In each subject at least 1 stimulus-related IC was identified in the active stimulation trials (coherence range between 0.55 and 0.91). Such components disappeared during the dummy stimulation session. In most subjects the stimulus-related IC identified the same brain regions. Frequency analysis of the neck suction stimulation signal in conjunction with ICA of fMRI identify the brain structures involved in the processing and integration of afferent signals from the carotid baroreceptors in healthy human subjects.

PC2

## Influence of Psychological Stress on QT Interval

Chandan Karmakar, Mohammad Hasan Imam*, Ahsan Khandoker and Marimuthu Palaniswami

University of Melbourne
Melbourne, Australia

This paper investigates the influence of psychological stress due to driving in city traffic condition on beat-to-beat QT interval. Electrocardiogram (ECG) signal of 16 subjects were analyzed from Physionet "drivedb" database. Total 32 segments of ECG signal was selected from all subjects. 16 of which were recorded during "Stressed" condition and rest 16 were in "Unstressed" states. Each segment was 5 minutes long and QT intervals were extracted using Berger's template matching algorithm. Heart rate corrected QT (QTc) intervals was calculated using methods proposed by Bazett, Fridericia and Framingham. The mean and standard deviation of each QTc interval time series was calculated as a feature describing average length and variability of QTc interval. The results showed that the mean QTc was lower in "Stressed" condition than "Unstressed", however none of the differences were statistically significant. In contrast, the variability of QTc intervals were higher in "Stressed" segments than the "Unstressed"ones and the difference was statistically significant. However, such difference was not present in RR intervals. In summary, QT was not prolonged due to stress but beat-to-beat QT variability increased in "Stressed" condition and this can be an effective marker to detect psychological stress.

PC2

# Cardiac Autonomic Reinervation Following Aorto-Coronary Bypass Evaluated by High Resolution Heart Rate Variability

D. Simov, M. Milanova, M. Matveev, V Krasteva, I. Christov*

Institute of Biophysics and Biomedical Engineering, Bulgarian Academy of Sciences, Sofia, Bulgaria

**Introduction:** Postoperative follow up of patients after operative coronary revascularization should be based on independent markers. The aim of the study is to assess cardiac autonomic reinervation after coronary artery bypass grafting (CABG) in patients with multivessel coronary artery disease (MCAD) by analysis of high resolution heart rate variability (HRV).

**Materials:** For 21 CABG patients (2-4 coronary arteries shunting) ECG at rest with sampling rate of 1000 Hz was recorded before the intervention and following on days 2 to 7. All patients are in sinus rhythm pre- and postoperatively.

**Method:** Using our software package for computing time and spectral frequency indices of HRV we evaluated standard deviation of all fluctuations (SDNN) and proportion of cumulative spectral power of frequency range of the three factors regulating sino-atrial activity: metabolic-humoral (VLF%), mostly sympathetic (LF%) and mostly parasympathetic (HF%) waves. For frequency analysis we use FFT and Hanning spectral window. A result of HRV analysis for one patient from the study group is shown on the figure.

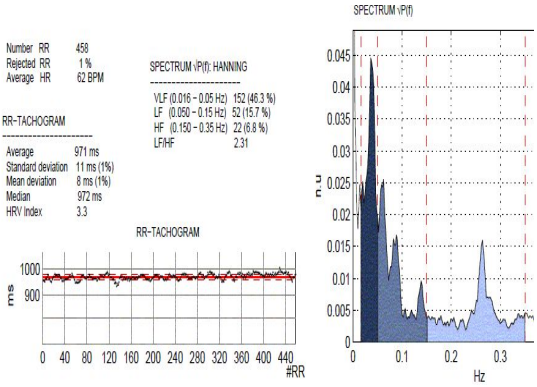


**Results:** Mean values of HRV indices before and after CABG are presented in the table. Postoperatively there is significant reduction of total variability (SDNN: from 39 to 24 ms; $p<0.05$) with still predominant humoral regulation (VLF% = 24.7) of rhythm. There is an increasing trend of protective vagal stimulation of cardiac pacemakers (HF%: from 7.7 to 8.6).

| HRV indices | Before CABG | 2-7 days after CABG |
|---|---|---|
| RRA (ms) | 903±93 | 651±111 $p<0.001$ |
| SDNN (ms) | 39±18 | 24±23 $p<0.05$ |
| VLF (%) | 34.9±8.5 | 24.7±7.4 $p<0.005$ |
| LF (%) | 13.8±5.1 | 10.9±4.9 $p<0.001$ |
| HF (%) | 7.7±3.1 | 8.6±5.7 *$p=0.263$; n.s.* |

PC2

# Linking a Novel Mutation to its Short QT Phenotype through Multiscale Computational Modelling

Chiara Bartolucci, Cristina Moreno, Alicia de la Cruz, Pier Lambiase, Stefano Severi* and Carmen Valenzuela

If you wish to designate a backup presenter (who must be one of the authors listed above) in the event that you are unable to present the work yourself, do so below. In this event, no award or reduction of registration fee will be given for this paper.

Cesena, Italy

**Aims:** The aim of this work was to assess the link between a newly identified KCNQ1 mutation and the short QT syndrome clinically observed in the patients. We applied two human Action Potential models, the ten Tusscher -Panfilov (TTP) and the O'Hara Rudy (ORd).

**Methods:** The index case of the family was a 37 years old man who died unexpectedly. A blood sample of his son was sent for genetic study of most prevalent genes related to channelopathies. To evaluate the electrophysiological results at the level of the cardiac action potential (AP) and of the pseudo ECG, we performed single cells and multicellular simulations with the TTP and ORd human ventricular cardiomyocytes model. We repeated all the simulations, with both models, by introducing the effects of β-adrenergic stimulation.

**Results:** Analysis of the KCNQ1 gene revealed a novel heterozygous mutation (F279I). To examine its effects in this physiologically relevant channel complex, either wild type Kv7.1 or the mutant subunit were co-transfected with KCNE1. Computer model simulations of the experimental data predicts a shortening of the AP consistent with the patient phenotype: using the TTP model the shortening was more pronounced (e.g. from 397 to 297 ms in M cells) while with ORd was less pronounced (e.g. from 332 to 318 ms in M cells). In addition, we performed also the pseudo ECG: the results confirmed the reduction of the QT interval caused by mutation.

**Conclusions:** The use of mathematical models to simulate mutant conditions proved useful in order to demonstrate its effects on the AP. The significant differences between the results with the two models is due to the different formulation of IKs. The weight of this current in human APD is actually still a matter of debate and deserves a detailed analysis.

PC3

# Ionic Mechanisms of Triggered Activity in Atrial Cell Models

Marta Varela, Nooshin Ghavami, Stuart James, Ross Morgan* and Oleg Aslanidi

King's College London, London,UK
London, United Kingdom

**Aims:** Spontaneous electrical activity of atrial myocytes is linked with the initiation of the commonest cardiac arrhythmia, atrial fibrillation (AF). However, the mechanisms of such triggered activity are not well understood. This study aims to explore changes in ionic channel currents that can lead to triggered activity, and link such changes with pathophysiological conditions associated with AF.

**Methods:** The Ramirez et al. (2000) model was used to simulate electrical activity of a canine atrial myocyte. Several pathological conditions associated with AF were considered: (i) enhanced Na+-Ca2+ exchange current, INaCa, resultant from sarcoplasmic Ca2+ leakage; (ii) increased late Na+ current, INaL, linked with heart failure; (iii) increased L-type Ca2+ current, ICaL, linked with β-adrenergic stimulation by isoproterenol (ISO); (iv) increased electrotonic load on atrial myocytes by fibroblasts, linked with fibrosis. Conditions (i)-(iii) were implemented by fitting the currents (INaCa, INaL, ICaL) to the respective experimental data; condition (iv) was implemented using the existing MacCannell et al. (2007) model for myocyte-fibroblast electrotonic coupling.

**Results:** Simulations of the models revealed a combination of conditions resulting in the generation of triggered activity: a 5-fold increase of INaL plus a 2.6-fold increase of ICaL by ISO (see Methods). This is in agreement with previous experimental observations that AF in dogs can be initiated by the application of ISO and stopped by blocking INaL. Enhanced Ca2+ leakage and INaCa did not result in triggered activity on their own. However, in a myocyte with the increased INaCa, the initiation of triggered activity required smaller increases of INaL and ICaL. Conversely, in a myocyte coupled with fibroblasts, triggered activity was initiated only with relatively larger increases of INaL and ICaL.

**Conclusion:** Triggered activity in atrial myocytes can be initiated by a combination of pathologically increased INaL and β-adrenergic stimulation, while other pathologies may play a secondary role.

PC3

# Solution of the Bidomain Equations with a Composite Backward Differentiation Formula

Wenjun Ying* and Craig Henriquez

Shanghai Jiao Tong University
Minhang, China

For numerically solving the bidomain equations, a semi-implicit or an operator splitting method is usually preferred than a fully implicit time integration method even though it is known that both semi-implicit and operator splitting methods are not L-stable methods for stiff problems, including the bidomain equations. As many (if not most) researchers in the community have an impression that a fully implicit method is too complicated for someone to implement and too expensive for the computer to run. In this talk, we will present a fully implicit time integration method for the bidomain equations in multiple space dimensions. We will show by numerical simulation results that the bidomain equations may be solved very efficiently with the implicit method. The method is a composite backward differentiation formula (CBDF), L-stable for stiff problem. It was first proposed for implicitly modeling cardiac dynamics along a cable in [Wenjun Ying, Donald Rose and Craig Henriquez, Efficient fully implicit time integration method for modeling cardiac dynamics, IEEE Trans. Biomed. Engrg, Vol 55 (12), pp. 2701-11, 2009]. The nonlinear equations resulting from the fully implicit discretization of the bidomain equations are solved with the Newton method. In multiple space dimensions, the linearized discrete equations are no longer tridiagonal and can not be solved with the Thomas algorithm. In our work, by a special arrangment of the equations, the discrete system has a very nice formulation. It is symmetric and non-negative definite and can be solved with a multilevel and multigrid iterative method. Some other techniques that we use to accelerate the Newton and multilevel/multigrid iterations will be reported in the talk.

PC3

# The Effect of Low Potassium in Brugrada Syndrome. A Simulation Study

Karen Cardona, Juan Francisco Gómez, Javier Saiz*, Wayne R Giles and Beatriz Trenor

Instituto Interuniversitario de Investigación en Bioingeniería y Tecnología
Valencia, Spain

Brugada Syndrome (BrS) is associated with an increased risk of sudden death due to ventricular arrhythmias. It is caused by ion channel abnormalities and is characterized by coved ST elevation, J wave appearance and negative T waves in the right precordial electrocardiographic lead. The changes in the electrocardiogram (ECG) in the setting of BrS can be due to (i) reduced inward currents (eg. INa and ICa,L), (ii) increased outward currents (Ito) and (iii) fibrosis. Some clinical reports relate hypokalemia to arrhythmic events (in the presence of other pathologies). Hypokalemia contributes to ST-segment elevation and changes in the T-wave morphology. It seems plausible that in patients with BrS, low extracellular potassium concentration ([K+]o) might increase repolarization gradients, especially in right ventricle (RV), setting the stage for ventricular arrhythmia. The main goal of this study is evaluate the effect of low [K+]o in BrS using a mathematical modeling approach. The O'Hara et al. ventricular action potential model (ORd) was modified to improve this behavior of right ventricle (RV) in hypokalemia. The electrical activity of a transmural RV strand of 165 cells was simulated. To simulate BrS, ICa,L was reduced by 50% and Ito was 6-fold increased. Our results show that transmural dispersion of repolarization (TDR) was increased in hypokalemic conditions. In control, TDR was 26 ms, for BrS TDR increased to 47 ms, and if hypokalemia ([K+]o=3.5mM) was also considered, TDR was 52 ms. Furthermore, Tpeak-Tend interval was calculated from the pseudo-ECG and was incresed by 14 and 51%, respectively, with respect to control. Aditionally, a prominent J wave was observed in BrS and this increased if hypokalemia was also introduced. In summary, our simulations show that hypokalemia increases repolarization gradients, increasing the risk of VT/VF in an in silico setting that mimics key aspects of BrS.

PC3

# Simple Ablation Guided by Approximate Entropy Mapping in a 2D Atrial Fibrillation Model

Catalina Tobón[1,2], Laura C Palacio[1], Juan E Duque[1], Esteban A Cardona[1], Juan P Ugarte[2], Andrés Orozco-Duque[2], John Bustamante[2], Javier Saiz[3]

[1]GI[2]B, Instituto Tecnológico Metropolitano, Medellín, Colombia
[2]Centro de Bioingeniería, Universidad Pontificia Bolivariana, Medellín, Colombia
[3]I3BH, Universitat Politècnica de València, Valencia, Spain

**Introduction:** Atrial fibrillation (AF) is the most common cardiac arrhythmia. AF is often sustained by rotors. Some studies suggest that fractionated electrograms (CFAE) are generated by the rotor tips and can be targets for ablation. Approximate entropy (ApEn) is a non-linear statistics method that can be used to quantify the complexity of a signal. We hypothesized that the simple ablation patterns guided by high ApEn regions could help to terminate rotors.

**Methods:** Electrical remodeling was introduced in the Courtemanche atrial cellular model in a 2D model of human atrial tissue. A rotor was generated by S1–S2 cross-field protocol. Pseudo-unipolar electrograms were simulated and ApEn was calculated for 5 s. Three different lineal ablation patterns were proposed and evaluated: 1) A line through the rotor tip and that ends before touching the tissue boundary (Panel 1B), 2) a line that does not pass through the rotor tip and that ends at the tissue boundary (Panel 1C), and 3) a line through the rotor tip and that ends at the tissue boundary (Panel 1D).

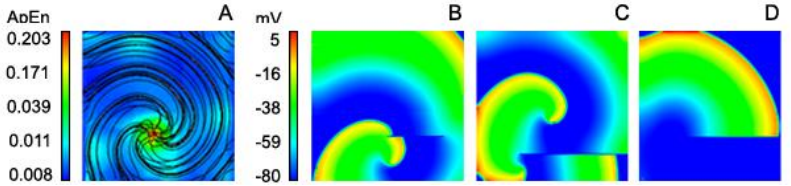


A) ApEn map and overlapped contour maps. Lineal ablation patterns not ending the rotor (B and C) and ending the rotor (D).

PC3

**Results:** The ApEn map showed an area with high ApEn values (0.164±0.014), which matched with the rotor tip as was confirmed by overlapped contour maps (red zone in Panel 1A). Only one of the three ablation patterns (pattern number 3) was effective in ending the AF activity, the rotor stopped at 200 ms.

**Conclusion:** ApEn may be effective in identifying rotor tips for ablation in permanent AF. The results suggest the importance to localize the rotor tip and identifying anatomical boundaries for effective ablation.

# The Modified Bidomain Model with Periodic Diffusive Inclusions

Yves Coudière, Andjela Davidović, Clair Poignard
Université de Bordeaux, INRIA CARMEN, LIRYC, IMB

**Introduction**: Bidomain equations are the standard way to model the electric potential in cardiac tissue. Even though they provide quite accurate results, they are based on the fact that active cardiomyocytes are present everywhere in the heart, while it is known that non-small regions exist where fibroblasts and other non-excitable cells or additional extracellular media take place. These regions, which play an important role in diseased hearts, are often taken into account through ad-hoc rough tuning of the tissue conductivities. In this work, we introduce a rigorous way to derive these conductivities from a microscopic description of the heterogeneities in the tissue.

**Method**: We assume a periodic alternation of the healthy tissue (bidomain model) and the fibrotic tissue (diffusive part). Such a microscopic model can be simulated directly, at the price of a very fine discretization and a high computational cost. Instead we derive a homogenized model at the macroscopic scale, following a standard multiscale technique. In order to study the model and illustrate its relevance, we computed numerical simulations of both the microscopic and homogenized models based on a non-physical linear model, and then on the Mitchell-Schaeffer ionic model.

**Results**: Interestingly, we recover a bidomain type model, but with modified conductivities, that depend on the volume fraction of the diffusive inclusions but also on their geometries. The numerical results confirm the convergence of the microscopic model to the homogenized equations in the linear case. We are currently working on the numerical simulations for the non-linear case, where we expect to observe the influence of the diffusive inclusions on the propagation of action potentials.

**Conclusion**: With the final non-linear model, we shall provide cheap modeling tools to account for tissue heterogeneities at intermediate scales, as can be observed, e.g., in the fibrotic tissue. The diffusive volume ratio, that enters the model, might be available through functional imaging, which enlightens the practical interest of the method.

# Myocardial Electrophysiological, Contractile and Metabolic Properties of Hypertrophic Cardiomyopathy: Insights from Modelling

Ismail Adeniran*, Gareth Jones and Henggui Zhang

The University of Manchester
Manchester, United Kingdom

Hypertrophic cardiomyopathy (HCM) is characterised by cellular dysfunction, asymmetric left ventricular hypertrophy, ventricular arrhythmias and sudden death. HCM is associated with mutations in sarcomeric proteins and is usually transmitted as an autosomal-dominant trait. Functional impacts of the mutant contractile proteins, particularly the cellular mechanisms underlying arrhythmogenicity is incompletely understood. The aim of this study was to investigate the mechanisms by which HCM alters electrophysiological activity, contractility and energy metabolism regulation at the single cell and organ levels, using in silico methods. We developed a human ventricular, electromechanical, mitochondrial energetics (EMME) myocyte model incorporating electrophysiology, metabolism and cytoplasmic ATP-consuming processes associated with force generation and ion transport. The model was validated by its ability to reproduce the experimentally observed kinetic properties of human HCM induced by a) remodelling of several ion channels and Ca2+ handling proteins arising from altered Ca2+/calmodulin kinase II signaling pathways; and b) increased Ca2+ sensitivity of the myofilament proteins. Our simulation results showed energy metabolism was markedly impaired, as indicated by a decreased phosphocreatine to ATP ratio (-29%), mitochondrial membrane potential was lowered, implying a lowered Electron Transport Chain oxygen radical and hence, energy expenditure beyond supply. With increasing heart rate from 1Hz to 3Hz, mimicking exercise conditions, there was a 3-fold increase in tension cost in HCM and less than ~1.5-fold in control, thus explaining one of the injurious effects of HCM in young athletes. 3D EMME human left ventricle model simulation incorporating septal hypertrophy showed ejection fraction was not significantly altered but contractile efficiency was reduced and the tissue's vulnerability to re-entry was increased. Our results show that HCM increases arrhythmia risk due to increased tissue vulnerability, electrophysiological abnormalities and impaired Ca2+ handling, which in combination facilitate maintenance of re-entry. Our results support the notion for inefficient energy utilisation as a unifying mechanism in HCM.

PC3

# Role of Fiber Orientation in Atrial Arrythmogenesis

Sanjay Kharche [1, 2], Jichao Zhao [3], Simon Castro [1], Michael Colman [1], Robert Stevenson [4], Jonathan Jarvis [4], Bruce Smail [3], Henggui Zhang [1]

[1]School of Physics and Astronomy, University of Manchester, Manchester, UK. [2]CEMPS, University of Exeter, Exeter, Exeter, UK. [3]Auckland Bioengineering Institute, University of Auckland, New Zealand, [4]Research Institute for Sport and Exercise Sciences, Liverpool John Moores University, Liverpool, UK.

**Background:** Electrical wave-front propagation in the atria is determined by local fiber orientation. Atrial fibrillation (AF) progresses with enhanced anisotropy. We illustrate AF due to myofiber structure.

**Methods:** A 3D rabbit atrial anatomical model at 20 μm resolution with realistic fiber orientation was constructed based on contrast-enhanced micro-CT imaging. The Fenton-Karma excitation cell model was adapted to reproduce rabbit atrial action potential period (APD) of 80 ms. Diffusivities were estimated for longitudinal ($D_p$ = 0.0065 $mm^2$/ms for CV = 0.5 mm/ms) and transverse directions ($D_p$ = 0.06 $mm^2$/ms for CV = 0.15 mm/ms) of the fiber orientation. The estimated diffusion constants were deployed in the 3D anisotropic atrial model (Figure) where pacing was conducted with a reducing S2 interval to facilitate initiation of atrial arrhythmia. Multiple simulations were conducted with varying values of diffusion anisotropy and stimulus locations to evaluate the role of anisotropy to evaluate propensity to initiate arrhythmia. BeatBox, a cardiac simulation package, was used throughout this work.

**Results:** Under physiological anisotropy conditions, a rapid right atrial activation was followed by the left atrial activation. Excitation waves reached the AV border where they terminated. Upon reduction of conduction heterogeneity, re-entry was initiated by the rapid pacing and the activation of both atrial chambers was almost simultaneous.

**Conclusions:** Myofiber orientation is an effective mechanism for regulating atrial activation. Modification of its myo-architecture is proarrhythmic.

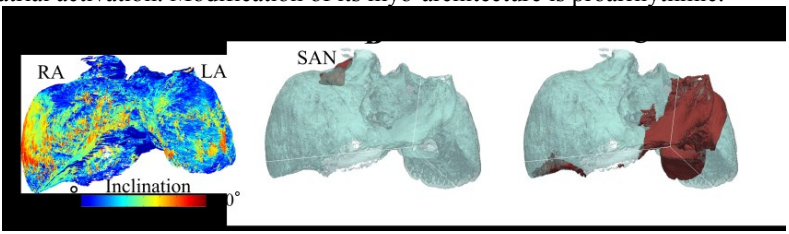


**Figure.** Rabbit atrial fiber directions (**A**) and atrial activation (pacing from sino-atrial node (SAN)) in rabbit atrial geometry with fiber orientation (**B, C**). RA=right atrium; LA= left atrium.

PC3

# Propagation Malfunctions due to Gap Junction Dysregulation

Inmaculada R Cantalapiedra*, Angelina Peñaranda and Blas Echebarria

niversitat Politecnica de Catalunya
Barcelona, Spain

Gap junctions are membrane channels that connect the cytoplasm of adjacent cells allowing the cell-to-cell electrical coupling necessary for action potential propagation. Pathological conditions, such as malformations in connexins, mutations affecting phosphorylation of regulatory sites of connexins, alterations in gap junction organization, and type and quantity of connexin expression, can impede the normal electrical propagation. All these malfunctions can produce a dispersion of repolarization, implicated in ventricular arrhythmias. In fact, ventricular tachycardia and spontaneous ventricular arrhythmia occurred in more than twice as many connexin deficient hearts than wild-type hearts. We perform numerical simulations of a human ventricular model in order to mimic some of these pathological conditions. In particular, we consider a diminished Cx43 connexin expression, as well as altered connexin conductance dynamics, i.e., modified maximum and minimum conductances gmax and gmin, half-inactivation voltage V1/2 and decay kinetics. Physiologically these modifications can appear due to mutations or to different connexin configurations, i.e., forming heteromeric channels. Under these conditions we study the change in action potential duration (APD) and CV-restitution properties. This allows us to define a critical conductance at which conduction block is produced depending on the pacing rate. Then, we study fibers with an inhomogeneous distribution of connexin expression. We observe that, although CV diminishes with decreased connexin expression, the APD remains almost constant up to the point of conduction block. Also, propagation differs for constant or time-dependent voltage conductance, conduction block occurring earlier for the former. While mutations resulting in a lower V1/2 produced an appreciable change in CV restitution, this effect was not so important when the mutations affected the delay time. Thus, our results suggest that a correct description of gap junctional conductance is of big importance for understanding conduction block under pathological conditions.

PC3

# Simulation of an Electro-mechanical Resuscitation Device for Cardiopulmonary Resuscitation

Alejandro Mendoza García, Stefan Eichhorn, Marcin Polski, Alois Knoll
Technical University Munich
Munich, Germany

**Introduction:** The application of cardiopulmonary resuscitation (CPR) to people suffering of cardiac arrest has become an effective way of increasing chances of survival. Current CPR is carried out manually with a compression depth of approx. 5 cm and a rate of 100 per minute. This however requires significant amount of force, producing fatigue, reducing the effectiveness of the procedure.

New electro-mechanical resuscitation devices (ERD) may solve this problem by providing constant compressions at a specific rate and depth. This additionally brings the possibility of generating different types of compressions.

The presented research is focused on the exploration of different compression curves and the effects in flow and pressure through simulation.

**Methods:** A mathematical model of the cardiovascular system was used to obtain hemodynamic behavior. Pressure in the heart and lung compartments was increased depending on the depth of the compression. Chest stiffness was represented by a spring-damper model. The ERD was composed of a DC motor coupled to a spindle drive shaft for vertical movement. A PID controller was used to control the position of the motor, receiving as input a compression curve (Sinuous, 30ms up/50ms down, 50ms up/30ms down) with a given rate and depth. Values of pressure and cardiac output (CO) were registered for the different types of compression curves and at different rates.

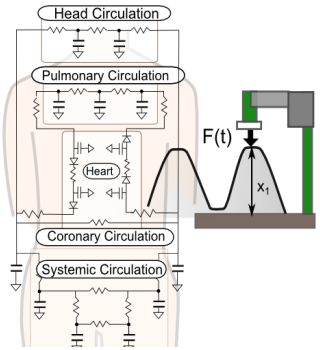

Cardiovascular and electro-mechanical resuscitation model

As implementation JSim was used for the evaluation of the differential equations of the cardiovascular model and Matlab was used to implement the controller.

**Results:** The constructed model was capable of representing chest compressions generated by the ERD. The curve with 30ms down /50ms up showed an increase of 7% compared to the sinuous wave form, while the 50ms down / 30ms up showed an increase of 12%. The next step will be to integrate this information into the controller of the ERD.

PC3

# Action Potential Abnormalities due to Loss- or Gain-of-Function Mutations in *KCNJ2*

Ronald Wilders*

Academic Medical Center, University of Amsterdam, Department of Anatomy, Embryology and Physiology
Amsterdam, The Netherlands

**Background:** Both Andersen–Tawil syndrome type 1 (ATS1) and short QT syndrome type 3 (SQT3) are associated with mutations in the *KCNJ2* gene, which encodes the Kir2.1 protein. Kir2.1 is the most abundant member of the Kir2.x family in the Kir2.x tetramers that constitute the cardiac inward rectifier potassium channel ($I_{K1}$ channel). The loss-of-function mutations in *KCNJ2* in ATS1 may cause QT prolongation and ventricular arrhythmias (extrasystoles and tachycardia), whereas the gain-of-function mutations in SQT3 shorten the QT interval and predispose the heart to develop reentrant arrhythmias.

**Aim:** We aimed to assess the effects of ATS1 and SQT3 related mutations in *KCNJ2* on the electrophysiological characteristics of human ventricular cells.

**Methods:** We carried out computer simulations using the updated ten Tusscher *et al*. human ventricular cell model. The model $I_{K1}$ was replaced with either wild-type or heterozygous mutant Kir2.1 current, the latter representing ATS1 (dominant-negative reduction of Kir2.1 current amplitude, as commonly observed in ATS1) or SQT3 (decreased inward rectification, as observed for the E299V and M301K mutations).

**Results:** In ATS1 simulations, the action potential was only modestly prolonged and calcium-driven spontaneous action potentials could be observed. The resting membrane potential was depolarized by 5–10 mV, thereby reducing sodium channel availability and contributing to a noticeable decrease in conduction velocity. In SQT3 simulations, effects on resting membrane potential and conduction velocity were relatively small. However, the action potential was markedly shortened, which facilitated ventricular conduction at high stimulation rates.

**Conclusion:** Our results explain the susceptibility to ventricular arrhythmias observed in ATS1 and SQT3 patients. The effects on the action potential are in line with the clinical observations on the ECG, except for the reduced conduction velocity in ATS1, which would be reflected in QRS prolongation. Such prolongation has been observed in transgenic mice, but not in ATS1 patients.

PC3

# Robust Derivative-Based Method to Determine Filtered QRS Limits in High Resolution Electrocardiography

Olivassé Nasario-Junior, Paulo R Benchimol-Barbosa, Jurandir Nadal

Biomedical Engineering Program, Federal University of Rio de Janeiro
Rio de Janeiro, Brazil

The accuracy of high resolution electrocardiogram (HRECG) as a risk stratification tool relies on QRS offset detection, which is subject to variation due to the signal residual noise level (RNL). This study proposed a technique for improving the accuracy of QRS complex limits detection, based on successive signal derivation (DER), and compared the results with the statistical method recommended by the American College of Cardiology (ACC).

Population: Control Group - 18 healthy volunteers (age: [mean ± SD] 52.1 ± 10.2 years) with no cardiac disease; SMVT Group - sustained monomorphic ventricular tachycardia: 18 subjects confirmed by electrophysiology study (58.7 ± 12.9 years). All were in sinus rhythm. HRECGs were analyzed according to ACC guidelines in vector magnitude (VM) high-pass filtered at 40 Hz, averaged to target RNL of 0.2 μV. In DER, HRECGs were successively derived toward the end of the ventricular activation seeking for next higher derivative inflection point, in which absolute amplitude was equal to RMS baseline noise (Figure 1). Sensitivity, specificity and predictive values were compared by $X^2$ test. QRS offset was assessed as function of different RNLs and linear correlation coefficient compared ($\alpha < 0.05$).

ACC and DER methods showed, respectively, 64.3% and 85.7% positive predictive value ($p < 0.05$), 58.6% and 59.1% negative predictive value ($p$ = NS), 50.0% and 33.3% sensitivity ($p$ = NS), and 72.2% and 94.4% specificity ($p < 0.05$). According to ACC and DER methods, QRS duration correlated to RNL respectively, in Control Group -0.98 ($p < 0.05$) and -0.32 ($p$ = NS) (Figure 2), and in SMVT Group -0.75 ($p < 0.05$) and -0.67 ($p$ = NS). DER showed higher accuracy and less sensitivity to RNL than ACC for QRS offset detection.

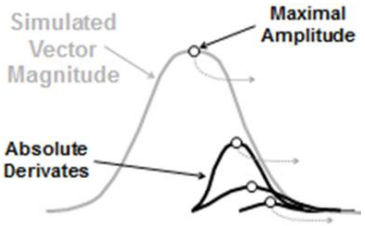


Figure 1: DER method logic showed in a simulated signal (cosine).

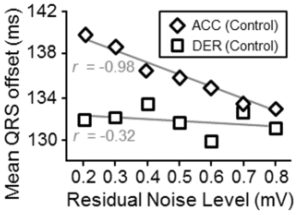


Figure 2: Mean QRS offset values as function of residual noise level for Control Group.

PC4

# Assessment of Electrocardiograms with Pretraining and Shallow Networks

Vicent Ribas Ripoll*, Anna Wojdel, Pablo Ramos, Enrique Romero and Josep Brugada

Centre Recerca Matemàtica
Spain

**Objective:** Clinical Decision Support Systems normally resort to annotated signals for the automatic assessment of ECG signals. In this paper we put forward a new method for the assessment of normal/abnormal heart function from raw ECG signals (i.e. signals without annotation) based on \textit{shallow} neural networks with pretraining. Methodology: this paper resorts to a prospective clinical study that took place at Hospital Clínic in Barcelona, Spain. This study took place in 2010-2012 and recruited 1390 patients. For each patient we recorded a 12-lead ECG and diagnosis was conducted by the Cardiology service at the same hospital. Two datasets were produced, the first contained the automatically annotated version of all input signals and the second contained the raw signals obtained from the ECG.

**Results:** The new method was tested through cross-validation with a cohort of 200 test patients. Performance was compared for both annotated and raw datasets. For the annotated dataset and a shallow network with pretraining we obtained an accuracy of 0.8639, a sensitivity of 0.9560 and specificity of 0.7143. The raw dataset yielded an accuracy of 0.8426, a sensitivity of 0.8977 and a specificity of 0.7785.

**Conclusion:** Shallow networks with pretraining automatically obtain a representation of the input data without resorting to any annotation and thus simplify the process of assessing normality of ECG signals. Despite the fact that sensitivity has decreased, accuracy is not much lower than that obtained with standard methods. Specificity is improved with the new method. These results open up a promising line of research for the automatic assessment of ECG signals.

PC4

# Variability of the Maximal Amplitudes of Impedance Cardiography and of its First Derivative during Supine, Standing, Controlled Breathing, and Exercise

Salvador Carrasco-Sosa and Alejandra Guillén-Mandujano*

División de Ciencias Biológicas y de la Salud, Universidad Autónoma Metropolitana-I, DF, México
Mexico City, Mexico

Despite the maximum value of the first derivative of impedance cardiography (dZmax) being used to compute the stroke volume and the Heather Index, its beat-to-beat variability remains unexplored. To address this issue, our aim was to examine the effects of four maneuvers that elicit different vagal activity levels on the time-frequency spectral measures of the maximal amplitude of impedance cardiography (Zmax) and dZmax. ECG, impedance cardiography (ICG) and respiration (Resp) were recorded from 17 healthy volunteers during 5-min supposedly steady-state conditions: lying position (L), controlled breathing (CB), standing (S) and dynamic exercise (E). Zmax and dZmax were computed from ICG and its first derivative traces respectively. Time-frequency spectra of RR intervals (RR), Zmax, dZmax and Resp series were estimated via the smoothed pseudo-Wigner-Ville distribution to compute their low-frequency (LFZmax, LFdZmax) and high-frequency powers (HFRR, HFZmax, HFdZmax, HFResp). Time-frequency coherences of HFZmax and HFdZmax with HFResp were also obtained. With respect to L condition: HFZmax power greatly increased in E ($p<0.01$) and remained unchanged in CB and S ($p>0.05$), showing coherences with HFResp greater than 0.8; LFZmax was similar among maneuvers ($p>0.05$) and its power was 20 times smaller than that of HFZmax; LFdZmax power was much larger in E ($p<0.01$) and decreased in S ($p<0.01$); HFdZmax power presented a large increment in E ($p<0.01$) and decreased in S ($p<0.01$), with coherences greater than 0.8 with HFResp. Remarkably, while LFZmax power is very small and unresponsive to the maneuvers and HFZmax only increases in E, LFdZmax and HFdZmax powers change significantly throughout the maneuvers, maximally in E condition. This suggests that LFdZmax is an index of left ventricular systolic function and HFdZmax reflects the non-neurally mediated respiratory influence. This study provides some evidence to document our hypothetical generalization that all cardiovascular variables present rhythmic variability correlated with autonomic and respiratory states.

PC4

# Post Extrasystolic T Wave Change in Subjects With Structural Healthy Ventricles – Measurement and Simulation

Gustavo Lenis, Yannik Lutz, Gunnar Seeman, Arcadi García-Alberola, José Luis Rojo-Álvarez, Óscar Baquero, Eduardo Gil, Olaf Doessel

Institute of Biomedical Engineering
Karlsruhe Institute of Technology, Karlsruhe, Germany

Risk stratification of sudden cardiac death after myocardial infarction plays an important role in cardiology. It has a significant impact on patients treatment and deciding on implantation of cardiac devices. However, the majority of well known methods for stratifying risk fail to accurately predict sudden cardiac death. The heart rate turbulence (HRT) delivers good prognostic results and could be complemented by analyzing the ECG morphology after a ventricular ectopic beat. Therefore, we studied post extrasystolic T wave change (PEST) in a group of 10 patients with structural healthy ventricles. Computer simulations of the human transmembrane voltages and posterior ECG reconstruction were also carried out. PEST and the dynamical restitution of the original T wave shape was quantified using 2 new parameters based on a similarity measure. A notorious PEST was measurable in every patient of this study (see figure). The patients presented diminished or alternating postectopic T waves and prolongation of T wave duration. However, the simulation does not present significant T wave changes. Furthermore, the new morphological parameters do not seem to correlate with the standard HRT parameters TO and TS. A weak correlation between PEST parameters and basal heart rate was observed.

PEST seems to be observable in every patient even if his heart is structurally healthy. In addition, the way T wave morphology changes in every patient is different. However, healthy subjects should present a rapid recovery of the original T wave morphology after the VEB. From the simulation we conclude that PEST cannot be entirely explained by pure electrical phenomena in the heart and that basal heart rate seems to play a significant role in the appearance of PEST. Finally, diagnostic information obtained from PEST is apparently independent from HRT.

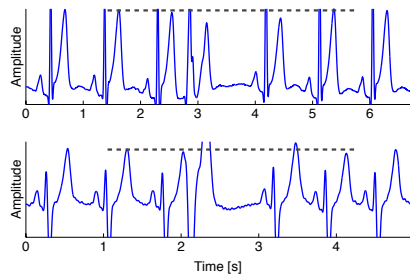


Different postectopic T wave changes in 2 patients with healthy ventricles.

PC4

# Comparative Study of Signal Decomposition Methods for Enhancement of the Accuracy of T-wave End Localisation

I. Christov, V.N. Batchvarov, I. Simova, N. Dimitrov, E.R. Behr,

Institute of Biophysics and Biomedical Engineering, Bulgarian Academy of Sciences, Sofia, Bulgaria

**Introduction:** Delineation of T-end alone and as a part of the measurement of the QT interval is a 'classical' problem in quantitative ECG, approached in many different ways, especially after the automation of the process. The **goal** of this study was to compare several ECG signal decomposition methods in order to enhance the accuracy of the T-wave end localisation.

**Materials:** We used the PTB Diagnostic ECG Database comprising 549 recordings which is freely available in PhysioNet.

**Method:** The idea was to combine the 8 independent leads (I, II, V1÷V6) of the standard 12-leads ECG into a single lead. The signal decomposition methods that were used were applied to reconstruct the combined T-wave in such a way as to obtain maximal accuracy of the automatic T-end localisation. Four signal decomposition methods were used (Figure): Dominant T-wave (DTW), Principle Component analysis (PCA), and 2 Spatial Vectors synthesized from the orthogonal x, y, and z vectors:

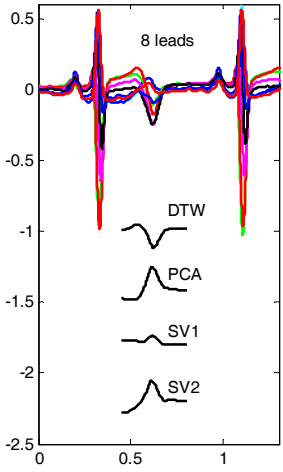


$$SV1 = \frac{1}{3}\sqrt{x^2 + y^2 + z^2}\ ,$$

$$SV2 = 0.5\left(x + y + z + 0.25(|\,x - y\,| + |\,x - z\,| + |\,y - z\,|)\right)$$

The four decomposition methods are shown in the Figure.

The T-ends were located using one and the same previously published software program. The results were compared to a published 'gold standard' dataset of manually determined T-ends. The 'gold standard' was obtained as a mean value of the markings of 5 experts working on the PTB Database.

**Results:** Mean and standard deviation of the difference between the automatic and manual T-end locations were calculated in [ms]:
DTW=8.72±14.19; PCA=10.30±12.69; SV1= -8.14±14.53; SV2=8.59±17.93

The best results (i.e smallest standard deviation) were obtained by PCA followed by DTW. Compared to the manual measurement, all signal decomposition methods except SV1 slightly overestimated the QT interval (i.e. moved the mean Tend location slightly to the right).

PC4

# A Portable Device for a Modular System of Patient Monitoring

Daniel Campillo*, Hector Torres, Rene Gonzalez, Katia Valdes and Rolando Lopez

ICID
Havana, Cuba

**Aims:** Discuss the main characteristics of a low cost and consumption portable device, which is part of a system for ambulatory monitoring of patients with heart diseases.

**Methods:** The solution is based on the microcontrollers MSP430F5419A and CC2540 (Bluetooth), both from Texas Instruments and the modem SIM908 from Simcom, which includes GSM/GPRS and GPS modules. The communication with the modem is done using a MSP430F5419A serial port by means of AT commands, which allow configuring it, transmitting and receiving information. There is a real time acquisition module which transmit ECG signal to the device using Bluetooth interface. Once ECG signal is acquired, the device can establish a data connection with any of the predefined phone numbers or establish a communication through GSM/GPRS module. Over the established connection, the device sends the acquired ECG signal and the GPS coordinate of the patient to a web page, where this information will be analyzed by specialized medical staff. The monitoring system can use a smartphone or the developed solution. This device is an attractive solution to use in systems where low cost is a critical issue.

**Results:** Three prototypes of the presented device in this paper were developed and tested. A total of 9 standardized ECG signals with different shapes, suggested by IEC 60601-2-25: 2011 for testing purpose were applied to the system. These signals were acquired and transmitted using a protocol which includes a cyclic redundancy code used for error checking. There was not any loss in the received signal.

**Conclusions:** The developed device allows to acquire and transmit the ECG signal in a safety way. According to the connectivity options of the device, it could be integrated as a part of different systems for ambulatory patient monitoring.

PC4

# Cardiac Telemetry System Intended for Flexible Patient Monitoring

Gay Meissimilly*, Mary Cartaya and Diolkis Ruiz

Cuba

Cardiac telemetry facilitates continuous ECG monitoring of patients in both inpatient and outpatient settings. This paper introduces a new flexible, low-power, short-range, real-time cardiac telemetry system designed to provide a monitoring solution for patients admitted either to a coronary care unit or to a cardiac rehabilitation exercise program. The custom firmware runs in real-time on a ZigBee-compliant platform. It uses a proprietary networking protocol on top of IEEE 802.15.4 PHY layer to optimally manage the system hardware regarding power saving and data processing. Finding and classifying arrhythmias on the ECG remain the benchmark method for identifying and preventing life-threatening heart conditions. The highly configurable application software can be set to effectively provide monitoring trends and alarm notification for up to 16 patients. A descriptive cross-sectional study conducted on 80 high-risk cardiac patients at the Cardiac Rehabilitation Centre, attached to the Institute of Cardiology & Cardiovascular Surgery of Havana, between July 2009 and April 2011 reported a considerable diagnostic accuracy [SPC>99%, TPR>80% and PPV>83%] of the dedicated algorithms for differentiating premature ventricular beats, as well as a remarkable correlation (>71%) between automatic and manual ST-segment depression measurements.

PC4

# Personalised System-on-chip for Standard 12-lead Reconstruction from the Reduced 3-lead System Targeting Remote Health Care

Utkalika Panda, Sidharth Maheshwari, Gayathri Padma, Murugaiyan Thendral, Agathya Jagirdar, Venkateswara Chowdary, Naresh Vemishetty, Amit Acharyya*, Paolo Emilio Puddu and Michele Schiariti

IIT Hyderabad
Hyderabad, India

Cardiovascular diseases(CVD) are the prime causes of human mortality and morbidity world wide. CVD can be prevented or cured ,if detected early or on-time, where technology can be of significant help. With the tremendous growth in the field of communication and mobile technology,sensing and chip design industry, the remote CVD health monitoring gradually become feasible. Concurrently, to take advantages of remote health care especially in the developing and underdeveloped nations, the affordability issue should also be addressed, without sacrificing the diagnostic accuracy of CVD. These pose two self contradicting requirements from the technical prospective to tackle CVD remotely: firstly, a tiny unobtrusive, noninvasive and low power consuming system running on battery backup yet giving medically accurate diagnosis results; secondly to reduce the number of on body ECG sensors yet to produce medically reliable standard 12 lead ECG for remote CVD diagnosis.In this paper we introduce a low power consuming and real time health care system-on-chip design methodology to reconstruct standard 12 lead ECG(medical perspective) from the reduced 3-leads(technological perspective) remotely and show that the system generates medically accurate ECG signal in a personalized manner .The system has been validated using 110 patients data from MIT-BTH database.The heart of the proposed system is the symmlet based wavelet trans-formation module, which has been designed to ensure low computational complexity by removing all multiplication from the design.The performance of the proposed system has been evaluated using R 2 -statistics, correlation and regression between the algorithm and architecture which came out to be more than 90%,95%and 92% respectively.The system generated output have been individually checked and compared by two cardiologists separately and the diagnostic accuracy have been endorsed.We believe the majority of population will get benefit from the proposed system in terms of accurate diagnosis,timely prognosis and intervention at an affordable cost world wide.

PC4

# QRS Complex Detection in Experimental Orthogonal Electrograms of Isolated Rabbit Hearts

Jiří Kozumplík, Marina Ronzhina, Oto Janoušek, Jana Kolářová*, Ivo Provazník and Marie Nováková

Brno University of Technology, Brno, Czech Republic
Brno, Czech Republic

**Aims:** Automated analysis of HRV and/or QT intervals of isolated rabbit heart electrograms requires reliable detection of QRS complexes. Spectral properties and quality of the electrograms differ from human ECG signals. Further, spectral properties and quality significantly vary during global ischemia experiments when voltage-sensitive fluorescence dye di-4-ANEPPS is applied to the heart tissue for optical recording of action potentials. All staining phases (control, staining, washout) and global ischemia phases (control, blocking perfusate flow, reperfusion) show large changes in electrical activity of the heart. Thus, reliable detection of QRS complexes requires a new algorithm robust from experimental phases.

**Methods:** The electrograms were recorded at sampling frequency of 2000 Hz from conventional orthogonal leads x, y, z placed around the isolated heart. The detection method is based on spatial velocity using differentiating all lead signals, the squaring, the adding and the square root in orders. Teager-Kaiser energy operator (TKEO) was applied after filtering spatial velocity with a standard pass-band filter. Reference (fiducial) points were detected in all three orthogonal lead signals at places where the TKEO signal excessed preset threshold.

**Results:** The algorithm was tested on 263 orthogonal electrograms that contained all experimental phases. It was necessary to include automated elimination of severe artifacts during detection. The major artifacts were mainly caused by heart movements (large baseline wander). Resulting values of both sensitivity and sensitivity of detection increased 99.1%.

**Conclusion:** It was proved that QRS complex detection in the signals from three orthogonal leads is more efficient and robust than detection based on signals of individual leads. The detection was more reliable even in the case of lead z failure when spatial velocity was calculated from x and y leads only.

PC4

# High-frequency Noise Filtration in Stress Test

G. Bortolan, I. Christov, I.

Institute of Biomedical Engineering, ISIB-CNR
Padova, Italy

**Background**. Electromyographic (EMG) noise is constantly present in stress test electrocardiographic (ECG) recordings, due to physical exercise. The main purpose of the research is to construct a filter that suppresses sufficiently the EMG noise, with minimal distortions of the high frequency content of the QRS complex.

**Materials**. We studied 106 patients: age 63±10 years, 61 male. Digital 12-lead electrocardiograms (ECG) were acquired during stress ECG test using veloergometer (GE Marquette Stress PC ECG Application) – 2-min stages 25W incremental workload. Median recording duration of 7.08 minutes and a mean number of 669 RR intervals.

**Method**s. The QRS onsets and offsets are identified by analysis of all the leads. Three lead groups: the 8 independent, the 12 standard and 15 (12 ECG + 3 VCG) leads have been considered for the development of optimal localization of QRS onsets and offsets. Two non linear combined leads have been considered in the identification problem, based on spatial differences ("spatial velocity") and product ("energy") of ECG intervals.

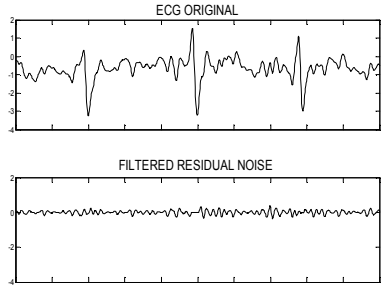


The EMG noise filter is based on the method of Savitzky-Golay, whose characteristics are dynamically changed inside and outside the QRS interval. The idea is to filter less inside the QRS and more outside for a minimal distortions of the high frequency informative content in the QRS complex. This can be obtained with appropriate constraints on the ratio between the power of filtered residual noise inside and outside the QRS complex . As a consequence, in absence of EMG noise, the filtering activity in QRS is not significant.

PC4

**Results and conclusions**. The considered EMG filter was tested, and the noise suppression out of QRS is 1.5 - 3 times higher than in QRS.

A comparison with previous results in the same database for the analysis of QRS and T wave alternans, produced significant increase of standard deviation of PCA index in QRS interval ($p<0.001$, paired sign-rank test).

# High Resolution ECG Differences between Hospital Survivors and Non-survivors of Out-of-Hospital Cardiac Arrest during Mild Therapeutic Hypothermia

Martin Rauber*, Dušan Štajer, Marko Noč, Todd Schlegel and Vito Starc

University of Ljubljana, Faculty of Medicine, Ljubljana, Slovenia
Slovenia

Out of hospital cardiac arrest (OHCA) is one of the leading causes of death in developed countries. Despite novel therapeutic strategies, management of patients resuscitated from OHCA is challenging for clinicians, and the mortality rate of those who achieve return of spontaneous circulation and hospital admission remains high. A number of factors and markers have been proposed for prediction of outcome after OHCA with higher or lower reliability, but none of them has been derived from electrocardiogram. The aim of our study was to evaluate electrocardiographic (ECG) differences between hospital survivors and non-survivors of OHCA and to identify among standard and advanced ECG parameters those, which might be used for early prediction of survival after OHCA. The study included 68 patients that suffered from OHCA. In all patients, serum arterial lactate on admission to the ICU was obtained as an index of ischemia during heart arrest and resuscitation. A 5-minute 12-lead high fidelity ECG recording was recorded dur¬ing mild therapeutic hypothermia (defined as core body temperature of 32-34°C). Custom soft¬¬ware pro¬¬g¬rams were used to cal¬culate con¬ventional and advanced spatial, repolarisation and interval varia¬bility ECG parameters. Survival at hospital discharge was considered as the outcome variable. There were 33 hospital survivors and 35 non-survivors of OHCA among our patients. Hospital survivors displayed significantly lower serum arterial lactate levels ($p = <0.001$) and lower values of beat-to-beat QT interval variability parameters - QTVI: QT variability index ($p = 0.041$); UTVI: index of unexplained part of QT variability ($p = 0.014$), uSDNN QT: unexplained component of the standard deviation from the mean of all normal-to-normal QT intervals ($p = 0.032$). We conclude that a relatively greater degree of anoxic injury in patients that fail to survive OHCA results in altered electrophysiological properties of the heart muscle leading to increased ventri¬cular repolarisation variability.

PC5

# Susceptibility of Isolated Rabbit Hearts with various Left Ventricular Mass to Short Ischemic Periods

Veronika Olejnicková*, Marina Ronzhina, Hana Paulova, Miroslava Hlavacova, Tibor Stracina and Marie Novakova

Faculty of Medicine, Masaryk University, Brno, Czech Republic
Brno, Czech Republic

**Aim:** Hearts with increased left ventricular (LV) mass show higher sensitivity to ischemic injury. The susceptibility to repeated short periods of ischemia in rabbit hearts with normal vs. increased LV mass was compared in this study.

**Methods:** Isolated hearts from 14 New Zealand adult rabbits were included in this study, subjected to 10 minutes of ischemia and 10 minutes of reperfusion, once or three times. Three orthogonal electrograms were recorded and total number of ventricular premature beats (VPBs) occurring as singles, salvos, and ventricular tachycardia were counted. The levels of CK, LDH, lactate, and 4-hydroxynonenal (HNE, marker of lipoperoxidation) in perfusate were analyzed. The hearts and their left ventricles were weighted and LV:heart weight ratio was calculated. Animals were distributed into groups with normal (A) and increased (B) LV:heart weight ratio (below and above 0.57, respectively).

**Results:** The total number of VPBs during the first ischemia was higher in group B (221± 9.9 vs. 21± 4.6 in group A). Both groups showed decrease of total number of VPBs during repeated ischemia (to 34 % and 11% in group B and 20 % and 21% in group A, respectively). Moreover, in both groups the onset of ectopic activity was delayed with repeated ischemia (from 6th minute in the first ischemia, to the 7th minute in the second, and the 9th minute in the third ischemia). Both groups exhibited increase in biochemical parameters after the first reperfusion as compared to end of stabilization; this increase was more pronounced in group B.

**Conclusions:** The rabbit hearts with increased LV mass show higher susceptibility to arrhythmias during short ischemic periods in comparison to normal rabbit hearts. Changes of biochemical parameters correspond to electrophysiological findings.

PC5

# Effects of Left Ventricle Enlargement on QRS of Rabbit Isolated Heart Electrogram

Marina Ronzhina*, Veronika Olejníčková, Oto Janoušek, Tibor Stračina, Tomáš Potočňák, Jana Kolářová, Marie Nováková and Ivo Provazník

Brno University of Technology
Brno, Czech Republic

**Introduction:** It is known that left ventricle (LV) enlargement may produce the changes in electrocardiogram, especially in QRS complex. Due to widespread use of rabbit isolated heart in experimental cardiology, the study of LV enlargement impact on electrogram (EG) shape could be useful for reliable interpretation of results and future experiments design. METHODS: The orthogonal EGs recorded from isolated hearts of nineteen New Zealand rabbits were analysed. Animals were divided into two groups (eLV - enlarged and nLV - normal) according to the LV weight/heart weight ratio (9 and 10 animals with the ratio above and below 0.57, respectively). During EGs recording the hearts were rotated around longitudinal axis in 10° steps in the range ±90°, covering LV region. Eight parameters were calculated: QRS width, maximal QRS deviation, area under QRS (AUCqrs), positive AUCqrs, negative AUCqrs, positive/negative AUCqrs ratio, angle of 2D QRS vector, and length of 2D QRS vector. Comparison of parameters in both animal groups was performed for all experiments together, as well as individually for two data sets obtained by further division according to the animal body weight (BW): 12 and 7 rabbits with the BW above and below 3 kg, respectively. RESULTS: Considering whole data set analysis, the differences were found in maximal deviation, AUCqrs, negative AUCqrs, and vector length. In case of BW-related analysis, there are differences between some parameters for eLV and nLV groups (maximal deviation and negative AUCqrs for both small and big animals, AUCqrs, positive AUCqrs, and vector length for small animals only, QRS width for big animals only). In both cases, the region of high values of maximal deviation calculated in eLV group is wider than that of nLV group. For some parameters, significant difference is present in narrow region of recording heart positions (i.e. for a few EG leads).

PC5

# Comparison of Time and Frequency Domain Methods for the Feedback on Chest Compression Rate

Digna González-Otero, Erik Alonso, Jesús Ruiz, Sofía Ruiz de Gauna, Elisabete Aramendi, Unai Ayala, James K. Russell, Mohamud Daya

University of the Basque Country, UPV/EHU
Bilbao, Spain

During cardiopulmonary resuscitation, quality of chest compressions (CC) is believed to be an important determinant for patient survival. Current resuscitation guidelines recommend CC-rates of at least $100\,\mathrm{min}^{-1}$, and feedback systems can guide rescuers towards this rate. Thoracic impedance (TI), available from defibrillation pads without additional sensors, fluctuates due to CCs, potentially supporting feedback.

**Aim:** To compare the feedback on CC-rate provided by a time-domain and a frequency-domain method using exclusively the TI.

**Materials:** Fifteen episodes were extracted from an out-of-hospital cardiac arrest database collected between 2006 and 2010 from a single EMS agency in Oregon (USA) using the Philips Heartstart MRx monitor/defibrillator equipped with Q-CPR meter. Each episode included the TI and the compression depth (used as gold standard to define a CC). Duration of the records was $2348 \pm 335\,\mathrm{s}$, with $1861 \pm 1207$ CCs per episode.

**Methods:** The *time domain method* identified the relative maxima of the preprocessed TI, and classified each fluctuation by features of amplitude and duration as compression or non-compression. The method reported the CC-rate as the median of the rates of the previous CCs. The *frequency domain method* computed the Fast Fourier Transform (FFT) with zero padding for short windows of the preprocessed TI, and it identified the highest peak in a frequency band. If the amplitude of this peak exceeded a dynamic threshold, its frequency was reported as the CC-rate for the analyzed window.

**Results:** Global root mean square errors of the estimated CC-rate were 3.2 and $3.1\,\mathrm{min}^{-1}$ for the time and the frequency domain methods, respectively. The proportion of false positives (CC-rate reported during CC-pauses) were 2.6% and 2.2%, respectively. The proportion of false negatives (no CC-rate reported during CC) were 1.7% and 1.9%, respectively.

**Conclusions:** Both methods reported high accuracy computing the feedback CC-rate and could be implemented without need for additional sensors.

PC6

# Three-dimensional Apex-seismocardiography

Samuel E Schmidt, Ask S Jensen, Jacob Melgaard, Claus Graff, John Hansen, Tanveer A Bhuiyan, Johannes J Struijk

Aalborg University
Aalborg, Denmark

Traditional apex-cardiography measures chest vibrations at the apex beat using an air-coupled microphone. Advantages of apex-cardiography include its relation to left ventricular pressure and the ability to identify markers of aortic valve and mitral valve openings in the signal. To provide additional insight in apex-cardiography and chest vibrations we estimated the three-dimensional displacement of the apex beat using a three-axis accelerometer.

**Methods:** A custom-built three-axis accelerometer unit was placed at the location of the apex beat in 5 healthy male subjects (Age: 29-42) lying in left lateral decubitus position. ECG, echo Doppler of the carotid artery and phonocardiography were recorded simultaneously with the accelerometer signals. The three-dimensional displacements of the apex beat were estimated by twofold integration of the accelerometer recordings and movements related to respiration were removed with a high-pass filter (cut-off at 0.5 Hz). Using the ECG as a reference, mean three-dimensional beats were constructed using an automatic segmentation algorithm. The most dominating displacement direction was estimated as the largest eigenvector in a principle component analysis (PCA).

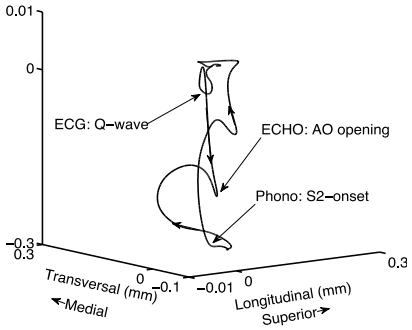


3D displacement loop at the apex

**Results:** The peak-to-peak displacements in the longitudinal, transverse and perpendicular dimensions were 0.39±0.35 mm, 0.28±0.15 mm and 0.38±0.12 mm (mean±std). The dominating displacement direction changed from subject to subject. On average it deviated from the downward perpendicular axis with 3.8±41 degrees toward the superior direction and with 18.4±30 degrees towards the medial line. The variance of the 1st PCA component corresponded to 85±17% of the total variance.

**Conclusion:** The longitudinal and transverse displacements show that single axis measurement along the perpendicular axis only reveals a part of the complex movements at the apex beat. The clinical relevance of adding the additional dimensions has to be investigated further.

PC6

# Filtering Chest Compression Artifacts Improves the Performance of VF-detection Parameters.

Unai Ayala, Unai Irusta, Jesús Ruiz, Felipe Alonso-Atienza, Erik Alonso, Digna González-Otero, Jo Kramer-Johansen, Trygve Eftestøl

University of the Basque Country (UPV/EHU)
Bilbao, Spain

**Aim:** Chest compressions of the cardiopulmonary resuscitation (CPR) induce artifacts in the ECG. Filtering techniques have not been successfully combined with commercial shock advice algorithms (SAA) to diagnose the rhythm during CPR. Recently, a promising new approach based on using SAAs especially designed to diagnose the filtered ECG has been introduced. This study evaluates the impact of filtering CPR artifacts on the shock/noshock decision for several well-known VF-detection parameters.

**Materials:** From retrospective resuscitation patients, we selected 1800 8-s artifact-free ECG segments, 318 shockable and 1572 nonshockable, and 5185 8-s ECG segments corrupted by CPR artifacts, 1185 shockable and 4000 nonshockable.

**Methods:** CPR artifacts were removed using an LMS filter. 22 VF-detection parameters were calculated for each segment, analysing time-domain (10), spectral (7), time-frequency (1) and complexity (4) features of the ECG. Performance was measured in terms of: (1) area under the curve (AUC) of the receiver operating characteristic curve, and (2) sensitivity/specificity for the shock/noshock decision.

**Results:** The AUC and the sensitivity/specificity for all parameters was largest for the artifact-free segments. Four parameters had an AUC and sensitivity/specificity values above 0.97 and 90%/95%, respectively. When compared before with after filtering, filtering improved the AUC values by up to 0.15 points, although the AUC of parameters analyzing the high-frequency bands of the ECG did not improve. After filtering, the best feature presented an AUC of 0.96 for a sensitivity/specificity of 88%/95%.

**Conclusions:** Filtering the CPR artifact improved the detection capacity of most parameters, and showed that combining features after filtering may be a successful strategy.

PC6

# Feasibility of Non-invasive Blood Pressure Estimation Based on Pulse Arrival Time: a MIMIC Database Study

Braiam Escobar* and Róbinson Torres

Escuela de Ingeniería de Antioquia
Envigado, Colombia

A novel technique for continuous non-invasive blood pressure (BP) estimation based on the pulse arrival time (PAT) has raised the attention of the research community over the last 15 years due to its suitability and convenience for either ambulatory or clinical implementation. The purpose of the present study was to evaluate the feasibility of BP estimation by means of PAT from data records of ICU patients available at the MIMIC public database. Datasets consisting of ECG, PPG and arterial BP waveforms from 8 subjects aged 64 ± 18 years were used for the analysis and the relationship of PAT with systolic, diastolic and mean blood pressure was assessed through a linear regression fit. PAT was calculated beat-to-beat as the time interval between the R-peak on the ECG and two characteristic points on the PPG waveform: the point of maximum amplitude (PAT_p) and the point of the steepest slope on the rising edge (PAT_d). The analysis was carried out on datasets of short (20 min) and long (60 min) duration in order to evaluate the temporal changes on the linear relationship. The results showed high correlation between systolic BP and PAT for both the short-term (PAT_p=-0.85, PAT_d=-0.89) and the long-term (PAT_p=-0.81, PAT_d=-0.89) analyses. The mean absolute error found between the true and estimated systolic BP values was above 5mmHg in 3 out of 8 subjects for both PAT_p and PAT_d on the short-time dataset; however, the error noticeably increased on the long-term dataset for all subjects. It is concluded that PAT could be potentially used for non-invasive BP estimation on ICU patients under certain limitations; nonetheless, further investigation needs to be addressed on the temporal degradation of the BP-PAT relationship in order to improve the technique reliability and accuracy.

# Measurement of Pulse Wave Velocity during Valsalva and Mueller Maneuvers by Whole Body Impedance Monitor

Magdalena Matejkova*, Vlastimil Vondra, Josef Halamek, Ladislav Soukup, Filip Plesinger, Ivo Viscor and Pavel Jurak

St. Anne's University Hospital, ICRC
Brno, Czech Republic

Elevated vascular stiffness of arteries is a marker of vascular aging and is connected with increased mortality. Noninvasive measurement of arterial stiffness is based on the measurement of pulse wave velocity (PWV), where PWV correlates with arterial stiffness. PWV depends on blood pressure (BP) and other physiological conditions. The aim of our study was to measure and analyze changes of PWVs between chest and limbs during Valsalva and Mueller maneuver and spontaneous breathing. We measured 30 healthy, 14 non-smoking men and 16 non-smoking women in age between 21-35 years. Simultaneous measurements of the whole body impedance, blood pressure and ECG were taken in supine position. Duration of maneuvers was 15 seconds. Spontaneous breathing with duration of 120 seconds was at the beginning and between maneuvers. PWVs were calculated beat-to-beat using Matlab and C# programs. PWVs for Valsalva and Mueller maneuver were computed as median values of 7 second long block situated in the middle part of the corresponding maneuver. PWVs for spontaneous breathing were calculated as median value of 61 seconds long area in the middle part of spontaneous breathing (at the beginning of the measurement). Relative changes of PWVs values (mean±standard deviation) during Valsalva maneuver and spontaneous breathing were: 0.82±0.11 (chest-thigh); 0.87±0.10 (chest-calf); 0.64±0.19 (chest-arm); 0.75±0.16 (chest-forearm), during Mueller maneuver and spontaneous breathing were: 0.92±0.11 (chest-thigh); 0.91±0.09 (chest-calf); 0.76±0.19 (chest-arm); 0.81±0.14 (chest-forearm). PWVs were lower during maneuvers than during spontaneous breathing (sign test, $p<0.001$), during Valsalva maneuver slightly lower than during Mueller maneuver. Changes in PWVs were corresponding with systolic BP which decreased during both maneuvers (Valsalva: 0.92±0.15; Mueller: 0.89±0.13). Diastolic BP during Valsalva maneuver increased (1.10±0.16) and during Muller maneuver decreased (0.91±0.08). Small differences in PWVs during maneuvers were corresponding with differences in pulse BP during these maneuvers.

PC6

# Analysis of Electrogram Complexity during Atrial Fibrillation for Ablation Procedure Duration Prediction

Katarzyna Kośna*, Piotr Podziemski, Lauren Wilson, Simon Stolcman, Prashanthan Sanders, Jan Jacek Żebrowski and Paweł Kuklik

Warsaw University of Technology
Poland

**Background** Atrial fibrillation (AF) is the most complex and the most common sustained arrhythmia. The isolation of Pulmonary Veins during an ablation procedure does not always lead to a cessation of the atrial fibrillation. Often an ablation of further sites is necessary, which complicates and lengthens the ablation procedure to unpredictable extent. The aim of this study was to assess the reliability of the algorithmic complexity analysis of single electrograms as an estimator of the length of the ablation procedure necessary for the cessation of the arrhythmia.

**Methods:** In the experimental part, left and right atrial endocardial bipolar electrograms were recorded during ablation procedure of AF in 28 patients. 5 second electrogram samples were measured at baseline, post ablation sites (LPV, roof, CFAE etc.) and prior to termination. A total of 101 recordings were examined. For all electrograms, algorithmic complexity was calculated based on algorithm proposed in [1].

**Results:** For patients, who had two or less ablation stages performed, the electrograms had significantly lower algorithmic complexity than for patients for whom more than one ablation stage was performed ($p = 0{,}000025$). ROC analysis revealed that 100% statistical sensitivity was obtained for 81% statistical specificity.

**Conclusions:** These results show that algorithmic complexity increases with number of ablation stages required for a given patient, thus with the length of the ablation procedure. We can only hypothesize at this point, that the effect is due to a higher complexity of atrial fibrillation in those patients. This hypothesis still requires further study. [1] Berkowitsch A, Erdogan A, Neuzner J, et al. New nonlinear approach to a quantitative assessment of atrial fibrillation mapping. Medical &Biological Engineering&Computing 1999;37 (Suppl 2):398±399.

PC7

# Frequency Spectrum Correlation along Atria to Study Atrial Fibrillation Recurrence

Raquel Cervigon*, Javier Moreno, Jorge García-Quintanilla, Julián Pérez-Villacastín, Francisco Castells and José Millet

UCLM
Cuenca, Spain

**Aims:** Atrial fibrillation (AF) is an abnormal heart rhythm originated in the top chambers of the heart. The goal of pulmonary vein ablation for AF is regaining a normal heart rhythm, nevertheless restoration sinus rhythm is difficult to prognostic.

**Methods:** Frequency spectrum was calculated from electrical activity registered along all the atria. We investigate whether there were differences between atrial electrical activity spectrum from both atria in recurrent and non-recurrent AF groups. The database includes intracardiac recordings from 45 paroxysmal and persistent AF patients submitted to an ablation procedure. Four electrodes were located at the right atrium (RA) and 4 more at the left atrium (LA). All patients were monitored after ablation, and were divided in 2 groups according to AF recurrence outcome: 28 of them remained in sinus rhythm, whereas the other 17 turned back to AF.

**Results:** It was found stronger correlation between atrial activity frequency spectrum from dipoles located in the left atrium in the non-recurrent group than in the recurrent AF group (0.78±0.12 vs. 0.71±0.26) with a statistical signification of p=0.001. Correlation between atrial activity frequency spectrum from dipoles located in the right atrium in the non-recurrent group than in the recurrent AF group (0.92±0.07 vs. 0.86±0.12) with a statistical signification of p=0.018. In addition, statistical significant differences were found between atrial activity frequency spectrum correlation from dipoles located in the left and right atria in the non-recurrent and recurrent AF groups (0.79±0.16 vs. 0.67±0.25, p=0.009). Moreover, right atrium dominant frequency differences were found, with 5.52±0.88 Hz in the non-recurrent AF group compared with 6.10±1.23 Hz in the patients with recurrences in the arrhythmia.

**Conclusion:** These findings show the more regular atrial activity along the atria in the patients with non recurrences in AF and lower main frequency in right atria compared with recurrent AF group.

PC7

# Loss of Transverse-Tubules Promotes the Development of Ectopic Activity in Guinea-pig Ventricle

Michael A. Colman[1], Sanjay Kharche[1,2], Henggui Zhang[1]
[1]University of Manchester and [2]University of Exeter, UK

**Introduction:** Intracellular calcium handling plays an important role in cardiac single cellular function. Dynamics of the membrane ion currents and intracellular calcium mechanisms are strongly coupled, and calcium dysfunction can promote arrhythmogenesis through the effect on the membrane system. The transverse-tubules (T-tubules) play an important role in bringing calcium to the interior of the cell and hence also have a large effect on calcium cycling. In this study we investigate the role of a loss of the T-tubule system in the generation of irregular spontaneous activity.

**Methods:** A stochastic model of the Guinea-pig ventricular myocyte, which accounts explicitly for the dynamics of dyads, is updated to account for the heterogeneous, coupled surface and T-tubular membrane system. Beta-stimulation is simulated based on previous models. Detubulation is simulated by removing the T-tubule ion currents, including those found in the dyad, and decoupling the surface and T-tubule action potential.

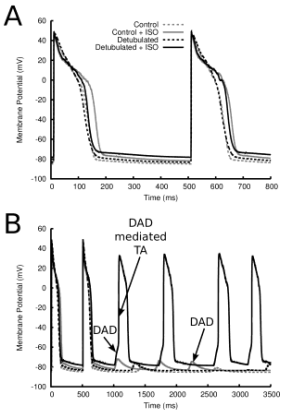


Triggered activity (TA) is observed in the presence of beta-stimulation (ISO) and detubulation.

**Results:** Beta-stimulation increased the magnitude of triggered calcium transients. Following a train of 100 applied stimuli, this resulted in a greater magnitude and frequency of spontaneous calcium sparks. Loss of T-tubules shortened the action potential at the surface membrane and resulted in a positive shift of the resting potential. This positive shift was accentuated by the presence of beta-stimulation. The combination of a positive shift in the resting potential and higher magnitude spontaneous calcium sparks resulted in delayed-after-depolarization mediated triggered activity, initiated by the sodium-calcium exchanger current. Both of these properties were necessary to result in such triggered activity, through promoting delayed-after-depolarizations of sufficient magnitude to cross the excitation threshold, although low amplitude delayed-after-depolarizations occurred in all cases.

**Conclusion:** Using a computational model of the Guinea-pig ventricle it has been demonstrated that loss of T-tubules promotes the development of triggered activity in the presence of beta-stimulation.

PC7

# Point-to-Pixel Tracking Cancellation Pipeline for Motion Artifact Compensation in Uncoupler-Free Non-Ratiometric Experimental Optical Mapping Studies

Jaime Yagüe-Mayans, Conrado J Calvo*, Francisco J Chorro and José Millet

BioITACA, Universitat Politècnica de Valéncia
Valencia, Spain

**Introduction:** Optical Mapping (OM) is a powerful technique for the study of cardiac physiology in the intact heart. Yet, those experiments require uncoupling cardiac contraction to avoid motion artifacts (MA) during registration. We propose a post-processing stepwise approach including point-to-pixel tracking cancellation in combination with blind source separation (BSS) to minimize optical distortion for accurate reconstruction of optical activation.

**Methods:** OM recordings were obtained from non-ratiometric studies in the absence of chemical or mechanical uncoupling. Sequence stacks were acquired with high resolution and pre-process for background noise reduction. Image registration via blob-matching maximum similarity strategy in preselected points was applied using normalized cross-correlation (NCCC) followed by distance weighted bilinear interpolation with sub-pixel resolution for MA tracking cancellation (MATC). MATC was validated using phantoms. Optical distortion was minimized by BSS (FastICA) in local patches. Performance was evaluated using time-space representations (TSP) and by measuring dispersion on action potential duration, activation times and conduction velocity as compared with the presence of the chemical uncoupler blebbistatine.

**Results:** MA was accurately tracked in all phantoms and applied to real sequences. MA tracked loops were heterogeneous spatially and across hearts. These were substantially minimized or abolished after image registration despite of persisting diastolic-coupled optical distortion. Dispersion on APD was minimized (98,7±32.1 vs 87.6±12.3, $p<0.05$) and comparable to that obtained under blebbistatine (89.3±10.8). Activation times and conduction velocity maps were correlated ($r>0.9$,$p<0.001$).

**Conclusion:** Our proposed pipeline for MA cancellation have shown to be a promising approach for accurate reconstruction of optical activation during sinus rhythm while keeping the scheme simple and of low computational cost. We believe this provides a novel framework for further investigation to fully suppress MA avoiding uncoupling techniques that modify cardiac physiology.

PC7

# The Effect of Scar Tissue on Complexity of Activation Patterns in Simulated Human Ventricular Fibrillation

Sathyavani Malyala* and Richard Clayton

University of Sheffield
Sheffield, United Kingdom

**Introduction:** Filament interactions and filament numbers can be used to quantify the complexity of activation patterns in simulated ventricular fibrillation (VF). In this study, we investigated how filament dynamics are affected by the presence of a simulated scar using computational models.

**Methods:** Electrical activation in cardiac tissue was simulated in a 3D monodomain model, with tissue geometry set to be a half ellipsoid representing the human left ventricle (base-apex 9.0 cm, wall thickness 1.1 cm). Scar was represented by a cylindrical region of inexcitable but diffusively coupled tissue with a radius of either 20 or 30 mm and extending either through the full width of the tissue, or half way through. The region of scar was either uniform, or contained a random mixture of excitable and inexcitable tissue. Re-entry was initiated by imposing a single scroll wave on the tissue and filaments were detected as lines of phase singularity. The location and configuration of filaments were detected and recorded throughout simulations of 2000 ms of activity.

**Results:** The initial re-entry broke up to form complex patterns of activity typical of VF. Overall the presence of scar resulted in a small increase in the number of filaments (20 %). Increased radius of half depth uniform scar region resulted in a higher number of filaments. The size and configuration of scar had a strong influence on the configuration of filaments. Increasing the radius in uniform and diffuse scar region resulted in more U-shaped filaments; a smaller radius resulted in more transmural filaments.

**Conclusions:** In simulated VF the presence of a scar region resulted in a modest increase in the number of filaments. The depth of the scar region did not play a significant role on filament configuration, but larger scars resulted in a higher proportion of U shaped filaments.

PC7

# Motion Analysis Method for Determining Cardiomyocyte Beating Properties Based on Digital Image Correlation and Templates

Antti Ahola*, Paruthi Pradhapan, Eeva Laurila, Katriina Aalto-Setälä and Jari Hyttinen

Tampere University of Technology
Tampere, Finland

The development of induced pluripotent stem cells (iPSC) has opened new avenues for in-vitro modelling for disease conditions and drug screening. With the advent of these new applications, there is an increased need for novel analysis methods. We have shown before that video based microscopy measurements provide a viable, non-invasive and label-free method for measuring beating dynamics of human iPSC derived cardiomyocytes. However, as the sarcomeric structure of iPSC derived cardiomyocytes is not fully organized, the displacement of cell is far from the uniform beating of the mature cardiomyocyte. Here, we demonstrate that by defining signal templates from displacement data we can improve the determination of specific beating characteristics of iPSC cardiomyocytes. Video recordings of human iPSC derived cardiomyocytes were performed with different frame rates. Using our in-house developed digital image correlation based video analysis method, beating patterns from different regions of the cell were calculated from displacement vector fields. The vector fields were divided into analysis sectors around the beating focus point. Radial and tangential components were calculated from the vector data, resulting in multiple signals per cell. A cross-correlation based template was then computed for individual cell sectors, representing their beating characteristics. By comparing the templates from different sectors, we observed inter-sector differences in the beating dynamics. Different frame rate and signal lengths were compared to create templates, which present the signal accurately and with enough detail. The template algorithm complemented well the sector division. It is able to classify areas with similar beating and determine areas with non-uniform beating. We showed that combining the sector approach of video analysis with template matching algorithm can provide additional information on the beating dynamics of cardiomyocytes. Our motion analysis has potential to provide valuable information for different disease models and in drug development studies.

PC7

# Discovering and Interpreting Dynamic Behaviors in Cardiovascular Time Series from a Heterogeneous Patient Cohort

Li-Wei Lehman*, Shamim Nemati, Matthew Johnson, George Moody, Thomas Heldt and Roger Mark

MIT
Cambridge, United States

Vital-sign time series of heart rate (HR) and blood pressure (BP) exhibit complex patterns of fluctuations, reflecting the underlying pathological and physiological states of patients. In this work, we adopt a nonparametric Bayesian switching Markov process framework to learn and discover a shared global library of vital-sign dynamical behaviors from a heterogeneous patient cohort. The premise of our approach is that complex physiological time series of a patient cohort can be described by a shared global library of phenotypic dynamic behaviors (or modes) with ``similar'' dynamical structure, and that the vital-sign time series of each individual patient exhibit a subset of these behaviors. Our previous work has demonstrated the utility of such a framework in discovering dynamic behaviors with prognostic values in hospital mortality prediction. In the current work, we adopt a data-driven approach to derive physiological and clinical interpretation of the discovered dynamic behaviors. Using human recordings of HR and BP time series as the subjects undergo a tilt-table protocol (10 subjects, six interventions each), we demonstrated that our technique is able to learn dynamic behaviors corresponding to different postural positions. Finally, using minute-by-minute vital sign recordings of over 450 ICU patient cohort from the MIMIC II database, we investigate the associations between different dynamical behaviors and clinical trajectories of ICU patients as revealed by daily lab values. Preliminary results indicate that the learned BP dynamics during the first 24 hours in the ICU are significantly associated ($p=0.003$) with deteriorating renal function as evidenced by a rise in patients' creatinine measured during the second day in the ICU.

MC

# Ethnic Variation in Prevalence of End QRS Notching and Slurring in Apparently Healthy Populations

Elaine Clark* and Peter Macfarlane

University of Glasgow
Glasgow, United Kingdom

Introduction The presence of end QRS notching or slurring (a characteristic of early repolarization) has been the subject of much recent study, with new guidelines being developed for its identification. The aim of the present study was to examine the prevalence of end QRS notching or slurring in apparently healthy populations of different races. Method New criteria for the detection of end QRS notching and slurring were implemented in the Glasgow resting ECG analysis program. 4223 ECGs (sampled at 500 samples/sec) from Caucasian, Black, Chinese and Indian cohorts were analysed using the same Glasgow program. The interpretations were then examined for the presence of end QRS notching and slurring. Counts were obtained and categorised by age, gender and race. The site of the notching/slurring, e.g. inferior, etc. was also recorded and analysed. Leads aVR,V1-V3 were excluded. Comparisons of proportions were made using a Chi-squared test. Results The prevalence of the phenomenon in the Caucasian, Black, Chinese and Indian data sets was 21%, 26%, 20% and 19% respectively. There was a significant difference ($p < 0.05$) between the prevalence in Blacks and each of the other races. When the prevalence between races was examined by gender, a significant difference between Blacks and each of the other races was found in females. For males, the only significant difference was between Blacks and Indians. There was a significantly higher prevalence in males than females in the Caucasian, Indian and Chinese cohorts. End QRS notching/slurring was most evident in the inferior leads. Conclusion There is a high prevalence of end QRS notching/slurring in normal populations with a significantly higher prevalence in Blacks. While the phenomenon is more evident in males than females in all races, the prevalence in Black women, and in particular, in young Black women, was significantly higher than in other races.

MC

# Bidomain Simulations of Subendocardial Ischemia: The Forward and Inverse Problems

Marius Lysaker, Bjørn Fredrik Nielsen and Samuel Wall*

Norwegian University of Life Sciences
Ås, Norway

ST depression in chest leads can indicate anterior subendocardial ischemia. Simulation studies have shown that it is difficult to replicate this phenomenon with the bidomain model. Such results, combined with additional biomedical knowledge, have raised the debate whether ST depression always occurs in the presence of anterior subendocardial ischemia, especially for subendocardial lesions covering a significant fraction of the endocardial-epicardial distance. We provide a mathematical analysis of the bidomain theory in relation to anterior subendocardial ischemia. Using the static bidomain model, this analysis explains why simulations do not produce ST depression when the ischemia is introduced into an anisotropic model. More precisely, if the ischemic border zone is represented as a smooth surface, then almost right angles between the normal vector of the border and the tangential plane of the fibers will lead to cancelling effects. The simulated transmembrane current flux, entering the ischemic region, will thus be underestimated, and the expected ST depression in chest leads may not occur. We propose to solve this problem by either representing the ischemic border zone as a zigzag surface or by specifying the transmembrane current flux along the border zone, instead of the shift in the transmembrane potential. We employ the latter approach and show that this method always yields ST depression in chest leads positioned above the lesion. A number of simulation studies will be presented, including clinical cases. Both the forward and the inverse problems of electrocardiography are addressed. We consider the inverse ECG problem in which ischemic heart disease is assumed to be the source of changes in the body surface potential maps (BSPMs).

MC

# Author Index

Aalto-Setälä, Katriina 316
Abächerli, Roger ..... 97, 166
Abbasi, Mitra ..... 54
Abry, Patrice ..... 221
Accardo, Agostino ..... 117
Acharyya, Amit ..... 67, 300
Acosta, Juan ..... 35
Addetia, Karima ..... 201
Adeniran, Ismail ..... 288
Agostinelli, Angela ..... 15, 46
Ahola, Antti ..... 316
Akematsu, Yuji ..... 68
Akoum, Nazem ..... 30
Alagoz, Celal ..... 59
Alcaine, Alejandro ..... 35
Ali, Rheeda L ..... 52
Almeida, Rute ..... 26, 210
Almeida, Tiago P ..... 189
Almeida, Tiago Paggi de ..... 188
Alonso, Erik ..... 7, 306, 308
Alonso-Atienza, Felipe ..... 308
Alvi, Mohsan ..... 151
Amandi, Ruhallah ..... 156
Amblard, Amel ..... 83
Amoore, John ..... 238
Amoud, Hassan ..... 39
Andreotti, Fernando .... 16, 91, 151
Andreu, David ..... 35
Ansaloni, Giovanni ..... 227
Ansermino, J Mark ..... 82
Antunes, Sofia ..... 1
Aquilina, Michele ..... 203
Aramendi, Elisabete ..... 7, 306
Aras, Kedar ..... 198
Arefin, Riadh ..... 14
Ariga, Rina ..... 110
Arini, Pedro David ..... 104, 114
Aslanidi, Oleg ..... 217, 283
Assanta, Nadia ..... 131
Aston, Philip ..... 121
Atienza, David ..... 227
Atienza, Felipe ..... 4
Atyabi, Seyyed Abbas ..... 74, 179
Au, Alexander ..... 30
Augiero, Giuseppe ..... 131
Augustyniak, Piotr ..... 129, 180
Ayala, Unai ..... 7, 306, 308
Babaeizadeh, Saeed .. 40, 170, 185
Babajani-Feremi, Abbas ..... 93
Badilini, Fabio ..... 45, 128, 167
Badtke, Piotr ..... 223
Baer, Karl-Juergen ..... 271
Bai, Jieyun ..... 242
Bai, Xiangyun ..... 242
Bai, Yong ..... 72
Bailón, Raquel ..... 80, 210
Balakrishnan, Minimol ..... 145
Baljepally, Raj ..... 165
Bandaru, Jagadish ..... 67
Baquero-Pérez, Oscar ..... 296
Baranowski, Rafał ..... 118
Barbieri, Riccardo ..... 23, 24, 137
Bargiotas, Ioannis ..... 8
Barizon, Gustavo ..... 260, 264
Baron, Lukas ..... 196
Barone, Valeria ..... 114
Bartolucci, Chiara ..... 282
Bartsch, Ronny P ..... 177, 222
Bashan, Amir ..... 177
Basile, Barbara ..... 279
Batchvarov, Velislav ..... 297
Bauer, Axel ..... 174
Bazarghan, Mahdi ..... 156
Becerra, Miguel A ... 138, 226, 286
Behar, Joachim ... 16, 78, 151, 224
Behar, Nathalie ..... 38
Behr, Elijah ..... 297
Behradfar, Elham ..... 2
Benchimol-Barbosa, Paulo ..... 293

Berenfeld, O ..... 150
Berenfeld, Omer ..... 4, 215
Berman, Adam ..... 230
Bermudez, L ..... 119
Bernini, F ..... 9
Bernus, Olivier ..... 235
Berruezo, Antonio ..... 35, 195
Bhuiyan, Tanveer A . 105, 169, 307
Bhuiyan, Tanveer Ahmed ..... 10
Biala, Taher ..... 275
Bian, Chunhua ..... 177
Blaber, Andrew ..... 5
Blanco-Velasco, Manuel ..... 126
Blauer, Joshua JE ..... 51
Bleda-Tomás, Andrés-Lorenzo 102
Bollache, Emilie ..... 8
Bond, Raymond ..... 100, 103, 109
Bonizzi, Pietro ..... 231, 251
Bonnemeier, Hendrik ..... 218
Bonomini, María Paula ..... 104
Bonomini, Marна Paula ..... 114
Boon Lim, Phang ..... 52
Bortolan, Giovanni ..... 113, 302
Bourenane, Hamed ..... 205
Bourke, John P ..... 232
Boyett, Mark R ..... 244
Bozzali, Marco ..... 279
Bragard, Jean ..... 142
Braojos, Rubén ..... 227
Brazdova, Ludmila ..... 84
Brennan, Thomas ..... 178, 229
Britton, Oliver J ..... 245
Brooks, Dana ..... 57
Brooks, Dana H ..... 234
Brotons, Daniel ..... 277
Brouse, Chris J ..... 225
Brugada, Josep ..... 294
Brunner-La-Rocca, Hans-Peter 133
Brüser, Christoph ..... 228
Bueno-Orovio, Alfonso .. 194, 216, 243, 245
Bullinga, John R ..... 59
Burattini, Laura ..... 15, 46, 48
Burrage, Kevin ..... 194
Burton, Brett ..... 57, 198
Bustamante, John ..... 286
Buyse, Bertien ..... 176
Cabasson, A ..... 9
Cadefau, Joan A ..... 277
Caetano dos Santos, Florentino ..... 259
Caicedo, Alexander ..... 172
Calcagnini, Giovanni ..... 279
Calvo, Conrado J ..... 314
Camara, Oscar ..... 35, 195
Caminal, Pere ..... 111, 277
Campillo, Daniel ..... 298
Cangioli, Giorgio ..... 135
Cantalapiedra, Inma R ..... 142
Cantalapiedra, Inmaculada R .. 290
Cantwell, Chris D ..... 52, 62
Cao, Yu ..... 89
Cardenes, Ruben ..... 195
Cardona, Esteban A ..... 286
Cardona, Karen ..... 285
Cardone-Noott, Louie ..... 194
Carducci, Tiziano ..... 131
Carrasco-Sosa, Salvador ... 81, 295
Carrault, Guy ..... 38, 39, 83
Carre, Francois ..... 39
Cartaya, Mary ..... 299
Casadei, Barbara ..... 216
Casanova Blancas, Ubay ..... 254
Casati, Daniela ..... 174
Cassin, Matteo ..... 134
Castells, Francisco ..... 312
Castro, Daniel ..... 160
Castro, Simon ..... 289
Cates, Joshua ..... 30

Censi, Federica ..... 279
Cerbai, Elisabetta ..... 243
Cerutti, Sergio ..... 1
Cervesato, Eugenio ..... 134
Cervigon, Raquel ..... 312
Chakravarthy, V Srinivasa..... 145
Chang, Eugene TY..... 146
Chang, Po-Cheng..... 211
Chen, Chi Hau..... 267
Chen, Diandian..... 197
Chen, Ji ..... 33
Chen, Yu ..... 225
Cherry, Elizabeth ..... 199
Chien, Simon C ..... 211
Chivukula, Krishna Bharadwaj... 67
Chladekova, Lenka ..... 120, 219
Chon, Ki ..... 80
Chorro, Francisco J ..... 314
Choudhury, Robin ..... 262
Chowdary, Venkateswara . 67, 300
Christie, Mark..... 121
Christopher, Monterola ..... 162
Christov, Ivaylo 113, 281, 297, 302
Chronaki, Catherine ..... 135
Chu, Gavin S ..... 188, 189
Chudбček, Vбclav..... 181
Cinquetti, Martino..... 117
Ciregia, Alessio ..... 131
Citi, Luca ..... 24, 137, 173
Ciuchciński, Kamil..... 70
Clark, Elaine..... 112, 318
Clayton, Richard ..... 54, 315
Clayton, Richard H..... 146
Clerx, Michael..... 61
Clifford, Gari..... 16, 143, 158, 178, 182
Clifford, Gari D..... 43, 78, 151, 224
Climent, AM ..... 150
Climent, Andreu M..... 4
Cluitmans, Matthijs JM ..... 3
Cochet, Hubert ..... 205
Cohen, Andrew R..... 59
Cohen, Gregory..... 41
Colantoni, Caterina..... 1
Coll-Font, Jaume ..... 57, 234
Collins, Pieter..... 61
Colman, Michael18, 217, 246, 289
Colman, Michael A..... 141
Colman, Michael Alan..... 313
Colombo, Sebastiano..... 1
Compas, Colin ..... 89
Coppini, Raffaele ..... 243
Corino, Valentina DA ..... 233, 250
Cornforth, David J ..... 27, 124
Corsi, Cristiana ..... 29, 31, 87, 203
Cosmi, Erich ..... 88
Couderc, Jean-Philippe ..... 191
Coudiere, Yves ..... 287
Coudière, Yves ..... 235
Crescencio, Julio Cesar ..... 115
Crescêncio, Júlio Cesar ..... 101
Crijns, Harry ..... 251
Cruces, Pablo Daniel ..... 104
Cybulski, Gerard..... 269, 270
Cygankiewicz, Iwona..... 47
Czippelova, Barbora 120, 123, 219
da Silva Filho, Antonio Carlos . 115
Dall'Armellina, Erica..... 194, 262
Daly, Michael ..... 100
Dastagir, Nawshin..... 189
Davidovic, Andjela ..... 287
Daya, Mohamud ..... 7, 306
De Cesare, Alain..... 8
de Chazal, Philip..... 208, 255
De Chazal, Philip ..... 41
De Cooman, Thomas ..... 71
de Graaf, Michiel ..... 200
de Jong, Monique MJ..... 3
De Jongh, Marjolein 106, 171, 184
de la Cruz, Alicia..... 282

De Marchi, Luca ..... 87
De Marco, Paola ..... 107
De Simone, Raffaele ..... 268
Dehkordi, Parastoo ..... 82
Delgado-Trejos, Edilson ..... 138
della Bella, Paolo ..... 1
Devine, Brian ..... 112
Di Marco, Luigi Yuri ..... 232
di Molfetta, A ..... 9
Di Nardo, Francesco ..... 48
Diciotti, Stefano ..... 24
Dimitrov, Nikolay ..... 297
Ding, Quan ..... 72
Dittrich, Andreas ..... 227
Doessel, Olaf ..... 65, 296
Doret, Muriel ..... 221
Dössel, Olaf ..... 37, 196, 212, 237
Dovancescu, Silviu ..... 274
Draeger, Erik ..... 58
Drijkoningen, Lenn ..... 239
Driscoll, Michael ..... 58
Duan, Wenfeng ..... 64
Dumont, Guy A ..... 82
Duque, Juan E ..... 286
Ebrahimi Orimi, Hamid ..... 157
Echebarria, Blas ..... 290
Eftestøl, Trygve ..... 127, 263, 308
Eggett, Christopher ..... 64
Eichhorn, Stefan ..... 291
Eilevstjønn, Joar ..... 127
Elorza, Jorge ..... 142
Elshrif, Mohamed ..... 199
El-Tatar, Aziz ..... 83
Emerek, Kasper ..... 10
Endo, Miyuki ..... 122, 136
Engan, Kjersti ..... 127, 263
Engelhardt, Sandy ..... 268
Enger, Steve ..... 233, 250
Erem, Burak ..... 57, 234
Erol, Yusuf ..... 72
Ersdal, Hege ..... 127
Escalona, Omar J ..... 92, 192
Escobar, Braiam ..... 309
Eskola, Hannu ..... 259
Esposito, Antonio ..... 1
Estelrich, Ana ..... 135
Faes, Luca ..... 176, 257
Falcao, Breno A A ..... 90
Falcao, Joao L A A ..... 90
Farhadi, Mohammad ..... 156
Fasano, Antonio ..... 13
Fazel-Rezai, Reza ..... 14
Felix de Castro, Antonio ..... 247
Félix, Paulo ..... 160
Feng, Mengling ..... 73, 229
Fenton, Flavio ..... 197
Fernandez-Aviles, F ..... 150
Fernández-Avilés, Francisco ..... 4
Ferrante, Alberto ..... 227
Ferrari, G ..... 9
Ferrazzi, Enrico ..... 174
Ferrer, A ..... 119
Ferrero, Jose M ..... 215, 247
Feuerstein, Delphine ..... 83
Finlay, Dewar .. 100, 103, 109, 168
Fioretti, Sandro ..... 48
Firoozabadi, Reza ..... 170
Fischer, Wolf-Joachim ..... 94
Flores-Yepes, Jose-Antonio .... 102
Flyrez Pacheco, Edward ..... 265
Fornasa, Elisa ..... 117
France, Jessie J ..... 148
Freeman, Daniel K ..... 225
Fresiello, L ..... 9
Fritz, Thomas ..... 196
Furuie, Sergio S ..... 90
Gadioli, Leonardo ..... 264
Galeotti, Loriano ..... 77
Gallo Júnior, Lourenço .... 101, 115
Galluzzo, Francesca ..... 87

Gangidi, Adithya G .....267
Gao, Xinpei .....200
Garcia Vicent, C .....119
García, Constantino A .....160
Garcia, N .....119
García, Ronald G .....23
García-Alberola, Arcadi ..102, 139, 296
García-Alberola, Arcadio .....34
García-Quintanilla, Jorge .....312
Garde, Ainara .....82
Gatzke, Ronald .....225
Gelzer, Anna RM .....193
Gerevini, Alfonso .....167
Ghaffari, Ali .....74, 179
Ghassemi, Mohammad ...229, 276
Ghavami, Nooshin .....283
Ghodrati, Alireza .....93
Ghosh, Shameek .....73
Gieraltowski, Jan .....144
Gierałtowski, Jan .....118
Gierałtowski, Jan Jakub .....70
Gierstorfer, Andreas .....209
Gil, Eduardo .....80, 296
Giles, Wayne R .....285
Giliбn, Zoltбn .....75
Gilmour Jr, Robert F .....193
Gimeno-Blanes, Francisco-Javier .....102
Gimeno-Blanes, Juan-Ramón ..102
Giovanni, Adriano .....247
Giuliani, Corrado .....15, 46
Godoy, E .....119
Gómez, Juan Francisco .....285
Gomis, Pedro .....111
Goncalves, Paulo .....221
Gong, Yinglan .....214
Gonzalez, Rene .....298
Gonzalez-Fernandez, Rene .....130
Gonzalez-Fernandez, Rene Ivan ..... 125
González-Otero, Digna ..... 7, 308
Gonzбlez-Otero, Digna M . 23, 306
Goodfellow, Jonathan ..... 92
Goovaerts, Griet ..... 50, 71
Gori, Andrea ..... 131
Graff, Claus . 10, 12, 105, 169, 307
Graindorge, Laurence ..... 83
Grau, Vicente ..... 262
Gray, Richard ..... 197
Gregg, Rich ..... 170
Gregg, Richard ..... 40, 185
Greisas, Ariel ..... 147
Grieten, Lars ..... 239
Griffiths, Clive ..... 240
Griffiths, Kerri ..... 112
Grisan, Enrico ..... 88
Grzegorczyk, Iga ..... 70
Guadiana, Juan ..... 128
Guerrisi, Maria ..... 24
Guez, Allon ..... 59
Guffanti, Giulia ..... 173
Guhathakurta, Soma ..... 145
Guillem, Maria S ..... 4
Guillem, MS ..... 150
Guillén-Mandujano, Alejandra 81, 295
Guldenring, Daniel . 100, 103, 109, 168
Gur, Yaniv ..... 148
Haex, Bart ..... 66
Halamek, Josef ..... 159, 310
Hall, Burr ..... 191
Hamilton, Emily F ..... 278
Han, Chengzong ..... 40, 236
Han, Fred ..... 51
Han, Frederick ..... 30
Hansen, John ..... 10, 169, 307
Hargittai, Sбndor ..... 252

Hatam, Nima ..... 55
He, Bin ..... 204, 236
Heldt, Thomas ..... 175, 317
Helfenbein, Eric ..... 211
Henriquez, Craig ..... 20, 284
Hernández Pérez, Eduardo ..... 254
Hernandez, Alfredo ..... 39
Hernández, Alfredo ..... 38, 83, 210
Hernando, David ..... 210
Hernбndez-Ortega, Jesъs ..... 102
Hitzeroth, Jens ..... 178
Hlavacova, Miroslava ..... 304
Hoeben, Bart ..... 162
Holmer, Mattias ..... 241
Honzikova, Natasa ..... 84
Hoog Antink, Christoph ..... 228
Hoshiyama, Asagi ..... 220
Hoshiyama, Masaki ..... 220
Hrstkova, Hana ..... 84
Hu, Xiao ..... 72
Huang, Dong ..... 162
Huang, Siyi ..... 32
Huang, Ying ..... 121
Hubbard, Marjorie ..... 20
Hyttinen, Jari ..... 21, 316
Imam, Mohammad Hasan. 25, 280
Ingallina, Fernando ..... 114
Iollo, Angelo ..... 235
Irurtia, Alfredo ..... 277
Irusta, Unai ..... 308
Ivanov, Plamen CH ..... 177, 222
Jaecques, Siegfried ..... 133
Jafarnia Dabanloo, Nader ..... 116, 187, 272
Jager, Franc ..... 79
Jagirdar, Agathya ..... 67, 300
Jalali, Ali ..... 6
Jalife, Jose ..... 215
James, Stuart ..... 283
Janíčková, Tereza ..... 181
Janoušek, Oto ..... 273, 301, 305
Jansen, Katrien ..... 257
Jarvis, Jonathan ..... 289
Javorka, Kamil ..... 120, 123, 219
Javorka, Michal ..... 120, 123, 219
Jaźwiec, Przemysław ..... 258
Jekova, Irena ..... 97, 166
Jelinek, Herbert F ..... 25, 27, 124
Jensen, Ask S ..... 169
Jensen, Ask Schou ..... 10
Jeon, Moongu ..... 161
Jeon, Taegyun ..... 161
Ji, Lizhen ..... 28
Jimenez, Joe A ..... 138
Johannesen, Lars ..... 77
Johnson, Alistair E W ..... 43, 78
Johnson, Chris R ..... 148
Johnson, Matthew ..... 317
Johnston, Barbara ..... 149
Johnston, Peter ..... 149
Johnston, Peter R ..... 53
Jones, Gareth ..... 288
Joseph, Bastin ..... 67
Joutsen, Atte ..... 259
Jurak, Pavel ..... 159, 310
Jurco, Juraj ..... 159
K, Abid ..... 154
Kabir, Muammar ..... 256
Kachenoura, Nadjia ..... 8
Kambova, Liliana ..... 113
Kanters, Joergen ..... 12
Kanters, Jørgen K ..... 105, 169
Kańtoch, Eliasz ..... 132
Karck, Matthias ..... 268
Karlen, Walter ..... 82
Karmakar, Chandan ..... 25, 280
Katova, Tzvetana ..... 113
Kaur, Jaspreet ..... 56
Keller, David UJ ..... 65
Keller, Matthias W ..... 37

Kelly, Christopher ..... 262
Kennedy, Alan ..... 109, 168
Kestler, Hans A ..... 17
Khalil, Mohamad ..... 39
Khandoker, Ahsan ..... 25, 122, 280
Khandoker, Ahsan H ..... 136
Kharche, Sanjay ..... 246, 289, 313
Kheirati Roonizi, Ebadollah ..... 95
Khodor, Nadine ..... 39
Kholmovski, Eugene ..... 30
Khosrow-khavar, Farzad ..... 5
Kimura, Yoshitaka ..... 122, 136
Kirby, Robert M ..... 148
Kitslaar, Pieter ..... 200
Knoll, Alois ..... 291
Kodoth, Vivek ..... 92
Kokosińska, Dorota ..... 118
Kolářová, Jana ..... 273, 301, 305
Kośna, Katarzyna ..... 70, 311
Kovács, Péter ..... 75
Kozumplнk, Jiřн ..... 301
Kramer, George C ..... 85
Kramer-Johansen, Jo ..... 308
Krasteva, Vessela ..... 97, 166, 281
Kresge, Scott ..... 186
Krug, Johannes W ..... 76, 209, 266
Kruger, Martin ..... 217
Kühl, Michael ..... 17
Kuklik, Paweł ..... 311
Kumar, Narendra ..... 231
Kyal, Survi ..... 191
Lagae, Lieven ..... 257
Laguna, Pablo . 35, 38, 47, 80, 104, 183, 206
Lam, Sera P ..... 124
Lamberti, Claudio ..... 203
Lambiase, Pier ..... 282
Lang, Roberto ..... 201
Langley, Philip ..... 64, 141, 232
Lankveld, Theo ..... 251
Latcu, Decebal G ..... 253
Laurila, Eeva ..... 316
Lausser, Ludwig ..... 17
Lazarova, Zuzana ..... 123, 219
Leber, Remo ..... 97, 166
Lechuga, Luis ..... 139
Lehman, Li-wei ..... 229, 317
Lehman, Li-Wei ..... 276
Leite, Argentina ..... 26
Lemos, Pedro A ..... 90
Lenaerts, Frederic ..... 239
Lenis, Gustavo ..... 296
Leonardi, Roberta ..... 29
Leonhardt, Steffen ..... 55, 228
Li, Dawel ..... 33
Li, Jinyan ..... 73
Li, Jue ..... 244
Li, Ke ..... 28
Li, Lei ..... 72
Li, Peng ..... 28
Li, Xin ..... 188, 189, 190
Liberos, A ..... 150
Liberos, Alejandro ..... 4
Lim, Chi-Wan ..... 202, 261
Lima, Gustavo Zampier dos Santos ..... 177
Linde, Jørgen ..... 127
Liu, Changchun ..... 28, 63
Liu, Chengyu ..... 28, 63, 238, 240
Liu, Kang KL ..... 177, 222
Liu, Xing ..... 216
Llamedo, Mariano ..... 99, 206
Loewe, Axel ..... 212
Lopez, J ..... 119
Lopez, Rolando ..... 298
López-Ayala, Jose-María ..... 102
Lopez-Cardona, Juan Dayron .. 130
Lopez-Creagh, Rolando ..... 130
Lopez-Reyez, Alejandro ..... 130
Lopez-Rodriguez, Rolando ..... 130

Lorenzini, Cinzia ..... 203
Lu, Haisheng ..... 186
Lu, Weigang ..... 19
Lubba, Carl Henning ..... 55
Luca, Adrian ..... 152
Luo, Cunjin ..... 19
Luo, Shen ..... 96
Lurbe, EF ..... 119
Lüsebrink, Falk ..... 266
Lutz, Yannick ..... 212
Lutz, Yannik ..... 296
Lysaker, Marius ..... 319
Lбzaro, Jesъs ..... 80
Ma, Qianli DY ..... 222
Maan, Arie C ..... 106, 171, 184
Mabo, Philippe ..... 38
Macabelli, Giuseppe ..... 1
Macfarlane, Peter ..... 112, 318
MacLeod, Rob ..... 30, 57, 198
MacLeod, Rob S ..... 51
Maestre-Ferriz, Rafael ..... 102
Maffessanti, Francesco ..... 201
Maheshwari, Sidharth ..... 300
Mahmood, Raziuddin ..... 86
Mainardi, Luca ..... 173
Mainardi, Luca T ..... 233, 250
Malberg, Hagen ..... 91, 218
Malek, Miroslaw ..... 227
Malik, Marek ..... 47
Malinowski, Krzysztof ..... 42
Malki, Guy ..... 213
Malyala, Pavana Ravi Sai Kiran .. 67
Malyala, Sathyavani ..... 315
Man, Sumche ..... 46, 48, 106, 171, 184
Mancini, Matteo ..... 279
Mann, Steffen A ..... 11
Manoharan, Ganesh ..... 92
Mantovan, Roberto ..... 29
Marianna, Meo ..... 253
Marino, Marco ..... 31
Mark, Roger ..... 229, 317
Markhasin, Vladimir S ..... 248
Marofkhani, Ahmad ..... 156
Marrouche, Nassir ..... 30
Marrouche, Nassir F ..... 51
Martín González, Sofía ..... 254
Martínez, Juan Pablo ... 35, 38, 99, 183, 206
Martinez, Laura ..... 215
Martínez-Fernández, Andrés .. 126
Martín-Yebra, Alba ..... 38
Martнn-Garcнa, Juan Francisco 34
Marzbanrad, Faezeh ..... 136
Masetti, Guido ..... 87
Matejkova, Magdalena ..... 310
Matelot, David ..... 39
Mattei, Eugenio ..... 279
Matveev, Mikhail ..... 281
Mayosi, Bongani ..... 178
McEneaney, David ..... 192
McGann, Chris ..... 30
McLaughlin, James ..... 109, 168
Meinzer, Hans-Peter ..... 268
Meissimilly, Gay ..... 299
Melgaard, Jacob ..... 10, 169, 307
Melgara, Marcello ..... 135
Melia, Umberto ..... 277
Mendoza Garcia, Alejandro .... 291
Menon, Carlo ..... 5
Merlo, Marco ..... 117
Meste, O ..... 9
Meste, Olivier ..... 253
Mestha, Lalit ..... 191
Michor, Franziska ..... 58
Mieke, Stephan ..... 238
Milanova, Maria ..... 281
Millet, J ..... 150
Millet, José ..... 4, 312, 314
Milosevic, Jelena ..... 227

Min, Wan.....261
Min, Xiaoyi .....33
Mincholé, Ana .....104, 194, 243
Mincholй, Ana.....110
Minter, Jan .....133
Mirmohamadsadeghi, Leila.....98
Miszalski-Jamka, Tomasz .....258
Młyńczak, Marcel.....269
Moharreri, Sadaf.....116, 272
Mollakazemi, Mohammad Javad .....74, 179
Moody, Benjamin E.....69, 153
Moody, George .....317
Moody, George B .....69, 153
Mora-Jiménez, Inmaculada.....34, 139
Mor-Avi, Victor.....31, 201
Moreno, Cristina .....282
Moreno, Javier .....312
Morgan, Ross .....217, 283
Morizzo, Carmela .....87
Morris, Alan.....30
Mortara, David .....45, 108
Mousseaux, Elie .....8
Muhammad, Syamil .....275
Mulet-Cartaya, Margarita125, 130
Müller, Andreas.....218
Murillo, Juan P.....226
Murray, Alan .....63, 64, 238, 240
Murta Junior, Luiz Otávio 260, 264
Murtagh, Gillian .....201
Murzi, Bruno .....131
Muszkiewicz, Anna.....216
Nabers, Diana.....268
Nadal, Jurandir .....293
Nadkarni, Vinay.....6
Naito, Yasuhiro.....22
Nam, Yunyoung.....80
Nandi, Manasi .....121
Nasario-Junior, Olivassй.....293
Nataraj, C ..... 6
Naumann, Tristan ..... 44
Navarro Mesa, Juan Luis..... 254
Nelwan, Stefan ..... 140
Nemati, Shamim ..... 276, 317
Neubauer, Stefan..... 110, 262
Ng, Andre G ..... 189
Ng, Fu Siong ..... 2, 62
Ng, G Andre ..... 190
Ng, G André ..... 188
Nguyen, Hung ..... 73
Ni, Haibo ..... 18
Nicolosi, Gian L ..... 134
Nielsen, Bjørn Fredrik ..... 319
Nielsen, Jimmi..... 105
Niewiadomski, Wiktor ..... 269
Noack, Alexander..... 94
Noč, Marko ..... 303
Nooriyan, Azadeh ..... 187
Nosakhare, Ehimwenma..... 175
Novakova, Marie ..... 304
Nováková, Marie .... 273, 301, 305
Novakova, Zuzana..... 84
Nuyens, Dieter ..... 239
Nygren, Anders ..... 2, 56
Oesterlein, Tobias..... 37
Olde, Bo ..... 241
Olejníčková, Veronika..... 305
Olejnickovб, Veronika..... 304
Oostendorp, Thom F..... 60
Orglmeister, Reinhold..... 11
Orłowska - Baranowska, Ewa . 118
Orozco-Duque, Andrés ..... 286
Orsolini, Stefano ..... 24
Oster, Julien ..... 16, 78, 151
Otani, Niels F..... 193
Otero, Abraham..... 160
Ottaviano, Giovanni..... 48
Pachamuthu, Rajalakshmi ..... 67
Paci, Michelangelo..... 21

Padma, Gayathri.....300
Palacio, Laura C.....226, 286
Palaniswami, Marimuthu.25, 122, 136, 280
Palmisano, Anna.....1
Pan, Jingwei.....32
Panda, Utkalika .....300
Pangerc, Urska .....79
Papa, Valéria .....115
Papastylianou, Tasos.....224
Parvaneh, Saman ....116, 187, 272
Passini, Elisa .....243
Patel, Amit.....31, 201
Paulova, Hana .....304
Pedron-Torrecilla, J .....150
Pedrón-Torrecilla, Jorge.....4
Peeters, Ralf .....231
Peeters, Ralf LM .....3
Peñaranda, Angelina .....290
Pépin, Jean-Louis.....83
Pereira da Silva, Fátima Maria Helena Simões.....101
Pereira da Silva, Fбtima Maria Helena .....115
Perera, Alexandre .....277
Perez Alday, Erick Andres.....141
Perez-david, E.....150
Pérez-Villacastín, Julián.....312
Peters, Nicholas S.....52, 62
Peterson, Derick.....191
Piazza, Rita .....134
Piccini, Giacomo.....131
Pilcher, Thomas.....198
Pimental, Marco.....229
Pimentel, Marco.....158
Pineda-Lypez, Flavio.....126
Piskulak, Piotr.....270
Pison, Laurent .....231
Platonov, Pyotr G .....233, 250
Plesinger, Filip .....159, 310
Pociask, Elżbieta ..... 42
Podziemski, Piotr ..... 70, 311
Pohl, Antje ..... 55
Poignard, Clair ..... 287
Poll, Rüdiger..... 94
Polski, Marcin ..... 291
Potočňák, Tomáš ..... 305
Potse, Mark..... 36
Potyagaylo, Danila ..... 237
Pradhapan, Paruthi..... 316
Presedo, Jesъs ..... 160
Proniewska, Klaudia Kinga..... 42
Proniewski, Bartosz ..... 42, 258
Provazník, Ivo..... 273, 301, 305
Puddu, Paolo Emilio..... 67, 300
Pueyo, Esther..... 38, 47, 183
Quintana Morales, Pedro ..... 254
Qureshi, Norman A..... 52
Raine, Daniel..... 232
Ramos, Pablo ..... 294
Ramos-Lopez, Javier ..... 139
Ramнrez, Julia..... 47
Randles, Amanda..... 58
Ranjan, Ravi ..... 30, 51
Rauber, Martin ..... 303
Ravanfar, Mohammadreza..... 14
Ravelo Garcнa, Antonio Gabriel ..... 254
Ravon, Gwladys ..... 235
Redheuil, Alban..... 8
Reiber, Johan ..... 200
Rellini, Gian L ..... 134
Reyes, Laura M ..... 23
Rhode, Kawal ..... 217
Ribas Ripoll, Vicent ..... 294
Ricci, Giorgio..... 131
Righini, Giovanni..... 134
Riistama, Jarno ..... 274
Rivolta, Massimo W..... 174
Rizzo, Giovanna ..... 1

Roca, Emma ..... 277
Rocca, Emiliano ..... 131
Rocha, Ana Paula..... 26
Rodrigo, M..... 150
Rodrigo, Miguel..... 4
Rodrigues, Paola A ..... 192
Rodriguez, Blanca... 110, 194, 216, 243, 245
Rohanova, Magdalena ..... 84
Rojas Quiros, Camilo ..... 227
Rojo-Álvarez, José Luis ..... 34, 126, 139, 296
Rojo-Álvarez, Jose-Luis..... 102
Romero, Daniel ..... 38, 183
Romero, Enrique ..... 294
Romero, Lucia ..... 215
Roney, Caroline H..... 52, 62
Ronkes, Mark ..... 140
Ronzhina, Marina ... 273, 301, 304, 305
Rose, Georg..... 76, 209, 266
Rossi, Irene..... 107
Rottmann, Markus ..... 37
Ruiz de Gauna, Sofía ..... 306
Ruiz, Diolkis ..... 299
Ruiz, Jesús ..... 306, 308
Russel, James K ..... 306
Russell, James K..... 7
Russell, Janice..... 124
Sadr, Nadi..... 255
Saiz, J ..... 119
Saiz, Javier ..... 215, 285, 286
Salas-Boni, Rebeca ..... 72
Salenius, Juha ..... 259
Sales, Fernando J R..... 90
Salinet, Angela..... 190
Salinet, Joao ..... 190
Salinet, Joao L..... 189
Salinet, João Loures..... 188
Samiee, Kaveh ..... 75
Sanchez-Cano, Alfonso ..... 139
Sandberg, Frida..... 241, 250
Sanders, Prashanthan..... 311
Sano, Hitomi ..... 22
Santos, Mauro ..... 158
Saoudi, Nadir ..... 253
Sassi, Roberto ..... 95, 128, 174
Schalij, Martin J..... 106, 171, 184
Scheer, Peter ..... 273
Schiariti, Michele ..... 300
Schlegel, Todd..... 303
Schlindwein, Fernando ... 190, 275
Schlindwein, Fernando S 188, 189
Schmid, Ramun..... 97, 166
Schmidt, André ..... 264
Schmidt, Marcus..... 209
Schmidt, Samuel ..... 12
Schmidt, Samuel E ..... 169, 307
Schmidt, Samuel Emil ..... 10
Scholte, Arthur..... 200
Scholz, Eberhard P ..... 212
Schotten, Ulrich ..... 251
Schou Jensen, Ask..... 12, 307
Schulte, Roman..... 76
Schulz, Steffen ..... 122, 271
Schulze, Walther..... 237
Schumacher, Autumn ..... 230
Scilingo, Enzo Pasquale..... 137
Scully, Christopher..... 77
Scully, Christopher G ..... 85
Sebastian, Rafael ..... 195
Seemann, Gunnar..... 37, 65, 196, 212, 217, 296
Selvaraj, Senthil Kumar..... 202
Senra Filho, Antonio Carlos ... 260, 264
Serrano-Balazote, Pablo ..... 139
Severi, Stefano.... 21, 29, 243, 282
Sfirakis, Petros ..... 143
Sherwin, Spencer J..... 52

Shi, Pengcheng ..... 199
Shiguemi Furuie, Sergio ..... 265
Siegle, Lea ..... 17
Siggers, Jennifer H ..... 52, 62
Silva Filho, Antϕnio Carlos ..... 101
Silva, Ikaro ..... 44, 69, 153
Silva, Maria Eduarda ..... 26
Silva, Marta João ..... 26
Simic, Ana ..... 142
Simões, Marcus Vinicius ..... 264
Simov, Dimiter ..... 281
Simova, Iana ..... 113, 297
Sinagra, Gianfranco ..... 117
Sison, Shiloh ..... 33
Smail, Bruce ..... 289
Smeets, Christophe ..... 239
Smolinska, Maria ..... 223
Soegaard, Peter ..... 10
Soguero-Ruiz, Cristina ..... 139
Solbrig, Harold ..... 135
Solem, Kristian ..... 241
Solinski, Mateusz ..... 144
Soliński, Mateusz ..... 70
Solovyova, Olga ..... 248
Sörnmo, Leif ..... 250
Soto-Iglesias, David ..... 35
Soukup, Ladislav ..... 310
Sparagino, Luca ..... 128
Speciale, Nicolò ..... 87
Speck, Oliver ..... 266
Spence, Ian ..... 124
Spilka, Jiri ..... 221
Spilka, Jiří ..... 181
Springer, David ..... 158, 178, 182
Stafford, Peter ..... 190
Štajer, Dušan ..... 303
Stampalija, Tamara ..... 174
Stapleton, Michelle ..... 133
Starc, Vito ..... 249, 303
Stastna, Jana ..... 84
Stevenson, Robert ..... 289
Stockbridge, Norman L ..... 128
Stolcman, Simon ..... 311
Storms, Valerie ..... 239
Stracina, Tibor ..... 304
Stračina, Tibor ..... 305
Strauss, David ..... 77
Strauss, David G ..... 85
Struijk, Johannes ..... 12
Struijk, Johannes J .. 105, 169, 307
Struijk, Johannes Jan ..... 10
Su, Honglian ..... 214
Su, Jianwei ..... 96
Su, Yi ..... 162, 202, 261
Sun, Zehui ..... 96
Sunderland, Kevin ..... 230
Svehlikova, Jana ..... 36
Swenne, Cees A . 46, 48, 106, 171, 184
Swenson, Darrell ..... 57
Syeda-Mahmood, Tanveer . 86, 89
Taddei, Alessandro ..... 131
Tan, May-Ling ..... 202
Tan, Ru-San ..... 202, 261
Tarassenko, Lionel ..... 178, 182
Tarroni, Giacomo ..... 31, 88
Tarvainen, Mika P ..... 27
Tasker, Robert ..... 175
Tate, Jess ..... 57, 198
Tavakolian, Kouhyar ..... 5, 14
Teijeiro, Tomás ..... 160
Teo, Soo-kng ..... 162
Teo, Soo-Kng ..... 202, 261
Teperino, Marcos Javier ..... 104
Ter Haar, C Cato ..... 106, 171, 184
Tereshchenko, Larisa ..... 49, 256
Tessa, Carlo ..... 24
Testelmans, Dries ..... 176
Testoni, Nicola ..... 87
Thendral, Murugaiyan ..... 300

Thomson, Stuart.....133
Thore, Maren .....55
Tiwari, Sandeep.....67
Tobon, Catalina .....215
Tobón, Catalina .....226
Tobyn, Catalina .....286
Toki, Tamami.....22
Tomita, Masaru.....22
Tonhajzerova, Ingrid120, 123, 219
Toninelli, Gianfranco.....167
Torres, Hector .....298
Torres, Róbinson .....309
Toschi, Nicola .....24
Trenor, Beatriz .....285
Treskes, Roderick ....106, 171, 184
Trivella, MG.....9
Tsanas, Athanasios.....143
Tsuji, Masatsugu .....68
Tu, Shengxian .....200
Tuan, Jiun .....190
Turianikova, Zuzana 120, 123, 219
Tveit, Arnljot.....233, 250
Tysler, Milan.....36
Ugarte, Juan P .....286
Uhrikova, Zuzana.....120
Ulimoen, Sara R.....233, 250
Vaglio, Martino .....167
Valdes, Katia.....298
Valentinuzzi, Max.....114
Valenza, Gaetano .....23, 24, 137
Valenzuela, Carmen .....282
Vallverdu, Montserrat.....277
van Dam, Eelco M .....60
van Dam, Peter.....57
van Dam, Peter M .....60
van Dam, Teus.....140
van den Berg, Jeroen.....140
Van der Auwera, Jo .....239
van der Heide, Maurits .....184
Van der Heide, Maurits ...106, 171
Van Huffel, Sabine 50, 66, 71, 133, 172, 176, 257
van Oosterom, Adriaan ..... 60
Vandenberk, Bert..... 50
Vander Sloten, Jos ..... 66
Vandervoort, Pieter ..... 239
Vanheusden, Frederique J ..... 189
Vanheusden, Frederique Jos .. 188
Varela, Marta..... 283
Varon, Carolina .... 50, 66, 71, 133, 172, 176, 257
Varro, Andras..... 245
Vartela, Vassiliki..... 143
Vasilyeva, Anastasia..... 248
Vemishetty, Naresh ..... 67, 300
Verghese, George ..... 175
Vernekar, Sachin..... 163
Veronesi, Federico..... 29, 31
Vesin, Jean-Marc ..... 98, 152, 207
Vicente, Jose..... 77
Vigmond, Edward ..... 56, 246
Vigmond, Edward J ..... 2
Vijayasenan, Deepu ..... 154, 163
Vikulova, Nathalie..... 248
Villani, Valeria..... 13
Ville, Nathalie ..... 39
Virag, Laszlo..... 245
Viscor, Ivo ..... 310
Visentin, Silvia..... 88
Visnovcova, Zuzana ..... 219
Volders, Paul GA ..... 3, 61
Vollmer, Marcus ..... 164
Vondra, Vlastimil ..... 310
Voss, Andreas ..... 122, 271
Vranken, Julie ..... 239
Vu, Huyen ..... 127
Wailoo, Michael..... 275
Wall, Samuel..... 319
Wallman, Mikael..... 194
Walsh, Philip R ..... 92, 192

Walton, Richard D ..... 235
Wang, Chun-Chieh ..... 211
Wang, Dafang ..... 57
Wang, Hongzhi ..... 89
Wang, John ..... 186
Wang, Kuanquan ..... 19, 242
Wang, Quan ..... 86
Warrick, Philip A ..... 278
Watermann, Niall ..... 192
Watkins, Hugh ..... 110
Wei, Meng ..... 32
Weinert, Lynn ..... 201
Wen, Ming-Shien ..... 211
Wensley, David ..... 82
Wessel, Niels ..... 218, 254
Westra, Ronald L ..... 3
Widjaja, Devy ..... 71, 176
Wierzba, Tomasz ..... 223
Wilders, Ronald ..... 292
Wilhelms, Mathias ..... 212
Willemen, Tim ..... 66
Willems, Rik ..... 50
Wilson, Brent ..... 30
Wilson, Lauren ..... 311
Wo, Hong-Ta ..... 211
Woie, Leik ..... 263
Wojdel, Anna ..... 294
Wolf, Ivo ..... 268
Xia, Henian ..... 165
Xia, Ling ..... 214
Xia, Xiaojuan ..... 191
Xie, Chaocheng ..... 96
Xu, Beilei ..... 191
Xu, Bo ..... 200
Xu, Liang ..... 200
Xue, Joel ..... 12
Y, Sivakrishna ..... 67
Yagье-Mayans, Jaime ..... 314
Yan, Chang ..... 28
Yang, Bo ..... 162
Yang, Xin ..... 32
Yazdani, Sasan ..... 207
Ye, Wenyu ..... 96
Ying, Wenjun ..... 284
Yu, Jiao ..... 96
Yu, Jongmin ..... 161
Yu, Lin ..... 32
Yu, Long ..... 204
Yuan, Yongfeng ..... 19, 242
Zajaczkowski, Stanislaw ..... 223
Zamaraev, Dmitry ..... 248
Zarzoso, Vicente ..... 253
Zaunseder, Sebastian ..... 91, 218
Zavodna, Eva ..... 84
Zebrowski, Jan ..... 144
Żebrowski, Jan ..... 118
Żebrowski, Jan Jacek ..... 311
Zeemering, Stef ..... 231, 251
Zemzemi, Nejib ..... 194, 205
Zenger, Brian ..... 30
Zengo, Beth ..... 170
Zhan, Heqing ..... 214
Zhang, Henggui .. 18, 19, 141, 242, 246, 288, 289, 313
Zhang, Xiaorong ..... 72
Zhao, Jichao ..... 289
Zhao, Lina ..... 63
Zhao, Xiaopeng ..... 165
Zheng, Dingchang ..... 63, 64, 214, 238, 240
Zhong, Liang ..... 202, 261
Zhou, Zhaoye ..... 204, 236
Zhu, Tingting ..... 224
Zhu, Yongwei ..... 155
Zibolen, Mirko ..... 120
Zimmermann, Norbert ..... 268
Zlochiver, Sharon ..... 147, 213
Zong, Wei ..... 186
Żyliński, Marek ..... 269